Characterisation of the Function, Sequence Polymorphism and Toxicity of the Yeast Rnq1p Prion Protein

By

Gemma Louise Staniforth

A thesis submitted to the University of Kent for the degree of Ph.D. in Biochemistry in the Faculty of Science

THESIS CONTAINS

CD

Declaration

No part of this thesis has been submitted in support of an application for any degree or qualification of the University of Kent or any other University or Institute of learning.

Gemma Staniforth

28th March 2011

Acknowledgements

A big thank you to all members of the Tuite, Gourlay and von der Haar labs who have helped me in so many ways throughout my Ph.D.

I would like to say thank you to my family also, for suffering the absence of a daughter, a sister and an aunty, but who were always there offering their support through the many ups and downs! And to Dan, the magic ingredient, who I must thank for keeping me sane, happy, focused and hopeful.

Finally, Professor Mick Tuite has been a wonderful mentor over the last four years. He has offered a great deal of guidance and insight, near inexhaustible patience, and has at every step been encouraging. I would like to say how grateful I am to him for all of these qualities and for making my Ph.D. a truly enjoyable and invaluable experience.

Abstract

The *Saccharomyces cerevisiae* Rnq1p prion protein plays an integral role in the dynamics of other aggregation-prone proteins, be they other prion proteins or glutamine-rich proteins. The conformational conversion of a prion protein to its prion state is often associated with changes to cellular physiology and two interesting questions arise from this. One, what impact do these physiological changes have on our ability to interpret experimental findings in this model organism? Two, are these changes non-random, representing a novel means of altering cellular physiology? An understanding of the cellular function of Rnq1p is important in addressing these questions. Further, the role of Rnq1p in its [*PIN*$^+$] prion state as a universal catalyst for amyloid-formation provides a useful model for dissecting mechanisms of amyloid toxicity, and once again, cellular function is one parameter of multiple that determine the final toxicity profile of a protein.

To identify a cellular function for Rnq1p both phenotypic assays and a mass spectrometry-based label-free quantitative proteomics analysis were performed. A role for Rnq1p as a negative regulator of translation termination was characterised and co-localisation of Rnq1p with P-bodies, tightly packed clusters of untranslating mRNA, was observed indicating that Rnq1p is intimately associated with mRNA dynamics within the cell. Additionally, evidence for a role in the maintenance of mitochondrial respiratory capacity pertaining to ATP-generation is presented, along with indications that this latter role may be through transcriptional regulation.

To further understand the mechanisms of toxic protein aggregation, two analyses were performed. One, a study on the impact of natural Rnq1p polymorphisms identified fifty-three novel *RNQ1* alleles and sequence features affecting Rnq1p toxicity. Two, a screen for genetic modifiers of both Rnq1p and mutant huntingtin demonstrated the role of P-bodies and mRNA degradation pathways in modulating amyloid or glutamine-based toxicity, along with a possible role for energy homeostasis.

The results presented in this thesis provided new insight into the functional roles of Rnq1p within the cell, and consequently the possible impact on cellular physiology associated with Rnq1p's [*pin*$^-$] to [*PIN*$^+$] conversion, and also identified novel modulators of toxic aggregation events in the cell.

Contents

List of abbreviations

ADP:	Adenosine Diphosphate
AMP:	Adenosine Monophosphate
ATP:	Adenosine Triphosphate
BLAST:	Basic Local Alignment Search Tool
cDNA:	complementary DNA
CJD:	Creutzfeldt-Jakob Disease
CFUs:	Colony Forming Units
CPEB:	Cytoplasmic Polyadenylation Element Binding
CREB:	cAMP Responsive Element Binding
DAPI:	4',6'-Diamidino-2-Phenylindole
dH_2O:	distilled H_2O
DNA:	Deoxyribonucleic Acid
EDTA:	Ethylenediaminetetraacetic acid
ELM:	Eukaryotic Linear Motif
ER:	Endoplasmic Reticulum
ES:	Embryonic Stem (cells)
EtBr:	Ethidium Bromide
FACS:	Fluorescence Activated Cell Sorting
$FADH_2$:	Flavin Adenine Dinucleotide ($+H_2$ = reduced, hydroquinone form)
FHA:	Forkhead-Associated
GdnHCl:	Guanidine Hydrochloride
GDP:	Guanosine Diphosphate

GTP:	Guanosine Triphosphate
GFP:	Green Fluorescent Protein
GO:	Gene Ontology
GPD:	Glyceraldehyde Phosphate Dehydrogenase
GPI:	Glycophosphatidylinositol
H_2O:	water (formula)
H_2O_2:	Hydrogen Peroxide (formula)
HCl:	Hydrogen Chloride
Htt:	Huntingtin
LB:	Luria Bertani
LC:	Liquid-Chromatography
LiOAc:	Lithium Acetate
MALDI-MS:	Matrix Assisted Laser Desorption Ionisation-Mass Spectrometry
MMS:	Methyl Methanesulfonate
mRNA:	messenger RNA
N:	Asparagine
NAD:	Nicotinamide Adenine Dinucleotide (+H = reduced form)
NADP:	Nicotinamide Adenine Dinucleotide Phosphate
NED:	N-terminal Extension Domain
°C:	degrees Celsius
OPR:	Oligopeptide Repeat Region
PBS:	Phosphate Buffered Saline
PCR:	Polymerase Chain Reaction

PEG:	Polyethylene Glycol
PfD:	Prion Forming Domain
PMSF:	Phenylmethanesulfonyl Fluoride
polyQ:	polyglutamine
PrP:	Protease Resistant Protein
Q:	Glutamine
QNR:	Glutamine and Asparagine Rich Region
RNA:	Ribonucleic Acid
RPM:	Rotations Per Minute
SDS:	Sodium Dodecyl Sulfate
SDS-PAGE:	SDS–Polyacrylimide Gel Electrophoresis
SDY:	Sainsbury's Dried Yeast
ssDNA:	Single Stranded DNA
T.E.:	Tris-EDTA
TAP:	Tandem Affinity Purification
TCA:	Tricarboxylic Acid
TEMED:	Tetramethylethylenediamine
TORC1:	Target of Rapamycin Complex 1
TPR:	Tetratricopeptide Repeat
tRNA:	transfer RNA
TSE:	Transmissible Spongiform Encephalopathy
TTC:	Triphenyltetrazolium Chloride
UAS:	Upstream Activating Sequence

Chapter I

Introduction

1.0 Prologue

It was the 19th century when Sir Francis Galton first proposed that one's identity, personality and fate could be ascribed entirely to the genes one had inherited. Within this statement, Galton encompassed everything from intelligence to criminality and disease. Although we are now aware that genetic traits are usually also environmentally conditional traits, obesity and cancer being fitting examples, it is the phenomena of epigenetics that has caused the greatest shift in our understanding of inheritance mechanisms.

Epigenetics describes "nuclear [[and cytoplasmic]] inheritance that is not based on differences in DNA sequence" (Holliday *et al.*, 1975). The field first gained recognition with coincident publications in 1975 by Holliday and Pugh, and by Riggs, suggesting that DNA methylation could mediate strong effects on the control of gene expression, pertaining in particular to the examples of development, X-chromosome inactivation and cancer (Holliday *et al.*, 1975; Riggs, 1975). The field of epigenetics has expanded significantly with the identification of additional mechanisms such as histone acetylation and methylation, and cytoplasmic epigenetics such as alternative splicing and editing of RNA transcripts, RNAi, and prions. The work contained within this thesis focuses on the latter of these cytoplasmic epigenetic factors, the prion.

The most unusual property of prions, in considering their contribution to heritable phenotypes in yeast, is that they are composed of protein, devoid of nucleic acid material. Most epigenetic events, as listed above, involve the modification of nucleic acids - be it DNA or RNA. Prion proteins however stand alone in their apparent sufficiency to propagate information in a DNA- and RNA-independent manner.

The epigenetic mechanism of prions, unfortunately, is not without wider context. There currently exists an inseparable link between those properties that allow prions to serve as hereditary units in yeast, and those properties that render prions aggregate-prone and consequently harbingers of disease. Indeed, it was as the causative agent of the rare but fatal class of neurodegenerative diseases Transmissible Spongiform Encephalopathies (T.S.E.s) that prions first claimed notoriety.

In the 1990s, fear of a T.S.E.-pandemic mobilised a significant level of financial resource for prion research. However, since Prusiner's seminal paper on the mammalian PrP prion in 1982 (Prusiner *et al.*, 1982) and Reed Wickner's later identification of the yeast [*URE3*] prion in 1994 (Wickner, 1994), the field has proceeded in a somewhat disjointed fashion. Mammalian-based research of prions has sought to understand the mechanisms underlying T.S.E.s, whereas in yeast, a seemingly more holistic approach has been adopted, with prions being studied both as epigenetic curiosities and as an efficient means by which to dissect mechanisms of protein misfolding, aggregation and propagation, relevant to both prion and non-prion proteinopathies.

The history of prion proteins and the events leading to their identification as causal agents of both an infectious disease and of dominantly heritable phenotypic traits represents a remarkable story of human endeavour and human error, and epitomises the inimitable contribution of the scientific process to our understanding of nature. I will briefly touch upon such beginnings throughout but primarily will discuss those aspects of prion biology that are immediately pertinent to this thesis.

1.1 What is a prion protein?

The word 'prion' was coined by Prusiner in 1982 to describe a novel, proteinaceous particle (Prusiner,1982) that consistently co-purified with scrapie infectivity; scrapie being the prototype of what was then deemed to be an infectious disease caused by slow viruses. Subsequently, prion proteins were found to exist in fungi such as *Saccharomyces cerevisiae* (Wickner, 1994)(Cox *et al.*, 1965) and *Podospora anserina* (Rizet *et al.*, 1952), and although to date they have not been identified in prokaryotic cells, it has recently been determined that *E. coli* can maintain a prion in

the infectious form (Garrity *et al.*, 2010). Despite the differences of prion proteins within and between species, in all cases, the term 'prion' describes a protein that is capable of existing in two physically and potentially functionally distinct states:

1 – a [*prion*$^-$] state: a soluble conformation associated with normal cellular activity, exhibiting an array of secondary structure, and which is sensitive to protease treatment.

2 – a [*PRION*$^+$] state: an insoluble state brought about by a stable conformational change that is enriched in β-structure and prone to aggregate into amyloid-like structures which are resistant to protease treatment.

The physical attributes of prion proteins alluded to above will be addressed in greater detail in section 1.2.

The inheritance mechanism of a prion protein is linked to its change in conformation from a [*prion*$^-$] to a [*PRION*$^+$] state, as any prion protein that undergoes this conformational change to the [*PRION*$^+$] state has the ability to induce the same conformational change in other homologous prion protein molecules presently of the [*prion*$^-$] state i.e. a [*PRION*$^+$] protein is 'infectious'. Therefore, [*PRION*$^+$] proteins transmit phenotypes via self-propagating structures that are immediately active and dominant, in contrast to the passive units of DNA inheritance which depend on elaborate decoding machinery.

In unicellular organisms, a prion protein in the [*PRION*$^+$] state will be transmitted from mother cell to daughter cell during mitosis and meiosis due to the division of 'infected' cytoplasm between the two cells (or the four spores). New prion protein synthesised by either the mother or the daughter cell(s) will be susceptible to conversion by existing [*PRION*$^+$] molecules, thus replenishing the pool of [*PRION*$^+$] proteins that might otherwise be 'diluted' out through continued cell division. Consequently, the [*PRION*$^+$] state is propagated through an 'infected' host cell lineage. In somatic cells of higher order eukaryotes, the mechanism by which the [*PRION*$^+$] state is transmitted from cell to cell has not been precisely defined.

1.2 Defining a prion protein

In order to fully characterise prion proteins and accurately dissect their infectious nature, it is important to be able to precisely identify, detect, isolate and monitor prion proteins *in vivo*, and to differentiate between the many subtleties of their form. The following sections introduce our current understanding of what a prion protein is, as most pertinent to (but not necessarily limited to) yeast.

1.2.1 Wickner's criteria

Criteria that allow prions to be distinguished from nucleic acid-based determinants of phenotype have been devised (Wickner,1994) and are as follows:-

1 – Expression of the nuclear gene encoding the prion protein must be essential to the establishment and maintenance of the [*PRION*$^+$] state.

2 – The [*PRION*$^+$] phenotype can also be achieved by mutations in that same gene.

3 – Non-DNA active mutagenic agents can reversibly eliminate the [*PRION*$^+$] state, and the consequential [*prion*$^-$] cells can be returned to the [*PRION*$^+$] state by cytoplasmic transfer from a [*PRION*$^+$] strain.

4 – Over-expression of the prion protein in a [*prion*$^-$] cell can greatly elevate the frequency of *de novo* appearance of the corresponding [*PRION*$^+$] state.

1.2.2 The prion-forming domain

Studies by Ter-Avanesyan and associates (Ter-Avanesyan *et al.*, 1993) revealed that the prion forming capacity of a prion protein is conferred by the presence of a modular domain, referred to as the prion-forming domain (PfD). The fusion of the PfD to another protein 'host' confers upon that host a prion-forming capacity. This was also elegantly illustrated by fusing the PfD of a yeast prion, Sup35p, with the rat glucocorticoid receptor – the result was both aggregation and transmission of the fusion protein (Li *et al.*, 2000). The PfD domain is typically longer than 60 amino acids in length.

1.2.3 Prion-forming domains are amyloidogenic

The infectious nature of a prion results from structural rearrangements that increase the abundance of β-strands within the PfD (Pan *et al.*, 1993). β-conformation is a major form of secondary structure consisting of stretched out regions of polypeptide, called a β-strand. Subsequently, two β-strands come together, forming a β-sheet, and are held by regular hydrogen bond contacts between the main chain C=O of one strand and the N-H group of the other strand. If strands align in the same direction (according to their termini), they are said to be 'in-parallel', if they align in opposite directions, they are 'anti-parallel', the latter of which seems to be more stable (Gailer *et al.*, 1997). Typically, more and more β-strands stack upon one another, or rather they 'polymerise', to form unbranching fibrils (polymers) collectively called amyloid.

Indeed, *in vitro* studies of the Sup35p PfD show that it polymerises spontaneously following an initial lag period that is inversely correlated with protein concentration (King *et al.*, 1997)(Glover *et al.*, 1997). The fibrils formed by Sup35p display characteristics indicative of amyloid: protease and heat resistance, binding to the dye Congo red, and β–rich structure (King *et al.*, 1997)(Glover *et al.*, 1997) - and the ability to transform cells to the prion state with *in vitro* generated fibrils further establishes the protein-only nature of prion inheritance (Sparrer *et al.*, 2000).

Recently, *in vivo* evidence for spherical Sup35-Gfp aggregates containing bundles of fibrillar structures was obtained (Kawai-Noma *et al.*, 2010). The probability that these *in vivo* fibrils are amyloid in nature is indicated by: the observed diameter of the fibrils (~20 nm) which is similar to the diameter observed for *in vitro* generated Sup35p fibrils (that showed amyloid characteristics); the fibrillar structures being resistant to 2 % SDS as is characteristic of amyloid structures; and that spherical aggregates of Sup35p formed *in vivo* (within which the fibril bundles were observed) have previously been shown to bind the amyloid-binding dye Thioflavin T (Kimura *et al.*, 2003).

The mechanism by which a PfD in the [*PRION*$^+$] conformation is able to template the conformational conversion of other homologous PfDs to the same β-rich

[*PRION*$^{+}$] form, propagating the amyloid state, has not yet been determined though models for conversion have been postulated (Prusiner, 1991; Jarret, 1993; Cohen, 1994).

Essential to prion dynamics therefore is the generic structure of the amyloid, placing prion diseases amongst a growing list of amyloidoses, for example Alzheimer's disease, Huntington's disease (section 1.8), Parkinson's disease and late-onset diabetes.

1.2.4 Prion-forming domains are glutamine and asparagine rich

Analysis of PfDs has revealed a bias in their amino acid composition. PfDs tend to be rich in the polar residues glutamine (Q) and/or asparagine (N), but depleted of charged residues and hydrophobic residues (Michelitsch *et al.*, 2000).

Asparagine and glutamine are unique amongst the twenty common natural amino acids in possessing carboxamide as the side chain functional group (O=CN) (Figure 1.1). The carboxamide functional group makes PfDs a rich source of hydrogen bonds – a major contributor to interfacial electrostatic interactions and this may be significant since Yun *et al* (Yun *et al.*, 2007) found that electrostatic interactions between pairs of charged amino acids promoted the formation of larger amyloid oligomers. Specifically, carboxamide groups are predicted to behave as "polar zippers" (Perutz *et al.*, 1994) which sees an increase in the abundance of hydrogen bond interactions between the main chain C=O and the side chain N-H groups, an association mentioned previously in section 1.2.3 as being important for β–sheet interactions. Water molecules binding hydrogen bonds can further stabilise these interactions (Prochnow *et al.*, 2007).

Testament to their potential for impact on cellular physiology, glutamine-rich proteins are responsible for a disease category called the 'polyglutamine diseases' (section 1.8). Studies of these diseases indicate a toxic aggregation of the polyglutamine-rich protein, implicating glutamine as an amino acid prone to aggregate.

While the lack of solubility in water has hindered efforts to characterise structural signatures of polyglutamine tracts, models suggest that glutamines possess random-coiled coil conformations in the presence of highly soluble carriers, but when expanded, they both destabilise native conformations and promote aggregation by forming intermolecular β-sheets (Perutz *et al.*, 1994).

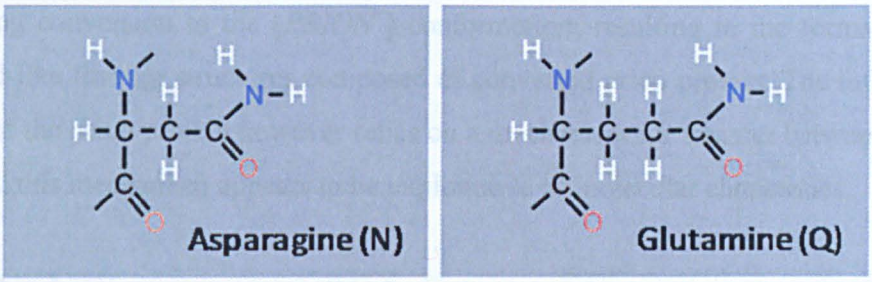

Figure 1.1: The functional group of asparagine and glutamine is carboxamide.
The polar amino acids glutamine and asparagine are referred to as the long- and short- amide, respectively.

It is not so surprising that asparagine is also an indicator of prion forming propensity, since it has properties and a structure most similar to that of glutamine. Additional support for the integral role of glutamine and asparagine residues in mediating the aggregation of PfDs is the finding that mutation of these residues, for example to charged residues, can resolubilise the associated protein and reverse the prion phenotype (DePace *et al.*, 1998)(Alberti *et al.*, 2009).

While Q/N-richness is a general characteristic of most prions identified to date, a notable exception to this rule is the PfD of HET-s, a protein of the fungus *Podospora anserina* discussed in section 1.4.2., which has been shown to propagate as a prion in *S. cerevisiae* indicating that the observed QN-richness of most fungal prions is not a specific requirement of *S. cerevisiae* (Taneja *et al.*, 2007). This may also suggest that non-QN-rich prion proteins exist in *S. cerevisiae*, and may represent another class of prion protein. Further, the propagation of HET-s as a prion in *S. cerevisiae* was found to be enhanced by the presence of the [*PIN*$^+$] prion (Taneja *et al.*, 2007) suggesting either that QN-rich and non-QN-rich prion (or aggregate prone) proteins

beneficially interact, or that the presence of QN-rich aggregates modifies protein homeostasis such that it creates a more aggregation-conducive environment.

1.2.5 The [*PRION*$^+$] state depends on interactions with chaperones

The prion forming domain of prion proteins has an inherent ability to self-associate following conversion to the [*PRION*$^+$] conformation, resulting in the formation of amyloid-like fibrillar structures composed of converted prion protein. The infectious nature of the prion protein however relies on a mechanism for transfer between cells. In yeast, this mechanism appears to be exploitative of molecular chaperones.

Molecular chaperones are responsible for maintaining the 'quality' of protein folding within the cell, and are particularly important following exposure to stresses that compromise the folding and stability of proteins. When [*PSI*$^+$], the prion form of the translation termination factor Sup35p (section 1.3.1) was found to be dependent on the molecular chaperone Hsp104p for its maintenance, this was deemed to be further support for the prion hypothesis and the notion that [*PSI*$^+$] was the result of a Sup35p misfolding event (Chernoff *et al.*, 1995). The explanation for this dependency of [*PSI*$^+$] on Hsp104p was that Hsp104p actively fragments Sup35p prion fibrils into smaller fibrils or oligomers, increasing the availability of 'recruiting' ends (Chernoff *et al*, 1995; Glover *et al*, 1997). Deletion of Hsp104p therefore leads to excessive growth of fibrils which become physically limited in their transmissibility to daughter cells (Satpute-Krishnan *et al.*, 2007), whereas over-expression of Hsp104p is predicted to over-fragment the fibrils.

Hsp104p has since been found to be critical for all yeast prions with the exception of Sfp1p/[*ISP*$^+$] (Rogoza *et al.*, 2010). One could speculate that this is due to the differential localisation of [*ISP*$^+$] foci relative to foci formed by the other yeast prion proteins; typical cytoplasmic foci formed by most yeast prion proteins identified to date are dependent on Hsp104p, but nuclear localised foci formed by Sfp1p may have established dependency on an alternative chaperone. If the Sfp1p sustaining chaperone were a nucleocytoplasmic shuttling chaperone, this would present a very interesting means of regulating [*ISP*$^+$] maintenance; conditions that relocalise the

chaperone predominantly to the cytoplasm or the nucleus would result in the loss or the maintenance of the [*ISP*$^+$] prion, respectively.

It should be noted that while deletion of *HSP104* or inactivation of Hsp104p *in vivo* is universally effective on yeast prion proteins, only the Sup35p [*PSI*$^+$] prion is lost by Hsp104p over-expression.

The *in vivo* inactivation of Hsp104p is achieved through exposure to the chaotropic agent guanidine hydrochloride (Ferreira *et al.*, 2001) which is believed to inhibit Hsp104p's ATPase activity required for the fragmentation of prion aggregates (Ferreira *et al.*, 2001) In support of this, a dominant ATPase-negative mutant of Hsp104p is also unable to maintain the [*PSI*$^+$] prion (Chernoff *et al.*, 1995). Exposure to guanidine hydrochloride by addition to yeast growth media is now a commonly employed method for prion 'curing'; the process of restoring a [*PRION*$^+$] cell to a [*prion*$^-$] state.

There is evidence however that guanidine hydrochloride also affects translation termination by a means other than Sup35p/[*PSI*$^+$] resolubilisation; guanidine hydrochloride reduces stop-codon readthrough brought about by missense mutations in *SUP35* or *SUP45* (Bradley *et al.*, 2003) although closer inspection of the published data reveals that read-through is also enhanced by guanidine hydrochloride in the [*psi*$^-$] control.

Chaperones other than Hsp104p are also influential in the dynamics of prion proteins. For example, the cooperativity in disaggregase activity observed between Hsp104 and members of the Hsp70/40 family of chaperones during thermotolerance also modulates prion maintenance and propagation (Sanchez *et al.*, 1990).

Specifically, reduced levels of the Hsp70 chaperones Ssb1/2 results in a higher frequency of [*PSI*$^+$] appearance, suggesting that Ssb1/2 normally antagonises [*PSI*$^+$] appearance (Chernoff *et al.*, 1999). In contrast, the Hsp70 chaperones Ssa1-4 appear to promote [*PSI*$^+$] appearance, with elevated levels of Ssa chaperones preventing [*PSI*$^+$] curing by Hsp104p over-expression (Newnam *et al.*, 1999). The Hsp40 family of chaperones function with and assist the Hsp70 chaperones. Amongst the Hsp40

members, Sis1p appears to be particularly important for prion dynamics. The interaction between Sis1p and Rnq1p is essential for maintenance of the [*PIN*$^+$] prion (section 1.5) (Sondheimer *et al.*, 2001), and it is believed that Sis1p generally is important for recruiting prion substrates to Hsp104p and for their subsequent translocation through the Hsp104p hexameric pore (Tipton *et al.*, 2008).

The interactions between the chaperones and the different prion proteins is complex however, for example Ssa1p overexpression cures [*URE3*] but as mentioned previously, enhances [*PSI*$^+$] formation (Schwimmer *et al.*, 2002) (Newnam *et al.*, 1999). Additionally, the co-existence of multiple prions within a cell can alter the relationship between certain prions and chaperones, for example the presence of [*PIN*$^+$] can allow Ssa1/2 overexpression to cure [*PSI*$^+$] (Mathur *et al.*, 2009).

1.3 Prion proteins of *Saccharomyces cerevisiae*

1.3.1 Translation termination: Sup35p and the [*PSI*$^+$] prion

The yeast Sup35p/eRF3 protein is an essential protein composed of 3 regions: an N-terminal region (1-123 aa) that is also the modular prion-forming domain, the highly charged middle (M) region (124-253 aa) of unknown function, and a C-terminal region (254-685 aa) containing a GTPase domain (Frolova *et al.*, 1996). Sequence comparison of eRF3s from different species (also called Gspt1/2 in higher eukaryotes) reveals that a significant degree of amino acid conservation, from yeast through to mammals, is found only in the C-terminus (Kisselev *et al.*, 1995). For this reason, the N- and M-regions can also be collectively referred to as the N-terminal extension domain (NED). Despite the divergent nature of the NED and their dispensability, almost all eRF3s possess an NED (Kodama et al., 2007).

Closer inspection of the primary sequence suggests that conservation between mammalian and yeast eRF3 begins with the start of the 'E-rich' region, within the yeast M-region, resulting in sequence conservation spanning 515-518 amino acids in length rather than the 431 amino acid region otherwise encapsulated by the currently

proposed C-region e.g. starting at yeast Sup35p residue E167 rather than M254 and thus encroaching 53 amino acids into the 3' end of the yeast M-region (Figure 1.2).

Presently, published functions for yeast Sup35p include cooperativity of the conserved C-region with another essential protein Sup45p/eRF1, to mediate the termination of translation upon arrival of a stop codon (UAA, UAG, or UGA) in the ribosomal A-site (Stansfield *et al.*, 1995), and in addition, the N-terminal region interacts with Pab1p (poly(A)-binding protein possibly to limit Pab1p multimerisation and allow for cyclical control of mRNA degradation or translation reinitiation (Cosson *et al.*, 2002). It is worth adding that the aforementioned release factor activity of Sup35p and Sup45p is not shared by any other yeast protein.

When Sup45p is accommodated by the ribosome in the presence of a stop codon, Sup35p is believed to bind to Sup45p and stimulate its release factor activity by virtue of Sup35p's C-terminal GTPase domain (Zhouravleva *et al.*, 1995). Specifically, Sup35p promotes better positioning of Sup45p within the ribosomal A-site, thus allowing for efficient hydrolysis of the peptidyl-tRNA linkage in the ribosomal P-site (Zhouravleva *et al.*, 1995). The efficiency of stop-codon recognition by the Sup35:Sup45 termination complex is sensitive to both the nucleotide sequence context surrounding the stop codon and the relative abundances of both Sup35p and Sup45p. As a deletion of the *SUP35* gene results in loss of cell viability (Ter-Avanesyan *et al*, 1993), the role of Sup35p in translation termination is deemed to be an essential one.

There exists however a slight paradox that suggests the essential function of Sup35p may not be attributed solely to its termination activity but to some other, as yet unidentified, function. This paradox arises from observations that a ~ 30 % depletion of Sup35p in the cell results in loss of viability (personal communication, Tobias von der Haar), yet conversion of Sup35p to the prion state via Sup35p's N-terminal prion-forming domain, believed to convert up to 90 % of Sup35p into an aggregated and presumably inactive or less active state, is not associated with any noticeable growth defect (personal communication, Tobias von der Haar). Furthermore, a mutation rendering Sup35p's GTPase domain essentially inactive only results in loss of cell viability in the presence of the N-terminus (Urakov *et al.*, 2006) suggesting an antagonistic action of the N-terminus on this mutation or *vice versa.*

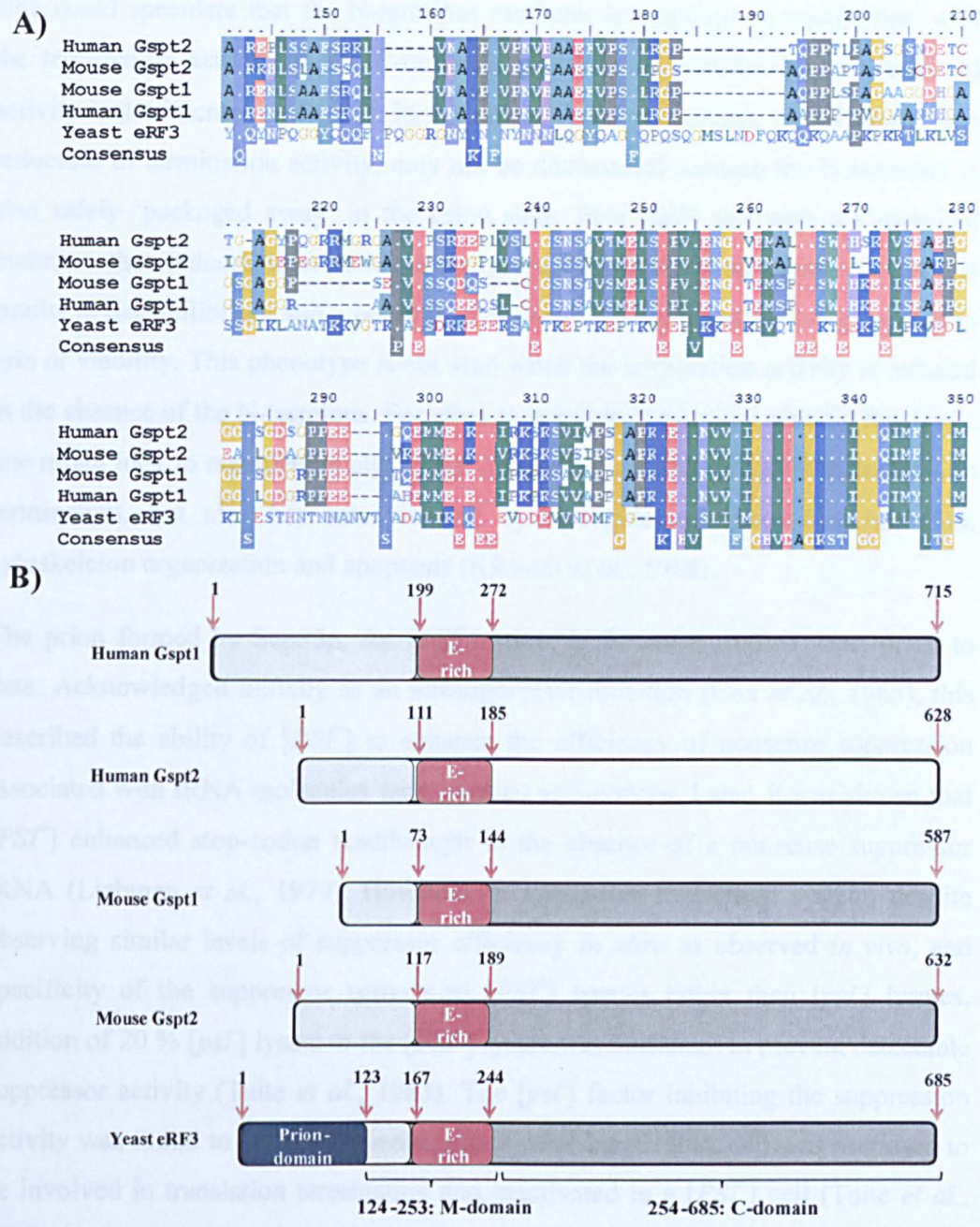

Figure 1.2: Alignment of yeast, mice and human eRF3/Gspt amino acid sequences.

A) The residue indicated at position 316 (M254, yeast) is considered the start of sequence conservation between the three species (eRF3 C-region) however conservation may encapsulate the E-rich region, starting at position indicated 229 (E167, yeast). B) cartoon indicating the suggested positions of sequence conservation.

One could speculate that the N-terminus mediates interactions in equilibrium with the termination activity of the C-terminus, and that an enrichment of N-terminal activity is detrimental to the cell. In this sense [*PSI*$^+$] conversion, which results in a reduction of termination activity, may not be detrimental because the N-terminus is also safely 'packaged away' in the prion state. In a [*psi*$^-$] cell with a C-terminal mutation that reduces termination activity, the presence of an active N-terminus results in disequilibrium and a possible enrichment of N-terminal activity, leading to loss of viability. This phenotype is not seen when the termination activity is reduced in the absence of the N-terminus. For clues to possible N-terminal specific functions, one might look to mammalian eRF3/Gspt1, which is not only involved in translation termination, but also has roles in cell cycle regulation, translation initiation, cytoskeleton organization and apoptosis (Kikuchi *et al.*, 1988).

The prion formed by Sup35p, the [*PSI*$^+$] prion, is the most studied yeast prion to date. Acknowledged initially as an allosuppressor mutation (Cox *et al.*, 1965), this described the ability of [*PSI*$^+$] to enhance the efficiency of nonsense suppression associated with tRNA molecules with mutated anti-codons. Later, it was shown that [*PSI*$^+$] enhanced stop-codon readthrough in the absence of a nonsense suppressor tRNA (Liebman *et al.*, 1979). However, in a cell-free translation system, despite observing similar levels of suppressor efficiency *in vitro* as observed *in vivo*, and specificity of the suppressor activity to [*PSI*$^+$] lysates rather than [*psi*$^-$] lysates, addition of 20 % [*psi*$^-$] lysate to the [*PSI*$^+$] lysate was sufficient to prevent detectable suppressor activity (Tuite *et al.*, 1983). The [*psi*$^-$] factor inhibiting the suppression activity was found to be ribosome-associated, heat-inactivated, and was proposed to be involved in translation termination and inactivated in a [*PSI*$^+$] cell (Tuite *et al.*, 1987).

The connection between Sup35p and [*PSI*$^+$] was established following Sup35p over-expression studies that 1) caused growth defects in a [*PSI*$^+$] but not in a [*psi*$^-$] strain (Dagkesamanskaya *et al.*, 1991)(Chernoff *et al.*, 1992), 2) caused a suppression phenotype in a [*psi*$^-$] cell (Chernoff *et al.*, 1992), and 3) induced the *de novo* appearance of [*PSI*$^+$] in a [*psi*$^-$] cell (Chernoff *et al.*, 1993). Additionally, the non-Mendelian inheritance of [*PSI*$^+$] (Cox *et al.*, 1965) indicated, and was subsequently confirmed, to be the result of a cytoplasmic determinant (Tuite *et al.*, 1982) though

mitochondria, plasmids and virus-like elements were found not to be the [*PSI*$^+$] determinant (review: Cox *et al.*, 1994).

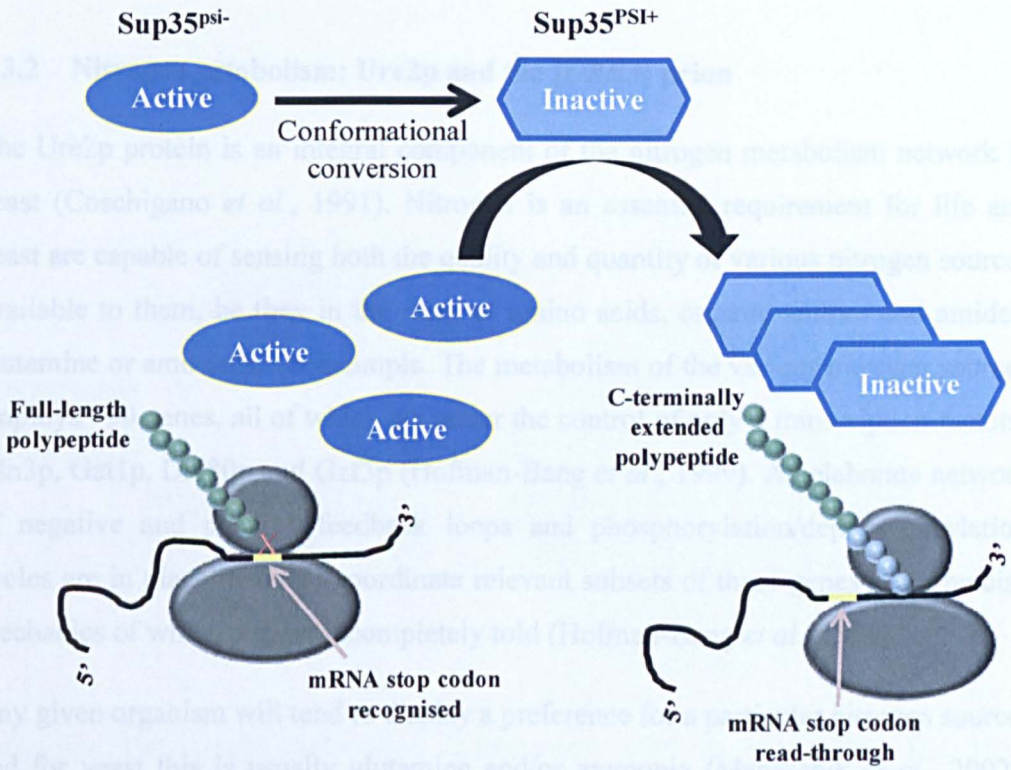

Figure 1.3: Conversion of Sup35p to the [*PSI*$^+$] state results in an increased read-through of mRNA stop-codons.
Sup35p is soluble and active in the [*psi*$^-$] state, efficiently forming a termination complex with Sup45p to recognise stop codons and terminate polypeptide synthesis. Sup35p in the aggregated [*PSI*$^+$] state results in a reduced formation or efficiency of the termination complex resulting in stop-codon read-through and the generation of C-terminally extended polypeptides.

In 1994, Reed Wickner proposed that the determinants of the [*PSI*$^+$] and [*URE3*] (sections 1.3.1, 1.3.2) elements were yeast prion proteins Sup35p and Ure2p, respectively (Wickner,1994). Conformational conversion of Sup35p to a prion conformation was proposed to reduce the functional pool of Sup35p available for translation termination, resulting in the nonsense suppressor phenotype associated with [*PSI*$^+$] presence (Wickner,1994) (Figure 1.3). Integral to the prion hypothesis was the ability of the prion form, [*PRION*$^+$], to catalyse the conversion of

homologous prion proteins in the non-prion conformation, [*prion*$^-$], to the same [*PRION*$^+$] state; allowing a rare event (conversion) to become conformationally dominant within the cell-lineage.

1.3.2 Nitrogen catabolism: Ure2p and the [*URE3*] prion

The Ure2p protein is an integral component of the nitrogen metabolism network in yeast (Coschigano *et al.*, 1991). Nitrogen is an essential requirement for life and yeast are capable of sensing both the quality and quantity of various nitrogen sources available to them, be they in the form of amino acids, organic amines and amides, glutamine or ammonia, for example. The metabolism of the various nitrogen sources employs ~90 genes, all of which are under the control of only 4 transcription factors: Gln3p, Gat1p, Dal80p and Gzf3p (Hofman-Bang *et al.*, 1999). An elaborate network of negative and positive feedback loops and phosphorylation/dephosphorylation cycles are in place to finely coordinate relevant subsets of these genes – the precise mechanics of which remain incompletely told (Hofman-Bang *et al.*, 1999).

Any given organism will tend to display a preference for a particular nitrogen source, and for yeast this is usually glutamine and/or ammonia (Magasanik *et al.*, 2002). Thus, in the presence of a preferred nitrogen source such as glutamine, repression of genes otherwise involved in the catabolism of less preferred nitrogen sources occurs. Similarly, when only poor nitrogen sources are available, the turn-over of specific amino acid permeases occurs and more general amino acid permeases are stabilised. Additionally under these conditions, autophagy is up-regulated, placing an emphasis on an internal supply of nitrogen for sustenance (Tsukada *et al.*, 1993).

The role of the Ure2p protein in the nitrogen metabolism network is to act as a cytoplasmic 'anchor' for one of the 4 aforementioned transcription factors – this being a favoured mechanism by which the cell regulates the so-called 'nitrogen discrimination pathway' (Courchesne *et al.*, 1988). Essentially, cytoplasmic anchors such as Ure2p can physically prevent their associated transcription factor from entering the nucleus, thereby preventing the transcriptional activation or repression of target genes. In the case of Ure2p, it binds to the transcription factor Gln3p during growth on glutamine, a high-quality nitrogen source (Courchesne *et al.*, 1988). In

poor nitrogen conditions however, both Gln3p and Ure2p are believed to be phosphorylated by TORC1 (target of rapamycin complex 1), triggering their dissociation and the nuclear import of Gln3p where, once in the nucleus, it is able to bind to the promoters of target genes (Figure 1.4) (Beck *et al.*, 1999). Accordingly, in a *ure2Δ* deletion strain, Gln3p resides within the nucleus where its target genes persist in a transcriptionally activated state, regardless of the available nitrogen source (Courchesne *et al.*, 1988).

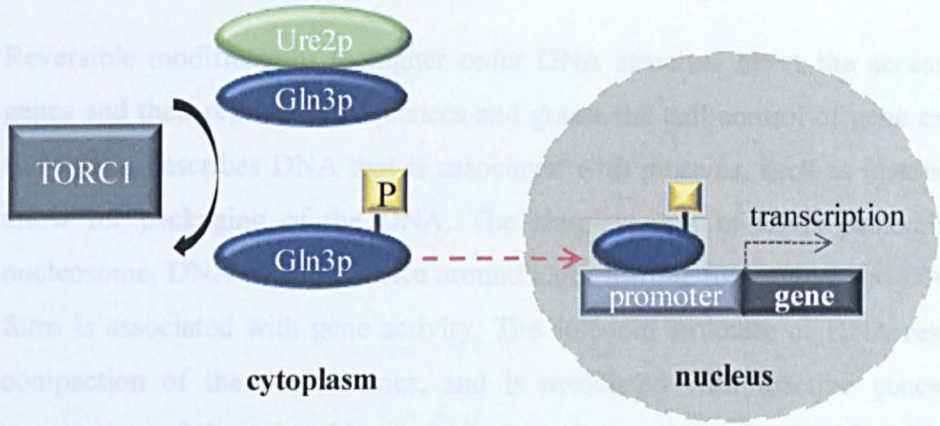

Figure 1.4: Ure2p acts as a cytoplasmic anchor, preventing Gln3p-mediated transcriptional activity.
In the presence of a high quality carbon source, the Ure2p protein binds to Gln3p in the cytoplasm. In the presence of poor quality nitrogen source, TORC mediated phosphorylation of Gln3p allows Gln3p to dissociate from Ure2p and enter the nucleus where it affects the transcription of metabolic genes.

The Ure2p protein exists as a homodimer in the cytoplasm and can be divided into 3 separate regions: an N-terminal region (1-70) that is also the prion-forming domain; a central 'tether' region (71-90) which is not incorporated into the prion aggregate but at the same time remains distinct from the C-region (91-354) which is responsible for binding to the Gln3p transcription factor (Masison *et al.*, 1995). The C-region also possesses a glutathione S-transferase (GST)–like fold, which groups Ure2p with a subset of GST proteins that do not possess typical GST activity; Ure2p possesses glutathione-dependent peroxidise activity against oxidant substrates such as hydrogen peroxide (Coschigano *et al.*, 1991).

The conversion of Ure2p to its prion conformation, [*URE3*], results in a reduction of Ure2p-associated functions, including a lack or reduction in nitrogen discrimination; a [*URE3*] cell will metabolise a poor nitrogen source in the presence of an otherwise preferred nitrogen source (Wickner,1994)(Baxa *et al.*, 2002). The [*URE3*] prion is also dependent on the molecular chaperones Hsp104p (Moriyama *et al.*, 2000) and Sis1p (Higurashi *et al.*, 2008) for its maintenance.

1.3.3 Chromatin remodelling: Swi1p and the [*SWI*$^+$] prion

Reversible modifications to higher order DNA structure alters the accessibility of genes and their regulatory sequences and grants the cell control of gene expression. Chromatin describes DNA that is associated with proteins, such as histones, which allow for packaging of the DNA. The simplest unit of DNA packaging is the nucleosome, DNA wrapped twice around eight histone molecules, and DNA in this form is associated with gene activity. The solenoid structure of DNA results from compaction of the nucleosomes, and is associated with inactive genes. Further compaction of the solenoid structure gives rise to the more familiar chromosome structure visible during cell division.

Protein complexes such as the SWI/SNF complex are used by the cell to remodel chromatin so that relevant regions of the DNA can be made accessible for control of gene expression (Peterson *et al.*, 1994). The chromatin remodelling complexes disrupt nucleosome structure, using the energy of ATP hydrolysis (Cote *et al.*, 1994), in one of three ways (Figure 1.5): A) nucleosome remodelling which alters the interactions of histones within the nucleosome to expose a region of DNA; B) nucleosome sliding which alters to position of the nucleosome to expose a region of DNA; and C) nucleosome displacement which dissociates the nucleosome from the DNA.

Swi1p is one of 11 subunits that form the conserved SWI/SNF chromatin remodelling complex, which in *S. cerevisiae* regulates the transcriptional activity of ~6 % of total genes. The target genes of the SWI/SNF complex are involved in a diverse range of processes for example cell growth, stress response and DNA

replication (Flanagan *et al.*, 1999), and in mammalian cells mutations of the SWI/SNF complex are linked to tumour malignancy (Neely *et al.*, 2002).

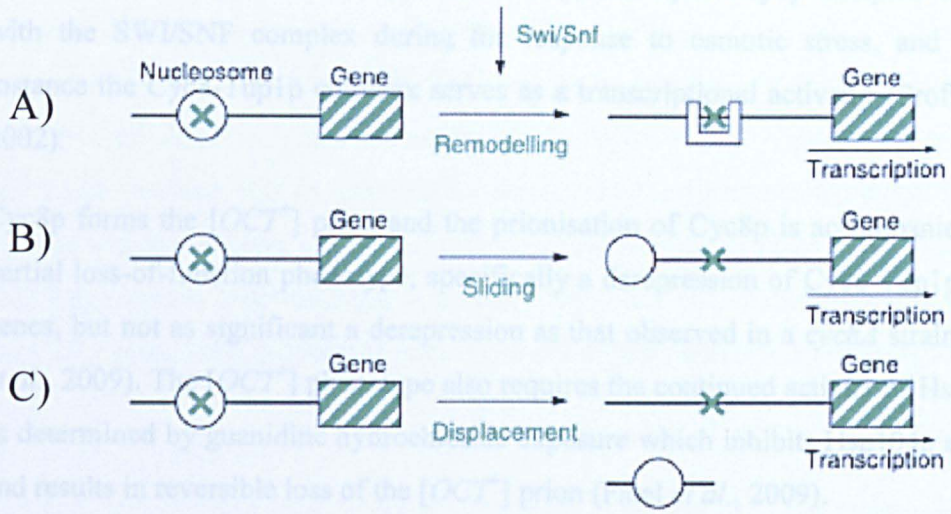

Figure 1.5: The SWI/SNF complex allows access of a regulatory protein to its target binding site (X).
A) the structure of the nucleosome is altered, in a process known as nucleosome remodelling; B) nucleosome sliding to a different position on the DNA is induced; or C) the nucleosome is displaced onto another DNA molecule. Image extracted from Latchman (Latchman, 2007).

In *S. cerevisiae*, Swi1p has been shown to spontaneously convert to the [*SWI*$^+$] prion, without Swi1p over-expression, indicating that this event may occur naturally in the cell (Du *et al.*, 2008). The conversion of Swi1p to [*SWI*$^+$] is accompanied by a partial loss-of-function phenotype, as is commonly observed for other yeast prion proteins converting to their prion form. A further likeness to other yeast prions was the dependency of [*SWI*$^+$] propagation on the chaperone Hsp104p, since guanidine hydrochloride inhibition of Hsp104p activity (Tuite *et al.*, 1981) or *HSP104* disruption caused a loss of the [*SWI*$^+$] prion (Du *et al.*, 2008).

1.3.4 Transcriptional repressor: Cyc8p and the [*OCT*$^+$] prion

The Cyc8p protein forms a co-repressor complex with the Tup1p protein for the repression of genes involved in mating-type, DNA repair and glucose-repression

(Smith *et al.*, 2000). The Cyc8-Tup1p complex does not bind DNA directly, but rather is recruited to promoters by its interaction with DNA-binding repressor proteins (Williams *et al.*, 1991). Additionally, the Cyc8-Tup1p complex interacts with the SWI/SNF complex during the response to osmotic stress, and in this instance the Cyc8-Tup1p complex serves as a transcriptional activator (Proft *et al.*, 2002).

Cyc8p forms the [*OCT*$^+$] prion and the prionisation of Cyc8p is accompanied by a partial loss-of-function phenotype; specifically a derepression of Cyc8-Tup1p target genes, but not as significant a derepression as that observed in a *cyc8Δ* strain (Patel *et al.*, 2009). The [*OCT*$^+$] phenotype also requires the continued activity of Hsp104p, as determined by guanidine hydrochloride exposure which inhibits Hsp104p activity and results in reversible loss of the [*OCT*$^+$] prion (Patel *et al.*, 2009).

1.3.5 Transcription regulator: Sfp1p and the [*ISP*$^+$] prion

The Sfp1p protein is a transcription factor that regulates the expression of ~ 10 % yeast genes, including those involved in ribosome biogenesis(Marion *et al.*, 2004) and the regulation of cell size (Jorgensen *et al.*, 2007). The activity and localisation of Sfp1p is regulated through TORC1 (target of rapamycin 1 complex) phosphorylation, and thus is responsive to both stress and nutrient signals (Marion *et al.*, 2004).

Sfp1p forms the [*ISP*$^+$] prion very efficiently (70 %) following Sfp1p over-expression, and the frequency of Sfp1p spontaneous conversion to [*ISP*$^+$] is higher than that observed for other yeast prions, 1.0 x 10^{-4}/cell/generation compared to 1.0 x 10^{-6}/10^{-7}/cell/generation (Rogoza *et al.*, 2010). An Sfp1-Gfp fusion in an [*isp*$^-$] strain was distributed between the cytoplasm and nucleus, and in an [*ISP*$^+$] strain Sfp1-Gfp formed nuclear localised foci (Rogoza *et al.*, 2010).

The [*ISP*$^+$] prion also differs from other yeast prions in that it is not influenced by the chaperone Hsp104p, either by overproduction or deletion of Hsp104p, yet the [*ISP*$^+$] prion is eliminated by growth on guanidine hydrochloride (Rogoza *et al.*, 2010).

A *sfp1Δ* deletion strain shows irreversible loss of [*ISP*$^+$], however while [*ISP*$^+$] is associated with a non-suppressor phenotype (efficient stop-codon recognition) and [*isp*$^-$] displays a suppressor phenotype (stop-codon read-through), the *sfp1Δ* strain does not show a non-suppressor phenotype (Rogoza *et al.*, 2010). This indicates that the non-suppressor function of [*ISP*$^+$] is not the result of Sfp1p depletion but due to an interaction or downstream consequence specific to the [*ISP*$^+$] prion. For example, one could speculate that an unidentified protein shuttling between the cytoplasm and nucleus which possesses suppressor activity could become trapped in the nucleus by [*ISP*$^+$] aggregates, thus resulting in an anti-suppressor phenotype in the presence of the [*ISP*$^+$] prion but a suppressor phenotype in the [*isp*$^-$] and *sfp1Δ* strain (figure 1.6).

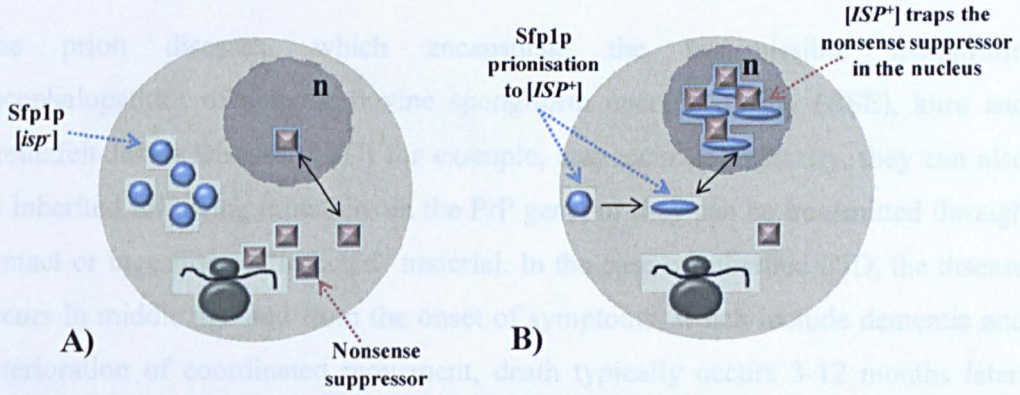

Figure 1.6: An explanation for why the [*ISP*$^+$] nonsense suppressor phenotype is not observed in an *sfp1Δ* strain.
A) cytosolic [*isp*$^-$] does not interact with the nonsense suppressor B) The [*ISP*$^+$] prion accumulates in the nucleus and may sequester the nucleocytoplasmic protein with nonsense-suppressor activity. Abbreviations: n = nucleus.

1.4 Prion proteins of other species

1.4.1 Mammalian PrP^{sc}

Stanley Prusiner had been studying the chemical nature of an agent responsible for scrapie, an ancient neurodegenerative disease of sheep that was clinically and pathologically very similar to several neurodegenerative diseases of humans, when in 1982 he proposed that a protease-resistant protein, PrP, was this elusive agent.

Controversially, the accompanying 'prion hypothesis' asserted that it was a mere isoform of PrP itself that was infectious (Prusiner,1982). The word 'prion' was a portmanteau derived from '**pro**teinaceous' and '**in**fectious'.

Scrapie infectivity was enriched from infected brain homogenate leading to the identification of a 27-30 kDa protease-resistant protein. Edman degradation was used to determine the sequence of the protein (Prusiner, 1982) before identifying from PrP cDNA and western blot analysis that the PrP 27-30 kDa molecule was a protease resistant core of a larger protein. The normal, cellular PrP was denoted PrP^{C}. A portion of PrP^{c} could undergo structural transition from an α-helical and coil structure to a β –sheet structure, and this modified isoform of PrP^{C} was called PrP^{Sc} (Pan *et al.*, 1993)(figure 1.7).

The prion diseases, which encapsulate the transmissible spongiform encephalopathies of scrapie, bovine spongiform encephalopathy (BSE), kuru and Creutzfelt-Jakob Disease (CJD) for example, can occur sporadically, they can also be inherited following mutations in the PrP gene, or they can be transmitted through contact or ingestion of "infected" material. In the case of inherited CJD, the disease occurs in middle age and from the onset of symptoms, which include dementia and deterioration of coordinated movement, death typically occurs 3-12 months later. Post-mortem histological analysis of a CJD patient's brain reveals PrP^{Sc} deposition in the form of amyloid plaques, spongiosis and neuronal loss. Additionally, disease symptoms and the pattern of PrP^{Sc} deposition in the brain vary depending on the specific structural conformation adopted by the PrP^{Sc} isoform, classed as prion 'strains' and analogous to the conformational 'variants' observed for some yeast prions (Derkatch *et al.*, 2001)(Schlumpberger *et al.*, 2001; Bradley *et al.*, 2002). The finding that oligomers of 14-28 PrP^{Sc} monomers represent the minimal infective unit (Silveira *et al.*, 2005) may also help explain the conformational variation of prion strains; where a monomer would be expected to exhibit fewer conformational differences than is possible with an oligomeric assembly (Morris *et al.*, 2006) .

The PrP sequence contains five variant octapeptide coding repeats in the N-terminus that are well conserved across mammals (Goldfarb *et al.*, 1991). The ability of the repeats to bind copper and zinc at physiologically relevant concentrations identifies a

role for PrP in metal ion homeostasis (Kramer *et al.*, 2001). In support of this, a 50 % reduction in copper, elevated zinc levels, and a 10x fold increase in manganese have been detected in the brains of CJD patients (Wong *et al.*, 2001).

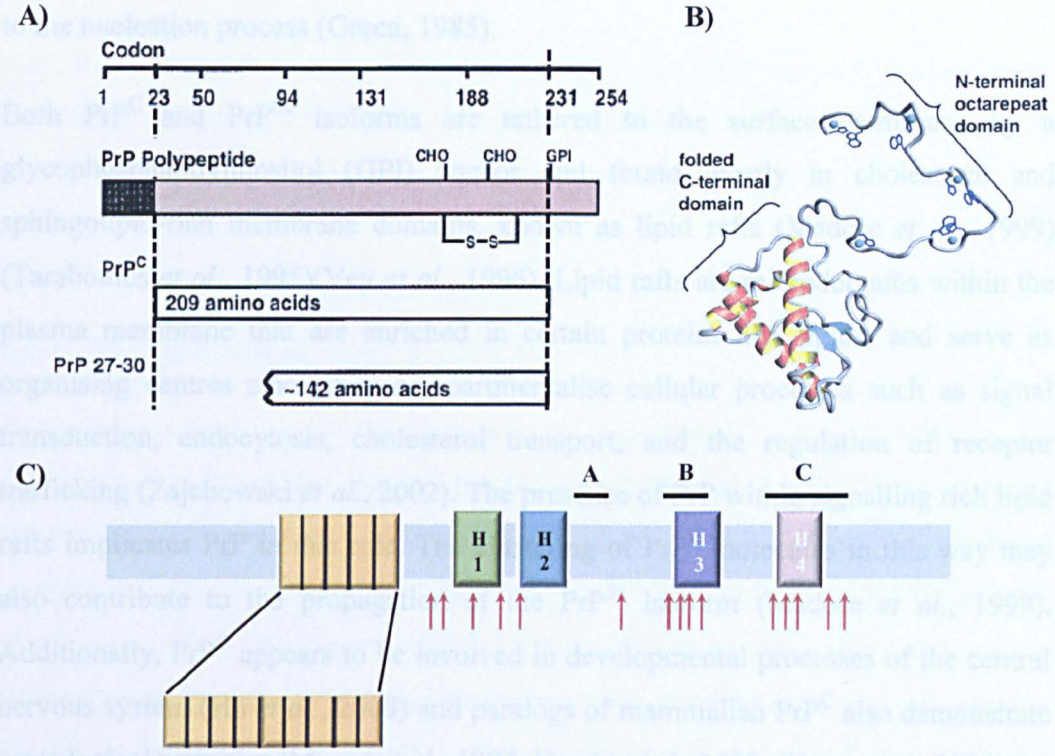

Figure 1.7: The PrP protein and secondary structure.
A) The PrP polypeptide is 254 residues long and is processed as depicted, resulting in a 209 residue PrP molecule. Proteolysis of PrP^{Sc} generates a 142 residue fragment (PrP 27-30). B) The PrP protein has a globular domain of three α-helices, two small anti-parallel β-sheet structures, and an extended flexible tail the conformation of which depends on the protein's environment. C) the segmented orange square represents the variable repeat region, susceptible to repeat expansion, and the red arrows (↑) indicate positions of PrP mutations relative to secondary structure elements that result in inherited prion disease. Images A&C adapted from Prusiner (Prusiner *et al.*, 2007). Image B copied from http://flipper.diff.org/app/items/info/1269.

The repeat region of the N-terminus is also unstructured when not bound to metal ions. Alternatively, this region has been shown to bind RNA *in vitro*, and may be responsive to extracellular RNA-mediated signalling (Dinger, 2008). However, instability of the repeats, particularly insertion mutations that increase the copy number of the repeats >10 has been associated with an earlier age of CJD onset

(Goldfarb *et al.*, 1991). Heptapeptide repeats found in two other proteins, the maize ribosomal protein S18 and RNA polymerase II, are involved in RNA binding and the maintenance of secondary structure respectively, and the presence of multiple octapeptide repeats is found in ice-nucleation proteins with each repeat contributing to the nucleation process (Green, 1985).

Both PrP^{C} and PrP^{Sc} isoforms are tethered to the surface membrane by a glycophosphatidylinositol (GPI) anchor and found mostly in cholesterol and sphingolipid-rich membrane domains, known as lipid rafts (Madore *et al.*, 1999) (Taraboulos *et al.*, 1995)(Vey *et al.*, 1996). Lipid rafts are microdomains within the plasma membrane that are enriched in certain proteins and lipids, and serve as organising centres since they compartmentalise cellular processes such as signal transduction, endocytosis, cholesterol transport, and the regulation of receptor trafficking (Zajchowski *et al.*, 2002). The presence of PrP within signalling rich lipid rafts implicates PrP in this role. The clustering of PrP^{C} molecules in this way may also contribute to the propagation of the PrP^{Sc} isoform (Madore *et al.*, 1999). Additionally, PrP^{C} appears to be involved in developmental processes of the central nervous system (Hu *et al.*, 2008) and paralogs of mammalian PrP^{C} also demonstrate neurological activities (Moore *et al.*, 1997; Hegde *et al.*, 1998; Watts *et al.*, 2007).

Recently, PrP^{C} has also been identified as a high affinity neuronal, cell surface receptor for soluble amyloid-β peptide (Aβ). Aβ is a 40-42 amino acid proteolytic fragment of the APP protein and is the causative agent in the neurodegenerative Alzheimer's disease. The absence of PrP^{C} or the use of PrP^{C} antibodies to block Aβ binding prevented Aβ-specific blockade of long-term potentiation and rescues synaptic plasticity (Lauren *et al.*, 2009). However, the inability of other research groups to reproduce these results has made the observations of Lauren *et al* highly controversial.

PrP^{C} is the only known protein involved in a misfolding disorder that possesses a GPI-anchor. The affect of GPI-anchoring aggregation-prone proteins has recently been assessed by expressing a GPI-anchored version of the yeast prion protein Sup35p (section 1.3.1) in neuronal cells, followed by subsequent exposure to preformed Sup35p fibrils to induce prion conversion of $Sup35p^{GPI}$ (Speare *et al.*,

2010). The Sup35p^{GPI} readily self-propagated, transferring between aggregate-negative and aggregate-positive cells and formed protease and detergent resistant aggregates. Thus, the GPI-anchor may contribute to the special infectivity of PrP (Speare *et al.*, 2010).

Despite the tremendous complexity, synchronicity and adaptiveness of the cell, prion proteins serve to remind us of the continued painstaking vulnerability of the cell to the ancient dilemma of a protein misfolding event.

1.4.2 Fungal *Podospora anserina* [HET-s]

Podospora anserina is a filamentous fungi that grows in hyphal form by tip extension, branching and hyphal fusion. The fusing of hyphae from different individuals gives rise to a vegetative heterokaryon, which describes the mixing of genetically different nuclei within the cytoplasm of a hyphal fusion cell (Saupe,2000; Glass *et al.*, 2003). However, genetic differences between the individuals at *het* (heterokaryon incompatibility) loci lead to rejection of the heterokaryon, in a process known as vegetative incompatibility (Saupe,2000)(Rizet *et al.*, 1952). Each of the 9 *het* genes is represented by one of at least 2 polymorphic alleles. The *het-s* locus encodes for a prion-forming protein, and it is the prion state of the encoded HET-s protein that determines the outcome of the heterokaryon reaction between a *het-s* and a *het-S* strain: vegetative incompatibility results when the HET-s protein is in the prion form [Het-s], whereas the hyphal fusion survives if the HET-s protein is in the non-prion form [Het-s*] (assuming complementarities at all other *het*-loci) (Rizet *et al.*, 1952).

1.4.3 *Aplysia californica* CPEB

The marine snail *Aplysia californica* has a simple nervous system composed of relatively large cells and is tractable to electrophysiological analysis; it has therefore become a popular organism in the study neurobiology.

In *Aplysia,* CPEB (Cytoplasmic polyadenylation element binding protein) has been found to facilitate the persistence of long-term memory (Si *et al.*, 2010). Specifically, CPEB activates dormant mRNAs in neurons by promoting the elongation of mRNA polyadenylation tails (Hake *et al.*, 1994). *Aplysia*, mice, humans and *Drosophila melanogaster* express an isoform of CPEB with an N-terminal domain that has prion-like sequence characteristics and initial studies of the *Aplysia* CPEB protein in yeast confirmed that by virtue of the N-domain, this protein could exist in two structurally distinct states, one of which was self-perpetuating, heritable and multimeric (Si *et al.*, 2003). The multimeric form of CPEB in yeast was also impaired in its propagation by over-expression or deletion of the chaperone Hsp104p; an effect of Hsp104p commonly observed with yeast prion proteins.

Recently, CPEB has been confirmed to form amyloidogenic, self-propagating structures in *Aplysia* following the stimulation of CPEB expression in neuronal synapses (Si *et al.*, 2010). It is the prion-form of CPEB that is active in memory persistence, facilitated by the self-sustaining nature of CPEB protein and which is also limited only to those synapses that were initially stimulated.

1.5 The *Saccharomyces cerevisiae* Rnq1p protein and the [*PIN*$^+$] prion

In the original studies of Sup35p, guanidine hydrochloride treatment of a [*PSI*$^+$] strain resulted in two distinct [*psi*$^-$] populations: those in which it was possible to reinduce [*PSI*$^+$] by Sup35p over-expression (in accordance with principle 4 of Wickner's criteria, section 1.2.1), and those where Sup35p over-expression was not effective in inducing [*PSI*$^+$] (Derkatch *et al.*, 1997). The difference between these two populations was [*PSI*$^+$] inducibility, and so a population was either positive for [***PSI***$^+$] ***in***ducibility ([*PIN*$^+$]) or negative for [***PSI***$^+$] ***in***ducibility ([*pin*$^-$]).

Like [*PSI*$^+$], [*PIN*$^+$] showed non-Mendelian inheritance and was dependent on the presence of the molecular chaperone Hsp104p for its maintenance (Derkatch *et al.*, 1997). However, despite Sup35p over-expression causing growth inhibition in both a [*PSI*$^+$] strain (Derkatch *et al.*, 1997) and a [*PIN*$^+$] strain, it was the ability of [*PIN*$^+$] to appear in the absence of the Sup35p's prion forming domain that led to the

suggestion that [*PIN*$^+$] was a different prion, and not simply a variant of the [*PSI*$^+$] prion (Derkatch *et al.*, 1997).

It was also noted that while the [*PSI*$^+$] and [*PIN*$^+$] prions could be lost independently, there was a correlation in their loss, in that most of the resultant [*psi*$^-$] cells were also [*pin*$^-$], and most that retained [*PSI*$^+$] also retained [*PIN*$^+$] (Derkatch *et al.*, 1997) (figure 1.8). However, [*PIN*$^+$] did not protect [*PSI*$^+$] from curing since a [*PSI*$^+$][*PIN*$^+$] and [*PSI*$^+$][*pin*$^-$] stain showed a similar frequency of [*psi*$^-$] conversion following brief exposure to guanidine hydrochloride (Derkatch *et al.*, 2000).

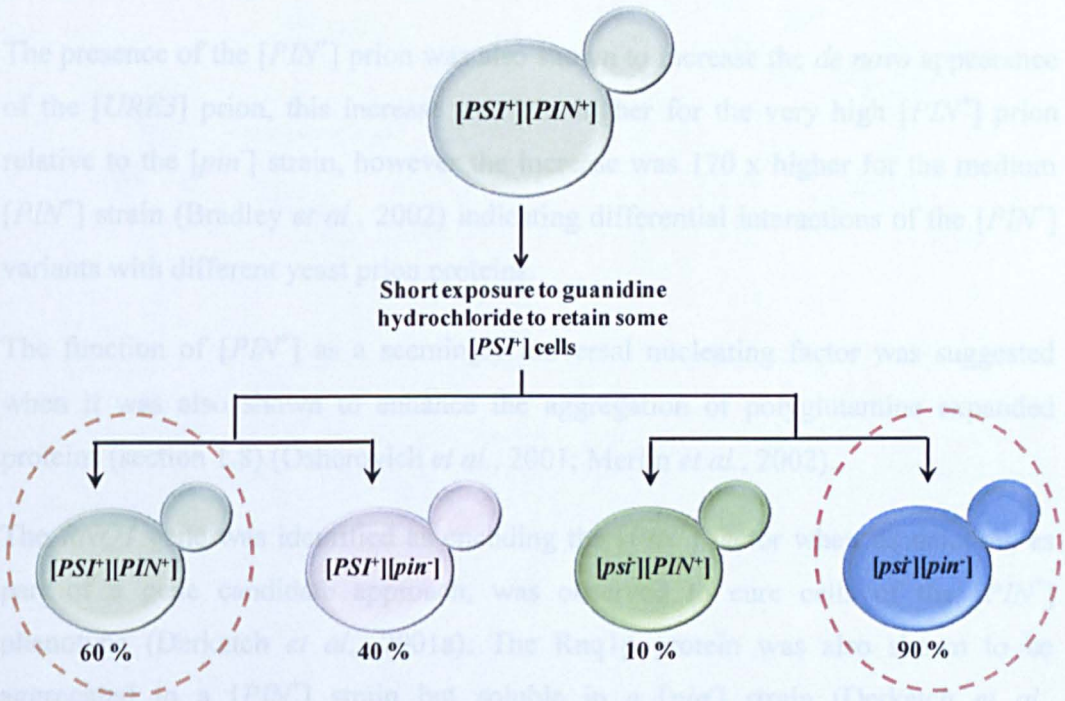

Figure 1.8: The loss of *PSI*$^+$] and [*PIN*$^+$] is correlated.
Short exposure to guanidine hydrochloride, which eliminates prions, demonstrated that 90 % of cells that lost [*PSI*$^+$] also lost [*PIN*$^+$], and that 60 % of cells that retained [*PSI*$^+$], also retained [*PIN*$^+$] (Derkatch *et al.*, 1997).

Reversible curing of [*PIN*$^+$] was also demonstrated when a [*psi*$^-$][*PIN*$^+$] strain was cured to the [*pin*$^-$] state by guanidine hydrochloride exposure, left for one month in stationary phase and assayed for [*PIN*$^+$] presence by Sup35p over-expression; [*PSI*$^+$] is readily assayable and would only be induced by Sup35p over-expression in a

[*PIN*$^+$] background. All cells appeared [*PIN*$^+$], demonstrating reversible curing of [*PIN*$^+$], though most of these were unstable (Derkatch *et al.*, 2000).

Different variants of [*PIN*$^+$] were subsequently identified that showed reproducible differences in the frequency with which [*PSI*$^+$] was induced *de novo*; the variants were [*pin*$^-$], low [*PIN*$^+$], medium [*PIN*$^+$], high [*PIN*$^+$] and very high [*PIN*$^+$], named according to their respective frequency of [*PSI*$^+$] induction (Bradley *et al.*, 2002). This property of the [*PIN*$^+$] variants is reproduced in figure 3.0. Excess Sup35p production also caused the greatest growth defect in the very high [*PIN*$^+$] variant, followed by the high, medium, and low [*PIN*$^+$] variants, with no growth defect in the [*pin*$^-$] strain (Bradley *et al.*, 2002).

The presence of the [*PIN*$^+$] prion was also shown to increase the *de novo* appearance of the [*URE3*] prion, this increase was 17x higher for the very high [*PIN*$^+$] prion relative to the [*pin*$^-$] strain, however the increase was 170 x higher for the medium [*PIN*$^+$] strain (Bradley *et al.*, 2002) indicating differential interactions of the [*PIN*$^+$] variants with different yeast prion proteins.

The function of [*PIN*$^+$] as a seemingly universal nucleating factor was suggested when it was also shown to enhance the aggregation of polyglutamine expanded proteins (section 1.8) (Osherovich *et al.*, 2001; Meriin *et al.*, 2002).

The *RNQ1* gene was identified as encoding the [*PIN*$^+$] factor when its deletion, as part of a gene candidate approach, was observed to cure cells of the [*PIN*$^+$] phenotype (Derkatch *et al.*, 2001a). The Rnq1p protein was also shown to be aggregated in a [*PIN*$^+$] strain but soluble in a [*pin*$^-$] strain (Derkatch *et al.*, 2001)(Bradley *et al.*, 2002).

Analysis of the *RNQ1* gene identified a C-terminus highly enriched for glutamine (Q) and asparagine (N) residues, a signature of yeast prion forming domains (PfD), and the region encapsulating amino acids 153 – 405 of the 405 residue protein was crudely designated the status of the Rnq1p PfD. (figure 1.10) (section 1.5.) (Sondheimer *et al.*, 2000; Vitrenko *et al.*, 2007).

Definitive proof that Rnq1p was the determinant of [*PIN*$^+$] was obtained when *in vitro* fibrils formed from the PfD of Rnq1p were transformed into a [*pin*$^-$] yeast strain

and shown to induce [*PIN*$^+$] (Patel *et al.*, 2007). Several *in vitro* studies also found that Rnq1p aggregates (but not soluble Rnq1p) could increase the polymerisation rate of Sup35-NM, albeit not as effectively as could homologous Sup35-NM aggregates (Derkatch *et al.*, 2004)(King *et al.*, 1997)(Glover et al., 1997) and similarly, that Sup35-NM fibres could stimulate polymerisation of the Rnq1p PfD (Vitrenko *et al.*, 2007).

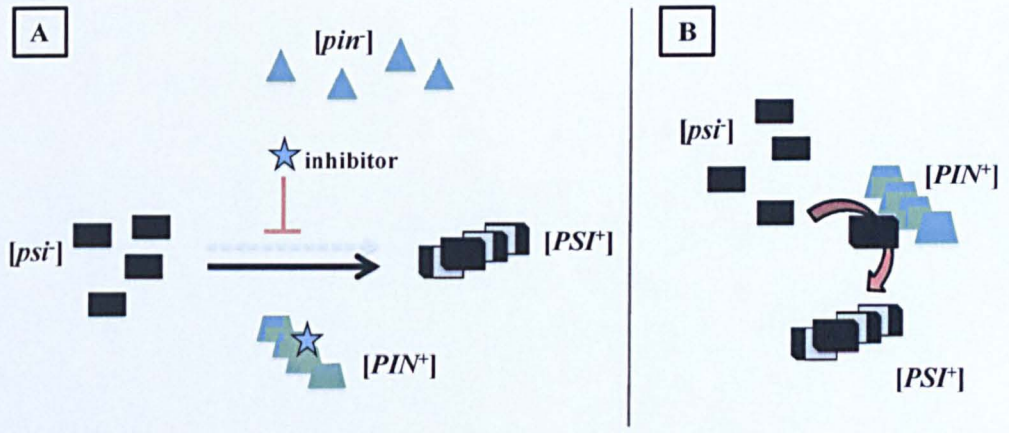

Figure 1.9: [*PIN*$^+$] 'Inhibitor Titration' and 'Direct Seeding' Models
The *de novo* appearance of [*PSI*$^+$] and [*URE3*] prions occurs only in the presence of the [*PIN*$^+$] prion. Two models could explain this [*PIN*$^+$]-dependent mechanism: (A) the titration of an inhibitor model and (B) the direct seeding model.

To explain how [*PIN*$^+$] might influence *de novo* [*PSI*$^+$] formation, two different models have been proposed (figure 1.9) (Derkatch *et al*, 2001):

1) Titration of an Aggregation Inhibitor

   A cellular factor that inhibits prion formation can itself be inhibited by sequestration into [*PIN*$^+$] aggregates, allowing other prion seeds, such as [*PSI*$^+$], to develop. Soluble Rnq1p is not predicted to be the inhibitor since [*PSI*$^+$] is also not observed in a *rnq1Δ* strain.

2) Direct Seeding

   Propagation is believed to involve prion seeds that act either as templates for conversion or that stabilise spontaneous conversion (Derkatch *et al*, 2001).

While conversion is thought to proceed by homologous prion seeding it may be that [*PIN*$^+$] can, albeit less efficiently, provide a seed for the *de novo* heterologous prion formation of [*PSI*$^+$] (Patel *et al.*, 2007).

Both models are mechanistically feasible explanations for how Rnq1p facilitates the generation of [*PSI*$^+$] and [*URE3*] prions.

The sequence of *RNQ1* and its PfD became particularly intriguing when it was discovered to be highly polymorphic (Resende *et al.*, 2003). Specifically, six diploid clinical isolate strains of *S. cerevisiae* were shown to harbour eight different *RNQ1* alleles generated from 6, 12, and 33 bp in-frame deletions and a 42 bp in-frame insertion, relative to the published *RNQ1* sequence (figure 1.12); three strains were heteroallelic for the *RNQ1* locus and one strain contained three *RNQ1* alleles indicating that it was either a triploid strain or trisomic for chromosome III (Resende *et al.*, 2003). The identified polymorphisms clustered to three regions (designated A, B and C on (figure 1.11) within the Pfd of Rnq1p (Resende *et al.*, 2003) and the consequence of these deletions and insertions was to alter the abundance most noticeably of glutamine within the PfD of Rnq1p, but also to a lesser degree the abundance of asparagine, glycine and tyrosine residues.

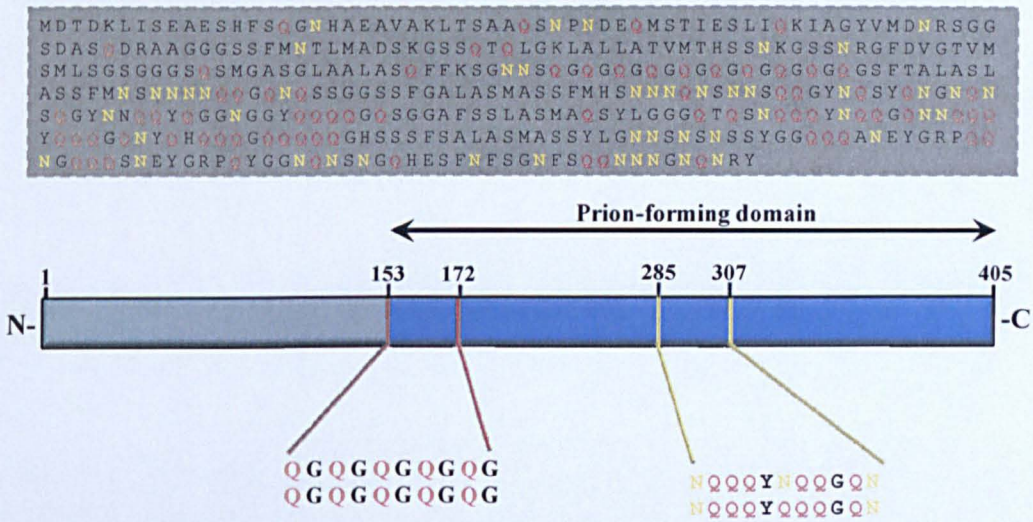

Figure 1.10: The Rnq1p prion-forming domain is C-terminally located and is rich in asparagine and glutamine residues.
The prion-forming domain falls between residues 153-405, and contains a number of repeating sequences throughout.

Since consecutive runs of glutamine within a protein are associated with increased aggregation propensities and in particular the neurodegenerative pathology of polyglutamine diseases (section 1.8), these differences between the *RNQ1* alleles might be expected to alter the frequency with which [*PIN*$^+$] can 1) arise *de novo* 2) induce the conformational conversion of other prion proteins to their prion state (Resende *et al.*, 2003) or 3) induce the aggregation of polyglutamine-rich proteins .

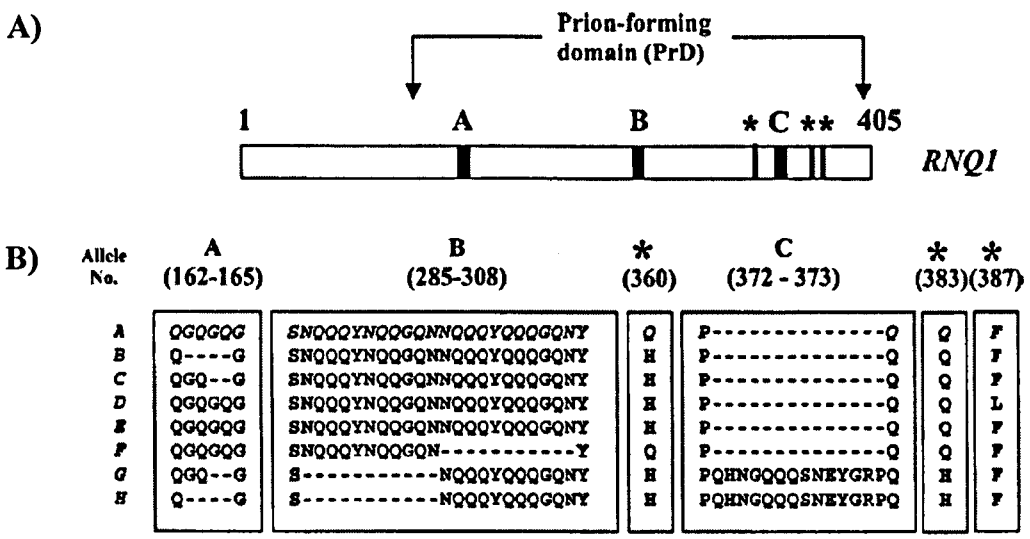

Figure 1.11: Three regions within the Rnq1p prion-forming domain are highly susceptible to polymorphism.
A) cartoon indicating polymorphic regions A, B and C and asterisks (*) indicating polymorphic residues. B) indicating sequence polymorphism occurring at each region identified in panel A. Image from Resende (Resende *et al.*, 2003a)

A separate study by Kadnar *et al* (Kadnar *et al.*, 2010) considered the Rnq1p sequence in terms of clusters of glutamine (Q), glycine (G) and asparagine (N) residues and by the presence of repeating sequences; thus in the PfD of Rnq1p, ten repetitions of the sequence QG (QG_{10}) exist between amino acids 153-172, in addition to four QN-rich regions designated QN_1 (185-198), QN_2 (218-263), QN_3 (279-319), and QN_4 (337-405) (Figure 1.12, panel A). These QG and QN clusters are interspersed with hydrophobic patches referred to in Figure 1.12 as A, B, C, D and E (Figure 1.12, panel A) (Kadnar *et al.*, 2010). A deletion analysis determined that no single QN-region was essential for [*PIN*$^+$] maintenance, though deletion of any QN

region except QN_1 resulted in a reduced frequency of [*PSI*$^+$] induction (Kadnar *et al.*, 2010).

Further, to determine whether any single QN-region was capable of driving prion-like aggregation, a second analysis was performed on multiple Rnq1p truncations that consisted of amino acids 1-172 but retained only one QN-region and the relevant 5' flanking hydrophobic region e.g. the QN_2 test protein consisted of the Rnq1p amino acid sequence 1-172 in-frame with Rnq1p amino acid sequences 199-263 (corresponding to QN_2 plus it's 5' hydrophobic region 'C') (Figure 1.12, panel B) (Kadnar *et al.*, 2010). These truncated proteins each lacking three of the four QN regions were purified and tested for their propensity to form amyloid *in vitro*, using the amyloid-specific shift in Thioflavin T (ThT) excitation spectrum as an indicator of amyloid formation. The QN_1 protein was unable to form amyloid; however a peptide corresponding to the QN_1 tract was capable of forming amyloid. The QN_2 and QN_4 proteins formed amyloid at a similar rate, though the lag time for QN_4 was slightly shorter than that required by QN_2. The QN_3 protein also formed amyloid but at a reduced rate relative to the QN_2 and QN_4 proteins. The authors concluded that since each QN region was able to drive prion-like aggregation, each QN region therefore represents an independent prion-determinant. The authors also noted that the longer the C-terminal truncation, the less able the protein was at maintaining [*PIN*$^+$] (Kadnar *et al.*, 2010).

The authors (Kadnar *et al.*, 2010) hypothesised from this and other data that transmission barriers, the inability of one prion protein to template conversion of another prion protein, were likely due to overall conformational differences, brought about by differential contributions of individual prion determinant regions to the final [*PIN*$^+$] conformation. They also proposed that the currently unknown function of Rnq1p may involve formation of oligomeric complexes (Kadnar *et al.*, 2010).

Analysis of the truncated proteins created in this study (Figure 1.12, panel C) reveals a general correlation between the size of the protein, Q, N and G content, and the ability of these proteins to form amyloid. Specifically, the largest proteins and those with the greatest abundance of Q, G and N residues tend to show the highest propensity to form amyloid, and vice versa. Proteins QN_2 and QN_4 have a similar abundance of residues Q, N and G, however the increased size of the QN_4 protein

may account for its reduced lag time in fibril formation relative to QN_2; essentially it would have longer 'arms' that may allow greater flexibility or ability to interact and therefore polymerise.

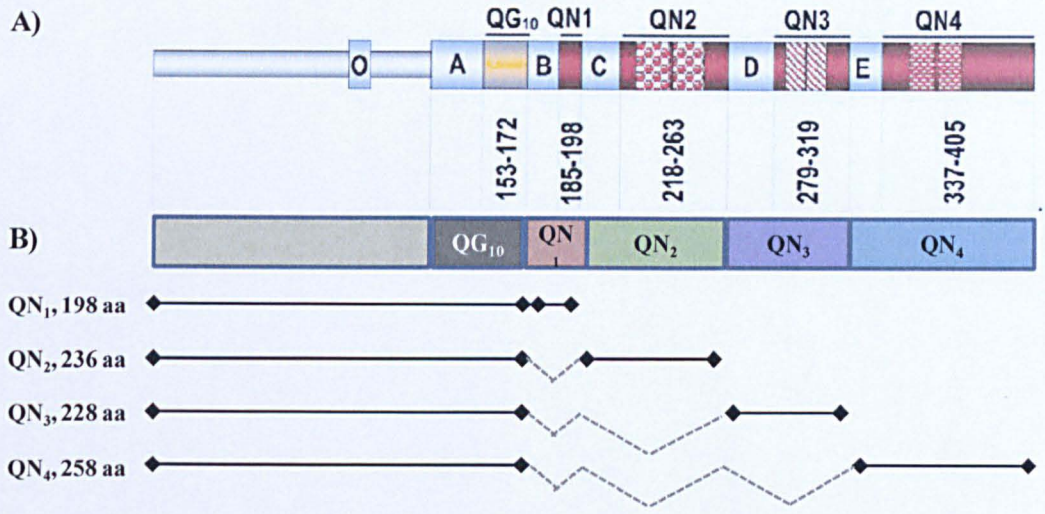

C)

Protein (region)	QN-Sequence	Size (aa)	#Q	#N	#G
QN_1 (+173-198)	SFTALASLASSFMNSNNNNQQGQNQ	198	4	6	1
QN_2 (+199-263)	SGGSSFGALASMASSFMHSNNNQNSNNSQQGYNQ SYQNGNQNSQGYNNQQYQGGNGGYQQQQGQS	236	15	13	11
QN_3 (+264-319)	GGAFSSLASMAQSYLGGGQTQSNQQQYNQ QGQNNQQQYQQQGQNYQHQQQGQQQQQ	228	25	5	8
QN_4 (+320-405)	GHSSSFSALASMASSYLGNNSNSNSSYGGQQQANEYGRPQQNGQ QQSNEYGRPQYGGNQNSNGQHESFNFSGNFSQQNNNGNQNRY	258	14	17	12

Figure 1.12: Further dissection of potentially significant regions of the Rnq1p prion-forming domain.
A) The prion forming domain of Rnq1p was further divided into four QN rich regions, one QG repeat region, and interspersing hydrophobic patches. B) Deletion analysis of the individual QN region with associated hydrophobic patches suggested that all served as prion determinants. C) Analysis of the truncated proteins suggest i*n vitro* aggregation may be positively correlated with protein size.

Despite intense analysis of Rnq1p, the function of this protein has not been identified. Rnq1p is not an essential protein. The primary phenotype associated with Rnq1p is its ability to enhance the *de novo* formation of other yeast prions, when in its own [*PRION*$^+$] conformation. [*PIN*$^+$] also causes increased aggregation and toxicity of the polyglutamine expanded exon 1 fragment of huntingtin protein

(Meriin *et al.*, 2002). Additionally, while the poor nitrogen discrimination of a [*URE3*] strain and the translation termination defect of a [*PSI*$^+$] strain are indicative of the cellular functions of Ure2p and Sup35p respectively, the increased appearance of other prions in a [*PIN*$^+$] strain appears not to indicate that Rnq1p is involved in suppressing their conversion, since [*PSI*$^+$] also cannot form in a *rnq1Δ* strain.

There is however a second phenotype associated with Rnq1p, and that is over-expression of Rnq1p is severely toxic in a [*PIN*$^+$] strain, though not in a [*pin*$^-$] or *rnq1Δ* strain (Douglas *et al.*, 2008). Studies by Douglas *et al* (Douglas *et al.*, 2008) showed that a 5-10x fold over-expression of Rnq1p results in death of 25 % of cells within 4 hrs, and toxicity is accompanied by an increase in amyloid-like aggregates. The toxicity of Rnq1p increased with expression level and in a [*PIN*$^+$] but not in [*pin*$^-$] strain, SDS-resistant high molecular weight aggregates assembled, though a soluble fraction remained (Figure 1.13). However, separate over-expression of the PfD of Rnq1p (amino acids 154-405) or the N-terminus (amino acids 1-153) was not toxic, despite the accumulation of PfD specific large SDS-resistant aggregates, therefore toxicity could not be attributed simply to the presence of large amyloid-like aggregates.

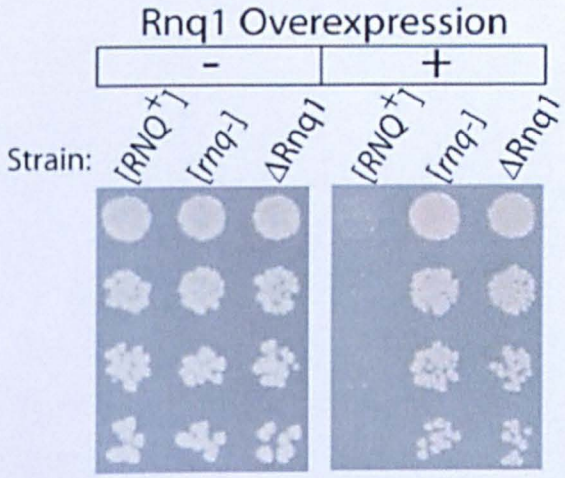

Figure 1.13: Rnq1p over-expression is toxic in a [*PIN*$^+$] but not in a [*pin*$^-$] background.
Over-expression of Rnq1p in a [*PIN*$^+$], [*pin*$^-$] and *rnq1Δ* strain results in [*PIN*$^+$] specific toxicity. Image from Douglas *et al* (Douglas *et al.*, 2008).

In the same study (Douglas *et al.*, 2008) a 3x fold elevation in the expression level of Sis1p, an essential Hsp40 chaperone required for [*PIN*$^+$] maintenance and propagation, was found to suppress the toxicity associated with Rnq1p over-expression in a [*PIN*$^+$] background. There is exceptional specificity to this effect of Sis1p in suppressing Rnq1p toxicity, since a screen of 4, 954 yeast genes from an expression library revealed Sis1p to be the only chaperone capable of conferring protection from Rnq1p toxicity (Douglas *et al.*, 2008). It remains to be seen if the authors identified other non-chaperone proteins that could suppress Rnq1p toxicity.

Since Sis1p is an essential protein which interacts in a 1:1 complex with the [*PIN*$^+$] prion (Lopez *et al.*, 2003), it was possible that Rnq1p over-expression was inducing cell death by sequestering Sis1p away from essential interactions in the cell. However Douglas *et al* (Douglas *et al.*, 2008) observed that direct Sis1p depletion caused a delayed lethality, compared to the 4 hrs for toxicity observed with Rnq1p over-expression. Nonetheless, one could speculate that the consequences of repressing Sis1p expression (for example via a titratable promoter) would depend on the rate of Sis1p turnover in the cell, its on-going interactions and its localisation. The effect of over-expressing Rnq1p would be expected to cause a more immediate depletion of Sis1p, and possibly a re-localisation of Sis1p to a less protected environment. One could speculate that these differences in the mode of Sis1p depletion could account for differences in the rate of cell death.

To invalidate sequestration of Sis1p as the cause of Rnq1p toxicity, two analyses were performed by Douglas *et al* (Douglas *et al.*, 2008), 1) over-expression of a Sis1p protein deleted for the Rnq1p interaction region, which was shown not to suppress the toxicity of Rnq1p, indicating suppression of Rnq1p toxicity by Sis1p was likely due to its direct interaction with Rnq1p, and 2) the Rnq1p Sis1p-binding site was mutated such that it impaired Sis1p association with Rnq1p, and over-expression of these Rnq1p mutants showed an increased level of toxicity relative to the wild-type Rnq1p protein – this indicated that Rnq1p toxicity was not due to sequestration of Sis1p, it also confirmed Sis1p's role in 'containing' Rnq1p toxicity (Figure 1.14). It was also noted by the authors that the Rnq1p mutants were impaired in their assembly of large amyloid-like aggregates, yet they were more toxic than the wild-type Rnq1p. These data indicated that the efficient conversion of Rnq1p into an

amyloid form was necessary to prevent the accumulation of toxic oligomers or conformers (Douglas *et al.*, 2008). Additionally, the Rnq1p mutant was toxic in a [*pin*$^-$] strain though the aggregates formed were not SDS-resistant, did not bind the amyloid indicator thioflavin-T and could not seed polymerisation of native Rnq1p *in vitro*, suggesting to the authors that suppression of Rnq1p toxicity requires both Sis1p over-expression and the presence of the [*PIN*$^+$] prion assembly pathway; where off-pathway conformations give rise to toxic species (Douglas *et al.*, 2008).

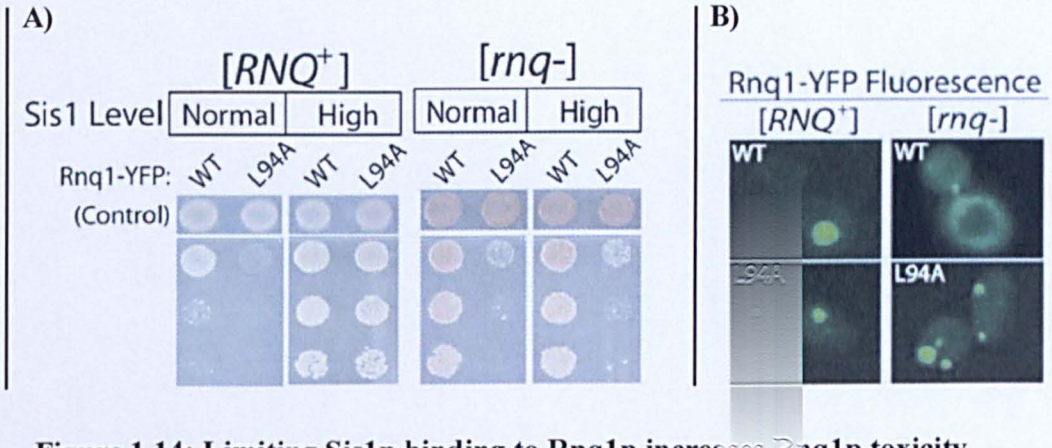

Figure 1.14: Limiting Sis1p binding to Rnq1p increases Rnq1p toxicity. The L94A mutant of Rnq1p, impairing the Sis1p:Rnq1p interaction, increases the toxicity of Rnq1p that in a [*PIN*$^+$] but not a [*pin*$^-$] strain, can be prevented by co-over-expression of Sis1p Douglas *et al* (Douglas *et al.*, 2008).

This explanation however is somewhat unsatisfying since it has been shown that only in the [*PIN*$^+$] state does Rnq1p interact with Sis1p (Sondheimer *et al.*, 2001) and also that Rnq1p over-expression is toxic only in a [*PIN*$^+$] background (Douglas *et al.*, 2008).. Rnq1p over-expression in a [*pin*$^-$] state also does not produce aggregates; the refolding of Rnq1p appears to be specific to the presence of the [*PIN*$^+$] prion, which triggers conversion of Rnq1p to the [*PIN*$^+$] state. In a [*pin*$^-$] strain, there are no pre-existing aggregates of Rnq1p available to trigger Rnq1p aggregation. Therefore while the L94A mutation of Rnq1p impairs its interaction with Sis1p, this should be inconsequential in a [*pin*$^-$] state since Sis1p does not bind Rnq1p in a [*pin*$^-$] conformation. This suggests that the L94A mutation may also destabilise Rnq1p; it may be this destabilisation that allows Rnq1p to misfold in a

[*pin*$^-$] background, giving rise to the observed aggregates. However, Sis1p over-expression did not rescue toxicity of the L94A mutant in a [*pin*$^-$] strain, where it was able to do so in a [*PIN*$^+$] strain (Figure 1.14), suggesting that in the absence of an efficient template (e.g. [*PIN*$^+$]) the Rnq1p L94A mutant gives rise to a conformation that is inaccessible to Sis1p. In support of this, the aggregates formed by the L94A Rnq1p mutant in a [*pin*$^-$] background were determined not to be amyloid.

Thus, the Rnq1p L94A mutant appears to give rise to toxic, non-amyloid aggregates that are conformationally inaccessible to Sis1p, since Sis1p was able to bind the L94A Rnq1p mutant in a [*PIN*$^+$] but not in a [*pin*$^-$] background. In addition, it suggests that the presence of the [*PIN*$^+$] prion may serve to mask alternative aggregation pathways.

If Rnq1p were a protein susceptible to destabilisation, the presence in the cell of the [*PIN*$^+$] prion may be a necessity, since destabilisation of Rnq1p in the absence of [*PIN*$^+$] could lead to misfolding aggregates that were toxic and inaccessible to Sis1p. Rnq1p is the only prion protein that has been found in non-lab strains; however it is not present in every strain suggesting that 1) Rnq1p is not an inherently unstable protein, 2) a mechanism exists to prevent Rnq1p destabilisation, or 3) a mechanism exists to handle the alternative aggregates formed by destabilised Rnq1p.

In summary, Rnq1p has become central to many investigations: mechanisms of prion conversion, where [*PIN*$^+$] is required in order for other prion proteins to convert to their [*PRION*$^+$] state; mechanisms of polyglutamine toxicity, particularly in the yeast model of Huntington's disease, where Rnq1p in the [*PIN*$^+$] state is required to drive aggregation of the expanded exon 1 of huntingtin and its associated toxicity; dissecting how repetitive sequences and protein composition contribute to prion/amyloid formation and transmission barriers between different prion proteins. Its own toxicity provides an opportunity to understand the pathways of protein misfolding, and how one might preferentially direct misfolding (where it is inevitable) down a non-toxic route.

1.6 The biological significance of prions

The context of their initial identification implicated prions as causative agents of disease, specifically neurodegenerative diseases of mammals. However, the subsequent identification of prion proteins in yeast and the absence of any noticeable growth defect in their presence suggested the original correlation between prion presence and toxicity was not the full story.

In the case of the yeast [*PSI*$^{+}$] prion for example, while the increase in termination errors that accompany Sup35p conversion to [*PSI*$^{+}$] leads to the production of C-terminally extended polypeptides (Inge-Vechtomov *et al.*, 1970), one significant corollary of this is the mass exposure of previously hidden genetic variation, which appears to be advantageous to cells under conditions of stress, allowing greater rates of stress adaptation than was seen to occur in [*psi*$^{-}$] cells (True *et al.*, 2000).

Further, it is becoming increasingly apparent that prion proteins, particularly in yeast, permeate many levels of cellular control, although a role in transcriptional processes seems increasingly over-represented. The question then becomes whether prions represent an additional level of epigenetic control over cellular processes, superimposed upon a backbone of cellular coordination determined by nucleic acid. One might expect that, were this to be the case, there would also exist some degree of coordination within this novel mechanism for control e.g. interactions between the different prion proteins, and so it may be that with time a network of prion-specific interactions within the cell will be recognised.

1.7 Prion-associated toxicity

Over-expression of Rnq1p is toxic in a [*PIN*$^{+}$] cell (section 1.5) and evidence suggests that this occurs when Rnq1p overwhelms the capacity of the Sis1p chaperone to assemble Rnq1p into the amyloid-specific pathway, since impairing the interaction between Sis1p and Rnq1p increases the toxicity of Rnq1p (Douglas *et al.*, 2008). Additionally, a Rnq1p mutant has been identified that displays [*PIN*$^{+}$]-independent toxicity, forming aggregates of a non-amyloid nature that are also non-responsive to the Sis1p chaperone (possibly due to the formation of a Sis1p-

inaccessible conformation). This latter example separates the toxicity of Rnq1p from its identity as both a prion, and a toxic amyloid, and allows one to question the contribution of its function, localisation and its abundance of glutamine and asparagine in general to this toxic misfolding event.

Sup35p has also been shown to cause cell toxicity when over-expressed in a [*PSI*$^{+}$] strain (Dagkesamanskaya *et al.*, 1991). Since Sup35p over-expression causes nonsense suppression in a [*psi*$^{-}$] cell, and [*PSI*$^{+}$] appearance also causes nonsense suppression (Cox *et al.*, 1965), it has been considered that Sup35p over-expression in a [*PSI*$^{+}$] background is toxic due to these additive detrimental effects on translational fidelity that lead to poor viability (Chernoff *et al.*, 1992). Recently however, it has been shown that it is the sequestration of Sup45p rather than functional Sup35p which leads to toxicity (Vishveshwara *et al.*, 2009).

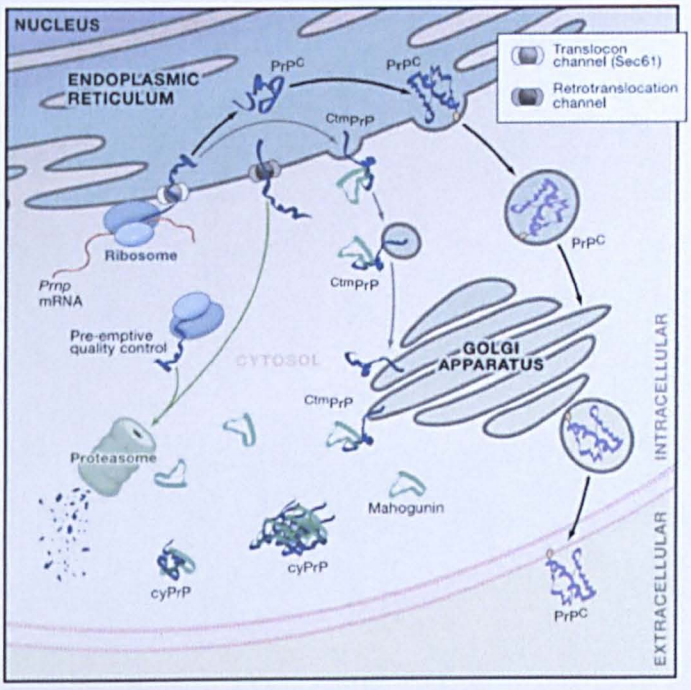

Figure 1.15: Co-translational entry of PrP into the secretory pathway. Toxicity of PrP may arise from cytoplasmic accumulation of a PrP:mahoguinin complex that has been linked to the spongiform pathology of CJD. Image extracted from Aguzzi *et al* (Aguzzi *et al.*, 2009).

Finally, the toxicity of the PrP^{Sc} isoform manifests as the neurodegenerative disease CJD (section 1.4.1.). At the molecular level, one source for PrP toxicity appears to be the accumulation of misfolded PrP in the cytosol. PrP normally enters the secretory pathway co-translationally for targeting to the cell surface however, PrP is not always efficiently translocated into the ER for this purpose and therefore must be degraded by the cytosolic proteasome (Rane *et al.*, 2004). Under burden, such as stress or with age, the capacity of the proteasome to degrade PrP is compromised and this can lead to the accumulation of neurotoxic PrP and the generation of PrP^{Sc} (Smallridge *et al.*, 2002). Additionally, a small proportion of PrP adopts a transmembrane conformation during co-translational import into the ER, with the aberrant projection of the PrP N-terminus into the cytosol; this form of PrP, along with any cytosolic PrP, has been shown to bind to an E3 ubiquitin ligase called mahoguinin and it is thought that this interaction between PrP and mahoguinin may be responsible for the spongiform pathology of CJD (Chakrabarti *et al.*, 2009) (Figure 1.15).

1.8 Polyglutamine-associated toxicity: Huntington's disease

Expansion of a CAG codon within a gene results in the production of a protein with an uninterrupted stretch of glutamine residues. There are currently nine known neurodegenerative diseases associated with an expanded polyglutamine (poly-Q) tract, including multiple Spino-Cerebellar Ataxias (SCA-1, -2, -3, -6, -7 and -17), Spinal and Bulbar Muscular Atrophy (SBMA), DentatoRubral and PallicloLuysian Atrophy (DRPLA) and Huntington's disease (section 1.8).

In all cases the polyglutamine disease manifests as a loss of select neuronal cells in specific regions of the brain. Symptoms usually present late in life and include the progressive deterioration of muscle coordination; however juvenile onset does also occur reflecting a strong correlation between age of onset and length of the poly-Q tract (Norremolle *et al.*, 1993). The critical threshold for expansion before pathological changes occur is 35-40 glutamines, indicating some commonality in the toxicity pathway of polyglutamine diseases, at least in the initial stages. However, the only sequence similarity between the different poly-Q expanded proteins resides

within the region conferring toxicity (the poly-Q tract); similar to how Q/N-richness of the prion-forming domain is the only unifying feature of yeast prion proteins.

Huntington disease is a progressive neurodegenerative disease caused by an expansion of the polyglutamine tract within exon-1 of the *IT15* gene (The Huntington's Disease Consortium, 1993) that encodes huntingtin (Htt) protein and as such is categorised as a polyglutamine disease.

Huntington disease affects 1/25,000 individuals (Schols *et al*, 2004) and is defined by loss of neurons in the striatum and cortex that lead to uncoordinated body movements and dementia. Following the onset of symptoms life-expectancy is ~ 15 yrs since there is currently no cure for Huntington's disease, with the primary causes of death being pneumonia, heart disease and suicide.

The mutant Htt protein is prone to aggregation due to the expanded poly-Q tract adopting β–rich fibrillar structure recognised as amyloid (Perutz *et al.*, 1994). The aggregates or 'inclusion bodies' that form accumulate mostly within, but also outside of, the nucleus and are a hallmark of polyglutamine diseases though their significance to etiology has been controversial. Recently however, compelling evidence for a primarily cytoprotective role of inclusion bodies and aggregates in general has been demonstrated by 1) protection from the toxicity of a Q/N-rich prion protein in yeast by chaperone-dependent amyloid assembly (Douglas *et al.*, 2008), 2) dramatic increases in neuronal survivability with the formation of mutant Htt inclusion bodies and the coincident reduction of dispersed mutant Htt (Miller *et al.*, 2010), 3) a gene-on:gene-off comparison study in an aged, late-stage mouse model of Huntington disease, revealing complete recovery of motor impairment in the gene-off mice, despite persistence of inclusion bodies (Diaz-Hernandez *et al.*, 2005).

Contributing to the difficultly in determining a cellular function for Htt protein, since its identification 17 years ago, has been the lack of sequence homology to other proteins (Landles *et al.*, 2004). Further, Htt is expressed in nearly all tissues, but highest levels of Htt are found in neurons of the central nervous system. Htt is present in the nucleus and the cytoplasm, and also associates with mitochondria, the Golgi apparatus and endoplasmic reticulum (Harjes *et al.*, 2003; Li *et al.*, 2004). Additionally, Htt is enriched in membrane-containing fractions, and its association

with microtubules indicates a role for Htt in vesicle-trafficking or cytoskeletal anchoring (Gutekunst *et al.*, 1995). Htt also has roles in clathrin-mediated endocytosis, neuronal transport, post-synaptic signalling, and protection from apoptotic stress (Nasir *et al.*, 1995)(Cattaneo *et al.*, 2001)(Rigamonti *et al.*, 2001).

A further unifying consequence of expanded poly-Q protein expression appears to be an elevated presence of the affected protein within the nucleus, indicating that nuclear events such as transcription could be altered by these diseases (DiFiglia *et al.*, 1997). Evidence supporting the transcriptional dysregulation brought about by expanded poly-Q and mutant Htt protein is now abound (Helmlinger *et al.*, 2006; Irwin *et al.*, 2005; Nucifora *et al.*, 2001; Luthi-Carter *et al.*, 2002). Indeed, similar to poly-Q disease proteins, several eukaryotic transcription factors also contain glutamine-rich domains. Specifically, the activation domains of transcription factors tend to be either acidic, proline-rich or glutamine-rich. The latter motif being essential for mediating protein-protein interactions required for transcriptional activation (Latchman *et al.*, 2007). Thus, the expanded polyglutamine tract of disease proteins may, by virtue of the enlarged glutamine-rich 'interaction domain', participate in spurious interactions with glutamine-rich transcription factors leading to the observed dysregulation of transcription (Truant *et al.*, 2007). In support of this, mutant Htt has been found associated with glutamine-rich members of the SP1 family of transcription factors and the CREB binding protein (CBP)/P300 proteins (Steffan *et al.*, 2000).

The threshold that must be exceeded for polyglutamine pathology to be observed is between ~35-40 residues, implying the existence of a molecular or functional barrier that can be breached by a common parameter (polyglutamine tract length) regardless of the affected protein's identity and flanking sequences. However, the mere existence of different polyglutamine-based diseases (section 1.8) indicates that the toxic structure formed by the expanded polyglutamine tract is not the only parameter influential in disease pathology. Thus, it is of great interest to dissect the toxicity mechanism by addressing the relative contribution to toxicity of the affected protein's function, cellular localisation(s), direct or complex-specific interactions, and flanking sequences, etc. Comparing the relative contributions of these parameters to toxicity for multiple disease proteins might indentify overlapping

features that could either elucidate mechanisms for disease progression or identify cellular components that may serve as broad-spectrum therapeutic targets for polyglutamine (or amyloid-based) diseases.

1.9 Aims of the project

1.9.1 Rnq1p function

The cellular function of Rnq1p is currently unknown, and Chapter 3 of this thesis describes experiments conducted to identify the possible role(s) of Rnq1p within the cell using a combination of approaches including basic phenotypic screens, growth analysis, bioinformatics and mass spectrometry-based label-free quantitative proteomics.

1.9.2 Rnq1p polymorphisms and toxicity

Rnq1p is a highly polymorphic protein, however publicly accessible sequence data for Rnq1p is limited to an analysis of six strains. Chapter 4 of this thesis describes experiments conducted to understand the extent of Rnq1p polymorphisms in nature by sequencing the *RNQ1* gene from multiple ecologically diverse *S. cerevisiae* strains. Additionally, studies of Rnq1p sequence polymorphism to date have considered the impact of laboratory generated polymorphisms on [*PIN*$^+$] maintenance and [*PSI*$^+$] induction, Chapter 5 of this thesis examines the functional consequences of natural *RNQ1* polymorphisms, identified in Chapter 4, on the toxicity profile of Rnq1p.

1.9.3 Modifiers of Rnq1p and Huntingtin toxicity

Rnq1p over-expression is toxic in a [*PIN*$^+$] cell (Douglas *et al.*, 2008), and the yeast model of Huntington disease also requires the presence of [*PIN*$^+$] for aggregation and toxicity (Meriin *et al., 2002).* Both Rnq1p and Huntingtin give rise to amyloid-like

fibrils in yeast, both appear to be nucleocytoplasmic proteins, and both are rich in glutamine residues - an elevated abundance of which appears to be a determinant for proteotoxicity. Thus, one might expect a considerable overlap in the toxicity pathways of these proteins. Differences in these pathways may be indicative of their separate cellular functions. To identify overlapping and unique suppressors of Rnq1p and Huntingtin toxicity in the [*PIN*$^+$] state, Chapter 6 of this thesis investigates potential genetic modifiers of Rnq1p toxicity and previously identified genetic modifiers of huntingtin toxicity. Additionally, it is likely that the [*PIN*$^+$] prion prevents the cell from exploring alternative aggregation pathways, masking the effect of certain genetic modifiers, therefore the same proteotoxicity screen is analysed in the [*pin*$^-$] state. .

Chapter II

Materials and Methods

Risk assessments including COSHH were carried out for all procedures involving use of hazardous chemicals or equipment and suitable control measures were employed. All work involving genetically modified organisms and pathogens were performed in an ACDP category two laboratory.

2.1 Media used for the culture of *Saccharomyces cerevisiae*

Unless otherwise stated, all media and sterile solutions were sterilised by autoclaving at 121 °C, 15 lb/sq.in for 11 min in a Prestige Medical benchtop autoclave.

2.1.1 YPD (complete) medium

Glucose 20 g per litre, Yeast Extract (Difco) 10 g per litre, Bactopeptone (Difco) 20 g per litre, Deionised water to 1 l final volume.

For solid medium, Granulated Agar (Difco) was added to a final concentration of 2 % w/v prior to autoclaving. For prion curing, guanidine hydrochloride (Sigma) was added after autoclaving to a final concentration of 5 mM from an 8 M stock solution in water.

2.1.2 Synthetic dextrose (minimal) medium

Glucose 20 g per litre, Yeast Nitrogen Base (without amino acids, with ammonium sulphate) (Difco) 6.7 g per litre, Deionised water to 1 l final volume.

For solid medium, Granulated Agar (Difco) was added to a final concentration of 2 % w/v prior to autoclaving. To select for cells carrying yeast plasmids the relevant nutritional marker was selected for by adding Yeast Synthetic Complete Drop-Out Media Supplement (Formedium) prior to autoclaving, which lacked the appropriate amino acid: for uracil drop-out media, 1.9 g per litre was added; for leucine drop-out media, 1.64 g per litre was added; for uracil and leucine drop-out media, 1.74 g per litre was added; for histidine drop-out media, 1.93 g per litre was added; and for adenine drop-out media, 0.78 g per litre was added. For prion curing, guanidine hydrochloride was added after autoclaving to a final concentration of 5 mM from an 8 M stock solution in water.

2.1.3 Synthetic 2 % raffinose medium

2 % Raffinose (Formedium) 26.7 g per litre, Deionised water to 1 l final volume.

For solid medium, Granulated Agar (Difco) was added to a final concentration of 2 % w/v prior to autoclaving. To select for cells carrying yeast plasmids the relevant nutritional marker was selected for by adding Yeast Synthetic Complete Drop-Out Media Supplement (Formedium) prior to autoclaving, which lacked the appropriate amino acid: for uracil drop-out media, 1.9 g per litre was added; for leucine drop-out media, 1.64 g per litre was added. For oxidative stress analysis, hydrogen peroxide (Sigma) was added to a final concentration of 3 mM in water.

2.1.4 Synthetic 2 % galactose medium

Galactose 20 g per litre, Yeast Nitrogen Base (without amino acids, with ammonium sulphate) (Difco) 6.7 g per litre, Deionised water to 1 l final volume.

For solid medium, Granulated Agar (Difco) was added to a final concentration of 2 % w/v prior to autoclaving. To select for cells carrying yeast plasmids the relevant nutritional marker was selected for by adding Yeast Synthetic Complete Drop-Out Media Supplement (Formedium) prior to autoclaving, which lacked the appropriate amino acid: for uracil drop-out media, 1.9 g per litre was added; for leucine drop-out

media, 1.64 g per litre was added. For oxidative stress analysis, hydrogen peroxide (Sigma) was added to a final concentration of 3 mM.

2.1.5 Synthetic 2 % galactose and 1 % raffinose medium

2 % Galactose, 1 % Raffinose (Formedium) 36.9 g per litre, Deionised water to 1 l final volume.

For solid medium, Granulated Agar (Difco) was added to a final concentration of 2 % w.v prior to autoclaving. To select for cells carrying yeast plasmids the relevant nutritional marker was selected for by adding Yeast Synthetic Complete Drop-Out Media Supplement (Formedium) prior to autoclaving, which lacked the appropriate amino acid: for uracil drop-out media, 1.9 g per litre was added; for leucine drop-out media, 1.64 g per litre was added; for uracil and leucine drop-out media, 1.74 g per litre was added; and for adenine drop-out media, 0.78 g per litre was added. For oxidative stress analysis, hydrogen peroxide (Sigma) was added to a final concentration of 3 mM.

2.1.6 Complete medium with variable carbon source

20 g of carbon source (dextrose, galactose, glycerol, sucrose, raffinose, fructose, maltose) Yeast Nitrogen Base (without amino acids, with ammonium sulphate) (Difco) 6.7 g per litre, Deionised water to 1 l final volume.

For solid medium, Granulated Agar (Difco) was added to a final concentration of 2 % prior to autoclaving. To select for cells carrying yeast plasmids the relevant nutritional marker was selected for by adding Yeast Synthetic Complete Drop-Out Media Supplement (Formedium) prior to autoclaving, which lacked the appropriate amino acid: for uracil drop-out media, 1.9 g per litre was added; for leucine drop-out media, 1.64 g per litre was added; for uracil and leucine drop-out media, 1.74 g per litre was added; for histidine drop-out media, 1.93 g per litre was added; and for adenine drop-out media, 0.78 g per litre was added.

2.2 Luria Bertani (LB) media for the culture of *Escherichia coli*

Bacto-tryptone (Difco) 10 g per litre, Yeast Extract (Difco) 5 g per litre, Sodium Chloride10 g per litre, Deionised water to 1 l final volume.

For solid medium, Granulated Agar (Difco) was added to a final concentration of 2 % w/v prior to autoclaving. To select for ampicillin resistant transformants, ampicillin was added to a final concentration of 100 μg/ml after autoclaving, from a 100 mg/ml stock solution in water. For the selection of kanamycin resistant transformants, kanamycin (Sigma) was added to the medium after autoclaving to a final concentration of 50 μg/ml from a 10 mg/ml stock solution in water.

2.3 Incubation conditions for *Saccharomyces cerevisiae* and *Escherichia coli* cultures

All strains of *Saccharomyces cerevisiae* were incubated at 30 °C unless otherwise indicated, with constant shaking at 200 rpm for liquid cultures. All strains of *Escherichia coli* were incubated at 37 °C, with constant shaking at 200 rpm for liquid cultures.

2.4 *Saccharomyces cerevisiae* strains

Table 2.1 ***Saccharomyces*** **cerevisiae strains used in this study**

Strain	Parent	Genotype	Source
SCI-1/ J941082		Clinical Isolate	Vaginal
SCI-2/ J940975		Clinical Isolate	Vaginal
SCI-3/ J941047		Clinical Isolate	Oral
SCI-4/ J940610		Clinical Isolate	Oral
SCI-5/ J940557		Clinical Isolate	Vaginal
SCI-6/ J940421		Clinical Isolate	Oral
SCI-7/ NCPF 8145		Clinical Isolate	Pleural effusion
SCI-8/ NCPF 8184		Clinical Isolate	Wound

SCI-9/ NCPF 8185		Clinical Isolate	Blood culture
SCI-10/ NCPF 8186		Clinical Isolate	Pancreatic drain
SCI-11/ NCPF 8290		Clinical Isolate	Serum
SCI-12/ NCPF 8313		Clinical Isolate	Blood culture
SCI-13/ NCPF 8328		Clinical Isolate	Peritoneal fluid
SCI-14/ NCPF 8348		Clinical Isolate	Blood culture
SCI-15/ NCPF 8363		Clinical Isolate	Pus from human bile duct
SCI-16/ NCPF 8372		Clinical Isolate	Human prosthetic aortic graft
NCYC 361		Natural isolate	Beer spoilage strain from wort in Irish brewery
NCYC 90		Natural isolate	Unknown, 1928
NCYC 110		Natural isolate	Ginger beer, Zingiber Officinale, West Africa, 1925
NCYC 187		Natural isolate	Kefir, 1921
NCYC 680		Natural isolate	Lager production strain, Holesovice brewery, 1966
NCYC 3452/ K11		Natural isolate	Scochu Sake strain, Japan
NCYC 3445/ Y12		Natural isolate	Palm wine strain, Africa
FBY		Natural isolate	Fresh Baker's Yeast, Henry's Bakery, Longfield
42-P04		Natural isolate	Portuguese wine yeast strain, University de Minho, Portugal
110-A42		Natural isolate	Portuguese wine yeast strain, University de Minho, Portugal
235-P119		Natural isolate	Portuguese wine yeast strain, University de

			Minho, Portugal
2-C30		Natural isolate	Portuguese wine yeast strain, University de Minho, Portugal
TH		Natural isolate	Theakston's Bitter
101-ACP10		Natural isolate	Portuguese wine yeast strain, University de Minho, Portugal
SDY		Natural isolate	Sainsbury's Dried Yeast
S288c		Mat α *SUC2, mal, mel, gal2, CUP1, flo1, flo8-1*	Rotting fig, California, USA
L1384		unknown	Y. Chernoff Lab.
BY4741		*Mat a his3Δ1 leu2Δ0 met15Δ0 ura3Δ0*	
BY4741		*Mat a his3Δ1 leu2Δ0 met15Δ0 ura3Δ0 rnq1::kanMX4, ppq1::URA3*	Klement Stojanovski
ATCC 201388		*MATa his3Δ1 leu2Δ0 met15Δ0 ura3Δ0 SIS1-GFP*	Invitrogen
ATCC 201388		*Mat a his3Δ1 leu2Δ0 met15Δ0 ura3Δ0 DCP2-GFP*	Invitrogen
R1158		*MATa his3-1 leu2-0 met15-0 URA::CMV-tTA kan^R-P$_{TET}$-SIS1*	Open Biosystems
BY4742		*MATα his3Δ1 leu2Δ0 lys2Δ0 ura3Δ0*	
W303		*Mat* a *leu2-3,112 trp1-1 can1-100 ura3-1 ade2-1 his3-11,15*	Thomas & Rothstein, Cell 56:619-630, 1989
74D-694		*MAT* a *ade1-14, trp1-289, his3Δ-200, ura3-52, leu2-3, 112.*	Patino *et al,.* (1996)
JSW508		*Mat a, leu2-3, -112, ur3-1, his3-11, -15, trp1-1, can1-100,*	J. Weissman Lab

		ade1-14	
JSW512		*Mat α, leu2-3, -112, ur3-1, his3-11, -15, trp1-1, can1-100, ade1-14*	J. Weissman Lab

Table 2.2 ***Saccharomyces cerevisiae*** **strains from the Yeast Knock-Out Collection (http://www.openbiosystems.com/GeneExpression/Yeast/YKO/) used in this study**

BY4741 (*Mat a his3Δ1 leu2Δ0 met15Δ0 ura3Δ0)* derivatives with *kanMX4* at locus of indicated gene:

aat2Δ	*ard1Δ*	*arg7*	*atp5Δ*	*bfr1Δ*
bmh1Δ	*bna4Δ*	*bub1Δ*	*bub3Δ*	*ccr4Δ*
cka1Δ	*ckb2Δ*	*ctt1Δ*	*cyk3Δ*	*dcp2Δ**
def1Δ	*dnm1Δ*	*ecm37Δ*	*edc3Δ*	*end3Δ*
far8Δ	*gad1Δ*	*get1Δ*	*get2Δ*	*get3Δ*
get4Δ	*get5Δ*	*grx1Δ*	*grx2Δ*	*hmg1Δ*
*hrp1Δ**	*hsp104Δ*	*hsp82Δ*	*inm2Δ*	*ino1Δ*
isy1Δ	*kip1Δ*	*lsb2Δ*	*lsm1Δ*	*lsm7Δ*
mbf1Δ	*met13Δ*	*mgt1Δ*	*mrp8Δ*	*mso1Δ*
nhp6b	*nth1Δ*	*nup170Δ*	*nup84Δ*	*ost4Δ*
paf1Δ	*pde1Δ*	*pep4Δ*	*pfk2Δ*	*pho87Δ*
pop2Δ	*ppn1Δ*	*ppz1Δ*	*ptc2Δ*	*rdh54Δ*
rnq1Δ	*rpd3Δ*	*rpn10 Δ*	*rxt3Δ*	*sdh1Δ*

sfp1Δ	*shs1Δ*	*smy2Δ*	*sna2Δ*	*snf2Δ*
sod1Δ	*sod2Δ*	*ssa1Δ*	*ssb1Δ*	*sse1Δ*
sti1Δ	*stp22Δ*	*swi3Δ*	*tdp1Δ*	*tel1Δ*
tom1Δ	*tor1Δ*	*tps1Δ*	*trx3Δ*	*tsa1Δ*
tsa2Δ	*ubc4Δ*	*ubc7Δ*	*ume1Δ*	*upf1Δ*
upf2Δ	*upf3Δ*	*vps1Δ*	*vps13Δ*	*vps53Δ*
wwm1Δ	*xrn1Δ*	*xrn1Δ*	*ymr082Δc*	*yap1Δ*
ybr016wΔ	*ycr051wΔ*	*ylr278Δc*	*yer185wΔ*	*yir003wΔ*
ymr244c	*ymr244c-aΔ*	*ypt31Δ*	*zap1Δ*	*ppq1 Δ*

BY4743 (*MATa/α his3Δ1/his3Δ1 leu2Δ0/leu2Δ0 LYS2/lys2Δ0 met15Δ0/MET15 ura3Δ0/ura3Δ0)* derivatives with *kanMX4* in locus of indicated gene:

kar2Δ	*las17Δ*	*not1Δ*	*pgk1Δ*	*tub2Δ*
ubc1Δ	*dcp2Δ**	*hrp1Δ*		

*** BY4743 heterozygous deletion**

2.5 *Escherichia coli* strains

Table 2.3 *Escherichia coli* strains used in this study

Strain	Genotype
DH5-α	F⁻ *deoR endA1 recA1 relA1 gyrA96 hsdT17*(r_k^- m_k^+) *phoA supE44 thi-1* Δ*(lacZYA-argF)U169* Φ80δ*lacZ*Δ*M15*
TOP10	F- *mcr*A Δ(*mrr-hsd*RMS-*mcr*BC) Φ80*lac*ZΔM15 Δ*lac*X74 *rec*A1 *ara*D139 Δ(*araleu*)7697 *gal*U *gal*K *rps*L (StrR) *end*A1 *nup*G

Mach1™-T1R	F- Φ80*lac*ZΔM15 Δ*lac*X74 *hsd*R(rk-, mk+) Δ*rec*A1398 *end*A1 *ton*A

2.6. Plasmids

Table 2.4 Plasmids used in this study

Plasmid	Description	Selectable markers[b]	Source
pYES2	Expression vector	2μ, P_{GAL1}, *URA3*	Invitrogen
pYES2-101-ACP10-1	See note 'a'	2μ, P_{GAL1}, *URA3*	This study
pYES2-101-ACP10-2	See note 'a'	2μ, P_{GAL1}, *URA3*	This study
pYES2-101-ACP10-b	See note 'a'	2μ, P_{GAL1}, *URA3*	This study
pYES2-101-ACP10-c	See note 'a'	2μ, P_{GAL1}, *URA3*	This study
pYES2-110-A42-1	See note 'a'	2μ, P_{GAL1}, *URA3*	This study
pYES2-110-A42-a	See note 'a'	2μ, P_{GAL1}, *URA3*	This study
pYES2-110-A42-b	See note 'a'	2μ, P_{GAL1}, *URA3*	This study
pYES2-110-A42-c	See note 'a'	2μ, P_{GAL1}, *URA3*	This study
pYES2-110-A42-d	See note 'a'	2μ, P_{GAL1}, *URA3*	This study
pYES2-2-C30-a	See note 'a'	2μ, P_{GAL1}, *URA3*	This study
pYES2-2-C30-b	See note 'a'	2μ, P_{GAL1}, *URA3*	This study
pYES2-2-C30-c	See note 'a'	2μ, P_{GAL1}, *URA3*	This study
pYES2-2-C30-d	See note 'a'	2μ, P_{GAL1}, *URA3*	This study
pYES2-42-PO4-a	See note 'a'	2μ, P_{GAL1}, *URA3*	This study
pYES2-42-PO4-b	See note 'a'	2μ, P_{GAL1}, *URA3*	This study
pYES2-42-PO4-d	See note 'a'	2μ, P_{GAL1}, *URA3*	This study
pYES2-74D-1B	See note 'a'	2μ, P_{GAL1}, *URA3*	This study
pYES2-74D-1Bii	See note 'a'	2μ, P_{GAL1}, *URA3*	This study
pYES2-74D-1Biii	See note 'a'	2μ, P_{GAL1}, *URA3*	This study

pYES2-74D-5A	See note 'a'	2μ, P_{GAL1}, *URA3*	This study
pYES2-74D-5Aii	See note 'a'	2μ, P_{GAL1}, *URA3*	This study
pYES2-BY4741-a	See note 'a'	2μ, P_{GAL1}, *URA3*	This study
pYES2-BY4741-c	See note 'a'	2μ, P_{GAL1}, *URA3*	This study
pYES2-FBY-b	See note 'a'	2μ, P_{GAL1}, *URA3*	This study
pYES2-FBY-d	See note 'a'	2μ, P_{GAL1}, *URA3*	This study
pYES2-HIGH-1	See note 'a'	2μ, P_{GAL1}, *URA3*	This study
pYES2-JSW512-a	See note 'a'	2μ, P_{GAL1}, *URA3*	This study
pYES2-JSW512-b	See note 'a'	2μ, P_{GAL1}, *URA3*	This study
pYES2-L1384-b	See note 'a'	2μ, P_{GAL1}, *URA3*	This study
pYES2- L1384-c	See note 'a'	2μ, P_{GAL1}, *URA3*	This study
pYES2- L1384-d	See note 'a'	2μ, P_{GAL1}, *URA3*	This study
pYES2-LOW-1	See note 'a'	2μ, P_{GAL1}, *URA3*	This study
pYES2-MED-1	See note 'a'	2μ, P_{GAL1}, *URA3*	This study
pYES2-NCYC-361-iii	See note 'a'	2μ, P_{GAL1}, *URA3*	This study
pYES2-NCYC-361-b	See note 'a'	2μ, P_{GAL1}, *URA3*	This study
pYES2-NCYC-361-d	See note 'a'	2μ, P_{GAL1}, *URA3*	This study
pYES2-NCYC-90-4	See note 'a'	2μ, P_{GAL1}, *URA3*	This study
pYES2-NCYC-90-D	See note 'a'	2μ, P_{GAL1}, *URA3*	This study
pYES2-SCI-1-c	See note 'a'	2μ, P_{GAL1}, *URA3*	This study
pYES2-SCI-1-d	See note 'a'	2μ, P_{GAL1}, *URA3*	This study
pYES2-SCI-2-a	See note 'a'	2μ, P_{GAL1}, *URA3*	This study
pYES2-SCI-2-c	See note 'a'	2μ, P_{GAL1}, *URA3*	This study
pYES2-SCI-2-d	See note 'a'	2μ, P_{GAL1}, *URA3*	This study
pYES2-SCI-3-b	See note 'a'	2μ, P_{GAL1}, *URA3*	This study
pYES2-SCI-3-c	See note 'a'	2μ, P_{GAL1}, *URA3*	This study
pYES2-SCI-3-d	See note 'a'	2μ, P_{GAL1}, *URA3*	This study
pYES2-SCI-4-b	See note 'a'	2μ, P_{GAL1}, *URA3*	This study

pYES2-SCI-4-c	See note 'a'	2μ, P_{GAL1}, *URA3*	This study
pYES2-SCI-4-d	See note 'a'	2μ, P_{GAL1}, *URA3*	This study
pYES2-SCI-5-c	See note 'a'	2μ, P_{GAL1}, *URA3*	This study
pYES2-SCI-6	See note 'a'	2μ, P_{GAL1}, *URA3*	This study
pYES2-SCI-7-a	See note 'a'	2μ, P_{GAL1}, *URA3*	This study
pYES2-SCI-7-b	See note 'a'	2μ, P_{GAL1}, *URA3*	This study
pYES2-SCI-8	See note 'a'	2μ, P_{GAL1}, *URA3*	This study
pYES2-SCI-9-a	See note 'a'	2μ, P_{GAL1}, *URA3*	This study
pYES2-SCI-9-c	See note 'a'	2μ, P_{GAL1}, *URA3*	This study
pYES2-SCI-10-b	See note 'a'	2μ, P_{GAL1}, *URA3*	This study
pYES2-SCI-10-d	See note 'a'	2μ, P_{GAL1}, *URA3*	This study
pYES2-SCI-12-1	See note 'a'	2μ, P_{GAL1}, *URA3*	This study
pYES2-SCI-12-2	See note 'a'	2μ, P_{GAL1}, *URA3*	This study
pYES2-SCI-12-2-b	See note 'a'	2μ, P_{GAL1}, *URA3*	This study
pYES2-SCI-12-a	See note 'a'	2μ, P_{GAL1}, *URA3*	This study
pYES2-SCI-12-A	See note 'a'	2μ, P_{GAL1}, *URA3*	This study
pYES2-SCI-12-B	See note 'a'	2μ, P_{GAL1}, *URA3*	This study
pYES2-SCI-12-C	See note 'a'	2μ, P_{GAL1}, *URA3*	This study
pYES2-SCI-12-D	See note 'a'	2μ, P_{GAL1}, *URA3*	This study
pYES2-SCI-12-E	See note 'a'	2μ, P_{GAL1}, *URA3*	This study
pYES2-SCI-13-b	See note 'a'	2μ, P_{GAL1}, *URA3*	This study
pYES2-SCI-13-c	See note 'a'	2μ, P_{GAL1}, *URA3*	This study
pYES2-SCI-13-d	See note 'a'	2μ, P_{GAL1}, *URA3*	This study
pYES2-SCI-14-a	See note 'a'	2μ, P_{GAL1}, *URA3*	This study
pYES2-SCI-14-b	See note 'a'	2μ, P_{GAL1}, *URA3*	This study
pYES2-SCI-14-c	See note 'a'	2μ, P_{GAL1}, *URA3*	This study
pYES2-SCI-15-a	See note 'a'	2μ, P_{GAL1}, *URA3*	This study
pYES2-SCI-15-b	See note 'a'	2μ, P_{GAL1}, *URA3*	This study

pYES2-SCI-15-c	See note 'a'	2μ, P_{GAL1}, *URA3*	This study
pYES2-SCI-16-a	See note 'a'	2μ, P_{GAL1}, *URA3*	This study
pYES2-SCI-16-b	See note 'a'	2μ, P_{GAL1}, *URA3*	This study
pYES2-SCI-16-c	See note 'a'	2μ, P_{GAL1}, *URA3*	This study
pYES2-SCI-16-d	See note 'a'	2μ, P_{GAL1}, *URA3*	This study
pYES2-SDY-2	See note 'a'	2μ, P_{GAL1}, *URA3*	This study
pYES2-SDY-a	See note 'a'	2μ, P_{GAL1}, *URA3*	This study
pYES2-SDY-b	See note 'a'	2μ, P_{GAL1}, *URA3*	This study
pYES2-SDY-D	See note 'a'	2μ, P_{GAL1}, *URA3*	This study
pYES2-TH-b	See note 'a'	2μ, P_{GAL1}, *URA3*	This study
pYES2-TH-c	See note 'a'	2μ, P_{GAL1}, *URA3*	This study
pYES2-TH-d	See note 'a'	2μ, P_{GAL1}, *URA3*	This study
pYES2-VERY-HIGH-3	See note 'a'	2μ, P_{GAL1}, *URA3*	This study
pYES2-W303-1-1B	See note 'a'	2μ, P_{GAL1}, *URA3*	This study
pYES2-W303-1-1C	See note 'a'	2μ, P_{GAL1}, *URA3*	This study
pYES2-W303-1-1D	See note 'a'	2μ, P_{GAL1}, *URA3*	This study
pYES2-Y12-a	See note 'a'	2μ, P_{GAL1}, *URA3*	This study
pYES2-Y12-c	See note 'a'	2μ, P_{GAL1}, *URA3*	This study
pYES2-Y12-d	See note 'a'	2μ, P_{GAL1}, *URA3*	This study
p6442-*SUP35NM-GFP*	*SUP35NM* region with C-terminal *GFP* tag under the control of the *CUP1* promoter	2μ, P_{CUP1}, *URA3*	T. Serio Lab
pENTR-*RNQ1*	*RNQ1* Gateway entry vector with stop codon	Kan^R	This study
pENTR-*RNQ1ns*	*RNQ1* Gateway entry vector without stop codon	Kan^R	This study
pAG426-*RNQ1-GFP*	*RNQ1* ORF, C-terminal *GFP* tag	2μ, P_{GAL1} *URA3*	This study

pAG426-*GFP-RNQ1*	*RNQ1* ORF, N-terminal *GFP* tag	2μ, P_{GALI}, *URA3*	This study
pAG425-*RNQ1-DsRED*	*RNQ1* ORF, C-terminal *DsRED* tag	2μ, P_{GALI} *LEU2*	This study
pAG425-*RNQ1*	*RNQ1* ORF	*CEN*, P_{GPD} *LEU2*	This study
pAG425-*RNQ1-N*	N-terminus of *RNQ1* aa 1 - 152	*CEN*, P_{GPD} *LEU2*	Tobias von der Haar
pTH460	Renilla and Firefly luciferase fusion	*URA3*, P_{PGK1}	Tobias von der Haar
pTH461	Renilla and Luciferase fusion interrupted by UAA stop codon	*URA3*, P_{PGK1}	Tobias von der Haar
pTH469	Renilla and Luciferase fusion interrupted by UAG stop codon	*URA3*, P_{PGK1}	Tobias von der Haar
pTH477	Renilla and Luciferase fusion interrupted by UGA stop codon	*URA3*, P_{PGK1}	Tobias von der Haar
pFRLuc(-)		P_{ADH1}	Tobias von der Haar
pRFLuc(*GCN4*)		P_{ADH1}	Tobias von der Haar

note a: All pYES2-based constructs contain the *RNQ1* gene were generated by PCR to include 46 bp of 5' UTR and 36 bp of 3' UTR of *RNQ1* and cloned into the *XhoI* and *HindIII* site of expression vector pYES2

note b: Selectable markers are abbreviated as follows:

bla : beta lactamase ampicillin resistance gene

kanMX4 kanamycin resistance gene

URA3: uracil biosynthesis gene from *Saccharomyces cerevisiae*

HIS3: histidine biosynthesis gene from *Saccharomyces cerevisiae*

LEU2: leucine biosynthesis gene from *Saccharomyces cerevisiae*

2.7 Oligonucleotide primers

Table 2.5 Oligonucleotide primers used in this study

Primer	Sequence (5' → 3')
GS-*RNQ1*-Exp-R	CCGCTCGAGCGTAAACAAAGGATAGAAGGC
GS-*RNQ1*-Exp-F-ne	CCCAAGCTTAAAAGAACGTACATATAGCGA
RNQ1-for	GAAATGGATACGGATAAG
RNQ1-rev	GTAGCGGTTCTGGTTGCC
PR1-F	TGCCTTGGCTTCTCAATTCT
PR1-R	CGGAGCTTTGATTTTGACCT
PR2-F	GGACAATCTGGTGGTGCTTT
PR2-R	GGAAGCCAAAGCTGAGAATG
PR3-F	CATTCTCAGCTTTGGCTTCC
PR3-R	GGTTCTGGTTGCCGTTATTG
pGTW-*RNQ1*-F	CACCATGGATACGGATAAG
pGTW-*RNQ1*-R	GTAGCGGTTCTGGTTGCC
pGTW-stop*RNQ1*-R	TCAGTAGCGGTTCTGGTT

All oligonucleotide primers were synthesised by Eurofins MWG Operon. The primers were stored as 100 pmol/µl stock solutions in sterile MilliQ water at -20 °C until required.

2.8 Introduction of DNA into host cells

2.8.1 Transformation of *Saccharomyces cerevisiae*

A fresh colony of yeast was picked using a sterile inoculating loop, and either streaked onto an agar plate of YPD complete media (Section 2.1.1) and incubated

overnight at 30 °C or was inoculated into 5 ml of appropriate medium and grown overnight at 30 °C with shaking. One loopfull volume was scraped from the YPD plate using a sterile inoculating loop and suspended in 1 ml of sterile water, or alternatively, 1 ml of the fresh overnight 5 ml culture was used. In both cases, cells were harvested by benchtop centrifugation at 13,000 rpm for 20 sec at room termperature. The supernatant was decanted and the pellet was resuspended after addition of the following reagents: 240 µl of polyethylene glycol (PEG)-4000 (50 % w/v), 36 µl of 1 M LiAc, 10 µl of freshly denatured single-stranded carrier DNA (salmon sperm DNA, 10 mg/ml), 5 µl of plasmid DNA (up to 1 ug), and 34 µl of sterile water. The transformation mix was vortexed at full speed for 1 min before incubating at 30 °C for 30 min with shaking, followed by incubation at 42 °C for 30 min, with shaking. Cells were harvested by benchtop centrifugation at 3, 000 rpm for 2 min at room temperature. The supernatant was decanted and the pellet resuspended in 200 µl of sterile water prior to plating 50-200 µl on the appropriate synthetic complete drop-out selection medium. Plates were incubated at 30 °C for 3-4 days, and the transformants subsequently restreaked onto fresh synthetic complete drop-out selection medium, as appropriate.

2.8.2 Transformation of *Escherichia* coli

The appropriate purchased competent bacterial strain was removed from -80 °C storage and thawed on wet ice. The cells were mixed gently by flicking the tube prior to aliquoting 50-100 µl of cells into a pre-chilled 1.5 ml Eppendorf tube. Up to 5 µl of DNA solution (≤ 1 µg) was added to the cell suspension per 50 µl of competent cells, and to mix the tube was then gently swirled to mix the contents. The transformation mix was incubated on ice for 30 min before transfer to 45 °C for a 45 sec heat-shock, without mixing, after which the reaction was immediately placed on ice for 2 min. The transformation reaction was diluted by addition of 900-950 µl of LB medium (Section 2.2) and then incubated at 37 °C for 1 hr, with shaking at 200 rpm. Between 50 – 200 µl of the mixture was plated on LB agar plates containing the appropriate antibiotic (Section 2.2), and the plates were incubated at 37 °C overnight.

2.9 DNA methods

2.9.1 Extraction and small-scale preparation of plasmid DNA from *Escherichia coli*

A single colony of *E. coli* bearing the plasmid of interest was inoculated into 5 ml LB medium supplemented with the appropriate antibiotic (Section 2.2) and grown overnight at 37 °C with shaking. Cells were harvested by centrifugation at 3, 000 rpm for 10 min at room temperature and the supernatant decanted. The resulting pellet was used to isolate the required plasmid DNA using a Qiagen QIAprep Spin Miniprep Kit according to manufacturer's instructions. To improve plasmid recovery yields, modifications to protocol were often included, consisting of reapplication of post-N3 buffer flow-through to the column before proceeding to the PE buffer wash step, and two separate PE buffer washes of 400 µl rather than one 750 µl wash with PE buffer. The DNA was eluted either with 50 µl of kit-supplied EB buffer or with sterile water.

2.9.2 Restriction enzyme digestion of plasmid DNA

DNA was digested using restriction endonucleases and buffers from either Roche or Promega. The basic reaction consisted of the following:

Buffer (10x) 2 µl, Bovine Serum Albumin (BSA) 0.2 µl, Enzyme 1 µl each, Plasmid DNA 1.5 µl, Sterile water to final volume of 22 µl.

Note that reagents listed above were added to the pre-determined volume of sterile water required for a 22 µl reaction mix. For double digests, the buffer was chosen according to manufacturer's recommendations. All digests were incubated at 37 °C for a minimum of 2 hr. The digestion reaction was stopped by 15 min incubation at 65 °C. To analyse the digestion products, 10 µl of the sample was loaded onto an agarose gel (see section 2.9.3).

2.9.3 Separation of DNA by agarose gel electrophoresis

DNA fragments were separated by electrophoresis on 1 % (w/v) agarose gel when the fragments were expected to be greater than approximately 1 kb in length. For samples containing fragments of a smaller size (i.e. <1 kb) a 1.5 % (w/v) gel was used. The analytical gels were made with 'molecular biology grade' agarose from Sigma, and were melted in 1x TAE buffer in a microwave oven for 2 min at full power.

1x TAE Buffer: Tris base 4.84 g, Glacial acetic acid 1.14 ml, 0.5 M EDTA, pH 8.0 2 ml, Milli-Q water to 1 l final volume.

The molten liquid agarose was cooled to about 50 °C before 5 µl of Sybr-Safe DNA stain per 50ml of gel was added. The gel solution was poured into a gel forming cassette. When the gel had solidified, it was placed in an electrophoresis tank and 1x TAE buffer was added in sufficient quantity to cover the gel surface by 2-3 mm. The DNA samples were prepared by adding 1/5 of a volume of 6x blue/orange loading buffer (Promega) to the samples, and pipetting the mix into the wells of the gel. For plasmid DNA preparations and PCR products, 5 µl of samples were loaded. For analysis of restriction digestion products, 10 µl samples were loaded. Electrophoresis was carried out at 100 V until the bands had migrated the desired distance. The DNA fragments were visualised by short wave length (312nm) UV transillumination.

2.9.4 Extraction and purification of DNA from agarose gels

The DNA fragments to be purified were visualised with short wave transillumination and excised using a sterile scalpel. The gel pieces were placed in a pre-weighed microfuge tube and the new weight used to calculate the volume of reagents required from Qiagen's 'QIAquick Gel Purification' kit. The kit was used as per manufacturer's instruction. The DNA was eluted with 30 µl of supplied EB buffer or with sterile water.

2.9.5 Ligation of DNA fragments

DNA ligations were carried out using Roche's 'Rapid DNA Ligation Kit' as per manufacturer's instructions. To determine the volume of digested insert and vector to use in the ligation reaction, an agarose gel of the insert and vector was used to assess the relative concentrations of each. Alternatively, a Thermo Scientific Nanodrop-1000 (Section 2.9.7) was employed that returned ng/µl measurements of the respective samples. 10 µl of the ligation reaction was used to transform 100 µl of competent *E. coli* cells (Section 2.6.2).

2.9.6 'Gateway® Systems Directional Cloning' reactions

Invitrogen's 'Gateway Systems pENTR™/D-TOPO® Directional Cloning' kit was used to create an initial *RNQ1* gene-based entry clone that was subsequently used to generate a range of *RNQ1* gene-based expression vectors. The cloning and LR reactions were performed according to manufacturer's (Invitrogen) instruction. DNA concentrations of the inserts, entry clones and destination vectors were determined using the Nanodrop-1000 (Section 2.7.7). For the cloning reaction to generate C-terminal *RNQ1* fusion constructs (entry clone lacking the *RNQ1* stop codon), 1.1 µl (7.6 ng/µl) of PCR product was used. For the cloning reaction to generate non-tagged and N-terminal *RNQ1* fusion constructs (entry clone with *RNQ1* stop-codon included), 1.8 µl (7.9 ng/µl) of PCR product was used. For the LR reaction to generate C-terminal *RNQ1* fusion constructs, 1 ul (142.4 ng/µl) of entry clone was mixed with 1 µl of diluted (150 ng/µl) destination vector(s). For the LR reaction to generate non-tagged and N-terminal *RNQ1* fusion constructs, 1 µl of entry clone was mixed with 1 µl of diluted (150 ng/µl) destination vector(s). All stages were verified by restriction digest (section 2.9.2) and PCR analysis (section 2.9.11)

2.9.7 Quantification of DNA fragments

The concentration of DNA in samples was measured using either an Eppendorf Biophotometer or a Thermo Scientific Nanodrop-1000. To determine the DNA concentration from the OD_{260} reading provided by the Biophotometer, the following

equation was used: DNA concentration (μg/ml) = OD_{260} x dilution factor. No dilution of sample was required for use of the Nanodrop-1000 and readings were obtained from an analysis of a 1 ul aliquot of sample.

2.9.8 Screening *Escherichia coli* transformants

Single colonies from the transformation plates were cultured and harvested as described in section 2.9.1. Plasmid DNA was isolated as described in section 2.9.1. and restriction digestion analysis (section 2.9.2) of the plasmid DNA was performed to confirm successful ligation of an insert. Alternatively, single colonies from the transformation plates were replated to designated positions on fresh LB agar medium containing the appropriate antibiotic (Section 2.2), incubated overnight at 37 °C and using a sterile inoculating loop. Cells from each colony were suspended in individual tubes of 50 μl sterile water. After vortexing the suspension for 10 sec, 5 μl was used as template DNA in a PCR reaction (section 2.9.11).

2.9.9 Screening *Saccharomyces cerevisiae* transformants

Single colonies from the transformation plate were replated to designated positions on fresh selective agar medium, incubated overnight at 30 °C and, using a sterile inoculating loop, cells from each colony were suspended in individual tubes of 50 μl sterile water. After vortexing the suspension for 10 sec, 5 μl was used as template DNA in a PCR reaction (Section 2.9.11).

2.9.10 Extraction and purification of genomic DNA from *Saccharomyces cerevisiae*

A single yeast colony was used to inoculate 1.5 ml of liquid YPD complete medium (Section 2.1.1) and grown overnight at 30 °C with shaking. Tubes were vortexed and the culture transferred to a clean 2 ml Eppendorf tube before centrifugation at 2, 000 rpm for 5 mins at room temperature. The supernatant was decanted and the pellet resuspended in 100 μl of TE/SDS, with shaking at room temperature for 15 min.

TE/(SDS Buffer): 10 mM Tris-HCl, 1 mM EDTA, (1 % SDS), pH 8.0.

A further 500 µl of TE buffer was added to the sample before commencing protein extraction by drop-wise addition of 1 volume (~600 µl) of phenol. The sample was centrifuged at 8, 000 rpm for 5 min at 4 °C. The upper colourless phase of the supernatant was carefully pipetted to a fresh eppendorf where 0.7 volumes (~420 µl) of pre-chilled isopropanol was added to precipitate the DNA. Tubes were subsequently kept chilled on ice for at least 30 min. To pellet the DNA, the sample was centrifuged at 13, 000 rpm for 30 min at 4 °C. The supernatant was decanted and the pellet allowed to air-dry at room temperature before being resuspended in 20 µl of sterile water.

2.9.11 PCR amplification of specific DNA

PCR was performed using the Roche 'High Fidelity PCR System' and a Techne TC-3000 thermal cycler. Either 1.5 µl of mini-prep plasmid DNA (Section 2.9.1), 5 µl of crude *E. coli* preparation (Section 2.9.8), 1 µl of yeast genomic DNA (Section 2.9.10), or 5 µl of crude *S cerevisiae* preparation (Section 2.9.9) was used as the source of the template for the PCR. The following reagents were mixed together on ice in a thin-walled 0.2 ml thin-walled Eppendorf PCR tube:

Reagent	Volume added	Final concentration
High Fidelity Buffer (10x) with 15 ml $MgCl_2$	5 µl	1x (1.5 ml $MgCl_2$)
dNTP mix, 10 mM each dNTP	1 µl	200 µM each dNTP
Forward primer, 100 pmol/µl	1 – 5 µl	300 nM
Reverse primer, 100 pmol/µl	1 – 5 µl	300 nM
Template DNA	1 – 5 µl	0.1 – 250 ng
High Fidelity Enzyme Mix	1 µl	3.4 U/reaction
Sterile Milli-Q water	Up to 50 µl	-

The contents of the tube were mixed thoroughly and briefly centrifuged to bring the contents to the bottom of the tube. The tube was placed into the PCR machine and the machine set up to carry a cycling programme specifically tailored to the size of the DNA being amplified and to the primers being used.

A 5 µl aliquot of the PCR product was run on an agarose gel (Section 2.9.3) and the remainder stored at -20 °C until needed. The products of preparative PCR reactions were purified with the Qiagen 'PCR Purification' kit, according to manufacturer's instructions, prior to any further manipulations. In cases where highly concentrated DNA was required, two PCR reactions were pooled before purification.

2.9.12 DNA sequencing

All DNA sequencing was performed by DBS Genomics (Durham University, UK). Purified plasmid DNA samples were sent for sequencing. Appropriate primers were sent with each sample (Table 2.7.1). The results from each primer and sample were received by e-mail and the sequence data was assembled using Bioedit software (Hall, T.A., 1999).

2.10 Protein methods

2.10.1 Separation of proteins by SDS-polyacrylamide gel electrophoresis (SDS-PAGE)

SDS-polyacrylamide gel electrophoresis (SDS-PAGE) when performed with precast gels used the NovexTris-Glycine electrophoresis system (Invitrogen) 10 % or 4-20 % gradient gels were typically used with SDS running buffer or the NuPAGE 10 % Bis-Tris gels with the NuPAGE MOPS SDS running buffer, according to manufacturer's instructions. In both instances an Invitrogen X-Cell Surelock gel tank was used The Tris-glycine gels were run at 150 V for 90 min; the NuPAGE gels were run at 200V for 50 min.

SDS-PAGE gels prepared by hand required preparation of a stacking gel and a resolving gel. The 10 % resolving gel was pipetted into 1 mm cassettes (Invitrogen) and 100 % ethanol was pipetted immediately above the resolving gel for the duration of its solidification. The ethanol was subsequently poured away and the remaining cassette volume was rinsed with water and blotted dry prior to pipetting in the stacking gel solution. The appropriate sized sample comb was inserted and only removed once the stacking gel was fully solidified. The SDS-PAGE gels were run at 150 V for 90 mins with SDS running buffer in both chambers of an Invitrogen X-Cell Surelock gel tank.

Resolving gel: 375 mM Tris pH 8.8, 0.1% SDS, 10% acrylamide, 0.15% ammonium persulphate, 0.05% TEMED.

Stacking gel: 250 mM Tris pH 6.8, 0.1% SDS, 0.23% ammonium persulphate, 0.07% TEMED.

SDS Running Buffer : 3 % w/v Tris-HCl, 14.4 % w/v glycine, 1 % w/v SDS.

2.10.2 Preparation of cell-free lysates for western blot analysis

A single colony of the strain to be studied was used to inoculate 10 ml of appropriate liquid medium. The culture was grown overnight at 30 °C with constant shaking. This starter culture was used to inoculate a further 10 ml of appropriate medium to an OD_{600} of 0.1. Depending on the strain being studied, a wash step was incorporated prior to sub-culturing. The wash step involved harvesting the cells by centrifugation at 3, 000 rpm for 5 min at room temperature, decanting the supernatant and resuspending the pellet in sterile water. This process was then repeated one more time. The sub-culture was incubated at 30 °C until an OD_{600} of 0.4-0.6 was reached. For certain strains, a 20 % galactose solution (to a 2 % final concentration) was added when cultures had reached an OD_{600} ~ 0.3, and the culture was then further incubated for a minimum of 3 hrs. The OD_{600} of each culture was measured and a volume equivalent to 4.0 OD_{600} units was removed and placed into a separate tube. The cells were harvested for 5 min at 3, 000 rpm and the cell pellet resuspended in 100 µl of lysis buffer.

Lysis Buffer: 100 mM NaCl, 2 mM PMSF, 1 complete protease inhibitor tablet in 1X PBS.

PBS: 137 mM NaCl, 2.7 mM KCl, 10 mM Na_2HPO_4, 1.76 mM KH_2PO_4, pH 7.4

100 µl of cell suspension was transferred to a Simport 2 ml round bottom micrewtube® screw-cap tube to which an equal volume of glass beads (diameter 425-600 µm) was also added. Cells were lysed in a Bertin Technologies Precellys® 24 lysis/homogenisation mill, on a programme that vortexed the sample tubes for 3 x 30 sec with 30 sec intervals between each pulse. Tubes were immediately placed on ice. For lysates intended for western blot, a further 100 µl of 100 mM PMSF was added to the lysis buffer and 50 µl of the lysis buffer was then added to each tube. The tubes were centrifuged for 1 min at 5, 000 rpm at 4 ^{0}C in a pre-cooled centrifuge and 50 µl of the supernatant was carefully pipetted to a clean pre-chilled tube. Protein concentration was determined using an Eppendorf Biophotometer, and 50 µl of a 1 µg/µl preparation was made by diluting an adequate volume of sample in the sample buffe. 15 µl of the preparation was loaded onto an SDS-PAGE gel (Section 2.10.1).

Sample Buffer: 60 mM Tris-HCl, 10 % glycerol, 2% SDS, 4% 2-mercaptoethanol, 0.2% Bromophenol blue, pH 6.8

2.10.3 Preparation of cell-free lysates for quantitative western blot analysis

Cultures were prepared as described in section 2.12.5 and grown in the 2 % galactose 1 % raffinose minimal media lacking uracil (section 2.1.5) until OD_{600} = ~0.7. An appropriate volume of culture was used to harvest OD_{600} = ~ 12.5 units via centrifugation at 3, 000 rpm for 5 mins at room temperature. The pellet was resuspended in 1 ml dH_20 and transferred to a 1.5 ml Eppendorf tube. The cell suspension was centrifuged at 3, 000 rpm for 5 mins at room temperature and resuspended in 200 µl lysis buffer: a 5 µl aliquot was immediately taken and added to 1 ml of dH_20 for cell counting via haemocytometer (section 2.12.2). The cells resuspended in lysis buffer were incubated for 10 mins at 90 °C. Subsequently, a 5 µl aliquot of 4 M acetic acid was added to neutralise the NaOH of the lysis buffer, vortexing for 30 sec to mix. A second incubation at 90 °C for 10 mins followed. To

the sample with the lowest cell number, 50 µl of sample buffer was added. A suitable volume of sample buffer was added to all other samples to ensure an equal number of cells per µl were present in each sample.

Lysis Buffer (final concentration): 100 mM NaOH, 50 mM EDTA, 2 % SDS, 2 % mercaptoethanol.

Sample Buffer: 250 mM Tris-HCl, 50 % glycerol, 0.05 % bromophenol blue, pH 6.8.

2.10.4 Preparation of cell-free lysates for sedimentation analysis

A single colony of the strain to be studied was used to inoculate 10 ml of appropriate liquid medium. The culture was grown overnight at 30 °C with constant shaking. This starter culture was used to inoculate a further 10 ml of appropriate medium to an OD_{600} of 0.1. Depending on the strain being studied, a wash step was occasionally incorporated prior to sub-culturing. The wash step involved harvesting the culture by centrifugation at 3, 000 rpm for 5 min at room temperature, decanting the supernatant and resuspending the pellet in sterile water. This process was then repeated one more time. The sub-culture was incubated at 30 °C until an OD_{600} of 0.4-0.6 was reached. For certain strains, galactose was added to final concentration of 2% v/v when cultures had reached an OD_{600} ~ 0.3, and the cultured was then further incubated for a minimum of 3 hrs. The OD_{600} of each culture was measured and a volume equivalent to 4.0 OD_{600} units was removed and placed into a separate tube. The cells were harvested for 5 min at 3, 000 rpm at room temperature and the pellet resuspended in 100 µl of lysis buffer.

Sedimentation buffer: 50 mM Tris-HCl, 10 mM KCl, 100 mM EDTA, 1 mM DTT, 1 % Triton X-100, 0.2 % SDS,1 complete protease inhibitor tablet, pH 6.8.

The 100 µl cell suspension was transferred to a Simport 2 ml round bottom microtube® screw-cap tube tube to which an equal volume of glass beads (diameter 425-600 µm) was also added. Cells were lysed in a Bertin Technologies Precellys® 24 lysis/homogenisation mill,, on a programme that vortexed the sample tubes for 3 x 30 sec with 30 sec intervals between each pulse. Tubes were immediately placed

on ice, and a further 50 µl of the lysis buffer was added to each tube which was then briefly vortexed and centrifuged for 3 min at 3, 000 rpm in a pre-cooled centrifuge. A 100 µl volume of supernatant was carefully pipetted to a clean pre-chilled tube. A 50 µl aliquot of this was transferred to a Beckman thick-walled polycarbonate tube which was placed into a pre-chilled TlA.100 rotor and centrifuged at 80, 000 rpm for 60 mins at 4 °C in a Beckman Optimax ultracentrifuge machine. The remaining 50 µl represented the total (T) lysate fraction. The 50 µl of supernatant collected from the polycarbonate tube following ultracentrifugation represented the soluble (S) lysate fraction and this was transferred to a pre-chilled tube. A 50 µl aliquot of lysis buffer was used to resuspend the pellet in the polycarbonate tube and this suspension represented the pellet (P) lysate fraction, which was also transferred to a pre-chilled tube. To each fraction, 20 µl of sample buffer was added and the samples incubated for 10 min at 100 °C before loading 5 µl of each onto an SDS-PAGE gel (Section 2.8.4).

Sample Buffer:

120 mM Tris-HCl, 4 % SDS, 20 % glycerol, 20 % 2-mercaptoethanol, 0.2 % Bromophenol blue, pH 6.8,

2.10.5 Preparation of cell-free lysates for proteomics analysis

Three single colonies from each 74D-694 *rnq1Δ* + pYES2, [*pin*$^-$] + pYES2 and [*pin*$^-$] + pYES2-*RNQ1* primary transformation plates were used to inoculate 5 ml dextrose minimal media lacking uracil (Section 2.1.2) for overnight growth at 30 °C with shaking giving 9 cultures in total. A 50 ul aliquot of the overnight culture was used to inoculate 10 ml 2 % raffinose minimal medium lacking uracil (Section 2.1.3) for overnight growth. Cell density of the raffinose-based culture was determined by haemocytometer (section 2.12.2) and an appropriate volume of overnight culture was used to inoculate 500 ml of 2 % galactose 1 % raffinose minimal medium lacking uracil (Section 2.1.7) with 1.15 x 10^8 cells/ml. Cultures were harvested at a cell density of ~ 2.1 x 10^7 cells/ml in a Beckman Coulter Avanti HC centrifuge with the JlA-10,500 rotor for 15 min at 3, 500 rpm at 20 ^{oC}. Supernatant was removed and the cell pellets were resuspended in residual supernatant fluid and transferred to a 50 ml

Falcon tube. An additional 25 ml dH_20 was added to wash the cell suspensions before centrifuging at 3, 000 rpm for 10 min at room temperature. Supernatant was removed, and the pellets were resuspended in ~ 1 ml of fresh lysis buffer. The cell suspensions were pipetted drop-wise into liquid nitrogen for rapid freezing.

The frozen cell balls were mechanically lysed using a SPEX SamplePrep® model 6770 Freezer/Mill with the settings i) precool-10 mins ii) grind-4 mins iii) cool-3 mins; steps i-iii were repeated through 4x cycles. Powder extracted from the freezermill vial was thawed and sonicated 5 x 30 sec with 1 min incubation on ice between each sonication cycle. Insoluble debris was pelleted by centrifugation at 13, 000 x g at 4 °C for 5 min, and the supernatant was collected for analysis.

Lysis Buffer: 0.1 M ammonium bicarbonate, 0.1 % Triton X-100, 6 M Guanidine Hydrochloride.

2.10.6 Preparation of cell-free lysates for ribosome association analysis

A single colony of a BY4741 [*PIN*$^+$] and a BY4741 [*pin*$^-$] strain were inoculated into 100 ml YPD complete medium (Section 2.1.1) until an OD_{600} of ~ 0.8 – 1.0 was obtained. Cycloheximide (Sigma) was added to a final concentration of 200 µg/ml 10 mins prior to harvesting. Cells were harvested for 10 mins at 3, 000 x g, 4 °C, and the pellets resuspended in 0.5 ml of chilled buffer to wash. Cells were reharvested by a 3 min centrifugation at 3, 000 x g at 4 °C and resuspended in chilled buffer. Cells were lysed with acid-washed glass beads for 6 cycles of 40 second vortexing, with 1 min on ice between each 40 sec breakage. Samples were checked under the light microscope to ensure at least 60-75 % lysis efficiency. Samples were microcentrifuged at 4 °C for 5 min at 3, 000 x g for glass bead removal and clarification of lysate. The supernatants were retained and centrifuged at 12, 000 x g for 15 mins at 4 °C to remove mitochondria and small fragments. The supernatants were retained and a 40-50 µl aliquot of each was kept to represent the total lysate fraction, and 300 ul of the supernatants were centrifuged for 3 hrs 28 mins at 4 °C , 35, 000 rpm in a Beckman thickwalled polycarbonate tube in a Beckman Coulter Optimax ultracentrifuge using the TIS-55 rotor. The post-ribosomal supernatants were retained as the soluble fraction. The tube and pellets was washed with 1 ml

chilled lysis buffer. The pellets were resuspended in 50 µl chilled lysis buffer (becomes cloudy). SDS-PAGE loading buffer was added to all fractions prior to 5 mins boiling at 100 °C, and then loaded onto an SDS-PAGE gel (section 2.10.1) followed by western blot analysis (section 2.10.2) to determine the distribution of Rnq1p across the fractions collected. To identify stronger protein:ribosome association, 0.5 M KCl was used in the ribosome buffer in place of 0.05 M KCl.

Ribosome Buffer (final concentrations): 25 mM Tris pH 7.2, i) 50 mM KCl or ii) 500 mM KCl, 5 mM $MgCl_2$, 5 mM 2-mercaptoethanol, 200 µg/ml cycloheximide, 1 x Complete protease inhibitor tablet (Roche), 1 µg/ml Pepstatin, MilliQ water.

2.10.7 Staining of SDS-PAGE gels

After electrophoresis, proteins within a gel were visualised following a 1hr incubation with Coomassie stain, followed by a 1 hr incubation with destain, and then an overnight destaining step in fresh destain solution at room temperature.

Coomassie Stain: 40 % (v/v) Methanol, 20 % (v/v) Glacial acetic acid, 0.1 % (w/v) Coomassie brilliant blue R250.

Destain: 10 % (v/v) Methanol, 10 % (v/v) Acetic acid.

2.10.8 Western blot analysis of SDS-PAGE gels

Proteins were separated on the basis of molecular mass by SDS-PAGE (Section 2.10.1). The wells and protruding foot of the gels were removed using a gel knife. The gels were either briefly rinsed in MilliQ water or were soaked in transfer buffer for 15 min. Six pieces of Whatmann 3mm paper were cut to approximately the same size as the gel and soaked in MilliQ water for 10 mins, and briefly in transfer buffer immediately prior to blotting. One piece of nitrocellulose membrane was briefly wetted in MilliQ water before a 5 min soak in transfer buffer immediately before blotting.

Western Blotting Buffer: 0.29 % (w/v) Glycine, 0.58 % (w/v) Tris-HCl, 0.037 % (w/v) SDS, 20 % Methanol.

2.11 Dual-Glo luciferase assay to measure translation termination efficiency

Translation termination efficiency was measured using the commercially available Promega 'Dual-Glo Assay' kit, with reagents being prepared according to manufacturer's instructions.

A strain of interest was transformed separately with 4 plasmids each encoding a Renilla-firefly luciferase fusion (pTH460) that in 3 of the plasmids had a UAA (pTH461), a UAG (pTH469), or a UGA (pTH477) stop codon separating the Renilla and firefly luciferase open-reading frames. A total of 4 transformant colonies were picked to represent each plasmid and each was inoculated into 150 µl of dextrose minimal media lacking uracil (Section 2.1.2), in a sterile 96-well microtitre plate, to give a total of 16 separate cultures. This was incubated at 30 °C overnight in a microplate thermoshaker (Grant Bio) set at 1000 rpm. After overnight growth, a 5 µl aliquot was used to inoculate 145 µl fresh dextrose minimal media lacking uracil, in a fresh 96-well sterile plate, and was incubated for ~ 4 hrs with shaking at 30 ^{0}C. A 25 µl aliquot was transferred to a Corning 96-well cross-talk free plate and 25 µl luciferase reagent was added to each sample well, followed by vigorous mixing for 5 sec, and an incubation period of 25 mins at 30 ^{0}C. A BMG labtech FlUOstar OPTIMA plate reader was used to read firefly luciferase luminescence. A 25 µl aliquot of the 'Stop and Glo' reagent was added to each sample well, mixed vigorously for 5 sec, and incubated for 25 min. The Renilla luciferase luminescence was then measured.

Read-through values were calculated by dividing firefly and Renilla values from each well, to provide *F/R* ratios. Percent read-through was calculated by dividing the *F/R* ratio of a construct containing the relevant stop codon, by the *F/R* ratio of the control construct without any stop codon (pTH460 strain). Values presented are the average of at least 2 experiments, each assaying four biologically independent replicates.

2.12 Growth analysis of *Saccharomyces cerevisiae* strains

2.12.1 Automated growth rate analysis

A single colony of yeast was inoculated into 5 ml of the relevant medium for overnight growth. Cell density was determined by absorbance at OD_{600}, and a volume of the overnight culture was used to inoculate 1 ml of fresh, appropriate media in a sterile 24-well plate to an OD_{600} ~ 0.1 units. A BMG labtech FLUOstar OPTIMA plate reader was used to measure growth rate of the culture with the following settings: double orbital shaking mode; 3 mM diameter shaking width; 1837 sec cycle time, 0.5 sec positioning delay.

The strain doubling time was determined with the following calculation: time in minutes was plotted against OD_{600} values using MS Excel, an exponential trend-line was applied to the graph along with the trend-line equation, the natural logarithm of 2 was divided by the equation x value to give the doubling time in minutes.

2.12.2 Growth rate determination using a haemocytometer

Aliquots are removed at specified time-points and used directly in the Neubauer haemocytometer or appropriately diluted beforehand. A 15 µl sample is pipetted under the coverslip of the haemocytometer and cells within a 25 square region (equivalent to $1mm^2$) are counted and multiplied by 10^4 to determine the cell number of the sample. Any dilution of the sample prior to counting was be factored into the final cell number. For greater accuracy, cells within multiple chambers were counted and the average cell count used to determine final cell number of the sample, as above. Doubling time was determined as described in section 2.12.1, plotting cell number instead of OD_{600} against time.

2.12.3 Measuring survival of yeast cell in prolonged stationary phase

BY4741 [*PIN*$^+$], [*pin*$^-$] and *rnq1Δ* strains were inoculated into 5 ml YPD complete media (Section 2.1.1) and cultured for 48 hrs. Cells from a 500 µl aliquot of each

culture were harvested by a 30 sec centrifugation at 13, 000 rpm at room temperature. The pellet was washed in 1 ml of sterile dH_20, harvested and resuspended in 1 ml sterile dH_20. A 200 µl aliquot of the washed cells was used to determine cell density with a haemocytometer and the volume of the aliquots adjusted to ensure equal cell density of each sample. The cell number adjusted samples were suspended in 50 ml sterile dH_20 in a 250 ml conical flask, to 0.06 OD_{600} units. Over a 25 day period, 10 µl aliquots were regularly removed from each culture at the same time, and each added to a 100 µl pool of sterile dH_20 on a YPD complete media agar (Section 2.1.1) plate which was spread into the agar until absorbed. Plates were incubated for 3 days at 30 °C before colony number was counted.

2.12.4 Growth analysis on different carbon sources

BY4741 [*PIN*$^+$] and [*pin*$^-$] strains were grown up overnight in 5 ml YPD complete media (Section 2.1.1). Cells from a 500 µl aliquot were pelleted by centrifugation at 13, 000 rpm for 30 sec at room temperature, washed in 500 µl sterile dH_20, pelleted and resuspended as before. An aliquot of the washed cells were used to establish a 5x fold dilution series in water, before a 96 well replica-plater was used for spotting onto complete agar medium containing various carbon sources (Section 2.1.6). Plates were incubated at 30 °C for 2-3 days.

2.12.5 Proteotoxicity assay

The pYES2 vector, pYES2-*RNQ1*, pYES2-*25Q* and pYES2-*103Q* constructs were used throughout the project to identify phenotypes associated with over-expression of Rnq1p or the polyglutamine expanded exon-1 of the Huntingtin protein.

For the plate assay a single yeast colony of the strain of interest transformed with the appropriate pYES2-based construct was used to inoculate 10 ml of 2 % dextrose medium lacking uracil (Section 2.1.2) , and incubated overnight at 30 °C with shaking. A 200 µl aliquot of the starter culture was transferred to a Corning 96-well plate and used to establish a 5-fold dilution series in liquid 2 % raffinose minimal

medium lacking uracil which was spotted using a 96 well replica-plater onto 2 % raffinose minimal medium agar lacking uracil (Section 2.1.3). Plates were incubated at 30 °C for 2 days. Cells taking from a colony on the 2 % raffinose plate were suspended in 200 µl 2 % galactose 1 % raffinose minimal media lacking uracil (Section 2.1.5), and used to establish a 5x fold dilution series in this media which was then spotted onto 2 % galactose 1 % raffinose medium agar lacking uracil (Section 2.1.5). The plates were incubated at 30 °C for 2-4 days.

For the liquid cultures a single yeast colony of the strain of interest transformed with the appropriate pYES2-based construct was used to inoculate 5 ml of 2 % dextrose medium lacking uracil (Section 2.1.2) and incubated overnight at 30 °C with shaking. A 50 µl aliquot of the overnight culture was used to inoculate 5 ml of liquid 2% raffinose minimal medium lacking uracil (Section 2.1.3) which was incubated overnight at 30 °C with shaking. The cell density of the overnight culture was determined by absorbance at OD_{600} and an appropriate volume used to inoculate 50 ml of 2 % galactose, 1 % raffinose medium lacking uracil (Section 2.1.4) to an OD_{600} of 0.15 units. Aliquots of culture were removed at the indicated time points and cell number and growth rate determined as described in section 2.12.2

2.12.6 pYES2-based viability assay

Cultures were prepared and incubated as described in section 2.12.5. Following pYES2 induction aliquots were taken for cell number assessment (section 2.12.2) at the indicated time points and were diluted appropriately so that an expected number of colony forming units between 200-300 would be plated onto 2 % glucose/dextrose minimal media agar lacking uracil (Section 2.1.2). Plates were incubated for 2-3 days at 30 °C prior to colony counting. Percent viability was calculated as follows: the number of observed colonies at each time point was divided by the number of expected colonies for the time point to give an *O/E* ratio which was then multiplied by 100.

2.12.7 Thermotolerance assay of the [*PIN*$^+$] variants

A single colony of each [*PIN*$^+$] variant was inoculated into 5 ml YPD complete medium (Section 2.1.1) and cultures were incubated overnight at 30 °C with shaking. Cell density was determined by absorbance at OD_{600}, and an appropriate volume of the overnight cultures were used to inoculate 5 ml fresh YPD complete medium to an OD_{600} of 0.15 units. Cultures were incubated for ~ 4 hrs before 4 x 1 ml aliquots from each [*PIN*$^+$] variant culture were transferred to sterile 2 ml Eppendorf tubes. The tubes were incubated 42 °C in a water bath for the indicated times. Following each heat-shock period, cells were immediately harvested at 3, 000 rpm for 5 mins at room temperature, resuspended in 500 µl of fresh YPD complete medium and used to establish a 5x fold dilution series which was spotted using a 96 well replica-plater on to YPD complete medium agar (Section 2.1.1) and incubated 2-3 days at 30 °C.

2.13 Mitochondrial dysfunction assays

2.13.1 TTC-overlay assay of respiratory deficiency

The chemical 2,3,5-triphenyl tetrazoliumn chloride (TTC) is reduced by the activity of the mitochondrial respiratory chain from a colourless to an insoluble red pigment (Ogul *et al*, 1957) and can therefore be used as an indicator of respiratory proficiency. Single colonies of BY4741 transformed with the pYES2 backbone or the pYES2-*RNQ1* plasmid were grown up overnight in 5 ml dextrose minimal media lacking uracil (Section 2.1.2), with shaking at 30 °C. The overnight cultures were diluted 1:50,000 in sterile dH_20 and 200 µl plated onto 2 % raffinose minimal media agar lacking uracil (Section 2.1.3). Plates were incubated for 2-3 days at 30 °C until colonies were well formed. Sterile filter paper was used to replica plate the colonies to fresh 2 % galactose 1 % raffinose minimal media agar lacking uracil (Section 2.1.5), which were then incubated for 2 days at 30 °C. The TTC at 0.5 % w/v was dissolved in pre-warmed 100 mM Tris-HCl pH 7.0 containing 1% granulated agar (Difco), and 10 ml of the solution per plate was overlaid on the yeast colonies. Following a 1-2 hr incubation at 30 °C, colony colour was noted and plates were scanned for record.

2.13.2 Ethidium bromide exposure assay

The pYES2 and pYES2-*RNQ1* or pYES2-*25Q* and pYES2-*103Q* group of BY4741 [*PIN*$^+$] transformants were grown up overnight in 5 ml of a minimal –uracil drop-out medium (Section 2.1.2) both with and without 5 µl of ethidium bromide from a 10 mg/ml stock solution. The cultures were used to establish a 5x fold dilution series in sterile water which was spotted using a 96 well replica-plater onto 2 % raffinose uracil drop-out agar (Section 2.1.3). Plates were incubated for 2 days at 30 °C. Cells from these colonies were used to establish a 5x fold dilution series in sterile water which was spotted onto 2 % galactose 1 % raffinose uracil drop-out agar (Section 2.1.5). Plates were incubated for 2 days at 30 °C. Cells from colonies representing each strain were suspended in 300 µl sterile water and cell density was determined using a haemocytometer. An equivalent cell number from each strain was then used to establish a 5x fold dilution series that was spotted onto 2 % glycerol complete agar medium (Section 2.1.6), which were then incubated for 2-3 days at 30 °C.

2.14 Trehalose heat-shock assay

The *tps1Δ* and *nth1Δ* deletion strains obtained from the Yeast Knock-out Collection were transformed with the pYES2 backbone and pYES2-*RNQ1* plasmid (section 2.6.). A transformant of each strain was inoculated into 5 ml dextrose minimal medium lacking uracil (Section 2.1.2) and grown overnight at 30 °C with shaking. A 200 µl aliquot of each overnight culture was used to establish a 5x fold dilution series in 2 % raffinose minimal media lacking uracil (Section 2.1.3), which was subsequently spotted using a 96 well replica-plater onto 2 % raffinose minimal media agar lacking uracil (Section 2.1.3). Plates were incubated for 2 days at 30 °C. A colony representing each strain was suspended in 250 µl sterile dH_20 and vortexed to mix. Cells were centrifuged for 20 sec at 13, 000 x rpm and resuspended in 210 µl of 2 % raffinose minimal medium lacking uracil. Cells were incubated in a 35 °C in a waterbath for 1 hr. The cell suspensions were then equally divided between two pre-warmed tubes; one set was incubated at 40 °C for 1 hr in a waterbath and the other set incubated at 30 °C for 1 hr in a waterbath. The treated cells were used to establish

a 5x fold dilution series in sterile dH_20, spotted onto 2 % galactose 1 % raffinose minimal media agar lacking uracil (Section 2.1.5) and incubated 2-3 days at 30 °C.

2.15 Microscopy

2.15.1 Sample preparation

Strains were grown overnight in appropriate selective media, sub-cultured the next day into fresh appropriate selective media and induced where necessary. Analysis was performed on log-phase cells. A suitable aliquot of log-phase culture was pelleted by a 30 second centrifugation at 13, 000 rpm, washed once with 1 ml 1X PBS, reharvested as before, and resuspended in an appropriate volume of 1X PBS (20-200 µl). For analysis, a 3.5 µl aliquot was spotted onto a microscope slide.

2.15.2 DAPI staining of yeast cells

A suitable aliquot (0.2 – 1 ml) of log-phase cells were pelleted by a 30 second centrifugation at 13, 000 rpm. Cells were resuspended in 0.5 ml 1X PBS buffer, and 1.5 ul of DAPI was added to 6X concentration. Cells were incubated with the dye for ~ 30 mins, with occasional gentle agitation. Cells were harvested as before, and the pellet resuspended in an appropriate volume of PBS (20 – 200 µl) (section 2.10.2). A 3.5 µl aliquot was spotted onto a microscope slide for analysis.

2.15.3 Analysis and induction of processing-bodies

To induce P-body formation in the BY4741 *DCP2-GFP.* strain (table 2.2) cells were grown to mid-log phase, cells were harvested in a microcentrfuge at 5, 000 rpm for 1 min, washed in fresh culture medium and either analysed directly, or exposed to 1 M KCl (osmotic stress) for 10 mins, or incubated in fresh culture medium lacking a carbon source (starvation stress) for 10 mins. All samples were spotted onto slides immediately prior to visualisation.

2.15.4 ImageJ processing of microscope images

The images to be merged were opened in ImageJ. The images were first converted to 32-bit type by selecting Image-> Type-> 32-bit. In the 'Plugins' tab, 'RGB Stack Merge2' was selected, and the appropriate colour assigned to the correct image before selecting the 'merge' option. Merged images were saved in the JPEG or PNG format.

2.15.5 Visualisation

All samples were visualised using an Olympus MT20 fluorescence microscope connected to a PC running CellR software.

2.16 Bioinformatics

2.16.1 *RNQ1* DNA sequence analysis

Using the free bioinformatics package 'BioEdit Sequence Alignment Editor', the nucleotide sequence of the *RNQ1* gene as published on the SGD website (http://www.yeastgenome.org/) was copied and pasted into a 'New Sequence' window. The nucleotide of the forward sequence read was also copied and pasted into a 'New Sequence' window of the same alignment file. The nucleotide read of the reverse sequence read was copied and pasted into the sequence box of the 'Gene/Sequence Resources' of the SGD website, and the reverse complement box ticked prior to submission. The returned sequence was copied and pasted into a 'New Sequence' window of the same alignment file. The accessory application 'ClustalW Multiple Alignment' was used to align the three sequences. Subsequently, the alignment option 'Create Consensus Sequence' option was selected and this was edited directly according to the aligned nucleotide reads. The sequence alignment was saved and the edited consensus sequence was exported as a FASTA file.

2.16.2 Generating interaction networks from FitDB using Cytoscape

The Yeast Fitness Database (http://fitdb.stanford.edu/), or simply FitDB, clusters each gene deletion strain of the Yeast Knock-Out Collection (http://www.openbiosystems.com/GeneExpression/Yeast/YKO/) with 10 other gene deletion strains according to the similarity of their chemical sensitivity profile. The table listing the identities of the top 10 interactors of *RNQ1* were copied to an Excel spreadsheet, as were the tables listing the top 10 interactors of *RNQ1*'s top 10 interactors. The Excel spreadsheet was saved as a tab delimited file and imported into the free bioinformatics software package 'Cytoscape' as a 'Network from MS Excel'. Prior to import, column-1 corresponding to geneA of the table was defined as the source interaction, column-2 corresponding to geneB of the table was defined at the target interaction, and column-3 corresponding to the similarity score was defined as the interaction type. To identify outliers of the network, the 'circular' layout of 'yfiles' layout option was selected. Gene ontology analysis of the interaction network was carried out omitting the identities of genes peripheral to the interaction network.

2.17 Creating *RNQ1* transgenic *Drosophila* melanogaster lines

The full-length *RNQ1* gene of Gateway entry clone pENTR-*RNQ1* was recombined by LR reaction (section 2.9.6.) with the *Drosophila* optimised Gateway destination vector pTW to create an untagged *RNQ1* expression clone with a *UASt* promoter. *E. coli* cells transformed with the products of the LR reaction that gave rise to ampicillin resistant colonies were cultured further to isolate plasmid DNA and this was subsequently digested with the restriction enzyme *Bam*HI to determine successful recombination events. Further confirmation of expression clone identity was obtained by *Sal*I restriction digest of the expression clones and PCR analysis for the presence of the *RNQ1* gene. Successful clones were sequenced (section 2.9.12), a mid-scale preparation of the plasmid DNA carried out (midi-prep, Qiagen) and the pTW-UAS-*RNQ1* construct was shipped to 'Genetic Services Inc' for larva injection.

Chapter III

Exploring cellular functions for Rnq1p

3.1 Growth analysis introduction

No function has yet been assigned for Rnq1p, except its ability in the [*PIN*$^+$] form to induce the *de novo* formation of the [*PSI*$^+$] and [*URE3*] prion. The [*PIN*$^+$] prion is also required for the aggregation of the Huntingtin 103Q construct used in the yeast model of Huntington's disease. This construct consists of exon1 of the Huntingtin gene and contains an expansion of the disease-associated polyglutamine tract to 103 glutamine residues. However, the role of Rnq1p in the above capacities is specific to the [*PIN*$^+$] form of Rnq1p, and does not necessarily inform us of a cellular function for the non-prion form of Rnq1p. Currently, the most that is known about the Rnq1p protein is that its function is not essential for viability, since a *rnq1Δ* strain is viable. In this chapter section I describe studies on effect on cell growth of deleting the *RNQ1* gene, of harbouring different [*PIN*$^+$] variants, and of existing in a [*pin*$^-$] state.

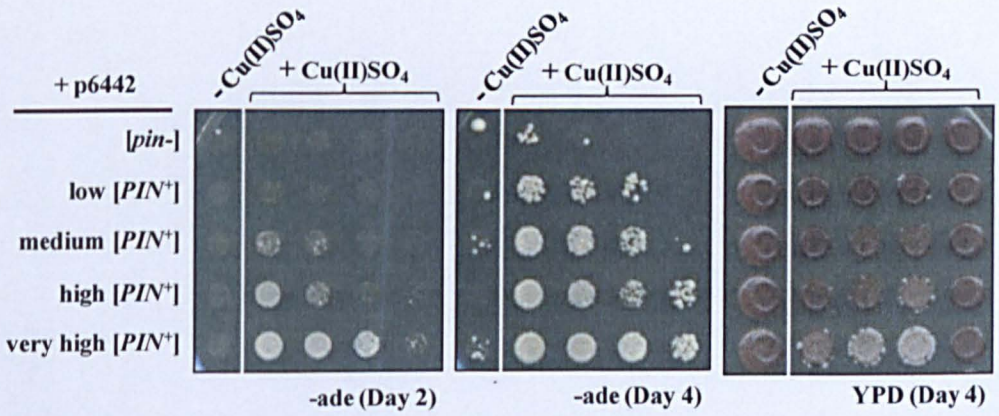

Figure 3.0: The [*PIN*$^+$] variants show reproducible differences in the frequency of [*PSI*$^+$] induction.
Over-expression of Sup35p (p6442-*SUP35NM*) in the [*PIN*$^+$] variants induces Sup35p conversion to [*PSI*$^+$] at different efficiencies. Only [*PSI*$^+$] cells can grow in the absence of adenine (-ade).

3.1.1 Deletion of the *RNQ1* gene results in a slight increase in doubling time

The growth properties of a 74D694 *rnq1Δ* strain, a [*pin*-] strain and of the low, medium, high and very high [*PIN*$^+$] variant strains were analysed in two independent experiments, each time in triplicate. The data reflect the average of 5 of these experiments after exclusion of outliers.

Deletion of the *RNQ1* gene resulted in a slight but statistically significant increase in doubling time of ~10 min relative to the [pin-] strain and all [*PIN*$^+$] variants, except the low [*PIN*$^+$] variant (figure 3.1). The doubling time of the low [*PIN*$^+$] variant was also statistically different to the [*pin*$^-$] strain and possibly also to the medium [*PIN*$^+$] and high [*PIN*$^+$] variants, but not the very high [*PIN*$^+$] variant. This result suggests that the *RNQ1* gene is required for optimal growth of the cell, possibly through an as yet undetermined function carried out by Rnq1p. However, deletion of the *RNQ1* gene can affect the divergently transcribed *BIK1* gene, a microtubule protein involved in sister-chromatid separation, which contains upstream regulatory sequences overlapping the *RNQ1* locus on chromosome III. Specifically, deletion of the *RNQ1* gene removes these regulatory sequences of *BIK1*. A *bik1Δ* strain is also decreased in fitness during fermentative growth. Therefore the slight growth disadvantage of the *rnq1Δ* strain may be attributed to either a reduction of transcription or a misregulation of the *BIK1* gene.

The results of the growth experiment also indicate that the presence of the low [*PIN*$^+$] variant had a slight negative effect on cell growth rate. The low [*PIN*$^+$] variant has the highest percentage of Rnq1p in soluble form in the presence of the [*PIN*$^+$] prion, compared to the other variant strains and it is possible that this elevated level of Rnq1p protein in the presence of the [*PIN*$^+$] prion can have a slight toxic effect in the cell, resulting in a slightly longer doubling time.

Overlaying the growth curves for the different strains reveals a slight difference in growth profile (figure 3.2A). The *rnq1Δ* strain and the high [*PIN*$^+$] variant strain deviated from the growth profile of the [*pin*$^-$] , low, medium and very high [*PIN*$^+$] variants as the strains entered diauxic shift. Diauxic shift describes the stage of growth where cells undergo dramatic metabolic changes, following the exhaustion of a fermentative carbon source such as glucose, in preparation for post-diauxic

respiratory growth where they consume the by-product of fermentative growth, ethanol (figure 3.2B). The growth experiment was terminated after apparent entry to diauxic shift, indicated in figure 3.2B.

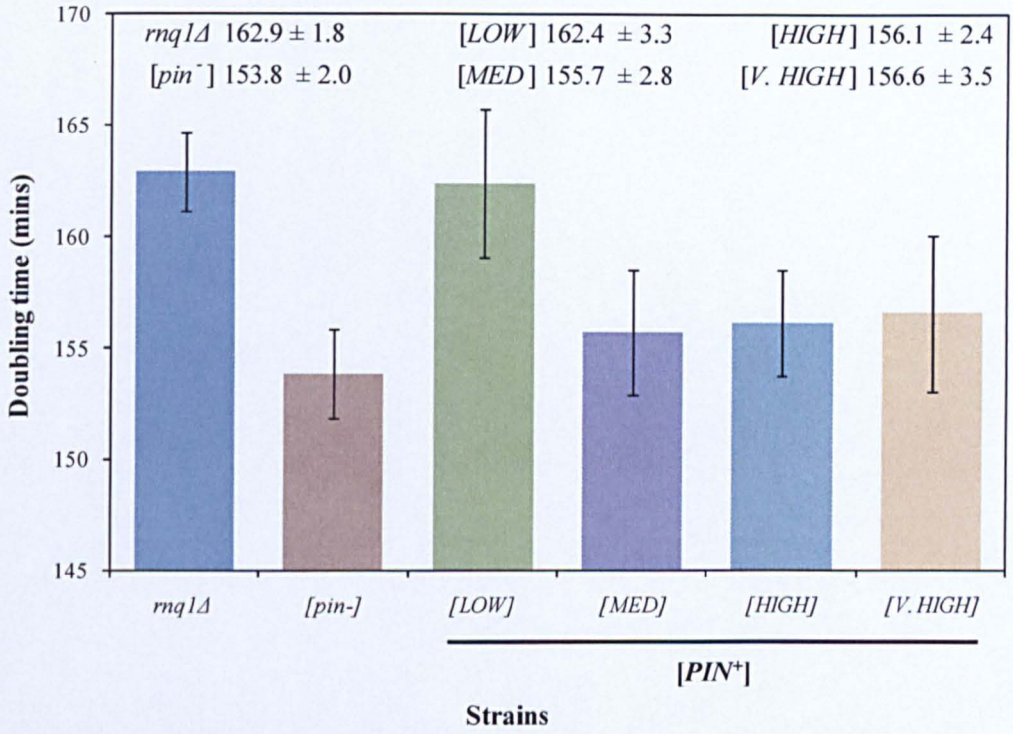

Figure 3.1: Doubling times as a consequence of changes in Rnq1p abundance and prion state.
The [*pin*⁻] form of Rnq1p is associated with the fastest doubling time, and both the absence of Rnq1p (*rnq1Δ* strain) or the presence of the low [*PIN*⁺] variant correlate with the slowest doubling times. Data reflect the average of 5 analyses over 2 experiments.

The *rnq1Δ* strain showed a slight growth advantage and the high [*PIN*⁺] variant a slight growth disadvantage, at the stage of diauxic shift compared to the other strains. By analysing a growth curve in terms of changes to the doubling time, over time, we can better appreciate the significance of the *rnq1Δ* strain's deviation from the 'average' curve. Specifically, as the [*pin*⁻] strain and the [*PIN*⁺] variants, including the high [*PIN*⁺] variant, rapidly increase in doubling time on approach to and transition through the reduced diauxic shift, the *rnq1Δ* strain undergoes only a steady increase in its doubling time, and as such the cell density increase for the *rnq1Δ* strain during this period was greater than that observed for the [*pin*⁻] and variant [*PIN*⁺] strains (figure.3.3). If the doubling time data (figure 3,3) for the

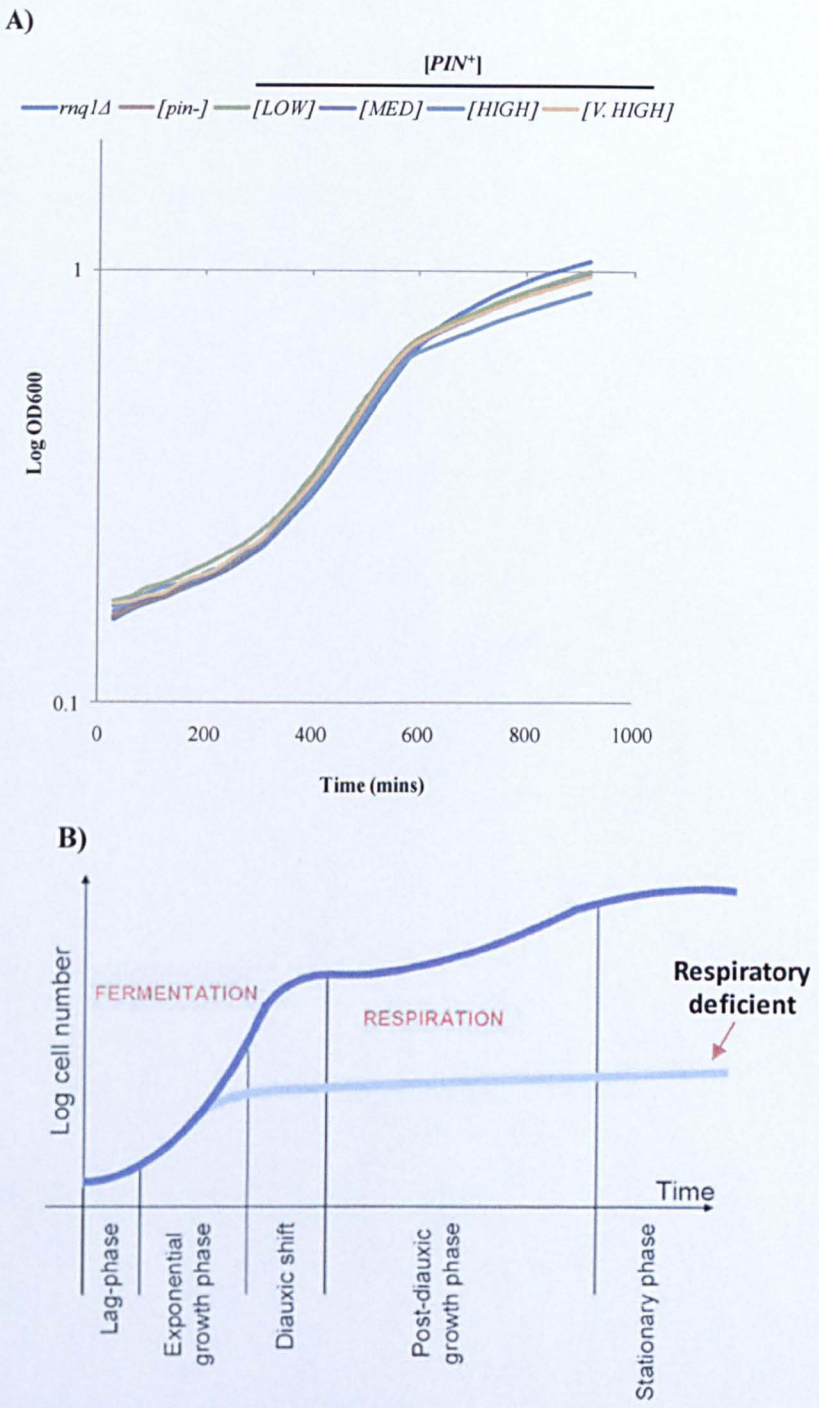

Figure 3.2: Growth profile of strains as a consequence of changes to Rnq1p abundance or prion state.

A) Comparison of growth profiles for the [*PIN*$^+$] variants, [*pin*$^-$] and *rnq1Δ* strains reveals a reproducible growth advantage of the rnq1 strain during diauxic shift, and a reproducible defect associated with the high [*PIN*$^+$] variant during diauxic shift. B) Example growth curve to indicate the multiple growth stages associated with a typical growth profile. Copied from Smets *et al* (Smets *et al.*, 2010)..

rnq1Δ, [*pin*$^-$] and high [*PIN*$^+$] strains is taken and overlaid with the standard deviation values onto the plot, this confirms that the growth difference is statistically significant, with non-overlapping error bars (figure.3.4).

One explanation for this result is that the *rnq1Δ* strain is better able to remodel the metabolic state of the cell in preparation for respiratory growth, and that for some as yet undetermined reason, the high [*PIN*$^+$] variant also specifically alters this function of Rnq1p during the diauxic shift. The data indicate that Rnq1p has a cellular role in metabolic processes which may be limited to the diauxic shift, or at least perform a non-redundant function at this stage. The fact that opposing phenotypes are observed when the *RNQ1* gene is deleted compared to the presence of the high [*PIN*$^+$] variant suggests that Rnq1p is integral to the changes noted at diauxic shift. Additionally, that the opposing phenotype (relative to the *RNQ1* deletion strain) is specific to the presence of the high [*PIN*$^+$] prion but no other variant indicates that Rnq1p may interact differently with the different [*PIN*$^+$] variant forms. Without data extending further into the stages of growth e.g. post-diauxic growth and stationary phase, it is -

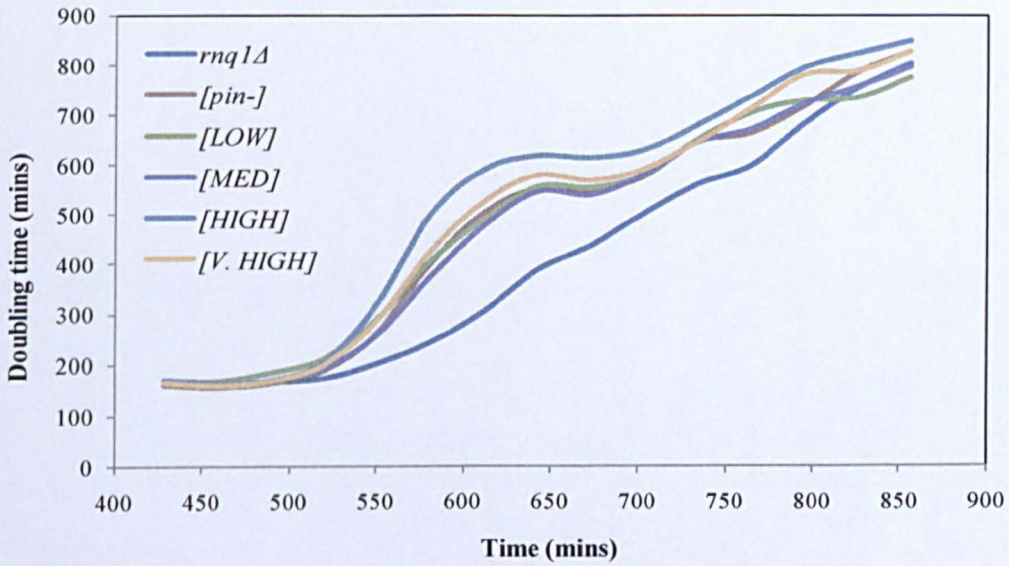

Figure 3.3: Changes in growth doubling times upon transition to diauxic shift for the Rnq1p [*PIN*$^+$] variants, *rnq1Δ* and [*pin*$^-$] strains.
The *rnq1Δ* strain shows a clear growth advantage during the diauxic shift relative to the [*PIN*$^+$] and [*pin*$^-$] strains. Average of 5 analyses over 2 experiments.

-not possible to comment on whether a deletion of *RNQ1* or the presence of the [*PIN*$^+$] prion is ultimately detrimental to the cell. However, it is unlikely that a slower transition through the diauxic shift, reflected either in terms of time or cell density, would be beneficial to a cell.

The presence of a phenotype for the *rnq1Δ* strain in diauxic shift may support a more direct role for Rnq1p in exponentially growing cells prior to diauxic shift, rather than attributing the slight growth defect during exponential phase to disruption of the regulatory sequences and subsequent transcriptional activity of the *BIK1* gene.

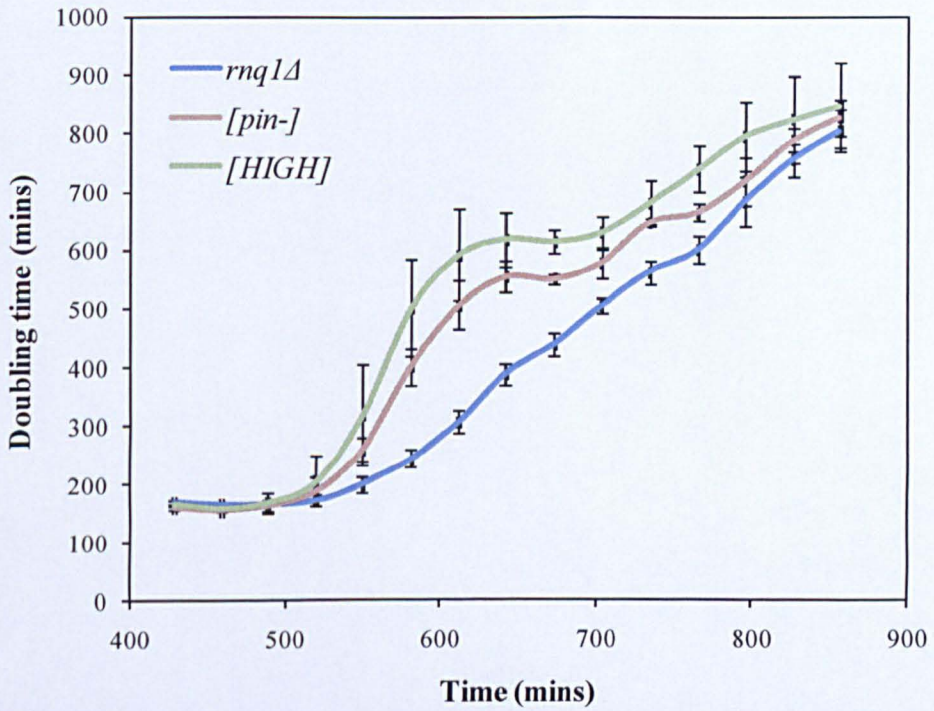

Figure 3.4: Changes in growth doubling times with standard deviation, upon transition to diauxic shift for the high [*PIN*$^+$] variant, *rnq1Δ* and [*pin*$^-$] strain.
Data from figure 3 plus standard deviation demonstrates the reproducible growth advantage of the *rnq1Δ* strain relative to the [*PIN*$^+$] and [*pin*$^-$] strains. Average of 5 analyses over 2 experiments.

3.1.2 The [*PIN*$^+$] prion negatively effects cell viability in stationary phase

In nature, yeast cells spend most of their life in the quiescent state known as stationary phase. It was therefore of interest to determine how Rnq1p and its prion form may influence the viability of cells while in stationary phase.

To do this, washed and counted cells from three YEPD stationary phase cultures of BY4741 *rnq1Δ*, [*pin*$^-$] and [*PIN*$^+$] were used to inoculate 50 mL sterile dH_2O. A small aliquot of suspension was removed on different days over a 25 day period post-inoculation and plated onto rich agar medium in order to measure the total colony forming units in each of the three different strains over time.

Fluctuation in the number of CFUs was observed for ~13 days, after which point CFUs steadily declined for all 3 strains (figure 3.5). This may indicate that the cell number originally used to inoculate the sterile water cultures was too high and created problems with cell clumping that would result in the variability of cell number per aliquot, until cell number was low enough for more accurate readings. It is also possible that after ~13 days in stationary phase, changes to the cell wall reduce cell-cell adhesion, allowing for better dispersion of cells throughout the suspension and therefore aliquots more accurately represent the number of individual viable cells within the cell suspension plated.

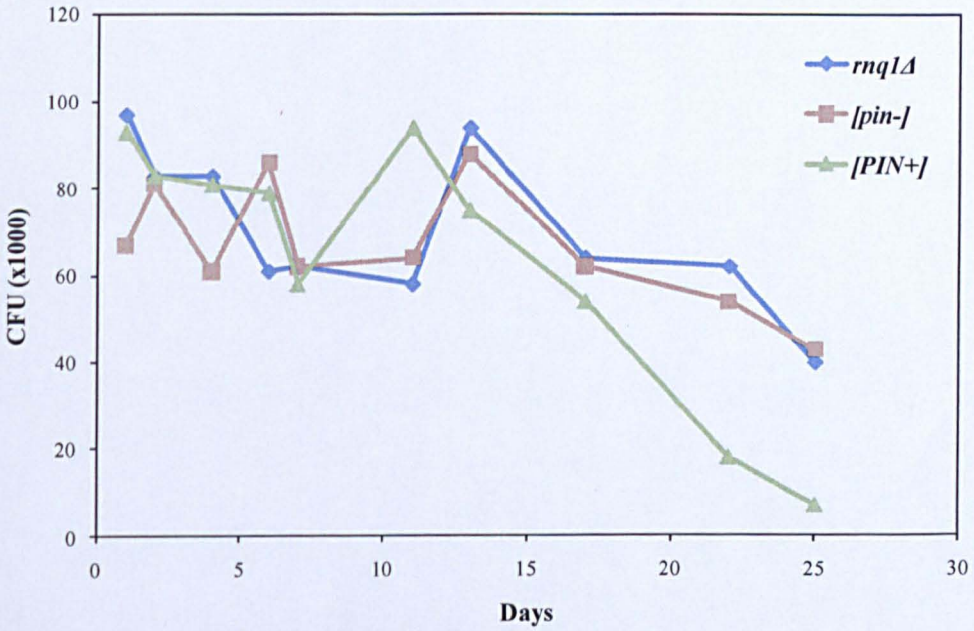

Figure 3.5: Stationary phase survival assay.
The change in colony forming units (CFU) with increasing time in stationary phase for three strains, BY4741 [*PIN*$^+$], [*pin*$^-$] and *rnq1Δ*, suggests that the presence of the [*PIN*$^+$] prion is detrimental to stationary phase survival.

The total CFUs of the *rnq1Δ* and [*pin*$^-$] strains decreased with a very similar profile by ~2x fold over 12 days, starting from day 13 of the experiment, in contrast, over

the same time period, the total CFUs of the [*PIN*$^+$] strain decreased ~ 12x fold. It is possible that the viability of the[*PIN*$^+$] strain started to decline 2 days before that of the *rnq1Δ* and [*pin*$^-$] strain, however even if this is taken into consideration the decline in CFUs of the [*PIN*$^+$] strain over ~ 11 days is still ~5x fold, higher than that seen for the *rnq1Δ* and [*pin*$^-$] strains.

These results indicate that cells harbouring the [*PIN*$^+$] prion, as opposed to the [*pin*$^-$] prion, may have a distinct disadvantage in the stationary phase. It is interesting that the decline in CFUs of the *rnq1Δ* strain did not differ from that seen for the [*pin*$^-$] strain, and suggests that the Rnq1p protein does not influence stationary phase viability; however the results do not preclude the possibility that Rnq1p protein acquires a toxic function in the presence of the [*PIN*$^+$] prion in stationary phase. The result is also interest in the context of ageing, since stationary phase starving yeast cells are similar to post-mitotic cells and are therefore be used to model age-related degeneration (Sokolov *et al.*, 2006). It may be that the [*PIN*$^+$] strain induces apoptosis more readily than the [*pin*$^-$] strain or that [*PIN*$^+$] cells age faster than [*pin*$^-$] cells., thus this could be an interesting system to analyse further.

3.1.3 Rnq1p is associated with no significant heat-shock resistance phenotype

In attempting to identify possible functions for Rnq1p via sensitivity or resistance phenotypes to certain stresses, and also to identify phenotypes that may distinguish between the [*PIN*$^+$] variants, the 74D694 rnq1Δ, and all [*pin*$^-$] and [*PIN*$^+$] variant strains were subjected to heat shock treatment as detailed in Materials and Methods section 2.12.7. Essentially cultures were adjusted to the same cell density with fresh medium, aliquoted to individual tubes and exposed to 42 °C for 0-20 min. Samples taken at 0, 5, 10, and 20 minutes were diluted and spotted on to YPD at 30 ^{0}C.

There was little to no significant difference in growth observed between the strains (figure 3.6). The low [*PIN*$^+$] variant also appeared to convert to the [*PSI*$^+$] state during the assay; this however cannot be attributed to heat-shock induction since the [*PSI*$^+$] phenotype was observed at 0 mins i.e. prior to heat shock.

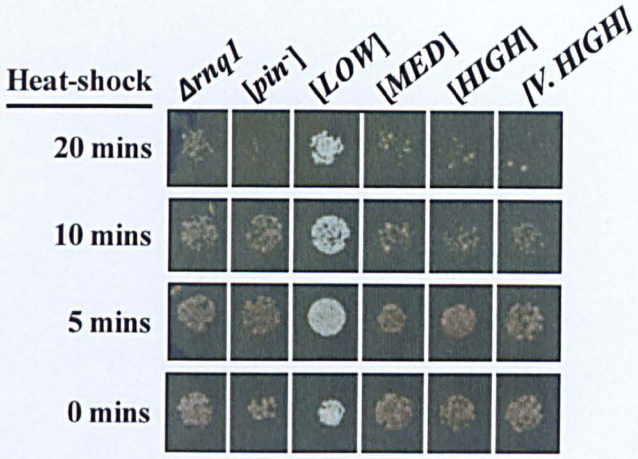

Figure 3.6: Thermotolerance assay of the [*PIN*$^+$] variants, a [*pin*$^-$] and *rnq1*Δ strain.
Exposure to 42 °C for increasing durations as indicated little to no difference in thermotolerance between the tested strains.

3.1.4 Growth analysis summary

A BY4741 *rnq1Δ* strain does not appear to have a defect in stationary phase that reduces cell viability relative to [*pin*$^-$] strain. Assuming this is not strain-specific behaviour, it would suggest that the apparent growth advantage detected in the 74D694 *rnq1Δ* strain during diauxic shift was not an indication of a metabolic failure to remodel in preparation for post-diauxic growth. However, it also suggests that the apparent growth advantage of the *rnq1Δ* strain during diauxic shift does not translate to improved cell viability during stationary phase, since in stationary phase the *rnq1Δ* strain showed a similar rate of loss of viability to that of the [*pin*$^-$] strain, which demonstrated no diauxic shift advantage. This does not mean that the increase in cell density of the *rnq1Δ* strain during diauxic shift is irrelevant, since the stationary phase experiment was commenced with equal cell density for all three strains. It is possible that in nature, the *rnq1Δ* strain would persist longer in the environment in stationary phase relative to the [*pin*$^-$] and [*PIN*$^+$] strain simply due to its increased cell density accumulated during the diauxic shift.

Alternatively, the increase in cell density of the *rnq1Δ* strain generated during diauxic shift could result in faster depletion of the respiratory carbon source ethanol

during post-diauxic growth, and therefore any benefit of elevated growth during diauxic shift relative to the [*pin*$^-$] and [*PIN*$^+$] strains would be balanced out by a relatively smaller increase in cell density in post-diauxic growth.

In terms of significance for understanding the function of Rnq1p, these data indicate a possible role for Rnq1p either (a) in the integration of cellular or environmental signals about nutrient availability (b) in the pathways that limit cell division in response to such environmental or cellular cues or (c) in the pathways that control activation or deactivation of fermentative or respiratory processes.

3.2 Rnq1p function: a bioinformatics approach

There are a number of online characterisation and functional prediction tools that, along with a multitude of data from published high-throughout screen, can be used to glean more information about any given protein of interest. In this chapter I present the results of a variety of analysis using these online resources, to potentially facilitate the identification of the function of the Rnq1p protein.

3.2.1 Evolution of the Rnq1p protein sequence

The budding yeast *S. cerevisiae* belongs to the phylum ascomycota and a phylogenetic tree in figure 3.7 depicts the evolutionary relationship amongst members of this phylum. The *RNQ1* gene is not present in the genome of all species of this group, and analysis of a few closely related species (indicated by blue boxes in figure 3.7) reveals that even in those species where the *RNQ1* gene is present, there is a great deal of sequence variation between them (figure 3.8).

Aligning the Rnq1p amino acid sequence from the species *Saccharomyces cerevisiae* against Rnq1p sequences identified in *Saccharomyces bayanus*, *Saccharomyces castelli* 1044, *Saccharomyces castelli* 1056, *Kluyveromyces polysporus*, *Candida albicans*, *Saccharomyces kluyveri*, *Kluyveromyces walti* and *Eremotheicum gossypii*, a 'consensus' sequence can be generated. The consensus sequence shows those residues that have been conserved in the Rnq1p protein as these species have evolved from a common ancestor over time. By removing species from the

alignment, usually the more distantly related species, the number of residues in the consensus sequence will increase as the sequence variation between the more closely related species decreases.

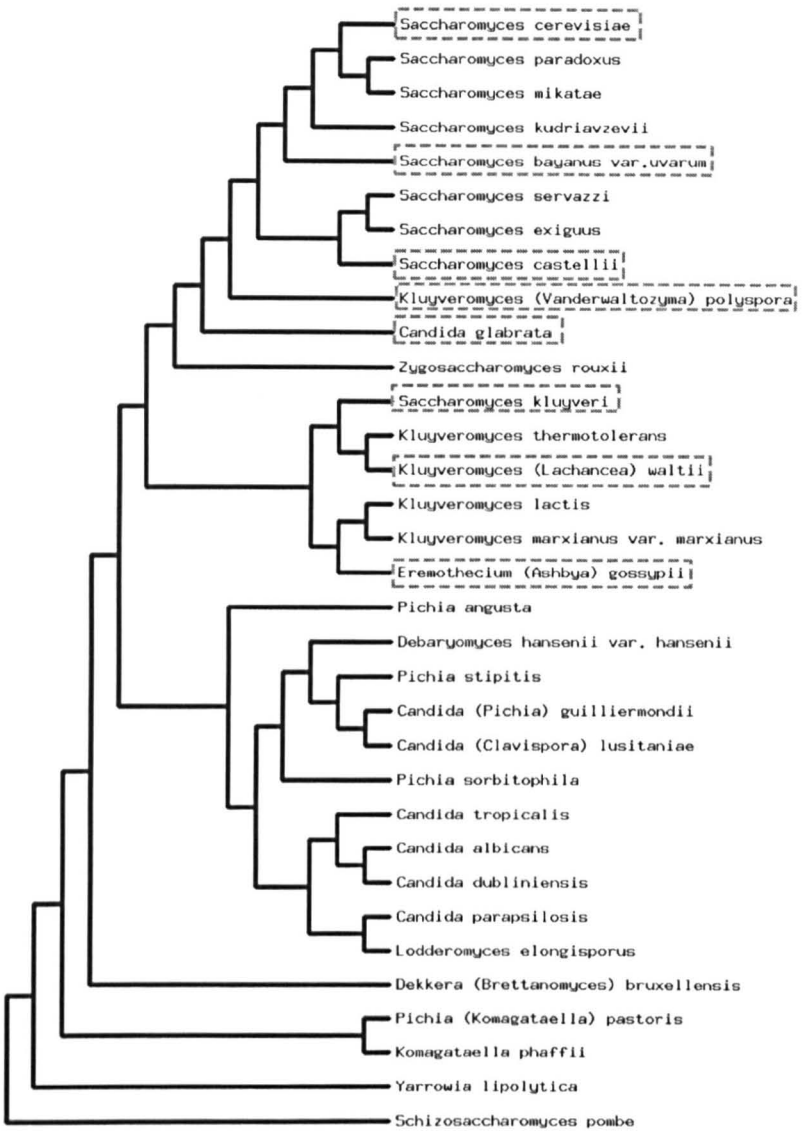

Figure 3.7 A phylogenetic tree depicts the evolutionary relationship between members of the ascomycota phylum.
Indicated in blue boxes are those members of the ascomycota phylum whose *RNQ1* gene sequence is examined within this thesis.

Starting with the 8 aligned sequences from the species listed above, 16 residues are conserved within the first 200 amino acids of the Rnq1p protein (figure 3.8). If *S. castelli* 1044 is removed from the alignment, the number of conserved residues in the consensus sequence increases to 28 residues. By taking *S. castelli* 1044 and *K. walti*

out of the alignment, the conserved residues increases to 33 and removing *S. kluyveri* increases the consensus sequence to 36 residues and removing *K.polysporus* as well, (essentially leaving an alignment between *S. cerevisiae*, *S. bayanus*, *C. glabrata* and *E. gossypii*), creates a consensus sequence with 44 residues in the first 200 amino acids of the Rnq1p protein. These highly conserved residues are likely to be important for the cellular function of Rnq1p. Indeed, none of the *RNQ1* alleles cloned and sequenced in this study (see Chapter 4) contained polymorphisms at the conserved residues (figure 3.8). It is also noteworthy that conservation appears to be limited to the N-terminus of Rnq1p, within the first 150 amino acids.

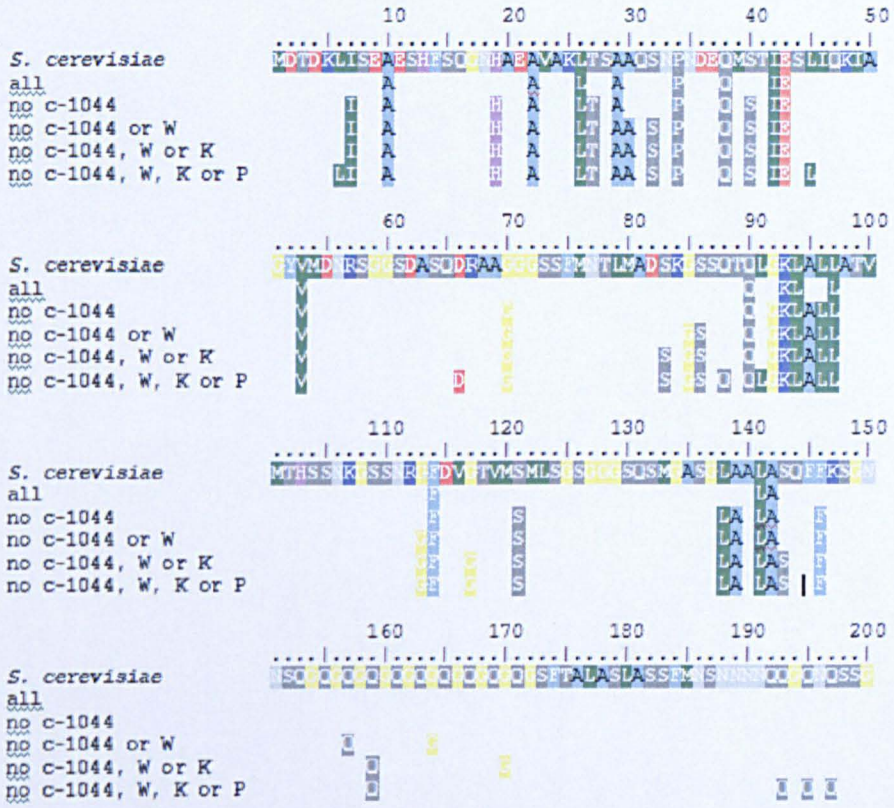

Figure 3.8 Identification of conserved Rnq1p residues.
Amino acid sequence of Rnq1p from multiple yeast species can be aligned to generate a consensus sequence, revealing residues of Rnq1p that are conserved. Excluding distantly related species from the alignment increases the number of residues in the consensus sequence. The alignment above demonstrates the persistence or appearance of residues in the consensus sequence as all species are aligned, to 'no c-1044' when all but castelli-1044 are aligned, and so on and so forth. (c-1044= *S. castelli* 1044; W= *K. walti*; K= *S. klyyveri*; P= *K. polysporus*; all = *S. bayanus*, *C. glabrata*, *S. castelli* 1056, *A. gossypii*, *S. castelli* 1044, *K. walti*, *S. klyyveri* and *K. polysporus*).

Despite conservation of the Rnq1p amino acid sequence being limited to the N-terminus, the general amino acid composition of the full-length Rnq1p protein from all of the species is similar (figure. 3.10). Specifically, the Rnq1p protein from all of the species is enriched for glycine, asparagine, glutamine and serine residues, relative to the expected abundance of these amino acids in a protein. Also, the relative amount of the amino acid tyrosine is, albeit only slightly for some, above the average. A similar trend can be seen for methionine, though only 5 of the 8 species are elevated for this amino acid.

In terms of properties, all of the enriched amino acids are aliphatic, except tyrosine. Four of these amino acids are also polar, including the two most common: glutamine and asparagine. Polar residues are typically on the surface of globular proteins and in combination with the known propensity of glutamine and asparagine to form protein-protein interactions (termed a 'polar zipper') (Perutz *et al.*, 1994) which can result in protein aggregation, their elevated abundance in Rnq1p may indicate that the ability to associate in this way is relevant to the function of Rnq1p

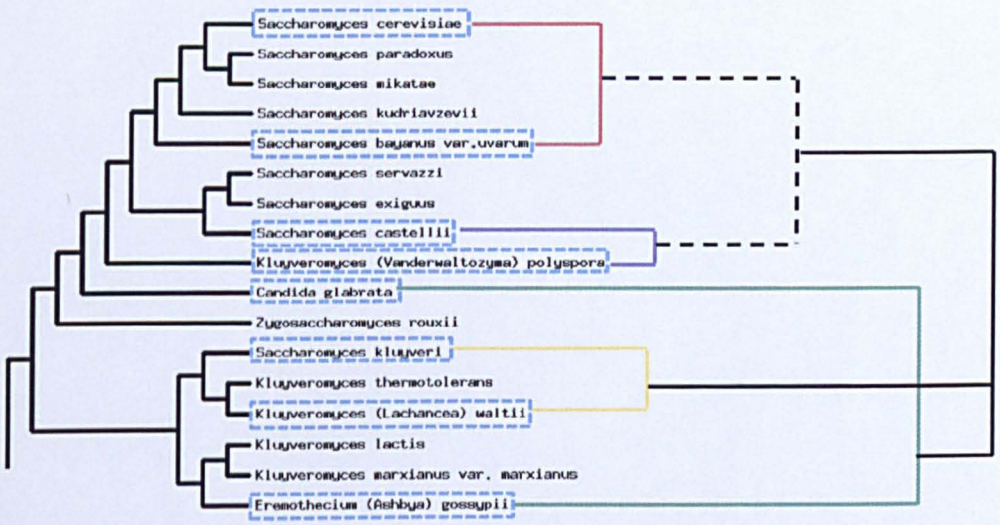

Figure 3.9 A phylogenetic tree as depicted in figure 3.7.
On the right-hand side, the relationship between the yeast species based on *RNQ1* sequence similarity is depicted for comparison to the species phylogenetic tree.

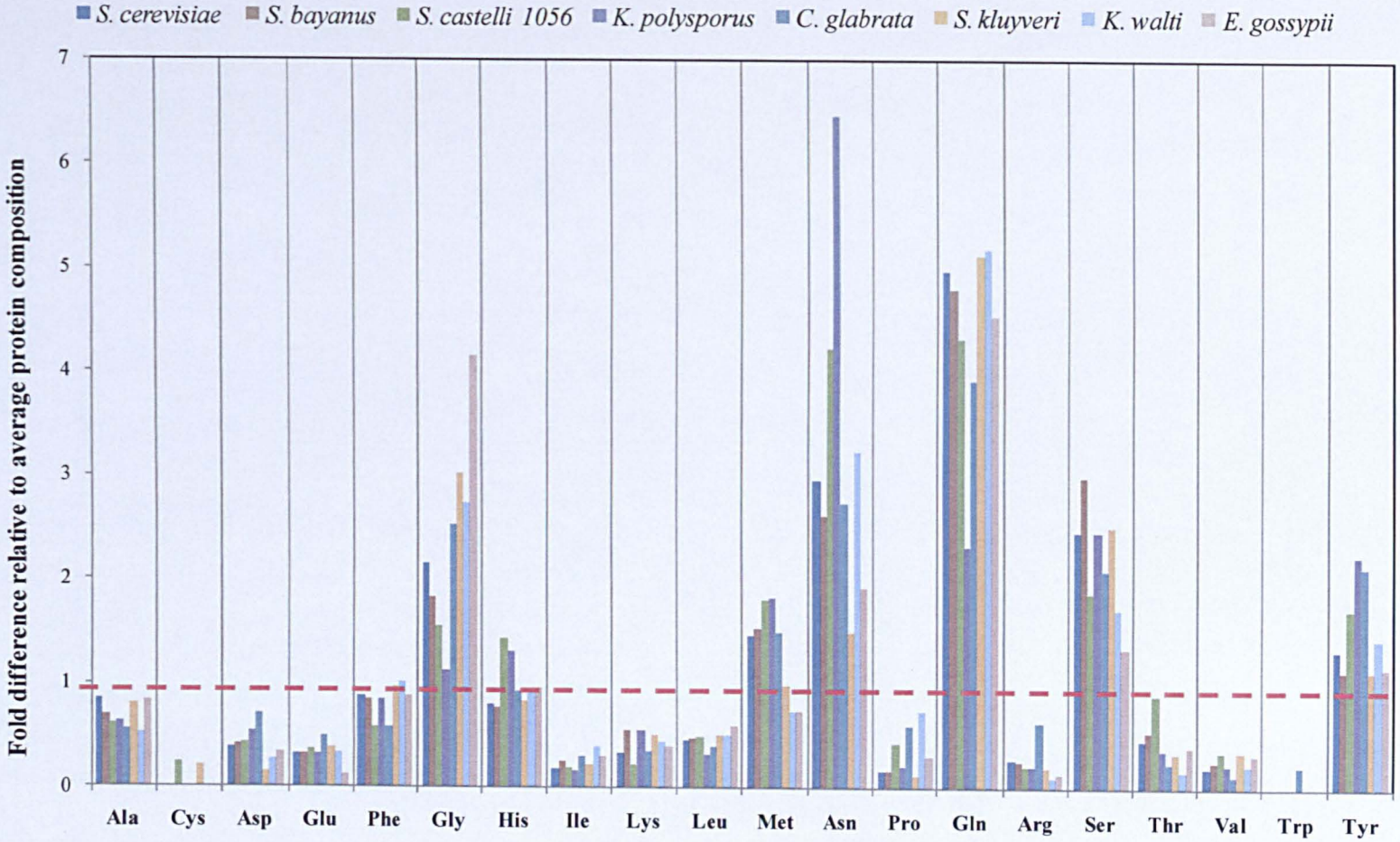

Figure 3.10 Amino acid composition of Rnq1p is similar across the different yeast species

Despite the significant difference in amino acid sequence between the Rnq1p protein of the different yeast species, particularly beyond the N-terminus, the overall composition of Rnq1p is very similar, all appear to be rich in glutamine, serine, asparagine and glycine.

3.2.2 Detection of functional sites in Rnq1p using ELM

Eukaryotic Linear Motif (ELM) an online tool for predicting functional sites within eukaryotic proteins was used to analyse the amino acid sequence of Rnq1p. Due to the shortness of the motifs, confidence levels were not assigned to any results, but rather were used merely as experimental guides.

An analysis of Rnq1p with the ELM tool indicated the presence of a forkhead-associated (FHA) domain between residues 1-7, representing the FHA motif: MDTDKLI. Proteins containing an FHA domain are involved in a wide variety of cellular functions, including signalling and vesicular transport in the cytoplasm, and cell cycle checkpoint, DNA repair and transcriptional regulation in the nucleus. Specifically, the FHA-domain recognises phosphothreonine, phosphoserine and phosphotyrosine containing sequences on target ligands. The discovery of an FHA domain in Rnq1p is particularly interesting, since other FHA-domain containing proteins in yeast induce the Pin4p protein, also known as Mdt1, which was identified as a [*PSI*$^+$]-Inducibility factor (Derkatch *et al.*, 2001a) and is the source for its name ([*PSI*$^+$] *IN*ducibility). The Pin4p protein is involved in cell cycle progression at the G2/M phase, it is hyperphosphorylated in response to DNA damage and it interacts with the protein kinase Rad53p – another FHA-containing protein of yeast also involved in cell cycle arrest and the response to DNA damage.

3.2.3 Rnq1p is predicted to be phosphorylated at serine-143

A multidimensional chromatography approach to identify low-abundance representatives of the phosphoproteome of *S. cerevisiae* was performed by Albuquerque *et al* (Albuquerque *et al.*, 2008). Specifically, they looked at the phosphoproteome following induction of DNA damage by 0.05 % methyl methanesulfonate (MMS). The study of proteins phosphorylated in this way was used to identify protein kinases involved in cellular signalling pathways.

Amongst the 2278 proteins identified was Rnq1p. The peptide of Rnq1p containing the phosphorylation was: L.AALASphosQFFK.S, via the target serine residue at amino acid position 143 of the Rnq1p sequence. This residue is conserved in the

different yeast species indicated by the blue boxes in figure 3.7, except *S. klyveri* and *K. walti* and *S. castelli*-1044.

The SQ/TQ phosphorylation motif is typically found in substrates for the Mec1 and Tel1 kinases involved in cell cycle checkpoints and the response to DNA damage, and these two redundant proteins are responsible for 26 % of all SQ/TQ phosphorylation events following MMS treatment (Albuquerque *et al.*, 2008).

3.2.4 A *rnq1Δ* strain is sensitive to Methyl Methanesulfonate (MMS)

The yeast gene deletion collection was screened by *Begley et al* (Begley *et al.*, 2002a) for sensitivity to various DNA damaging agents, testing multiple doses in triplicate, and the results are published in the form of a searchable database online (http://genomicphenotyping.mit.edu/). The study identified the *rnq1Δ* strain as sensitive to MMS treatment in two of the three experiments, growing <67 % of the wild-type each time and therefore considered significant.

While genes involved in DNA repair and cell cycle control are expected to show MMS sensitivity, strains deficient in protein and amino acid metabolism (degradation, synthesis, targeting) also influence recovery post-MMS exposure (Begley *et al.*, 2002a). Specifically, importing the 420 gene deletion strains sensitive to MMS (Begley *et al.*, 2002a) into the 'Saccharomyces Genome Database' gene ontology tool 'SlimMapper' showed clustering to processes such as response to stress (20.2%), unknown biological process (20.2%) transport (17.6%), RNA metabolic process (14.3%), DNA metabolic process (13.1%), cell cycle (12.6%), protein modification (11.2%), chromosome organisation (11.0 %) and transcription (10.5%).

3.2.5 Rnq1p is predicted to be ubiquitinated

UbPred is an online tool used to predict potential ubiquitination sites within proteins. The prediction is based on an analysis of 266 experimentally verified ubiquitination sites and 2 large-scale proteomic surveys. The results presented (figure 3.12) are a screen-shot summarising an analysis of the Rnq1p protein by the UbPred tool.

Lysine residues at position 5 and 84 are high-confidence ubiquitination targets predicted by UbPred. In terms of conservation, the lysine at residue 5 is present only in *S. cerevisiae*, *S. bayanus*, *S. castelli*-1056 and *A. gossypii*; the lysine at residue 84 is only found in *S. cerevisiae* and *S. bayanus*.

Ubiquitination is used by the cell to target proteins to the proteasome for degradation, and is thus a way of regulating protein levels. The most abundant targets of ubiquitination are proteins involved in the cell cycle, transcriptional regulation, stress response and the secretory pathway (Glickman *et al.*, 2002).

3.2.6 Structure prediction for Rnq1p

An online tool called 3Dpro (http://scratch.proteomics.ics.uci.edu/) can be used to make predictions of the 3D structure of a protein by accepting or rejecting conformational moves of fragments, based on a PDB fragment library, using energy function as its guide. From the multiple models generated, the final predicted structure is the one with the lowest overall energy. The tool is only able to compute proteins with 400 amino acids or less. Since Rnq1p is 405 amino acids, the 5 amino acids at the extreme C-terminal were excluded, given that conservation of this protein is concentrated on the N-terminus. The predicted structure in figure 3.13 shows the C-terminus in red at the bottom of the stem, and the N-terminus in dark blue at the top right overhang. The structure show some degree of similarity with tRNA molecules and other proteins involved in translational elongation and termination, which are themselves tRNA mimics.

MDTDKLISEAESHFSQGNHAEAVAKLTSAAQSNPNDEQMSTIESLIQKIAGYVMDNRSGGSDASQDRAAGGGSSFMNTLM
ADSKGSSQTQLGKLALLATVMTHSSNKGSSNRGFDVGTVMSMLSGSGGGSQSMGASGLAAALASQFFKSGNNSQGQGQGQG
QGQGQGQGQGQGSFTALASLASSFMNSNNNNQQGQNQSSGGSSFGALASMASSFMHSNNNQNSNNSQQGYNQSYQNGNQN
SQGYNNQQYQGGNGGYQQQQGQSGGAFSSLASMAQSYLGGGQTQSNQQQYNQQGQNNQQQYQQQGQNYQHQQQGQQQQQG
HSSSFSALASMASSYLGNNSNSNSSYGGQQQANEYGRPQQNGQQQSNEYGRPQYGGNQNSNGQHESFNFSGNFSQQNNNG
NQNRY

Output:

Residue	Score	Ubiquitinated
5	0.84	Yes High confidence
25	0.77	Yes Medium confidence
48	0.50	No
84	0.86	Yes High confidence
93	0.55	No
107	0.79	Yes Medium confidence
147	0.73	Yes Medium confidence

Legend:

Label	Score range	Sensitivity	Specificity
Low confidence	0.62 ≤ s ≤ 0.69	0.464	0.903
Medium confidence	0.69 ≤ s ≤ 0.84	0.346	0.950
High confidence	0.84 ≤ s ≤ 1.00	0.197	0.989

Figure 3.12 UbPred prediction of Rnq1p ubiquitination.
The Rnq1p amino acid sequence was imported into the online form at http://www.ubpred.org/. A screen shot of the result is shown; Rnq1p is predicted to be ubiquitinated at residues 5 and 84.

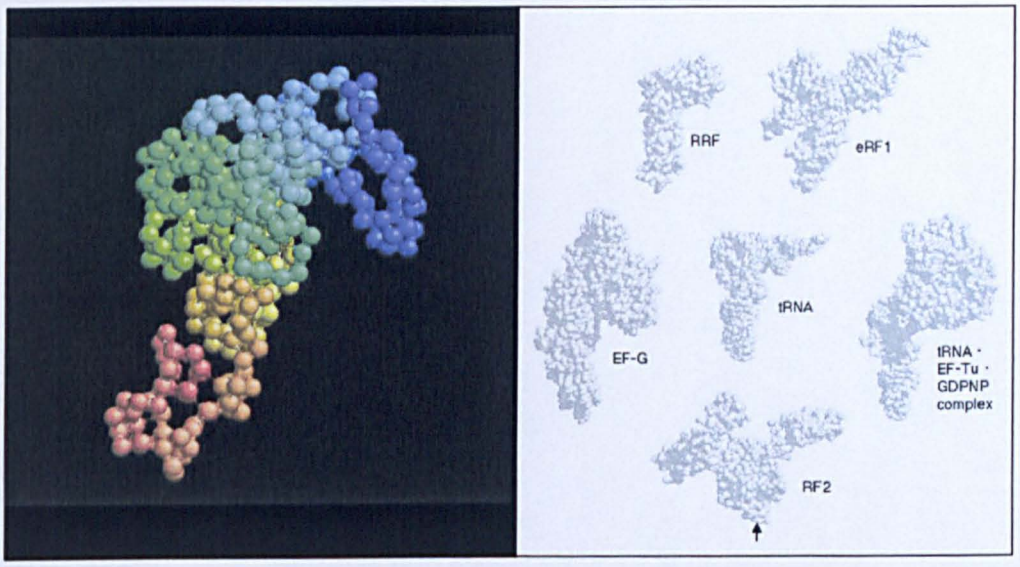

Figure 3.13 Scratch Protein Predictor 3Dpro prediction of Rnq1p structure.
The Rnq1p amino acid sequence (residues 1-400) was imported into the online form of the 3Dpro tool, at the Scratch Protein Predictor website, http://www.ics.uci.edu/~baldig/scratch/. The structure (left panel) has been visualised with RasMol freeware (Sayle, 1995) and resembles a tRNA molecule, similar to other tRNA mimics (right panel).

3.2.7 There are no proteins with significant amino acid homology to Rnq1p

A BLAST search of the full-length or N-terminus (amino acids 1-153) of Rnq1p against the *S. cerevisiae* open-reading frame database does not identify any proteins in *S. cerevisiae* that are sequence related to Rnq1p. Searching in terms of amino acid composition, the full length protein is most similar to the yeast nucleoporin proteins and other transcription factors (figure 3.14).

The closest SWISS-PROT entries (in terms of AA composition)
for the species YEAST:

Rank	Score	Protein	(pI	Mw)	Description
1	0	RNQ1_YEAST	6.13	42580	[PIN+] prion protein RNQ1.
2	212	NU116_YEAST	9.36	116234	Nucleoporin NUP116/NSP116.
3	271	MSS11_YEAST	7.34	85050	Transcription activator MSS11.
4	281	NUP49_YEAST	5.77	49142	Nucleoporin NUP49/NSP49.
5	287	NAM8_YEAST	8.59	56972	Protein NAM8. /FTId=PRO_0000081659.
6	287	NUP57_YEAST	9.59	57498	Nucleoporin NUP57. /FTId=PRO_0000204877.
7	291	IXR1_YEAST	7.84	67856	Intrastrand cross-link recognition
8	296	PUB1_YEAST	4.95	50659	Nuclear and cytoplasmic polyadenylated
9	299	NU100_YEAST	9.40	99988	Nucleoporin NUP100/NSP100.
10	301	SGF73_YEAST	9.03	72878	SAGA-associated factor 73.
11	303	GTS1_YEAST	7.05	44407	Protein GTS1. /FTId=PRO_0000074226.
12	308	PIN4_YEAST	5.82	73776	RNA-binding protein PIN4.
13	310	DAT1_YEAST	9.84	27067	Oligo(A)/oligo(T)-binding protein.
14	314	MIC17_YEAST	5.40	14313	Mitochondrial intermembrane space
15	318	PIN3_YEAST	6.82	23539	[PSI+] inducibility protein 3.
16	325	HRP1_YEAST	5.42	59650	Nuclear polyadenylated RNA-binding
17	335	WHI3_YEAST	8.53	71253	Protein WHI3. /FTId=PRO_0000082005.
18	342	CBK1_YEAST	7.72	86946	Serine/threonine-protein kinase CBK1.
19	345	POP2_YEAST	5.77	49682	Poly(A) ribonuclease POP2.
20	346	MED15_YEAST	9.81	120309	Mediator of RNA polymerase II

Figure 3.14 Swiss-prot clustering of proteins from *Saccharomyces cerevisiae* with amino acid composition most similar to Rnq1p.
Ranked according to score, a measure of overall amino acid composition similarity, Rnq1p appears to be compositionally rare, though is most like yeast nucleoporin and transcription factor proteins.

However, Rnq1p is more similar in amino acid composition to proteins of other species (apart from Rnq1p in yeast), for example the calcium-responsive transactivator protein found in cows or other ungulates, the mouse, human, frog and rat and the pqn-8 prion-like protein of *C. elegans* (figure 3.15)

The closest SWISS-PROT entries (in terms of AA composition)
for any species:

Rank	Score	Protein	(pI	Mw)	Description
1	0	RNQ1_YEAST	6.13	42580	[PIN+] prion protein RNQ1.
2	165	CREST_BOVIN	6.07	43329	Calcium-responsive transactivator.
3	166	CREST_XENLA	6.08	44217	Calcium-responsive transactivator.
4	167	PQN8_CAEEL	5.35	43472	Prion-like-(Q/N-rich) domain-bearing
5	173	CREST_MOUSE	6.08	43729	Calcium-responsive transactivator.
6	176	CREST_HUMAN	5.96	42990	Calcium-responsive transactivator.
7	177	SAS2_BACSU	5.01	7332	Small, acid-soluble spore protein 2.
8	182	PNT1_DROME	6.21	66866	ETS-like protein pointed, isoform P1.
9	185	SEUSS_ARATH	9.20	96232	Transcriptional corepressor SEUSS.
10	188	HDC_DROME	8.43	117448	Headcase protein. /FTId=PRO_0000021402.
11	193	SCR_DROME	9.05	44263	Homeotic protein Sex combs reduced.
12	195	EAF_DROWI	6.56	59127	Ell-associated factor Eaf.
13	200	CREST_RAT	6.62	43999	Calcium-responsive transcription
14	202	EAF_DROMO	6.75	56617	Ell-associated factor Eaf.
15	208	POLG_FMDVO	4.03	8776	Protein VP4 (Potential).
16	208	POLG_FMDVT	4.03	8776	Protein VP4 (Potential).
17	208	POLG_FMDVZ	4.03	8776	Protein VP4 (Potential).
18	209	SAS1_BACSU	5.01	7068	Small, acid-soluble spore protein 1.
19	210	Y014_HELHP	5.58	19230	UPF0323 lipoprotein HH_0014.

Figure 3.15: Swiss-prot clustering of proteins from any species with amino acid composition most similar to Rnq1p.
Ranked according to score, a measure of overall amino acid composition similarity, Rnq1p appears to be compositionally most like the calcium-responsive transactivator protein from multiple species and a prion-like protein, pqn-8, of *C. elegans*.

3.2.8 Interaction networks for Rnq1p

A systematic screen of the *S. cerevisiae* heterozygous and homozygous diploid deletion collection for sensitivity and resistance phenotypes to 1140 chemicals and assayable stress conditions was performed by Hillenmeyer *et al.* (Hillenmeyer *et al.*, 2008). Each mutant tested was assigned a fitness score for growth in each of the conditions. The assignment of fitness scores per assayed condition allowed mutants to be grouped according to their shared sensitivity or resistance profiles, where it is expected that proteins involved in similar activities within the cell will be similarly sensitive or resistant to particular stresses.

The data from this screen (http://www.fitdb.stanford.org) was interrogated to identify mutant strains that displayed similar phenotypes to the *rnq1Δ* strain in both the heterozygous and homozygous states. Interestingly, there was little overlap between the top 10 deletion strains that behaved similarly to the *rnq1Δ* strain in the heterozygous or homozygous state. It may be that in the homozygous *rnq1Δ* deletion

strain, which is missing both copies of the *RNQ1* gene, redundant processes come into play which may represent a more radical, but probably more stable, substitution of the role normally played by Rnq1p e.g. alternative pathways are up-regulated to compensate for the loss of Rnq1p. In the heterozygous *rnq1Δ* strain however, missing only one copy, the pathways and processes that Rnq1p is involved in are

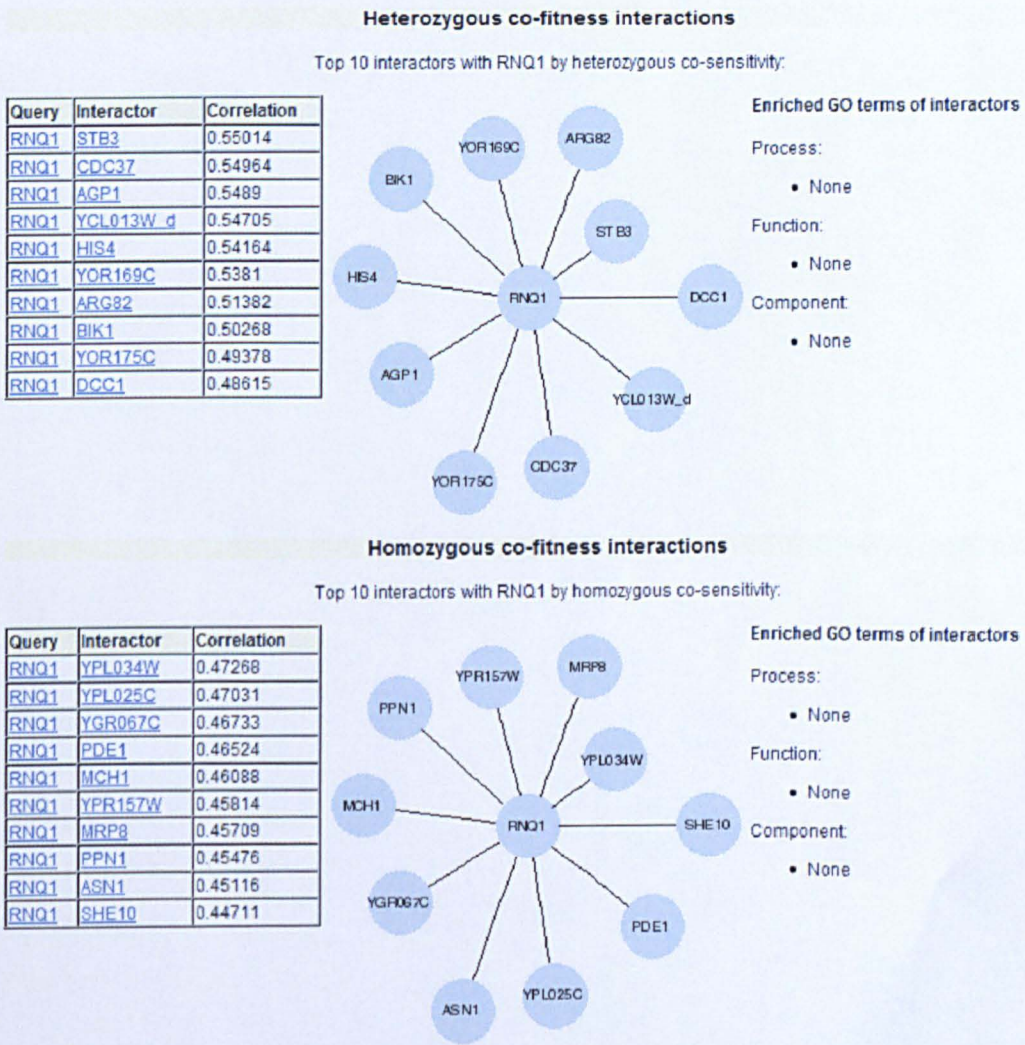

Figure 3.16 Chemical sensitivity clustering.
The Fitness Database (http://www.fitdb.stanford.edu/) clusters gene deletion strains of *Saccharomyces cerevisiae* according to similar chemical sensitivity profiles, as depicted by the above screen shots identifying gene deletions most similar to a homozygous and a heterozygous deletion of the *RNQ1* gene.

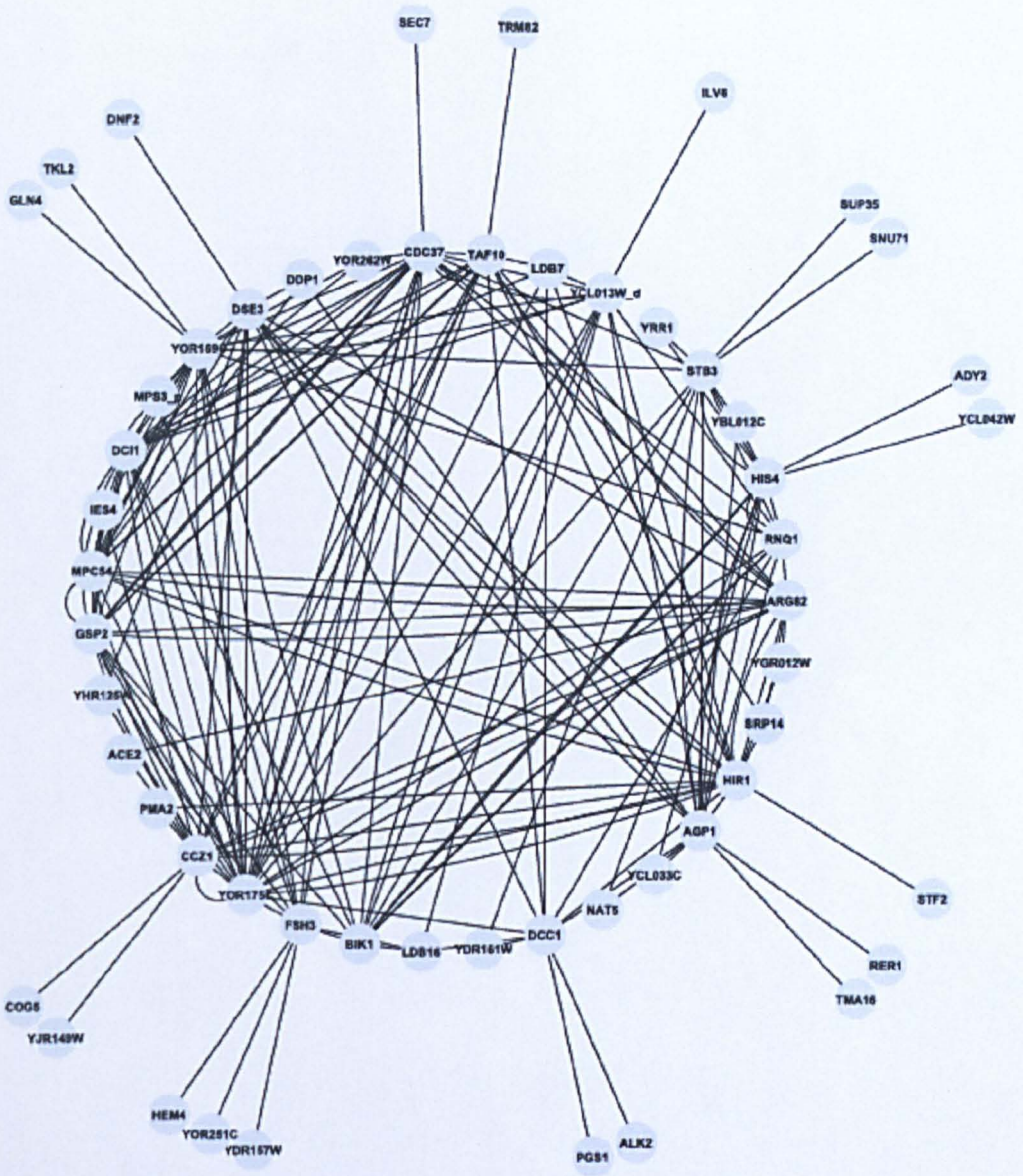

Figure 3.17 A heterozygous interaction network for Rnq1p.
Ten heterozygous deletion strains with chemical sensitivity profiles most similar to the *rnq1Δ* strain (revealed in the Fitness Database, http://www.fitdb.stanford.edu/) were assembled into a network by importing into Cytoscape software (http://www.cytoscape.org) along with their own ten most similar deletion strains. Repeating members that form the circular network are considered significant within the interaction network. Those that only appear once are peripheral to the circular network, and considered less significant.

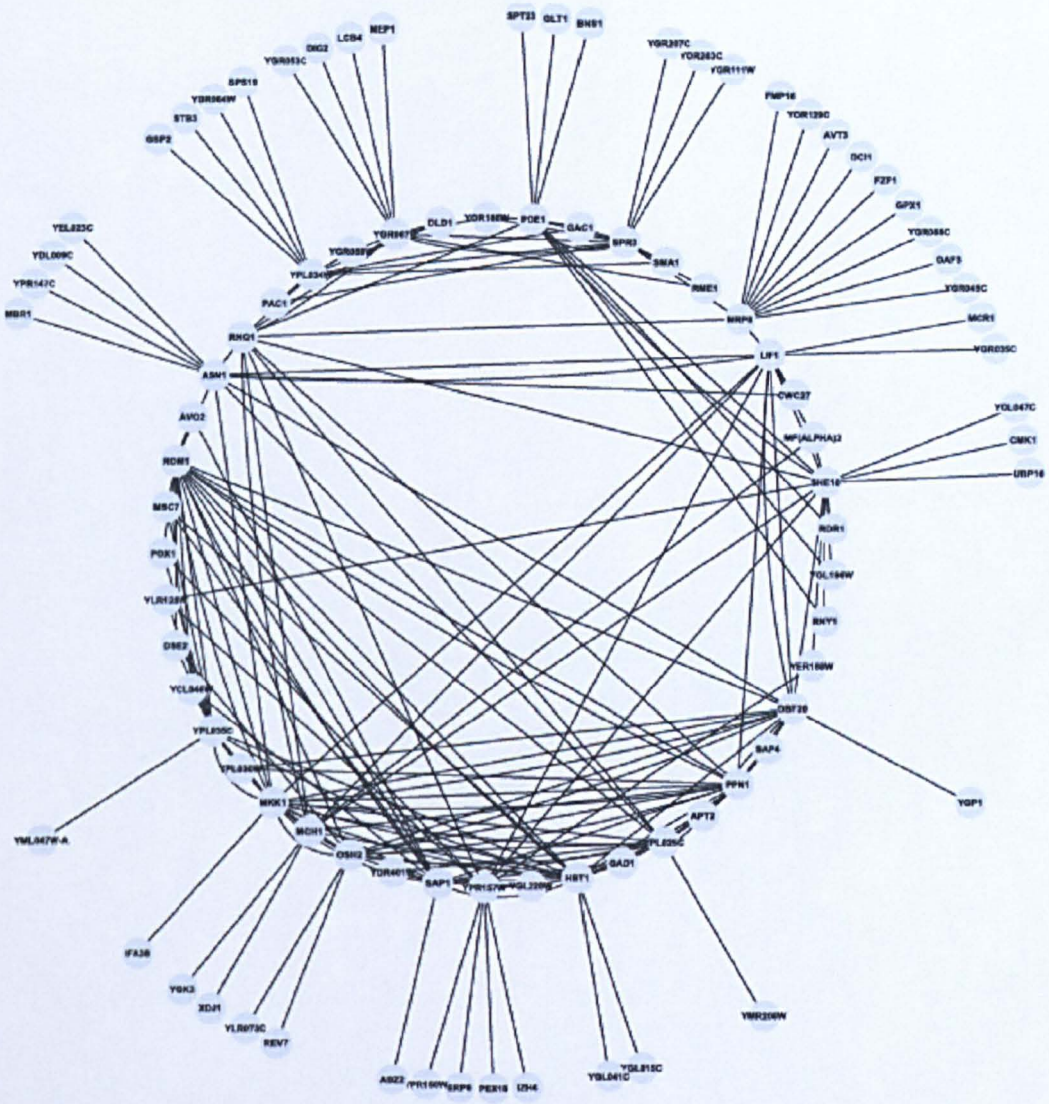

Figure 3.18 A homozygous interaction network for Rnq1p.
Ten homozygous deletion strains with chemical sensitivity profiles most similar to the rnq1Δ strain (revealed in the Fitness Database, http://www.fitdb.stanford.edu/) were assembled into a network by importing into Cytoscape software (http://www.cytoscape.org) along with their own ten most similar deletion strains. Repeating members that form the circular network are considered significant within the interaction network. Those that only appear once are peripheral to the circular network, and considered less significant.

probably made more vulnerable to perturbation, since the activities associated with Rnq1p are not fully diverted to other redundant pathways.

By identifying the top 10 interactions of the *rnq1Δ* strain's own top 10 interactions, it should be possible to identify shared interactions and build up a network of interactions for Rnq1p.

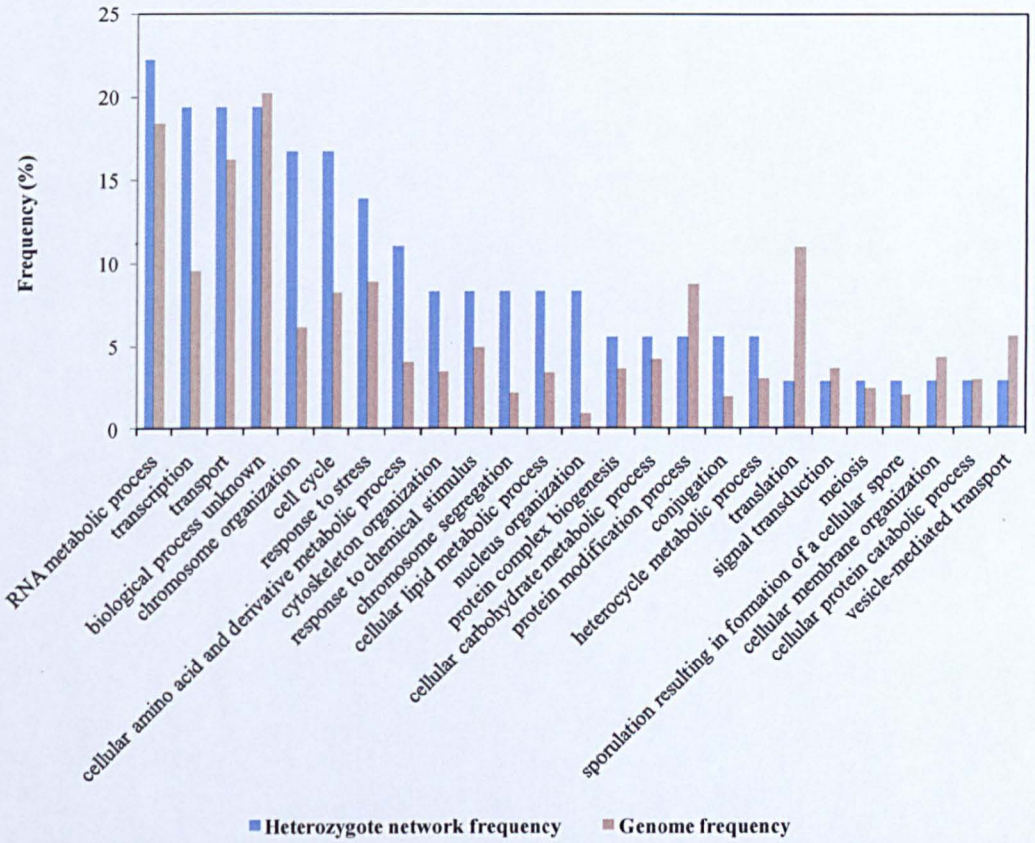

Figure 3.19: 'Slim Process' gene ontology analysis of the heterozygous interaction network.
Members of the heterozygous circular network were imported into the Saccharomyces Genome Database (http://www.yeastgenome.org/) gene ontology tool 'SlimMapper' and the abundance of different process terms associated with the heterozygous interaction were determined.

The list of deletion strains and their interactions were uploaded to Cytoscape as a network (http://www.cytoscape.org/). Cytoscape is a freely downloadable bioinformatics tool for visualising network interactions and for superimposing gene expression data on molecular interaction networks. In the context of this work, Cytoscape allows one to visualise those members with multiple interactions within

the member list. Those that only form one interaction are likely to be outliers and not relevant to the function of Rnq1p, and these are depicted peripherally to the circular network (figures 3.17, 3.18).

The identities of those genes with multiple interactions within the network were isolated and this list analysed for enrichment of any particular gene ontology category. This essentially considers all activities assigned to each of the individual listed members, and can reveal whether particular activities are over-represented. The outcome of this is an ability to associate your original target protein, in this case Rnq1p, with a particular, or multiple, functions. Such an analysis for Rnq1p, and analysis of the GO terms enriched in the heterozygous network indicate possible roles for Rnq1p in RNA metabolic processes, transcription, transport, chromosome organisation, the cell cycle and response to stress (figure 3.19).

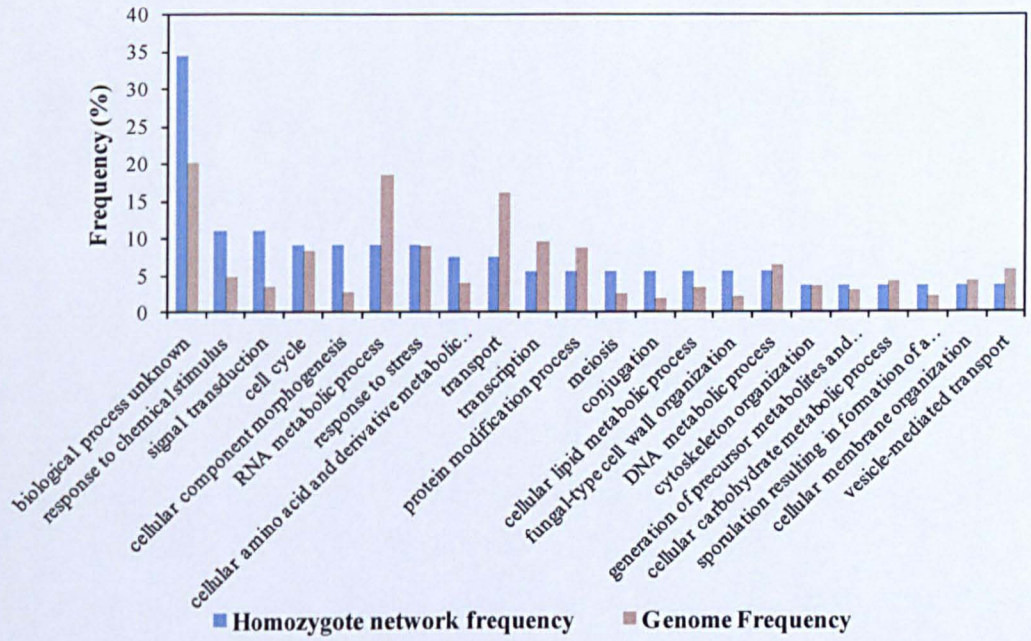

Figure 3.20 'Slim Process' gene ontology analysis of the homozygous interaction network.

Members of the homozygous circular network were imported into the Saccharomyces Genome Database (http://www.yeastgenome.org/) gene ontology tool 'SlimMapper' and the abundance of different process terms associated with the homozygous interaction were determined.

Similarly, an analysis of GO terms enriched in the homozygous network indicated roles for Rnq1p in response to chemical stress, signal transduction, the cell cycle, RNA metabolic processes, the response to stress, and cellular amino acid and metabolic processes – the most abundant term associated with the homozygous network however was biological process unknown (figure 3.20)..

3.2.9 Rnq1p is predicted to contain a TPR domain

A TPR domain is a degenerate sequence of ~ 34 amino acids loosely based around a tandem array of the consensus sequence W-LG-Y-A-F-A-P. A Pfam motif TPR_2 has been predicted in the N-terminus of the Rnq1p protein (figure 3.21).

Figure 3.21: Prediction of Rnq1p N-terminal TPR domain.
The Rnq1p amino acid sequence was imported into the free web-tool TPRpred (http://www. toolkit.tuebingen.mpg.de/tprpred/). Rnq1p residues 3-36 were predicted to form a TPR domain.

Proteins containing these domains tend to serve as scaffolds for the assembly of multi-protein complexes. TPR domains were originally identified in yeast where they mediate protein-protein interactions of cell cycle proteins, they are however also present in proteins involved in other functions, for example the co-chaperones Sti1p and Cpr6p, and the phosphatase Ppt1p contain TPR-domains. A particularly interesting idea proposed by a colleague (T.v.d.Haar) was that the prionisation of Rnq1p might create an array of TPR domains, a functional interaction surface that would represent a gain of function for the [*PIN*$^+$] prion.

3.2.10 Summary

There exists a wealth of information publicly available from many high-throughput studies that can be interrogated for information to assign function to a proteins of interest. Alongside this, the increasing accessibility and annotation of sequence data

has allowed for the creation of many prediction and characterisation tools. In this section, a number of these tools were used to advance our understanding or guide subsequent analyses into the cellular function of Rnq1p. The major findings that emerge from these analyses were as follows:

(a) Analysis of the Rnq1p sequence from different yeast species revealed that conservation of primary amino acid sequence of this protein is limited to the N-terminus, however overall composition of the protein is maintained and therefore may indicate that such composition rich in glutamine and asparagine also plays a role in Rnq1p function.
(b) The prediction of an FHA-domain, associated with proteins involved in cell cycle checkpoints and response to DNA damage amongst other roles, in combination with the finding that Rnq1p is phosphorylated at an SQ/TQ motif in response to DNA damage suggests Rnq1p may have a direct or indirect role in these processes.
(c) Rnq1p was predicted to be ubiquitinated, suggesting that the cell may find it necessary to control Rnq1p activity by rapid degradation, possibly in response to environmental or cellular changes.
(d) BLAST searches did not find any potential homologue for Rnq1p.
(e) A published systematic chemical-genomics screen that co-clustered deletion strains by shared phenotypic profiles has been useful in learning more about the roles that Rnq1p may be involved in, highlighting RNA metabolic processes, transcription, transport, chromosome organisation, response to stress and cell cycle processes as areas for further investigation.

3.3 The role of Rnq1p in translation termination

A possible link between Rnq1p and translation termination was indicated by experimental data obtained by Nadia Koloteva-Levine within the Tuite group. Specifically, Nadia discovered a positive interaction between Rnq1p and Sup45p using a yeast-2-hybrid growth assay, and this interaction was further validated by co-immunoprecipitation of Sup45p with a Rnq1p-TAP construct. An interaction between Rnq1p and Sup45p, the latter of which is known to interact intimately with Sup35p to mediate translation termination (see section 1.3.1), suggested that Rnq1p

might be capable of modulating Sup45p participation in translation termination, and therefore the level of stop-codon readthrough, thus revealing a possible role for Rnq1p in the cell.

3.3.1 The efficiency of translation termination is compromised in a [*PSI*$^+$] cell

Translation termination efficiency can be assayed *in vivo* by measuring the levels of a chosen reporter whose production depends on stop-codon read-through. In the studies presented here, the production of luciferase was monitored using the commercially available 'Dual-Glo Luciferase Assay Kit' (Promega) (see materials & methods 2.11) .

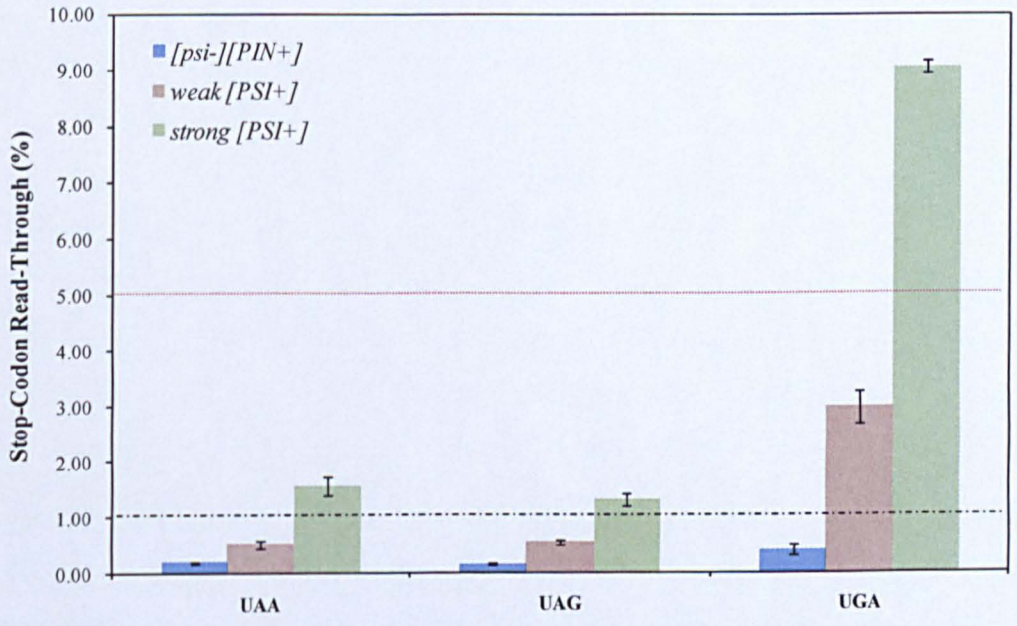

Figure 3.22: The effect of the [*PSI*$^+$] prion on translation termination efficiency at three stop codons.
Three strains differing in their [*PSI*$^+$] status were assayed for stop-codon read-through (UAA, UAG and UGA). The strong [*PSI*$^+$] strain was the most compromised in its ability to terminate translation, relative to the weak [*PSI*$^+$] and [*psi*$^-$] strains, with the latter [*psi*$^-$] strain demonstrating the greatest efficiency at stop-codon recognition. The dashed black line represents the read-through scale at 1 %, the dotted red line at 5 %.

Stop-codon read-through levels were assayed in a 74D [*psi⁻*][*PIN⁺*], 74D weak [*PSI⁺*] and 74D strong [*PSI⁺*] strain to validate the nonsense-suppression assay. In-line with previous findings, the strong [*PSI⁺*] strain correlated with the greatest level of stop-codon read-through, and the [*psi⁻*][*PIN⁺*] strain showed the greatest degree of termination efficiency at all stop-codons i.e. lower levels of read-through. Also as predicted, all three strains demonstrated enhanced read-through at the UGA stop codon, relative to the UAA and UAG stop codons.

3.3.2 Rnq1p over-expression increases stop-codon read-through

In order to determine the effect of Rnq1p over-expression on translation termination activity, it was necessary to employ a strain with the N-terminus of Sup35p deleted. The N-terminus of Sup35p is responsible for the aggregation propensity of this protein, and as shown in figure 3.22 in its aggregated state, as exemplified by [*PSI⁺*], this decreases the efficiency of stop-codon recognition and therefore increases stop-codon read-through. Therefore, to ascertain the effect of Rnq1p over-expression on termination efficiency that did not also reflect Rnq1p-induced changes to the aggregation state of Sup35p, a strain with the N-terminus of Sup35p deleted was used. In addition, Rnq1p over-expression causes toxicity in a [*PIN⁺*] state and since this deterioration of cell viability may have downstream consequences on termination activity not directly attributable to Rnq1p function, the *RNQ1* gene was deleted from these strains.

The 74D694 Sup35*ΔN rnq1Δ* strain was transformed with either full-length *RNQ1* under the control of the constitutive GPD promoter (pAG425-Rnq1, 2μ) or the N-terminus (aa 1 – 152) of Rnq1p also under the control of the GPD promoter (pAG425-NRnq1, 2μ). The backbone plasmid (pAG425, 2μ) was used as a control to demonstrate the translation termination activity of this strain prior to manipulations in Rnq1p level.

The control strain carrying the pAG425 plasmid showed similar read-through levels to the 74D [*psi⁻*][*PIN⁺*] strain as shown in figure 3.22 (figure 3.23). Both the N-terminus of Rnq1p and the full-length protein increased the percentage read-through of stop-codons, though the defect was about 2x fold greater for the full-length

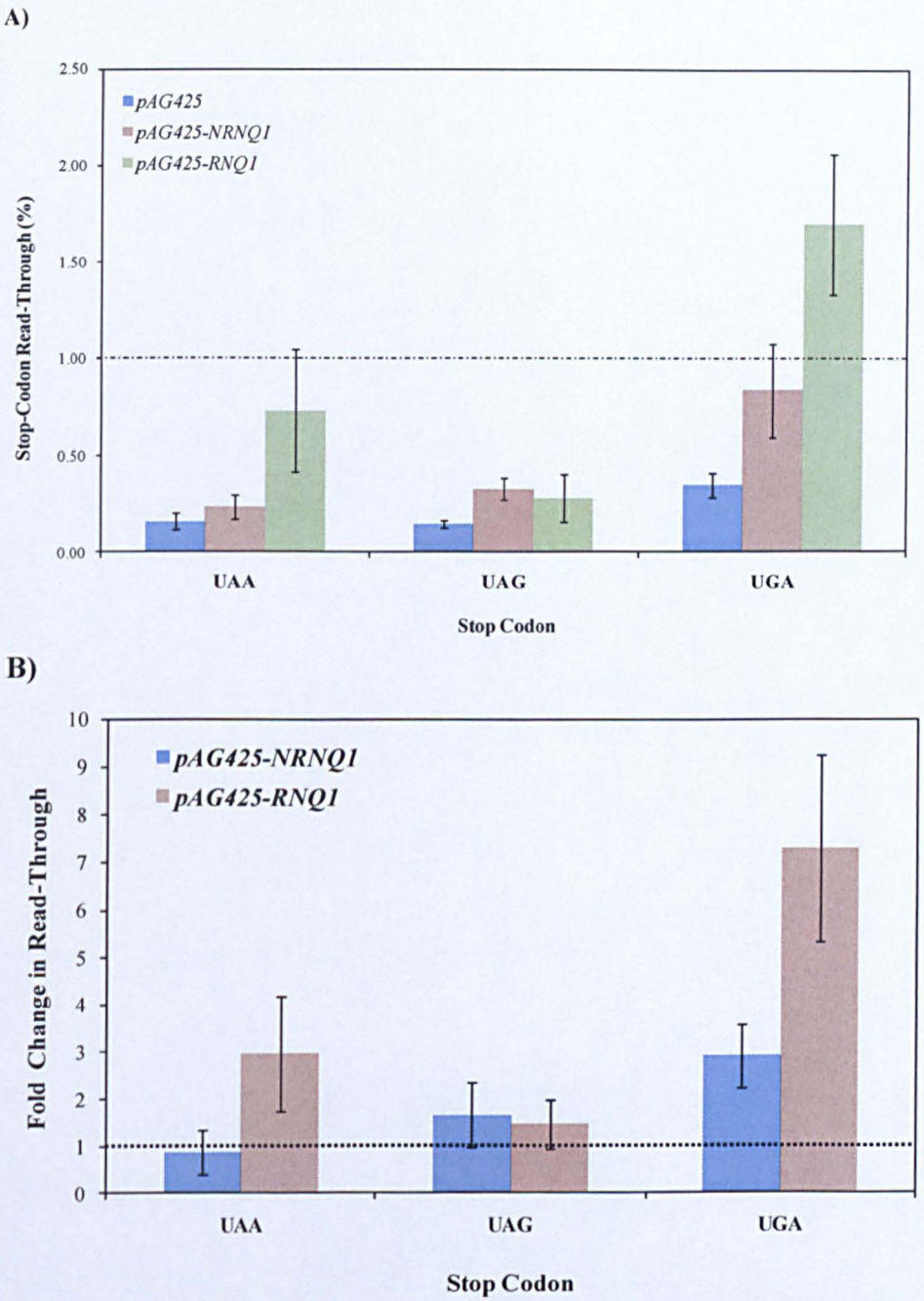

Figure 3.23: The effect of Rnq1p on translation termination efficiency.
A) Three strains were assayed for stop-codon read-through (UAA, UAG, UGA): one expressed the N-terminus of Rnq1p representing residues 1-152 (pAG425-NRnq1); another expressed the full length Rnq1p protein (pAG425-Rnq1); and the last carried the vector backbone (pAG425). The dashed black line represents the read-through scale at 1 %. B) The fold-change in stop-codon read-through relative to the control (vector backbone, pAG425). Full-length Rnq1p (pAG425-Rnq1) increases UGA stop-codon read-through 7x fold, relative to the control. The N-terminus of Rnq1p causes a less pronounced defect, with a 3x fold increase in UGA stop-codon read-through. Results reflect the average of 8 analyses over 2 separate experiments.

protein relative to the N-terminus alone (figure 3.23). Over-expression of full-length Rnq1p gave rise to a ~7x fold increase in read-through relative to the control strain, carrying the pAG425 plasmid (figure 3.23). The termination defect brought about by full-length Rnq1p was not as significant as the termination defect associated with Sup35p existing in a weak [*PSI*$^+$] state (refer to figure 3.23).

These data suggest that Rnq1p antagonises the activity of the termination factors in recognising stop-codons and/or terminating polypeptide synthesis.

3.3.3 Over-expressing the N-terminus of Rnq1p is not sufficient for toxicity

In the 74D [*psi*$^-$][*PIN*$^+$] strain, full-length Rnq1p over-expressed from the pAG425-Rnq1p construct caused a growth defect that was not observed when the N-terminus of Rnq1p was expressed from pAG425-NRnq1 (figure 3.24). This may indicate 1) that the toxicity of Rnq1p is associated with the C-terminus; 2) that toxicity requires full-length Rnq1p; 3) that any residual toxicity of the N-terminus is not sufficient to bring about a growth defect; 4) That the N-terminus was not expressed at the same level as full-length Rnq1p. Expression of the C-terminus of Rnq1p would confirm whether toxicity required the C-terminus or full-length Rnq1p.

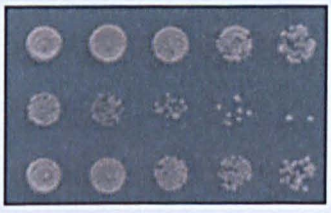

Figure 3.24 Determining the toxicity of the Rnq1p N-terminus and the full-length Rnq1p protein expressed from the pAG425 construct.
The pAG425 constructs were expressed in a 74D [*psi*$^-$][*PIN*$^+$] strain and full-length Rnq1p, but not the N-terminus of Rnq1p, was toxic.

When the same pAG425-based constructs were expressed in the Sup35*ΔN rnq1Δ* strain or a Sup35*ΔN* strain, again no toxicity was associated with the N-terminus of Rnq1p (figure. 3.25). In the Sup35*ΔN rnq1Δ* strain, over-expression of full-length

Rnq1p did not cause any growth defect, as expected, since Rnq1p-mediated toxicity is usually dependent on [*PIN*$^+$]. Repeated attempts failed to generate transformants for full-length Rnq1p in the Sup35*ΔN* strain. This may indicate a synthetic lethality between Rnq1p when the protein is constitutively over-expressed in the cell and the absence of Sup35p's N-domain, since the same plasmid could be introduced into the 74D strain where the Sup35p protein was intact.

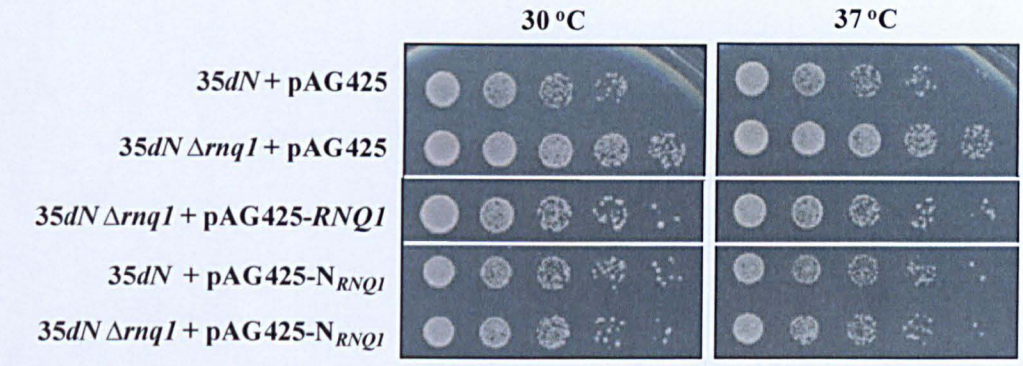

Figure 3.25 The effect on Rnq1p toxicity of deleting the Sup35p N-terminus

A plate assay to determine the effect of deleting the N-terminus of Sup35p, alone and in combination with a deletion of the *RNQ1* gene, on the toxicity of full-length Rnq1p and the N-terminus of Rnq1p (1-152 residues) when expressed from a 2μ plasmid under the control of a constitutive GPD promoter.

3.3.4 Rnq1p over-expression is toxic in the absence of Sup35p's N-terminus.

Over-expression of Rnq1p is toxic in a [*PIN*$^+$] cell, and continues to be toxic when the N-terminus of Sup35p is deleted (figure.3.26). This would suggest that Rnq1p toxicity is not dependent on the Sup35p N-terminus; however in contrast to the result shown in figure 3.25 with the pAG425-based construct, full-length pYES2-based Rnq1p demonstrated toxicity in the combined absence of Sup35p's N-terminus and the *RNQ1* gene (figure 3.26). The pYES2-103Q huntingtin construct was also toxic in the absence of Sup35p's N-terminus and the *RNQ1* gene. The difference between pAG425-Rnq1p and pYES2-Rnq1p may be expression level, with pYES2-Rnq1p expressing considerably more Rnq1p than the pAG425 construct – this could be determined by quantitative western blot analysis. In support of this suggestion was the observed toxicity of the pYES2-103Q huntingtin construct which also normally requires [*PIN*$^+$] presence for toxicity. Differences in expression level could account

for the difference in results obtained between the two plasmids pAG425 and pYES2. The presence of Rnq1p and 103Q toxicity in the absence of the *RNQ1* gene when the N-terminus of Sup35p is also removed may indicate a role for the N-terminus of Sup35p in suppressing polyglutamine or aggregation-associated toxicity – doing sufficiently well in a wild-type [*pin*-] cell, but ineffective in a wild-type [*PIN*$^+$] cell. Specifically, it may be that once the suppressing function of Sup35p's N-terminus is removed, Rnq1p or 103Q over-expression causes [*PIN*$^+$]-independent toxicity. To determine if this phenotype is specific to the absence of the N-terminus of Sup35p, it would be necessary to reintroduce the N-terminus of Sup35p in trans via a plasmid. If this were the case, one would expect expression of the N-terminus to restore growth in the *rnq1Δ* strain while co-expressing either pYES2-Rnq1p or pYES2-103Q.

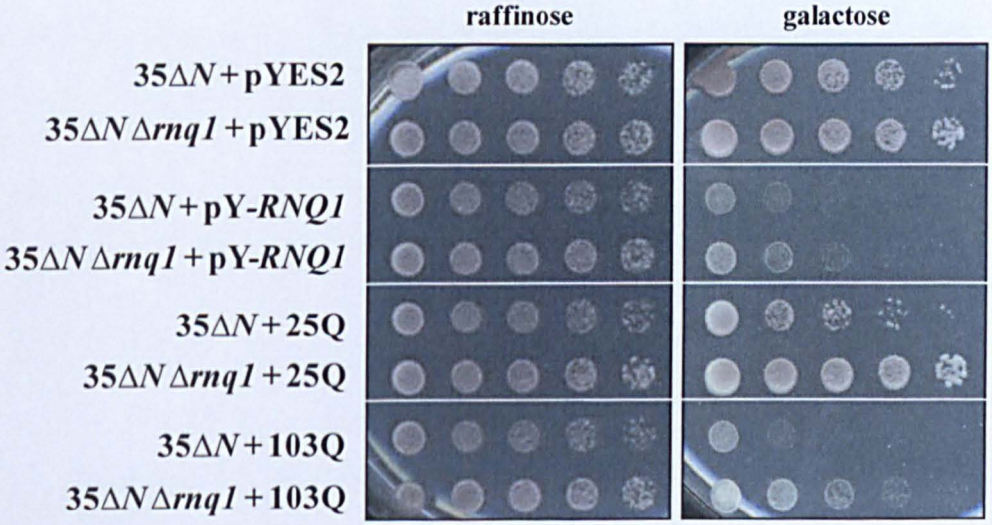

Figure 3.26: The effect on Rnq1p and 103Q toxicity of deleting the Sup35p N-terminus.
A plate assay to determine the effect of deleting the N-terminus of Sup35p, alone and in combination with a deletion of the *RNQ1* gene, on the toxicity of full-length Rnq1p and the 103Q-huntingtin fragment expressed from the 2μ plasmid pYES2, under the control of the *GAL*-promoter. (pYES2 = vector backbone, pYES2-25Q = control plasmid for pYES2-103Q).

3.3.5 Rnq1p induces growth defects in the presence of the *sup45-2* allele

Since Rnq1p was shown to be a negative regulator of translation termination, it was of interest to determine the effect of Rnq1p over-expression in a strain compromised

in translation termination activity, specifically, a mutant allele of *SUP45*, *sup45-2*, derived from yeast strain MT604 was tested. The mutant shows detectable stop-codon read-through though there is no growth defect at 30 °C.

Over-expression of Rnq1p in the *sup45-2* mutant resulted in a growth defect that was not observed when Rnq1p was over-expressed in an otherwise isogenic strain (carried the wild-type *SUP45* gene) (figure 3.27). This result suggested that over-expression of Rnq1p further antagonised the termination defect of the *sup45-2* mutant, leading to decreased cell viability.

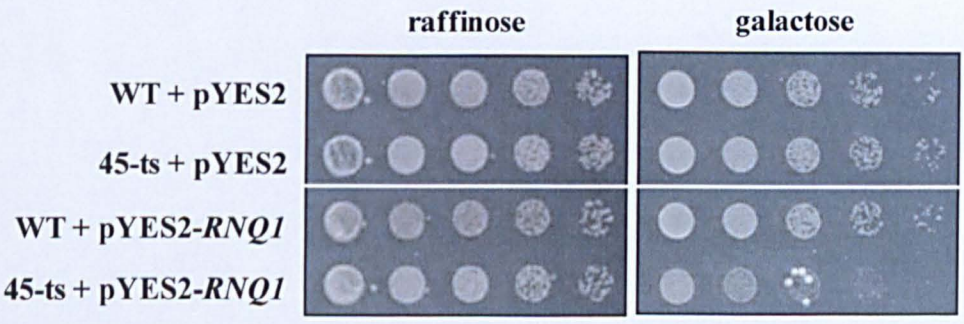

Figure 3.27 Rnq1p over-expression causes a growth defect in a strain with impaired Sup45p translation termination activity.
A plate assay demonstrating that Rnq1p over-expression in a strain harbouring a temperature sensitive allele of *SUP45*, *sup45-2* (45-ts), relative to an isogenic but *SUP45* wild-type strain (WT), results in a growth defect.

3.3.5 Rnq1p and the carbon source specific modulation of translation termination

The translation termination activity, of yeast strain BY4741, varied considerably on carbon source, with termination being more accurate on glucose, and significantly less efficient on galactose and sucrose (figure 3.28, C. Solcheid). The link between Rnq1p and carbon source was of interest, given results from the proteomics project (Chapter 3). To determine whether Rnq1p was influencing the carbon source specific translational defects, suppression of *ade1-14* was tested in [*PIN*$^+$][*psi*$^-$] and [*pin*$^-$][*psi*$^-$] derivatives of the 74D strain on the different carbon sources. Cultures of 74D, were grown overnight, washed, and a serial dilution in water was spotted onto agar plates differing in their carbon source: glucose, fructose, galactose, maltose, glycerol and sucrose (figure 3.29). No homogenous colour differences were observed, indicating

the absence of significant translation termination differences on the carbon sources, however white sectors appeared on sucrose and galactose, and to a lesser degree fructose, and these events only occurred in a [*PIN*$^+$] background. Therefore one hypothesis that could explain the read through levels shown in figure 3.28 was that the white sectors represented [*PSI*$^+$] *de novo* formation events, and that the degree of stop-codon read-through (figure 3.28) represented populations of [*PSI*$^+$] cells that occurred at different frequencies on the various carbon sources. To test this, it was first necessary to determine the read-through levels of a [*PSI*$^+$] strain on the various carbon sources – if the differences previously observed for BY4741 ([*PIN*$^+$]) were attributed to [*PSI*$^+$] conversion events, then read-through levels should be equivalent in a [*PSI*$^+$] strain regardless of carbon source.

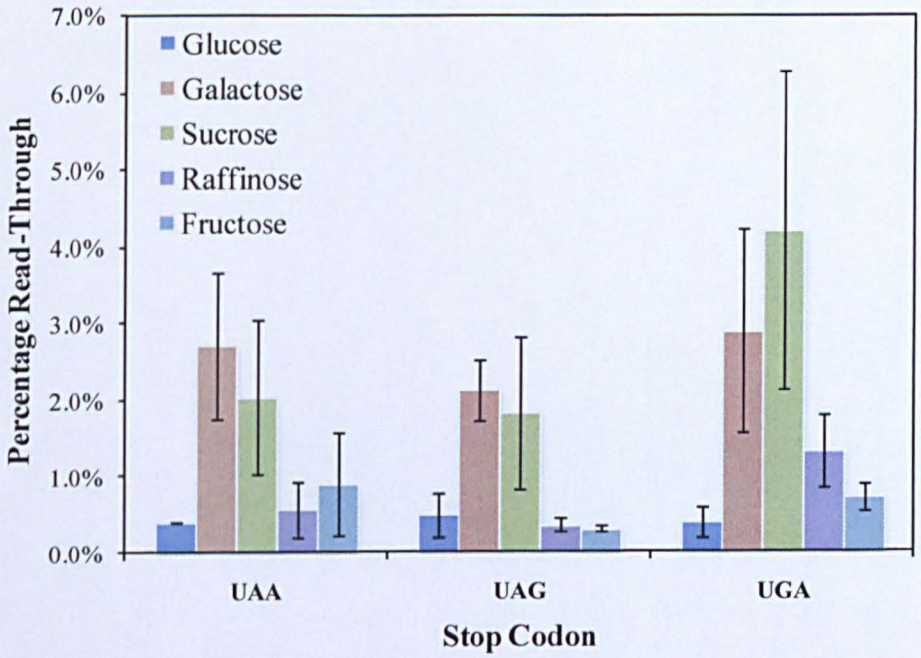

Figure 3.28: The effect of carbon source on termination efficiency in a [*PIN*$^+$] strain.
Stop-codon read-through levels of BY4741 [*PIN*$^+$] when grown on different carbon sources: glucose, galactose, sucrose, raffinose and fructose. Glucose displays the lowest level of stop-codon read-through, while sucrose and galactose show considerably higher levels of read-through. Data provided by C. Solscheid.

The 74D [*PSI*$^+$] strain however, did show differences in read-through on galactose when compared to glucose, suggesting that the data shown in figure 3.28 was not indicative of carbon-specific differences in [*PSI*$^+$] conversion. However, while the 74D [*PSI*$^+$] demonstrated a familiar level of read-through on glucose, in contrast to results obtained with BY4741 [*PIN*$^+$], read-through levels on galactose were roughly 2x fold less i.e. there was increased stop codon-read-through on glucose than galactose (figure 3.30).

Comparing these results (table 3.1) suggests either: 1) that there are strain specific differences in the influence of carbon source on translation termination activity; or 2) that while conversion from [*psi*$^-$] to [*PSI*$^+$] results in increased read-through on glucose, the same conversion results in a decrease (UAA, UAG) or no change (UGA) on galactose.

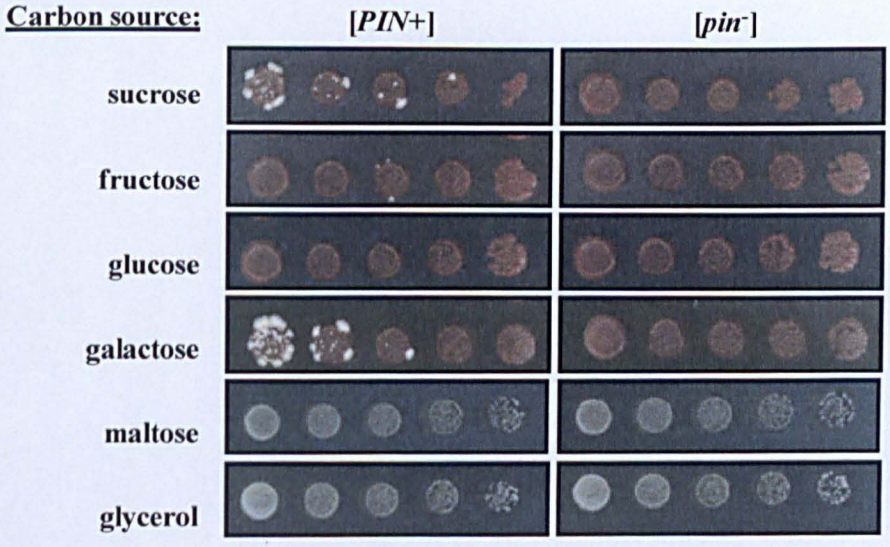

Figure 3.29 Interaction between carbon source and the [*PIN*$^+$] prion.
A 5x fold serial dilution of 74D [*PIN*$^+$] and [*pin*$^-$] cells spotted onto different carbon sources reveals [*PIN*$^+$]-specific white sectoring on sucrose, galactose and fructose.

The appearance of white sectors on different carbon sources, thought to be indicative of [*PSI*$^+$] conversion events, were subsequently restreaked onto YPD agar containing 5 mM GdnHCl three times in order to confirm whether they were indeed the result of [*PSI*$^+$] prion appearance (reversible phenotype following growth on GdnHCl). The

inability to obtain red colonies indicated that the white sectors were non-curable and therefore most probably represented genetic suppressor events.

To address the issues raised here, the 74D [*PIN*$^+$] [*psi*$^-$] strain was assayed on galactose. If the 74D [*PIN*$^+$] strain demonstrated little change or enhanced read-through on galactose relative to the read-through seen in the 74D [*PSI*$^+$] strain, then this would indicate that [*PSI*$^+$] conversion causes reduced or little change to read-through on galactose, in contrast to the change seen in read-through on glucose (much increased). If however, the 74D [*PIN*$^+$] strain showed reduced levels of read-through on galactose relative to the [*PSI*$^+$] strain, this would suggest that the results seen here represents strain specific differences in and the effect carbon source has on translation termination activity. Unfortunately, the transformants failed to grow reliably and results for this experiment were not obtained.

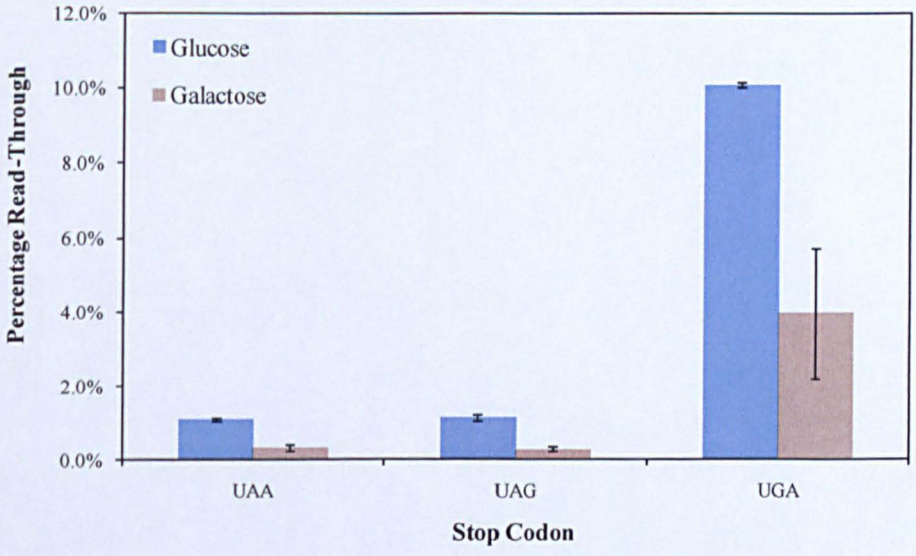

Figure 3.30 The effect of carbon source on stop-codon read-through in a [*PSI*$^+$] strain.
Stop-codon read-through levels of a 74D [*PSI*$^+$] strain when grown on galactose or glucose. Read-through was at least 2x fold higher on glucose than on galactose for this strain in the [*PSI*$^+$] state.

In addition, the original question of whether a BY4741 [*pin*$^-$] strain would generate the same carbon source –specific termination defects as the standard BY4741 [*PIN*$^+$]

strain, and therefore the exact contribution of Rnq1p (if any) to this phenotype remains to be addressed.

Condition	glu	gal	trend
BY4741 [*PIN*$^+$]	0.6	2.9	↑
74D [*PSI*$^+$]	10.09	3.96	↓

Condition	glu	glu	trend
BY4741 [*PIN*$^+$] → 74D [*PSI*$^+$]	0.6	10.09	↑

Condition	gal	gal	trend
BY4741 [*PIN*$^+$] → 74D [*PSI*$^+$]	2.9	3.96	↑↓

Table 3.1: Comparing the effect of carbon source on 74D [*PSI*$^+$] and BY4741 [*PIN*$^+$] UGA stop-codon read-through levels.
Either [*PSI*$^+$] only elevates read-through on glucose but not on galactose, or carbon source effects translation termination activity of the BY4741 and 74D yeast strains differently. (↑↓) indicates over-lapping error bars therefore non-significant trend.

3.3.6 A subset of Sup35p mutations do not modulate Rnq1p toxicity

With access to a range of 74D Sup35p mutants, I was interested to determine whether mutations in Sup35p would modulate the toxicity of Rnq1p. As shown in figure 3.2.6 Rnq1p is toxic even in cells expressing a Sup35pΔN mutant; however there were indications that the N-terminus may normally play a role in suppressing polyglutamine or aggregation-associated toxicity in a [*pin*$^-$] cell.

To determine the impact of these mutations on the termination activity of Sup35p through a stop-codon read-through assay. Both a deletion of the repeat region 3 (R3) and deletion of the entire oligopeptide repeat (OPR) region resulted in increased levels of stop-codon read-through, with an error level similar to that of a weak [*PSI*$^+$] strain.

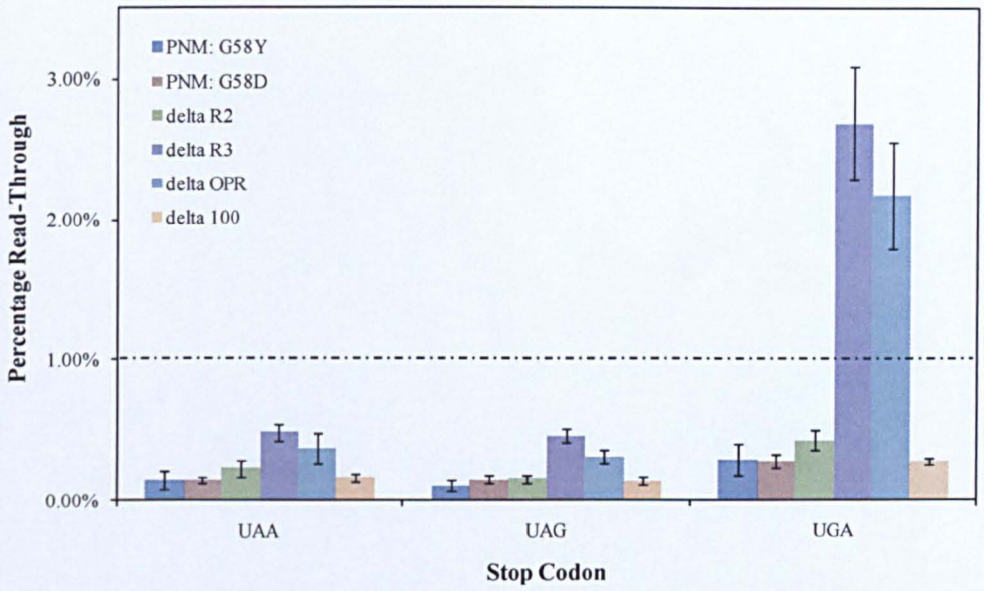

Figure 3.31: Differing levels of stop-codon read-through associated with mutations of the N-terminus of Sup35p.
A deletion of the repeat region 3 (R3) or the oligopeptide repeat (OPR) region appear to result in an increased rate of stop-codon read-through.

The toxicity of Rnq1p in the various Sup35p mutants was determined by comparing growth of the mutants with and without the over-expression of Rnq1p, using the pYES2 and pYES2-*RNQ1* constructs, respectively (figure 3.32).

Rnq1p was toxic in all deletion mutants tested, therefore in terms of growth defects, these N-terminal deletions of Sup35p did not affect the toxicity of Rnq1p. It would be of interest to determine whether these mutants affect the toxicity of Rnq1p in the [*pin*$^-$] state, by curing the transformed strains and repeating the above growth assay. If the N-domain suppresses Rnq1p toxicity in the [*pin*$^-$] state, the N-terminal mutants may indicate a region of the N-terminus responsible for this activity.

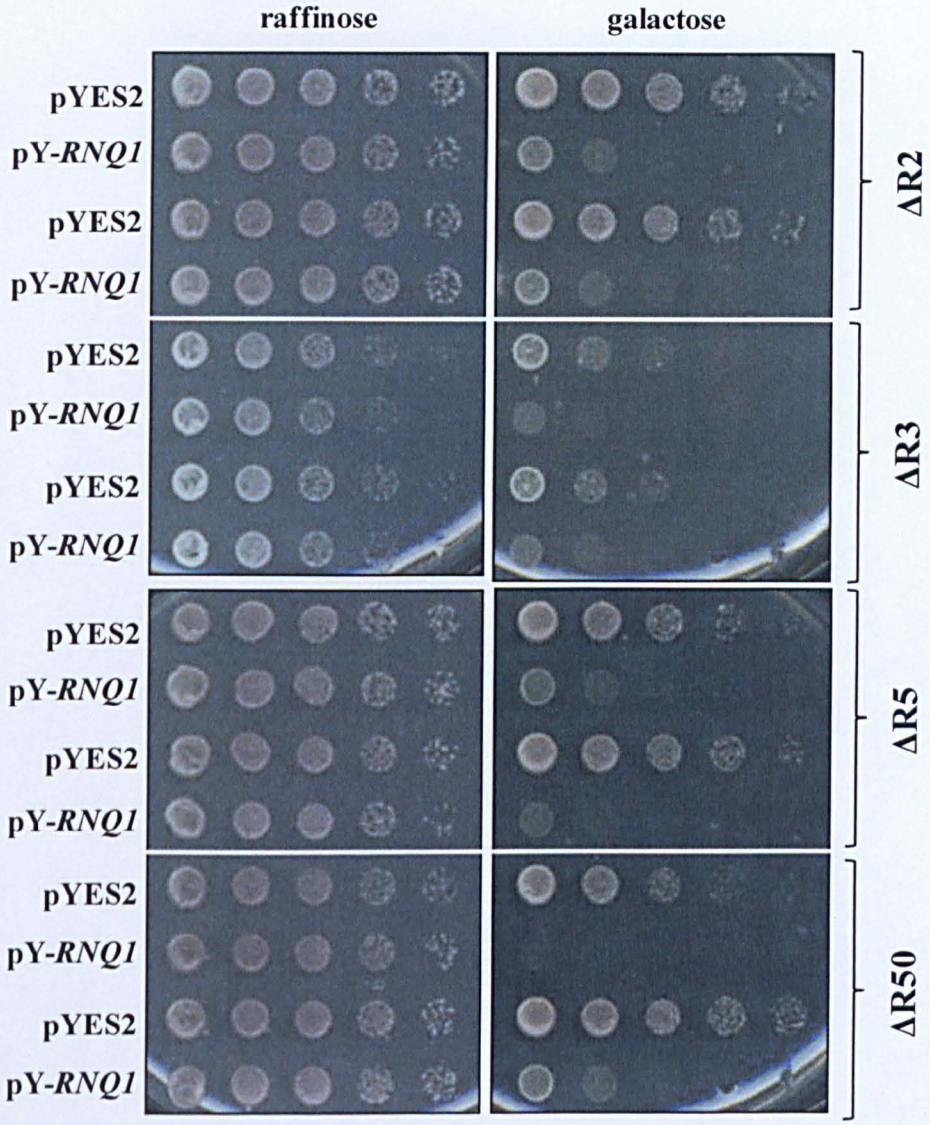

Figure 3.32: The effects of Sup35p N-terminal mutants on Rnq1p toxicity. Over-expression of Rnq1p (pYES2-*RNQ1*) in a range of N-terminal mutants of Sup35p does not affect Rnq1p associated growth defects or toxicity, in a [*PIN*$^+$] background. Duplicates shown.

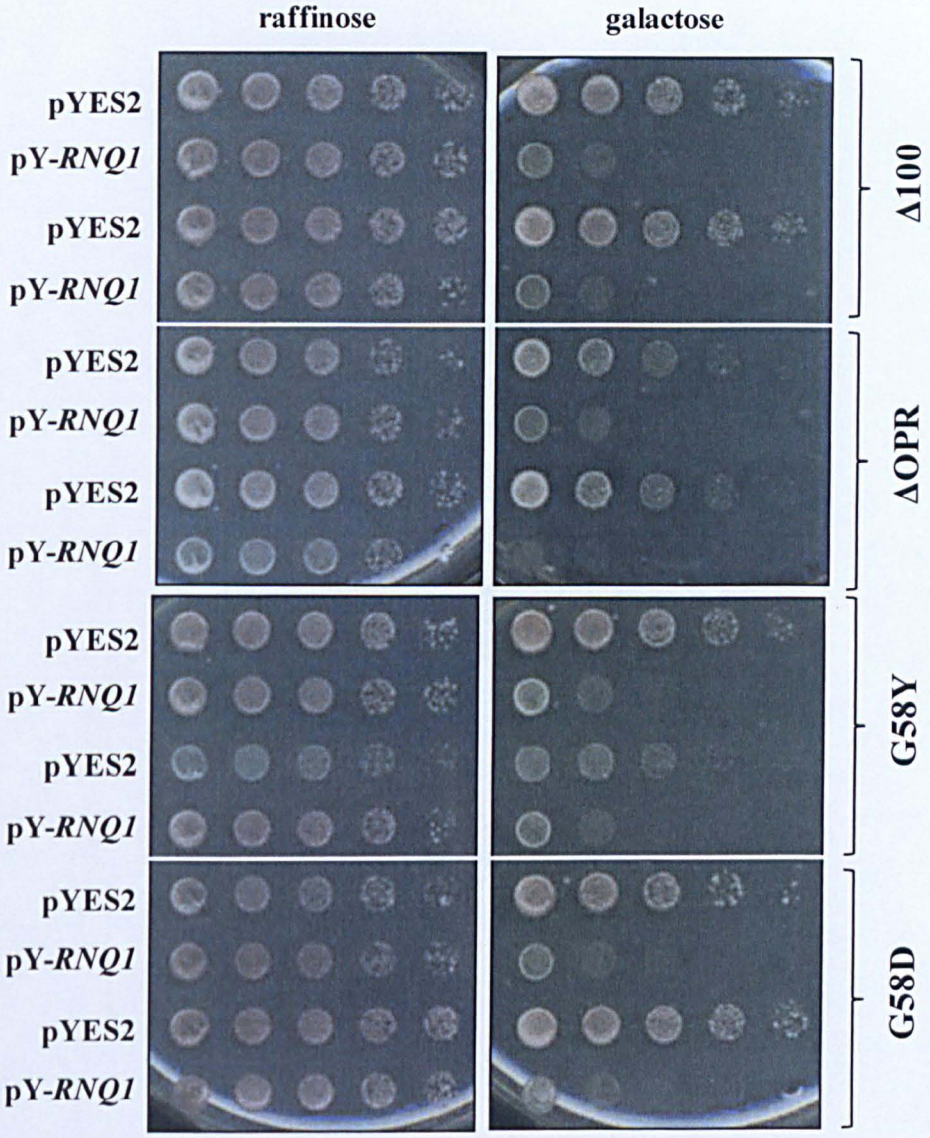

Figure 3.33: The effects of Sup35p N-terminal mutants on Rnq1p toxicity. Over-expression of Rnq1p (pYES2-*RNQ1*) in a range of N-terminal mutants of Sup35p does not affect Rnq1p associated growth defects or toxicity, in a [*PIN*$^+$] background. Duplicates shown.

3.4 A proteomics approach to identifying Rnq1p function

Rnq1p is a prion protein of the yeast *S. cerevisiae* and the subject of many experiments that seek to understand the mechanism(s) by which Rnq1p induces the *de novo* conversion of other yeast prion proteins from their [*prion*$^-$] to their [*PRION*$^+$] state. Despite this familiarity with Rnq1p in the literature, its cellular function remains unknown. Increasing evidence for yeast prion proteins permeating all levels of cellular function (Nemecek *et al.*, 2009; Tuite *et al.*, 2009), possibly an indication of their importance for long or short-term cellular dynamics, has made identifying the role of Rnq1p in the cell similarly compelling.

A yeast strain harbouring a deletion of the *RNQ1* gene is viable, yet over-expression of the Rnq1p protein leads to a loss of cell viability (Douglas *et al.*, 2008c). The toxicity of Rnq1p however is attributed to prion-specific amyloid or oligomer accumulation, since the toxicity phenotype is only observed when the endogenous Rnq1p protein exists in its prion ([*PIN*$^+$]) state; no toxicity is observed when Rnq1p is over-expressed in a cell lacking the prion form of Rnq1p. It cannot, however, be dismissed that Rnq1p also acquires a toxic gain-of-function in the presence of the [*PIN*$^+$] prion.

Since it is expected that each protein encoded by the yeast genome performs at least one function in the cell, the removal of any single protein or an increase in the abundance of any single protein, should be expected to perturb the function to which it is prescribed. The absence of perturbation would only be expected from those proteins involved in a redundant function, where redundancy serves to mask the role of the particular protein in question. Additionally, a functional perturbation will not be detected for a protein whose activity is required only in rare functional events e.g. a particular stress or growth condition, unless the relevant condition is factored into the investigation. In contrast, a protein possessing many non-redundant, central functions would be expected to perturb many functions if the respective protein is made unavailable, or produced to excess. Thus, it is possible to identify the function(s) of a single protein if one has the ability to identify functional perturbations brought about by this protein, within the cell.

One way to identify functional perturbation(s) resulting from changes in the levels of a single protein is to perform high resolution analyses of the cellular proteome across

these changes. Constituents of the proteome in their entirety encapsulate every possible function within a cell; individually, the constituents of the proteome represent subsets of functions. Presently, roughly two-thirds of yeast proteins are annotated according to their respective function(s) and therefore, identifying changes to the levels of these functionally annotated proteins is synonymous with identifying a "functional" perturbation.

The high-resolution proteomic approach adopted in this study to identify functional perturbations of the proteome brought about by changes in the expression level of Rnq1p was quantitative, label-free liquid chromatography (LC) matrix-assisted laser desorption ionisation (MALDI) mass-spectrometry (MS).

3.4.1 Quantitative LC/MALDI-MS analysis of Rnq1p induced changes to the yeast proteome

In an attempt to identify the cellular function(s) of Rnq1p within the cell, where no function is currently known, collaboration was initiated with colleagues at the pharmaceutical company Pfizer Ltd. and the mass-spectrometry company Bruker. The division of labour was as follows:

1 – I prepared the required yeast strains and provided extracts of yeast lysate

2 – Colleagues at Pfizer performed sample preparation for analysis and preliminary screening of the samples

3 – Colleagues at Bruker performed the LC/MALDI-MS analysis of the prepared samples and extracted statistically significant quantitative data

4 – I performed bioinformatic analyses to extract biological significance from the quantitative data and performed wet lab analyses to validate biological indications.

3.4.1.1 Strain and extract preparation

Crude cell yeast lysates were prepared from biological triplicates of three 74D [*pin*$^-$] yeast strains differing only in their expression of Rnq1p: a strain in which Rnq1p

was over-expressed via the pYES2-*RNQ1* plasmid in addition to expression from the endogenous *RNQ1* gene locus; a strain transformed with the pYES2 backbone and therefore with expression of Rnq1p only from the endogenous *RNQ1* gene locus; and a strain transformed with the pYES2 backbone but carrying a deletion at the endogenous *RNQ1* locus and therefore with no expression of Rnq1p.

A [*pin*$^-$] background was chosen for this study since proteomic changes would be expected to arise only as a consequence of changes to the level of Rnq1p expression between the three strains. In contrast, a *RNQΔ1* deletion strain when compared to the pYES2 and pYES2-*RNQ1* transformed [*PIN*$^+$] strains would differ not just in the abundance of Rnq1p, but also the prion status since a *rnq1Δ* strain would also not be [*PIN*$^+$] – thus introducing two variables into the study rather than one. Further, Rnq1p over-expression in a [*PIN*$^+$] background causes toxicity and it would not be possible to separate proteomic changes resulting from increased cellular abundance of Rnq1p from those changes associated with prion-specific toxicity events and the non-specific downstream consequences of this toxicity. In summary, a [*PIN*$^+$] strain would not have allowed us to confidently identify changes to the proteome that were specific only to the expression level of Rnq1p in the cell.

Triplicate 0.5 L 2% galactose 2 % raffinose selective minimal media cultures of each strain were harvested when a cell density of between 2.1 – 3.7 x 10^7 cells/mL was reached. The cell pellets were resuspended in 1 mL of lysis buffer (section 2.10.5) before pipetting 200 µl aliquots of the cells into liquid nitrogen for rapid freezing. The frozen cells were stored at – 80 °C overnight before mechanical lysis and protein lysate extraction as detailed in materials & methods section 2.10.5. The protein lysates were subsequently handed over to colleagues at Pfizer.

An aliquot from each of the harvested cultures of the pYES2 and the pYES2-*RNQ1* transformed strains was retained for sedimentation analysis to confirm the [*pin*$^-$] status of the cells post-culture (figure 3.34). The pYES2 cultures appeared to be [*pin*$^-$], since most of the Rnq1p protein was in the soluble (S) fraction rather than the pellet (P) fraction. For the pYES2-*RNQ1* transformed cultures, there was also signal for Rnq1p in the pellet fraction, however in strains pYES2-*RNQ1*-1 and pYES2-*RNQ1*-3 the pellet fraction signal was still clearly weaker than the soluble fraction signal for Rnq1p, indicating that these strains were also likely to be [*pin*$^-$]. The extra

Rnq1p in the pellet fraction for the strains over-expressing Rnq1p may represent a normal distribution for Rnq1p that due to the low abundance of Rnq1p in the cell is not normally detectable. Alternatively, the pelleted Rnq1p protein may represent some degree of Rnq1p aggregation in the [*pin*$^-$] state however, since Rnq1p over-expression is toxic in a [*PIN*$^+$] but not in a [*pin*$^-$] background, this would imply that either (1) Rnq1p aggregates formed in a [*pin*$^-$] background are structurally distinct from those formed in a [*PIN*$^+$] background such that the former are non-toxic (2) the folding intermediates of Rnq1p are different in a [*PIN*$^+$] and [*pin*$^-$] background, resulting in toxic oligomers only in a [*PIN*$^+$] background or (3) Rnq1p acquires a toxic gain of function in a [*PIN*$^+$] background but not in a [*pin*$^-$] background.

The sample pYES2-*RNQ1*-2 appeared to have a higher level of Rnq1p in the pelleted fraction and indicated this strain may have converted from [*pin*$^-$] to [*PIN*$^+$]; this would have been an early event in the culturing of this strain, or prior to inoculation, given the degree of Rnq1p observed in the pellet fraction for this sample.

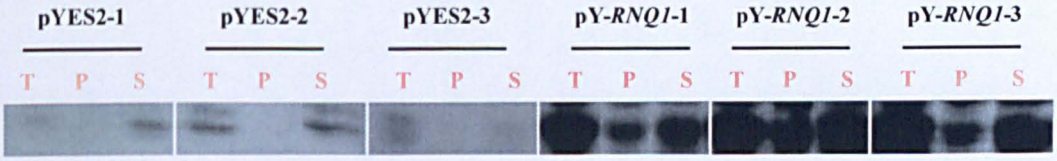

Figure 3.34 Sedimentation analysis of lysates used in the proteomics study.
An aliquot of the three [*pin*$^-$] + pYES2 cultures and three [*pin*$^-$] + pYES2-*RNQ1* cultures used in proteomics investigation were tested by sedimentation analysis to determine the solubility state of Rnq1p in these strains. 'T' = total fraction; 'S' = soluble fraction; 'P' = pellet fraction.

3.4.1.2 The technique employed: quantitative LC/MALDI-MS

The yeast cell proteome is very complex, for it encapsulates not only the many thousands of proteins that may be present in a cell at any one time, but also the different forms of each protein if subjected to post-translational modification or splicing. In addition, complexity arises from the dynamic range of protein abundance: some proteins exist with fewer than 50 copies per cell, others with more than 1, 000, 000 copies per cell (Weissman, 2003), and this copy number can vary

with the stages of the cell cycle, or with the environment in which the yeast cell finds itself.

To analyse the yeast proteome, it is first necessary to reduce this complexity, since it is very easy for lower abundant proteins to be 'masked' by the more abundant proteins, obscuring an accurate view of proteome dynamics. Therefore to overcome the complications of accurate proteome analysis concomitant with complex samples, techniques have been developed to reduce this complexity prior to analysis. The method for reducing complexity very much depends on the intended methods for downstream analysis of the sample. In this study, liquid chromatography was used to reduce sample complexity, and MALDI-MS used to identify the components of the proteome and changes therein.

Determining the molecular weight of a protein is not sufficient for its identification. Instead, the individual masses of peptides generated from a protein by protease digestion can be used to identify the protein in a process called 'peptide mass fingerprinting' (PMF). Proteases such as trypsin can be used to cleave between specific amino acid sequences and therefore, if the sequence of a protein is known, the peptides generated by digestion of the protein with a particular protease can be predicted. Since most protein sequences are unique, the peptide mass fingerprint is also unique to each protein. The more peptides identified whose masses correspond to the predicted fragments of the digested protein, the more confidence there will be in the identification of the protein.

MALDI-MS is used to identify the masses of peptides present within a digested protein lysate and involves the ionisation and evaporation of peptides from a discrete position on the surface of a metal target plate. A small aliquot of the sample to be analysed is deposited at a precise position on the target plate and mixed with a 'matrix' solution which crystallises within the sample upon drying. Under the focus of a laser, the matrix absorbs a great deal of energy which it imparts to the sample, ionising the peptides within it and allowing for their evaporation from the surface of the target place: hence the method is referred to as '*matrix-assisted laser desorption ionisation*' (MALDI).

The gaseous, ionised peptides can be separated by charge, and this charge is also exploited to accelerate the peptides through a vacuum where the peptides then

separate by mass, the peptides with greater mass travel slower through the vacuum than the peptides of smaller mass. Thus, the mass of each peptide can be determined by the time taken for it to reach a detector.

However, if the crude digested protein lysate is deposited on to the MALDI target plate and analysed by MALDI-MS, the mass spectra will be dominated by peaks corresponding to the peptides of the most abundant proteins, masking the identity of lower abundant peptides. The ability to detect a greater number of peptides in the mix requires that the digested protein lysate be fractionated into many separate fractions. Each fraction will be deposited on to the MALDI target plate occupying a position dedicated to each fraction. Therefore, a more manageable cluster of peptides, as present in each fraction, will be analysed at any one time.

For the experiments with Rnq1p the fractionation of peptides from the digested protein lysates was performed by reversed-phase liquid chromatography. Essentially, the peptides were loaded onto a column packed with beads of a chosen size and pore size, and a non-polar resin termed the stationary phase which consists of hydrophobic alkyl chains of a selected length. Before the peptide mix was loaded onto the column, it was reconstituted in a polar mobile phase, ensuring that the hydrophobic properties of the peptides were attracted to the hydrophobic stationary phase, and bind to it. As the mobile phase is made increasingly hydrophobic, the less hydrophobic peptides dissociate from the column in favour of interactions with the mobile phase, and this will result in their elution from the column. The peptides eluted from the column were collected in fractions, with the earlier fractions corresponding to the least hydrophobic peptides and the later fractions, that demonstrated increased retention time, corresponding to the most hydrophobic peptides. These fractions were spotted directly onto specific positions of the MALDI target plate, which was pre-coated with matrix solution, and then analysed by MALDI-MS.

In this study, it was not necessary to assign an identity to each peptide. The interest was in identifying reproducible changes between the spectra obtained from the three different sample conditions, since varying spectral features correspond to peptides that differ between the three conditions. The spectral regions identified as varying were then selected for further study and identification. This retrospective analysis

was possible since the spectra were associated with a particular retention time, which was associated with a known position on the MALDI target plate. Given the abundance of peptides derived from a digestion of a protein lysate however, it was still necessary to obtain greater sequence detail about the peptides of interest beyond the PMF, and this is achieved by tandem mass-spectrometry (MS/MS). This involves repeated MS analysis of the interesting fraction, isolation of the precursor ion/peptide of interest, and further fragmentation in a second mass analyser to obtain greater mass detail for accurate identification of the corresponding protein. This process is summarised in figure 3.35.

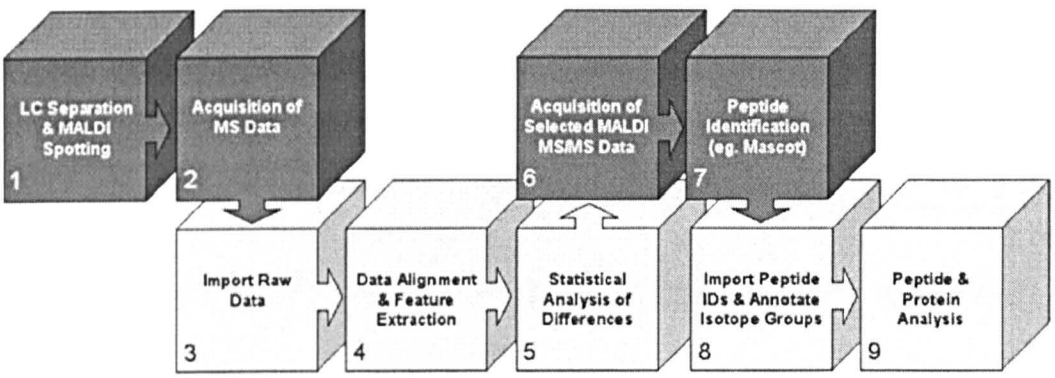

Figure 3.35 Workflow for label-free quantitative proteomics based on LC/MALDI mass spectrometry.
Following LC separation, fractions were spotted onto the MALDI target and MS data was acquired (1, 2). All MS raw spectra were imported into the elected analysis tool (3) for retention time alignment of the mass spectral intensity maps and subsequent feature extraction (4). This was followed by statistical analysis of the spectral differences (5) to generate a list of masses for targeted acquisition of MS/MS spectra (6) to facilitate peptide identification (7). Figure copied from Neubert *et al* (Neubert, 2008).

3.4.2 Extracting biological significance from quantitative data

In total, 483 proteins were identified as reproducibly altered in their expression level as a consequence of changes to the expression level of Rnq1p (Appendix 1). Results received from Bruker were in the form of expression level ratios, or fold-differences, for each identified protein in three different conditions:

- ***rnq1Δ*:pYES2**
  the protein abundance in the *rnq1Δ* strain compared to the protein abundance in the [*pin*$^-$] pYES2 strain.
- ***rnq1Δ*:pYES2-*RNQ1***
  the protein abundance in the *rnq1Δ* strain compared to the protein abundance in the [*pin*$^-$] pYES2-*RNQ1* strain.
- **pYES2:pYES2-*RNQ1***
  the protein abundance in the [*pin*$^-$] pYES2 strain compared to the protein abundance in the [*pin*$^-$] pYES2-*RNQ1* strain.

An example of the data received and how the three conditions differ is further illustrated in figure 3.36.

Most of the expression changes identified in the three conditions represented increases in protein abundance as Rnq1p became more abundant: 66.7% of expression values showed up-regulation compared to 33.3 % that showed decreasing expression (figure 3.37). The range of expression change that was most common to the data-set was an increase between 0.51 – 0.75, which corresponds to ~ 1.3 – 2.0x fold increase in protein expression.

The proteins that showed the greatest fold change in abundance are listed in table 3.2: specifically 12 proteins whose abundance decreased the most as Rnq1p expression increased, and 9 proteins whose abundance increased the most as Rnq1p expression increased.

For those showing the greatest decrease in expression, there is no function or activity in which they all partake, however: 4 of the proteins (Gut2p, Idh1p, Tal1p and Ymr315w) are involved in cofactor metabolic processes; 3 of the proteins (Atp5p, Glc7p and Idh1p) are involved in the generation of precursor metabolites for energy process; a further 3 (Glc7p, Gut2p and Tal1p) are involved in the cellular carbohydrate metabolic process; and 4 of the proteins (Bdh1p, Gut2p, Idh1p and Ymr315w) possess oxidoreductase activity. Of these proteins, 3 of the 12 are associated with the mitochondria, 3 with the membrane component, 3 with the nucleus and 10 with the cytoplasm. In combination, these overlapping processes

might suggest that Rnq1p is involved in the negative regulation of certain aspects of cellular metabolism.

A

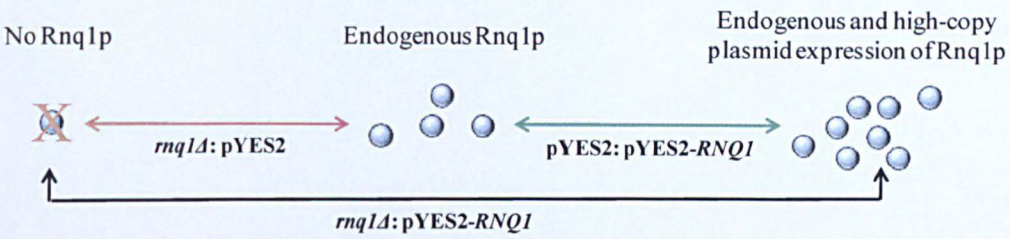

B

	Strain pair		
Accession	***rnq1Δ* : pYES2**	***rnq1Δ* : pYES2-*RNQ1***	**pYES2 : pYES2-*RNQ1***
ABP1_YEAST	1.83	1.86	0.97
ACAC_YEAST	1.06	1.37	1.23
ACH1_YEAST	2.17	0.72	0.34
ACON_YEAST	2.33	0.7	0.33
ACON2_YEAST	0.94	0.61	0.61

Figure 3.36 Illustrating differences and data associated with each strain.
Three strains varying in their level of Rnq1p expression (panel A) and the quantitative pair-wise comparison of their associated proteome (panel B) allowed for the identification of proteins (assigned Uniprot accession name) whose expression was co-regulated with Rnq1p.

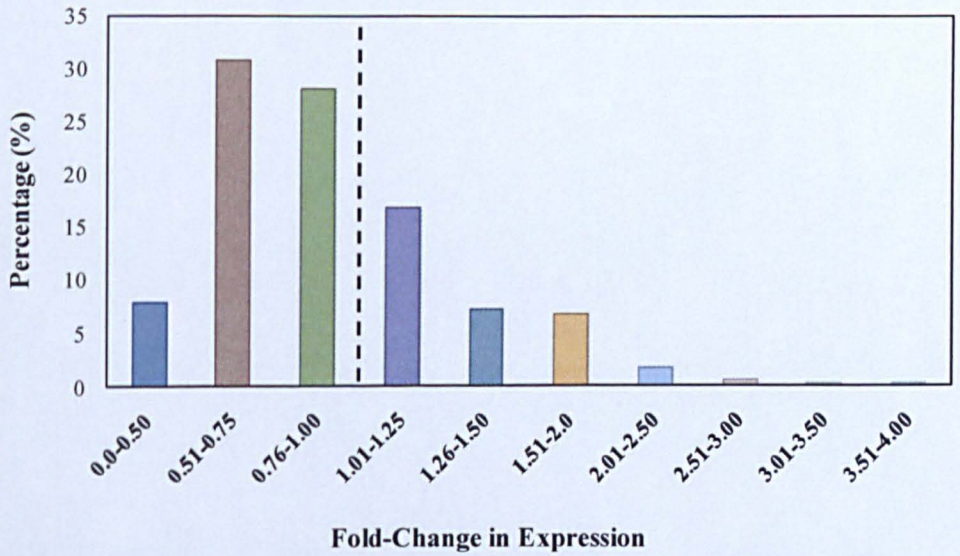

Figure 3.37: The distribution of fold-change values in the abundance of Rnq1p co-regulated proteins.
The three pair-wise comparisons of the three strains used in the study revealed a range of expression changes. More proteins were positively (<1) rather than negatively (>1) regulated as Rnq1p abundance increased in the cell.

Fold-Change	Protein	Condition	Function
↓2.55	Atp5	dr:Y	Subunit 5 of the stator stalk of mitochondrial F1F0 ATP synthase, which is an evolutionarily conserved enzyme complex required for ATP synthesis; homologous to bovine subunit OSCP (oligomycin sensitivity-conferring protein); phosphorylated
↓2.6	Bdh1	Y:R	NAD-dependent (R,R)-butanediol dehydrogenase, catalyzes oxidation of (R,R)-2,3-butanediol to (3R)-acetoin, oxidation of meso-butanediol to (3S)-acetoin, and reduction of acetoin; enhances use of 2,3-butanediol as an aerobic carbon source
↓2.6	Zps1	dr:R	Putative GPI-anchored protein; transcription is induced under low-zinc conditions, as mediated by the Zap1p transcription factor, and at alkaline pH
↓2.67	Idh1	dr:Y	Subunit of mitochondrial NAD(+)-dependent isocitrate dehydrogenase, which catalyzes the oxidation of isocitrate to alpha-ketoglutarate in the TCA cycle
↓2.87	Gut2	Y:R	Mitochondrial glycerol-3-phosphate dehydrogenase; expression is repressed by both glucose and cAMP and derepressed by non-fermentable carbon sources in a Snf1p, Rsf1p, Hap2/3/4/5 complex dependent manner
↓2.88	Gis2	Y:R	Protein with seven cysteine-rich CCHC zinc-finger motifs, similar to human CNBP, proposed to be involved in the RAS/cAMP signaling pathway
↓2.95	Zps1	dr:Y	Putative GPI-anchored protein; transcription is induced under low-zinc conditions, as mediated by the Zap1p transcription factor, and at alkaline pH
↓2.96	Glc7	Y:R	Type 1 serine/threonine protein phosphatase catalytic subunit, involved in many processes (eg: glycogen metabolism, sporulation, mitosis); accumulates at mating projections by interaction with Afr1p; interacts with many regulatory subunits
↓3.36	Nup170	dr:Y	Subunit of the nuclear pore complex (NPC), required for NPC localization of specific nucleoporins; involved in nuclear envelope permeability and chromosome segregation; has similar to Nup157p; essential role, with Nup157p, in NPC assembly
↓3.37	YMR315W	dr:Y	Protein with NADP(H) oxidoreductase activity; transcription is regulated by Stb5p in response to NADPH depletion induced by diamide; promoter contains a putative Stb5p binding site
↓3.46	Fra1	dr:Y	Protein involved in negative regulation of transcription of iron regulon; forms an iron independent complex with Fra2p, Grx3p, and Grx4p; cytosolic; mutant fails to repress transcription of iron regulon and is defective in spore formation
↓3.75	Tal1	dr:R	Transaldolase, enzyme in the non-oxidative pentose phosphate pathway; converts sedoheptulose 7-phosphate and glyceraldehyde 3-phosphate to erythrose 4-phosphate and fructose 6-phosphate

Fold-Change	Protein	Condition	Function
↑0.29	Rpn1	dr:Y	Non-ATPase base subunit of the 19S regulatory particle of the 26S proteasome; may participate in the recognition of several ligands of the proteasome; contains a leucine-rich repeat (LRR) domain, a site for protein-protein interactions
↑0.29	Idh1	Y:R	Subunit of mitochondrial NAD(+)-dependent isocitrate dehydrogenase, which catalyzes the oxidation of isocitrate to alpha-ketoglutarate in the TCA cycle
↑0.27	His4	dr:R	Multifunctional enzyme containing phosphoribosyl-ATP pyrophosphatase, phosphoribosyl-AMP cyclohydrolase, and histidinol dehydrogenase activities; catalyzes the second, third, ninth and tenth steps in histidine biosynthesis
↑0.27	Gut2	dr:Y	Mitochondrial glycerol-3-phosphate dehydrogenase; expression is repressed by both glucose and cAMP and derepressed by non-fermentable carbon sources in a Snf1p, Rsf1p, Hap2/3/4/5 complex dependent
↑0.26	Rpl26a	dr:Y	Protein component of the large (60S) ribosomal subunit, nearly identical to Rpl26Bp and has similarity to *E. coli* L24 and rat L26 ribosomal proteins; binds to 5.8S rRNA
↑0.25	Glr1	Y:R	Cytosolic and mitochondrial glutathione oxidoreductase, converts oxidized glutathione to reduced glutathione; mitochondrial but not cytosolic form has a role in resistance to hyperoxia
↑0.13	Ykl033w	dr:Y	Putative protein of unknown function; subunit of the ASTRA complex which is part of the chromatin remodeling machinery; similar to *S. pombe* Tti1p; detected in highly purified mitochondria in high-throughput studies
↑0.07	Ykr064w	dr:Y	Zinc cluster protein; regulates transcription in response to oleate levels; the authentic, non-tagged protein is detected in highly purified mitochondria in high-throughput studies
↑0.06	Ykl033w	dr:R	Putative protein of unknown function; subunit of the ASTRA complex which is part of the chromatin remodeling machinery; similar to *S. pombe* Tti1p; detected in highly purified mitochondria in high-throughput studies

Table 3.2: Proteins associated with the greatest changes in abundance, either increasing or decreasing, determined by pair-wise comparison of the strains.

'dr' refers to the *rnq1Δ* strain; 'Y' refers to the pYES2 strain; 'R' refers to the pYES2-*RNQ1* strain. Descriptions of protein function were extracted from the *Saccharomyces* Genome Database website (http://www.yeastgenome.org).

Of those proteins that were up-regulated the most when Rnq1p was also elevated, listed in table 3.2, two of these proteins (His4p and Idh1p) are involved in cellular amino acid and derivative metabolic processes; 2 more proteins (Gut2p and Idh1p) are involved in co-factor metabolic processes; 4 proteins (Glr1p, Gut2p, His4p and Idh1p) possess oxidoreductase activity; 2 proteins (His4p and Rpn1p) possess hydrolase activity; 5 of the 8 are associated with the mitochondria, while 4 of the 8 are associated with the nucleus, and 7 of the 8 with the cytoplasm.

Similar to the proteins that were most down-regulated when Rnq1p was over-expressed, we saw for this group of up-regulated proteins that they also appear to suggest a metabolic regulatory role for Rnq1p. Therefore, Rnq1p may have both activating and repressing roles in metabolic processes. The mitochondrial component may be more significantly affected by Rnq1p over-expression, since there were more proteins associated with the mitochondria in the up-regulated group of proteins compared to the down-regulated group.

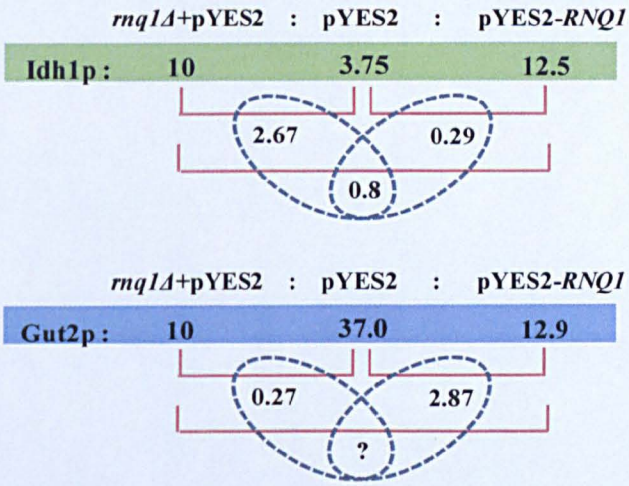

Figure 3.38 An example of using assigning arbitrary values to reflect expression ratios.
Arbitrary values can be assigned to each protein in each strain pair to reflect the significance of ratio values obtained from the pair-wise comparisons. The values below the red horizontal brackets indicate the determined expression differences between the indicated strains. The values in the green box are arbitrarily assigned values that reflect the significance of the expression values for the respective protein's abundance.

It was interesting that 2 of the discussed proteins, Idh1p and Gut2p, both appeared amongst the most up-regulated and the most down-regulated proteins, of all proteins

identified in the proteomics data set. The expression profile for Gut2p and Idh1p is depicted in figure 3.38, and a more in-depth description of this format for presentation is explained in section 3.4.3.

The Idh1p protein was increased in expression whether Rnq1p was increased (pYES2-*RNQ1*) or absent (*rnq1Δ*). The Gut2p protein was decreased in expression whether Rnq1p was increased (pYES2-*RNQ1*) or absent (*rnq1Δ*).

It was observed for these two proteins, Idph1p and Gut2p, that their expression was either highest (Gut2p) or lowest (Idh1p) in the strain expressing Rnq1p at its endogenous level, and that the expression of these proteins either decreased (Gut2p) or increased (Idh1p) if Rnq1p was over-expressed (in the pYES2-*RNQ1* strain) or absent (in the *rnq1Δ* strain).

Idh1p and Gut2p are both mitochondrial dehydrogenases. Closer inspection of the list of proteins that varied in expression as a consequence of changes to Rnq1p abundance revealed the presence of many mitochondrial proteins, particularly those involved in the TCA cycle. Since the TCA-cycle is one of the three central metabolic pathways of the cell, the other two being glycolysis and the pentose phosphate pathway, an analysis of the proteomics data set in terms of changes to these and related pathways was carried out.

3.4.2.1 The effect of Rnq1p on metabolic pathways

The TCA-cycle, also known as the Krebb's cycle, is a process used by the cell during respiratory growth on non-fermentative carbon source, but is also used at a reduced level at all times to supply the cell with biosynthetic intermediates . The TCA-cycle is responsible for the oxidative decarboxylation of acetyl-co-A, which supplies the respiratory complexes with reducing equivalents e.g. NADH and $FADH_2$.

Glycolysis is the central pathway metabolising fermentable sugars for the production of ATP and precursor metabolites used in the synthesis of other small and macromolecules, the by-products of glycolysis are ethanol and carbon dioxide. Gluconeogenesis is essentially the reverse of glycolysis and is used to generate

glucose from simpler molecules, such as pyruvate and lactate. The pentose phosphate pathway redirects glucose-6-phosphate from glycolysis for the generation of a variety of sugars used in biosynthetic reactions, and is also responsible for ~ 60 % of NADPH production in the cell which is an essential cofactor, a source of reducing energy and important for the protection against oxidative stress.

Many proteins involved in the gluconeogenesis and glycolysis pathways were altered due to changes in the abundance of Rnq1p (table 3.3). It appeared that gluconeogenesis was down-regulated in both the *rnq1Δ* and Rnq1p over-expressing strain (trend 'low-high-low') and that glycolysis through to ethanol production was up-regulated in both the *rnq1Δ* and Rnq1p over-expressing strain (trend 'high-low-high'): this arrangement between the gluconeogenesis and glycolysis pathways, places an emphasis on the catabolism of glucose to pyruvate, rather than the anabolism of pyruvate and simpler molecules to glucose.

The pentose phosphate pathway showed a reduction in the conversion of glucose-6-phosphate or fructose-6-phosphate to ribulose-5-phosphate, otherwise required for purine, pyrimidine and histidine synthesis, due to a decrease in Zwf1p, Pgl p and Gnd1p in both the *rnq1Δ* and Rnq1p over-expressing strains. Additionally, enzymes that metabolise ribulose-5-phosphate such as Tkl1p were up-regulated in the same strains, again reducing the pool of ribulose-5-phosphate in the cell. The reaction catalysed by Tkl1p generates glyceraldehyde-3-phosphate and sedoheptulose-7-phosphate; the Tal1p enzyme that converts these intermediates to erythyrose-4-phosphate and fructose-6-phosphate was substantially down-regulated, which would result in an increase in glyceraldehyde-3-phosphate and sedoheptulose-7-phosphate availability and prevent the unnecessary regeneration of fructose-6-phosphate.

Surprisingly, 10 of the 14 TCA-cycle proteins for which expression data was obtained in the dr:Y ratio showed an increase in their expression level in the absence of Rnq1p, and similarly 12 of the 15 TCA-cycle proteins for which expression data was available in the Y:R ratio also showed an increase in expression when Rnq1p was over-expressed. This was an unexpected result for two reasons, 1) as for the pathways mentioned thus far, it appeared that any deviation in Rnq1p abundance from the endogenous expression level was sufficient to disrupt this central metabolic pathway, and 2) the active fermentation of glucose via the glycolysis pathway is

usually accompanied by a repression of the TCA-cycle, which is up-regulated only for respiratory growth during metabolism of non-fermentable carbon sources. It appeared here that not only was glycolysis up-regulated in the *rnq1Δ* and Rnq1p over-expressing strain, but the TCA-cycle was also up-regulated in these strains. It should be noted that Sdh1p and Sdh2p, two subunits of the succinate dehydrogenase complex that couples oxidation of succinate with the transfer of electrons to ubiquinone in the respiratory chain, were not up-regulated in line with other TCA-cycle proteins when Rnq1p was over-expressed and in fact were slightly down-regulated – this would have resulted in reduced activity of the respiratory chain, affecting ATP generation and cellular redox homeostasis, and possibly caused an accumulation of early TCA-cycle intermediates.

		Expression Ratios			Expression Trend
Pathway	**Gene**	**dr:Y**	**Y:R**	**Function**	**dr-Y-R**
Glycolysis/ Gluconeogenesis	*PGI1*	0.73	1.2	β-D-glucose to G6P or F6P	
	YMR099C	0.56	0.98	β-D-glucose to G6P	
	HXK1	0.71	1.4	α-D-glucose to G6P	low-high-low except Hxk2p and Ymr099c
	HXK2	0.71	0.89		
	GLK1	0.79	1.46		
	GAL10	0.66	1.45		
	PFK1	0.5	1.59	F16P2 to F6P	
	PFK2	0.72	1.18		
	FBA1	1.34	0.9	reversible F16P2 to G3P	high-low-high
	TPI1	1.21	0.69	reversible glycerone to G3P	
	TDH1	1.5	0.86	reversible G3P to PEP reactions	high-low-high except Ykr043c
	TDH2	1.15	0.93		
	TDH3	1.18	0.86		
	PGK1	1.41	0.67		
	GPM1	1.28	0.68		
	YKR043C	0.51	1.19		
	ENO1	2.06	0.61		
	ENO2	1.57	0.59		
	PYK1	1.22	1.14	PEP to pyruvate	consistent decrease
	PYC1	0.49	1.24	pyruvate to oxaloacetate	low-high-low
	PDC1	0.76	1.61	pyruvate to acetyl-coA or acetaldehyde	high-low-high
	PDA1	0.8	0.89		consistent increase
	PDB1	0.79	1.04		high-low-high
	LPD1	0.78	0.65		consistent increase
	ADH1	0.67	1.23	acetaldehyde to ethanol	high-low-high
	ADH3	0.8	1.21		
	ALD4	0.5	1.1	acetate to aldehyde	low- high-low
	ALD6	1.52	0.68		high-low-high
Pentose Phosphate Pathway	*PGI1*	0.73	1.2	G6P or F6P to ribulose-5-phosphate	low-high-low
	ZWF1	0.91	1.02		
	GND1	0.69	1.52		
	TKL1	0.98	0.64		consistent increase
	TAL1	2.22	1.39	E4P and F6P production	consistent decrease
	PRS3	1.25	1.23	R5P production	consistent decrease

TCA-Cycle	*CIT1*	1.31	0.48	citrate production	high-low-high except Aco2p
	ACO1	2.33	0.33	citrate to isocitrate	
	ACO2	0.94	0.61		
	IDP1	1.74	0.67	alpha-ketoglutarate production	
	IDH1	2.67	0.29		
	IDH2	1.74	0.65		
	KGD2	1.13	0.67	succinyl-coA production	consistent increase
	LPD1	0.78	0.65	dihydrolipoyl dehydrogenase	low-high-low consistent increase
	LSC1	0.58	1.19	succinate production	
	LSC2	0.83	0.63		
	SDH1	1.49	1.05	ubiquinol production	consistent decrease
	SDH2	1.16	1.01		
	FUM1	/	0.54	L-malic acid production	?-low-high
	MDH1	1.55	0.51	reversible malate to oxaloacetate	high-low-high
	MDH3	1.11	0.75		
Electron Transport Chain	*NDI1*	1.71	0.81	Complex I	high-low-high
	NDE1	1.14	1.3		
	SDH1	1.49	1.05	Complex II	consistent decrease
	SDH2	1.16	1.01		
	COR1	1.54	0.71	Complex III	high-low-high
	QCR2	1.21	0.7		
	QCR7	2.11	0.86		
	CYC1	1.77	0.71		
	COX4	1.11	0.99	Complex IV	high-low-high
	COX6	2.47	0.62		
	ATP11	1.07	0.54	Complex V	high-low-high except Atp1p
	ATP1	0.92	0.97		
	ATP2	1.22	0.67		
	ATP16	/	0.55		
	ATP3	1.67	0.81		
	ATP5	2.55	0.47		
	PMA1	1.24	0.55		
Galactose Metabolism	*GAL1*	0.73	1.48	galactose to G1P	low-high-low consistent increase
	GAL7	0.88	0.94		
	GAL10	0.66	1.45	reversible UDP-gal to UDP-glu	low-high-low
	UGP1	1.53	0.61	reversible UDP-glu to G1P	high-low-high
	HXK1	0.71	1.4	reversible G6P to glucose	low-high-low consistent increase low-high-low
	HXK2	0.71	0.89		
	GLK1	0.79	1.46		
Fatty Acid Metabolism	*ERG10*	0.81	0.81	acetyl-group transfer	consistent increase
	FAA1	0.34	2.06	long-chain fatty acid synthesis	low-high-low consistent-decrease
	FAS1	0.82	1.39		
	FAS2	1	1.16		
	FAS3	1.06	1.23		
	ADH1	0.67	1.23	reversible alcohol to aldehyde	low-high-low
	ADH3	0.8	1.21		
	ALD4	0.5	1.1	fatty acid to aldehyde	low-high-low high-low-high
	ALD6	1.52	0.68		

Oxidative stress	*CTT1*	0.71	1.57	Protection against H_2O_2	
	PRX1	0.93	1.08	Mitochondrial peroxiredoxin	low-high-low
	GND1	0.69	1.52	Adaptation to O.S.	
	SOD1	0.59	1.21	Superoxide dismutase	
	AHP1	0.54	0.95	Thiol-specific peroxiredoxin	consistent increase
	GLR1	0.53	0.25	Glutathione oxidoreductase	consistent increase
	DOT5	1.76	0.64	Nuclear thiol-peroxidase	
	TSA1	1.54	0.84	Thioredoxin peroxidase	high-low-high
	GRX3	1.14	0.69	H_2O_2/superoxide oxidoreductase	

Table 3.3 Pathway mapping of the regulated proteins and associated expression ratios.

Expression ratios from dr:Y (*rnq1Δ*:pYES2) and Y:R (pYES2:pYES2-RNQ1) pair-wise comparisons can be clustered to cellular pathways to reveal functional patterns in the expression data. Abbreviations: G6P, Glucose-6-phosphate; F6P, fructose-6-phosphate; F16P2, fructose-1-6-phosphate; G3P, glyceraldehyde-3-phosphate; PEP, phosphoenol pyruvate; R5P, ribose-5-phosphate; G1P, glucose-1-phosphate; UDP, uridine diphosphate ; H_2O_2, hydrogen peroxide.

Proteins of the electron transfer chain mirrored the expression trend noted for the glycolysis and TCA-cycle, namely an increase in their abundance in both the *rnq1Δ* and Rnq1p over-expression strain: with the exception of Sdh1p, also a component of the TCA-cycle, which consistently decreased in expression as Rnq1p increased in expression.

The *rnq1Δ* and Rnq1p over-expression strains appeared less inclined to metabolise galactose to a glycolytic intermediate. There was also a reduction in fatty acid metabolism in the *rnq1Δ* and Rnq1p over-expression strains. Finally, enzymes involved in the protection from oxidative stress were also observed to vary in their expression with changes to Rnq1p. A further observation was made relating to the TCA-cycle: this pathway is also important for the synthesis of amino acids, supplying intermediates that are directed into amino acid biosynthetic pathways. Analysis of the protein list revealed that many proteins involved in amino acid synthesis were either up-regulated as Rnq1p increased in abundance (trend ↑ in table 3.4) or that their expression was up-regulated if Rnq1p abundance differed from the endogenous wild-type level e.g. the proteins were up-regulated in the *rnq1Δ* strain and the [*pin*$^-$] + pYES2-*RNQ1* strain. An example of pathway mapping of Rnq1p-induced proteins relevant to the valine, leucine and isoleucine biosynthetic pathway

is illustrated in figure 3.39. Most of the proteins that catalyse flux through these pathways are present in the proteomics list of regulated proteins (green boxes).

Protein	Trend	Function
Arc1		Binds tRNA and methionyl- and glutamyl-tRNA synthetases
Arg1		Arginine biosynthesis pathway
Arg4	↑	Arginine biosynthesis pathway
Aro4	↑	Aromatic amino acid biosynthesis
Aro8	↑	Aromatic aminotransferase I, regulated by general control of amino acid biosynthesis
Bat1	↑	Mitochondrial branched-chain amino acid aminotransferase
Frs1		Phenylalanyl-tRNA synthetase
Gdh1		Synthesizes glutamate from ammonia and alpha-ketoglutarate
His4	↑	Histidine biosynthesis
Hom2	↑	Methionine and threonine biosynthesis; regulated by Gcn4p and the general control of amino acid synthesis
Hom6	↑	Methionine and threonine biosynthesis
Ils1	↑	Cytoplasmic isoleucine-tRNA synthetase
Ilv2	↑	Isoleucine and valine biosynthesis, under general amino acid control
Ilv3	↑	Biosynthesis of branched-chain amino acids
Ilv5		Branched-chain amino acid biosynthesis; required for maintenance of wild-type mitochondrial DNA
Ilv6	↑	Branched-chain amino acid biosynthesis
Krs1	↑	Lysyl-Trn
Leu1	↑	Leucine biosynthesis pathway
Leu4	↑	Leucine biosynthesis pathway
Lys1		Lysine biosynthesis pathway
Lys12		Biosynthesis of lysine
Lys20		Lysine biosynthesis pathway
Lys4		Lysine biosynthesis pathway
Met6	↑	Methionine biosynthesis and regeneration
Sam2		S-adenosylmethionine synthetase
Thr1		Threonine biosynthesis; regulated by the Gcn4p-mediated general amino acid control pathway
Trp2	↑	Tryptophan biosynthesis
Trp5	↑	Tryptophan biosynthesis; regulated by the general control system of amino acid biosynthesis
Tys1		Tyrosyl-tRNA synthetase
Ydr341c	↑	Arginyl-tRNA synthetase

Table 3.4: Many aminoacyl-tRNA synthetases (highlighted beige) and proteins involved in amino acid biosynthesis were co-regulated with Rnq1p.

Pair-wise comparison of protein abundances in each of the three strains showed an increase in aminoacyl-tRNA synthetases and proteins involved in amino acid biosynthesis, as the abundance of Rnq1p increased in the cell. Trend '↑' indicates consistent increase of protein abundance as Rnq1p is increased, all others increased in abundance whether Rnq1p was absent or over-expressed.

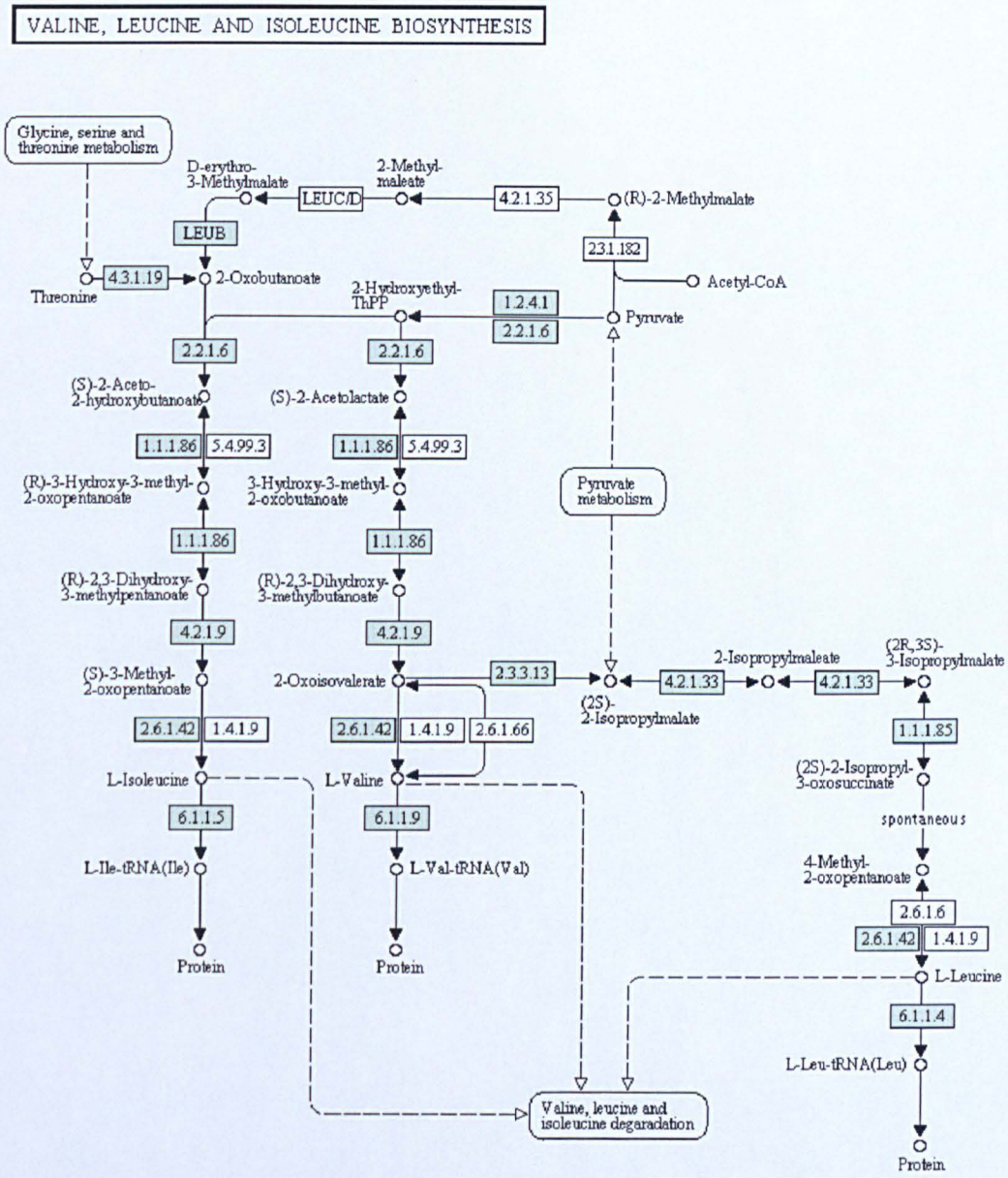

Figure 3.39 KEGG pathway map listing enzymatic steps (indicated by boxes) through the valine, leucine and isoleucine biosynthetic pathway.
The number is the Enzyme Commission (EC) number which classifies proteins according to the chemical reactions they catalyse. Boxes highlighted in green represent proteins detected in this study which change in their abundance as a consequence of changes to Rnq1p abundance.

3.4.2.2 Gene Ontology analysis of the gene list

The website for the '*Saccharomyces Genome Database*' provides a gene ontology tool for analysing lists of genes/proteins and clustering members of the list according

to their cellular functions, processes or components. Since all proteins encoded by the genome will also demonstrate a specific distribution of terms, with some functions, processes and components being more or less represented than others, there is expected to exist an inherent bias toward this distribution within gene/protein lists of interest. For this reason the frequency of a term within a gene/protein list is considered relative to the frequency with which that term occurs in the genome. However, this comparison is not always appropriate; for example when the gene/protein list is *not* generated by a method that relies on detecting protein abundance (or a signal that identifies the protein).

The gene/protein list generated by the proteomics study was based primarily on an ability to detect proteins, and secondly on the reproducible variation in each proteins detection across the three strains studied. For this reason, it was necessary to consider the influence that GO term abundance had on an ability to detect changes to those GO term abundances; however this does not invalidate the significance of terms that are abundant in both the gene/protein list of interest and the genome list. An analysis of the proteomics gene list relative to genome frequency would indicate changes to terms for processes, functions and components that are less abundant and therefore less likely to have been detected; these terms are as significant if not more significant than terms that are abundant in both the gene/protein list and the genome list.

For the proteomics gene/protein list the most abundant processes, functions and components relative to their genome frequency are presented in figure 3.40 and 3.41. Due to changes in the abundance of Rnq1p, proteins involved in the process of protein folding were 4x more likely to be affected than one might expect given the frequency of this term within the genome. This was also true for processes such as cellular amino acid and derivative metabolic process (3.65x more than genome frequency, 'gf'), generation of precursor metabolites and energy (3.57x more than gf), cellular respiration (2.94x more than gf), cofactor metabolic process (2.67x more than gf), translation (2.38x more than gf) and cellular carbohydrate metabolic process (2.21x more than gf).

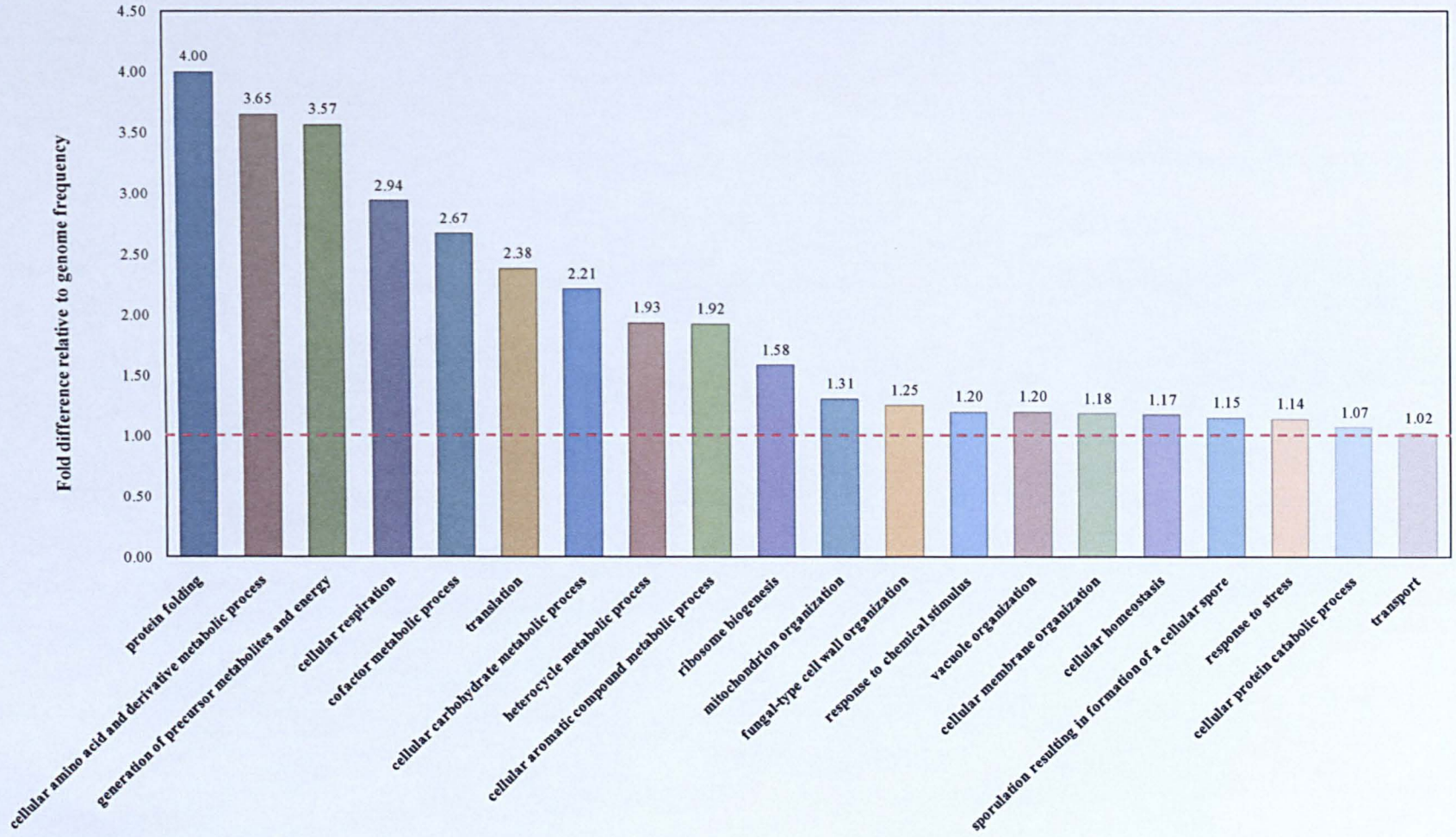

Figure 3.40: Gene ontology process terms associated with the proteomics dataset.
Plotted is the abundance of each term associated with the gene list relative to the genome frequency for that term, expressed as a ratio. SlimMapper is an online gene ontology tool available on the *Saccharomyces Genome Database* website (hhtp://www.yeastgenome.org)

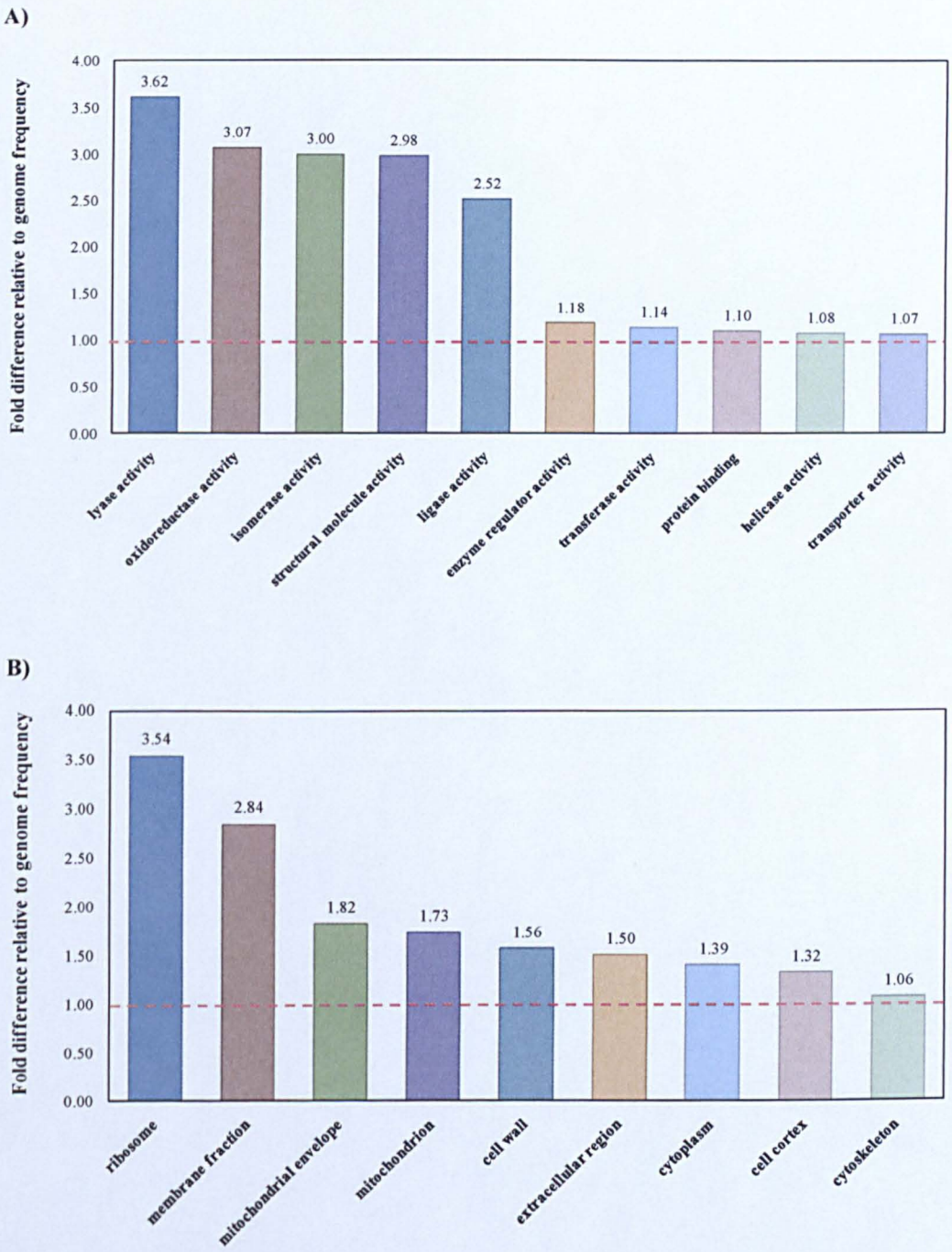

Figure 3.41: Gene ontology function and component terms associated with the proteomics dataset.

Plotted is the abundance of each term associated with the gene list relative to the genome frequency for that term, expressed as a ratio for A) SlimFunction, and B) SlimComponent. SlimMapper is an online gene ontology tool available on the *Saccharomyces Genome Database* website (hhtp://www.yeastgenome.org)

For function terms, lyase activity was most enriched relative to its normal genome frequency (3.62x more than gf). A lyase catalyses C-C, C-O or C-N bond cleavage by a means other than hydrolysis or oxidation, or the addition of a double bond to a group. Proteins with oxidoreductase activity were also commonly altered in their expression as Rnq1p expression level was varied (3.07x more than gf), and this refers to the catalysis of any redox reaction within the cell. Similarly, isomerase activity (3.00x more than gf) – the catalysis of structural rearrangements within a molecule, structural molecule activity (2.98x more than gf) – proteins that contribute to structural integrity of complexes, and ligase activity (2.52x more than gf) – proteins that ligate 2 substances together, were also over-represented in the list of proteins that vary as a consequence of changes to Rnq1p abundance.

The analysis of the gene/protein list for component terms revealed that many proteins co-regulated with/by Rnq1p were associated with the ribosome (3.54x more than gf), the membrane fraction (2.84x more than gf), the mitochondrial envelope (1.82x more than gf) and the mitochondria (1.73x more than gf).

3.4.2.3 Transcription factors associated with the gene list

The list of all identified proteins that vary in expression with the abundance of Rnq1p were also analysed to determine whether there was a majority transcription factor responsible for transcription of their source gene. If many of the genes encoding the identified proteins are represented by a particular transcription factor, it might indicate that Rnq1p was activating this transcription factor in some way and would explain why certain proteins were altered in their expression level as a consequence of Rnq1p abundance.

To identify the transcription factors associated with the list of proteins of the proteomics project, or more specifically associated with the genes encoding the proteins, the list was uploaded to the 'GeneCodis' web-tool which groups genes in a species dependent manner to their associated transcription factors (Nogales-Cadenas, 2009; Carmona-Saez, 2007).

The results revealed that 14.7 % of the genes are responsive to the transcription factor Rap1p (figure 3.42). The Rap1p transcription factor is required for the

regulation of a diverse array of processes; however genes encoding ribosomal proteins represent the largest group of target genes that Rap1p activates (Lieb, 2001). Since ribosomal proteins represent the largest component group of proteins within the data set, this result was not unexpected.

The Fhl1p transcription factor was also well represented by the data set, with 11.8 % of all of the genes on the list being responsive to Fhl1p, and relative to its representation of the genome, Fhl1p showed the greatest enrichment in the Rnq1p dataset. The Fork-head like 1 (FhL1) transcription factor is responsible for regulating genes encoding ribosomal proteins and requires Rap1p for its recruitment to the promoters of genes encoding ribosomal proteins (Zhao *et al.*, 2003).

Genes that are transcriptionally regulated by Abf1p, the third most represented transcription factor of the gene set at 10 % coverage, are also involved in many different cellular processes such as ribosomal function, carbon source utilisation,

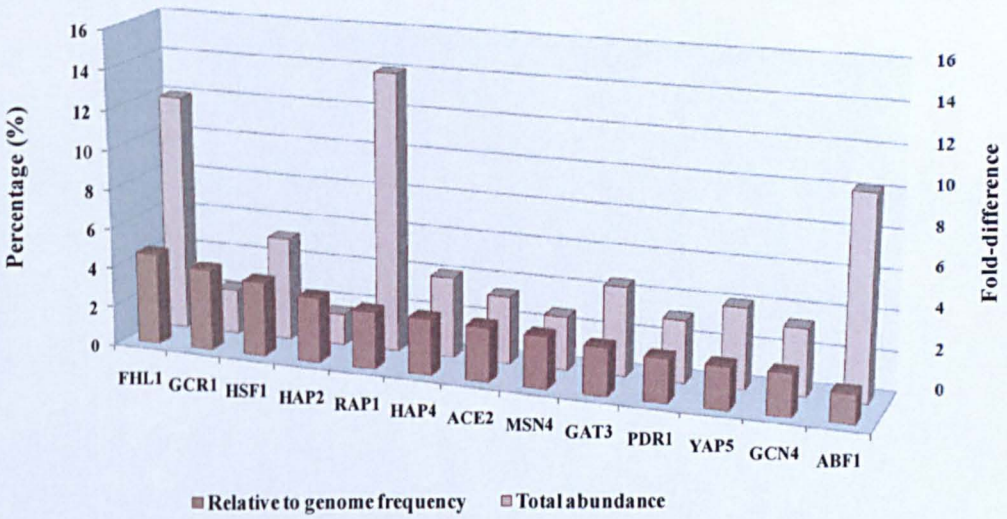

Figure 3.42 Transcription factor representation of the regulated proteins. Protein abundance within a cell is partly controlled by the transcriptional regulation of the encoding gene. Certain transcription factors control genes whose proteins cluster to distinct cellular processes. Using the GeneCodis web-based tool, genes encoding proteins co-regulated with Rnq1p (442 analysed) were found to be associated with the above transcription factors.

sporulation and meiosis (Miyake *et al.*, 2004). However the percentage of genes represented by Abf1p transcription factor in the genome relative to the dataset shows the lowest fold difference.

Rnq1p resides both in the nucleus (Douglas *et al.*, 2009a)(Weissman, 2003) and the cytoplasm (Sondheimer *et al.*, 2000b), and it is possible that Rnq1p affects the control of specific transcription factor target groups by either interacting with the relevant transcription factor or by binding to transcription factor-interacting partners in a way that modulates the activity of the transcription factor e.g. Fhl1p, Rap1p and Abf1p. For example, Rnq1p is predicted to contain an FHA (forkhead-associated) domain (section 3.2.2) at its N-terminus; these recognise phosphorylated residues on target ligands to affect transcriptional regulation. Rnq1p may thus use this FHA-domain to mediate interactions that have an effect on Rap1p, Fhl1p or Abf1p transcriptional regulation. Alternatively, it may be through sequestration of a nucleocytoplasmic shuttling protein with a more direct transcriptional role that Rnq1p is able to influence transcriptional dynamics – this would make Rnq1p analogous to the Ure2p prion protein, which acts as a cytoplasmic 'anchor' for the transcription factor Gln3p(Beck *et al.*, 1999) .

Rnq1p however is not an essential protein and it was lost rapidly in evolution. Therefore its role, if any, in the capacity of a transcription regulator must be a partially redundant one at most.

3.4.3 Expression profiles across the three test strains

Arbitrary values can be assigned to the strains in order to visualise the significance of the fold-change values. For example, in panel A of figure 3.43, the fold change of a protein between the *rnq1Δ* strain and the pYES2 strain is 0.5: this means that the abundance of the protein is 2x fold higher in the pYES2 strain relative to the *rnq1Δ* strain. We could therefore assign an arbitrary value of 10, representing the expression level of the protein, to the *rnq1Δ* strain and an arbitrary value of 20 to the pYES2 strain, since the protein is 2x more abundant in the pYES2 strain than in *rnq1Δ* strain. If this particular protein increases in expression as the level of Rnq1p increases, we would expect that the arbitrary value assigned to the pYES2-*RNQ1*

would be greater than 20, to represent an increase in abundance of the protein between pYES2 and pYES2-*RNQ1* in parallel with the increase in Rnq1p protein. If we assign an arbitrary value for the protein of 30 to the pYES2-*RNQ1* strain, we can calculate the fold-difference ratios expected for the remaining two pairs: the *rnq1Δ* and pYES2-*RNQ1* strains would have a fold difference of ~0.33, and the pYES2 and pYES2-*RNQ1* strains would have a fold-difference of ~0.66. Thus, in the condition where a protein increases in expression as the abundance of Rnq1p increases, the greater the change in protein expression level that occurs within a strain pair, the smaller the fold-difference value will be (<1).

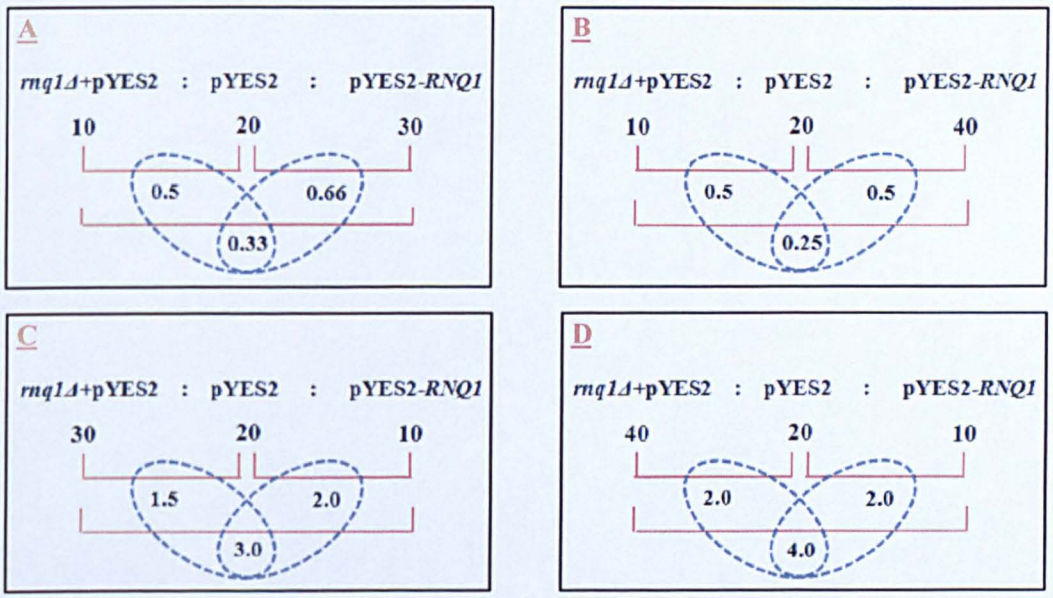

Figure 3.43: Spotting trends in protein abundance across the three test strains based on pair-wise ratio values.
A protein's fold-difference value from pair-wise comparison can also be represented by an arbitrary value. Assigned to each strain, the arbitrary values make it easier to spot trends in expression changes across the three strains. Fold-difference values >1 represent decreases in protein expression as Rnq1p is increased in expression, values <1 represent increases in proteins expression as Rnq1p is increased in expression.

For a protein that decreased as the expression level of Rnq1p increased, we could predict a scenario as depicted in panel C and D of figure 4. The protein would be at its most abundant when the level of Rnq1p was at its lowest; therefore we would assign the higher arbitrary value to the *rnq1Δ* strain. Subsequently, we would expect

a decrease in the arbitrary value for the pYES2 strain, and the smallest arbitrary value of protein expression would be in the pYES2-*RNQ1* strain – in accordance with a protein that decreased as the abundance of Rnq1p protein increased. In the case where a protein decreased as Rnq1p increased, we can see that the greater the difference in protein expression between a strain pair, the greater the fold difference number is (>1).

Analysis of the fold-difference values for each identified protein across the three conditions revealed the following changes:

- 28 proteins decreased in expression level as Rnq1p increased in abundance:
    - 21 of these proteins showed a consistent decrease in expression level across all three conditions
    - 2 proteins only decreased in expression level between the *rnq1Δ*:pYES2 and *rnq1Δ*:pYES2-*RNQ1* conditions
    - 5 proteins decreased only between the *rnq1Δ*:pYES2-*RNQ1* and pYES2:pYES2-*RNQ1* conditions.

- 220 proteins increased in expression level as Rnq1p increased in abundance:
    - 118 of these proteins showed a consistent increase in expression across all three conditions
    - 12 proteins only increased in expression between the *rnq1Δ*:pYES2 and *rnq1Δ*:pYES2-*RNQ1* conditions
    - 100 proteins increased only between the *rnq1Δ*:pYES2-*RNQ1* and pYES2:pYES2-*RNQ1* conditions.

Since many yeast proteins are functionally annotated it is possible to consider the groups of proteins that increased or decreased in expression in terms of their functions, and therefore to identify whether these groups are associated with an enrichment of particular functions. The website for the '*Saccharomyces Genome Database*' provides a gene ontology tool for such a purpose: the 'GO SlimMapper' tool. The relevant list of genes are uploaded to this tool and a search is performed on the members of the gene list by the GO SlimMapper so as to cluster genes within the list by shared functions – some genes have multiple functions in the cell and therefore will add significance to multiple GO terms. Additionally, since some

functions are over-represented in the genome, it is expected that by chance there will also be a functional bias within gene lists of interest. For example, 11 % of all yeast genes thus far annotated are associated with the GO process term 'translation', consequently for the process of translation to be significant within a gene list of interest the term translation would ideally be associated with more than 11 % of the uploaded genes. Therefore, functions associated with the gene list were considered in terms of their expected frequency within the genome.

3.4.3.1 Expression profiles: GO Process

A comparison of GO process terms associated with the 28 proteins that decreased in expression as Rnq1p expression increased and the 118 proteins that consistently increased in expression as Rnq1p expression increased revealed significant functional differences between these two groups of proteins.

The proteins that decreased in expression as Rnq1p increased in expression were highly enriched for processes such as cofactor metabolic process (9.59x more than genome frequency, 'gf'), cellular carbohydrate metabolic process (5.16x more than gf), and generation of precursor metabolites and energy (6.37x more than gf), in comparison to abundance of this function within the yeast genome (figure 3.4.4). Other processes that were also decreased considerably were cellular lipid metabolic process (3.26x more than gf), heterocycle metabolic process (3.7x more than gf), cellular respiration (4.6x more than gf) and nuclear organisation (3.7x more than gf).

The GO process terms associated with the proteins that increased in expression level as Rnq1p expression increased included translation (3.67x more than gf), ribosome biogenesis (2.4x more than gf), cellular amino acid and derivative metabolic process (3.3x more than gf), and protein folding (7.5x more than gf) (figure 3.4.5).

The processes RNA metabolic process and transport featured highly in both the groups that increased and decreased in expression as Rnq1p levels increased, however these processes are also well represented within the genome and so it was difficult to discern the significance of these processes, if any, to the functional influence of Rnq1p within the cell.

Analysis of the GO process terms associated with these two groups of proteins, one group that increased with Rnq1p abundance and the other group that decreased with Rnq1p abundance, suggested a possible logical compatibility. An increase in translational processes might instigate an increase in ribosome biogenesis, or an increase in ribosome biogenesis might allow for an increase in translational processes. In turn, an increase in both translation and ribosome biogenesis would require an increase in protein folding capacity to ensure efficient folding and assembly of the newly synthesised protein. The translational process consumes a great deal of energy within the cell, and the down-regulation in particular metabolic processes may indicate differential compatibilities or requirements between cellular events (such as translation) and the various metabolic pathways.

Alternatively the decrease in certain metabolic processes was not linked directly to the increase in cellular translation processes. An increase in translational processes might indicate an actively growing cell, yet processes such as cell wall organisation, cellular lipid metabolism and nuclear organisation were down-regulated and, in addition the down-regulation of certain metabolic processes represented a combination of events that appeared to be less than optimal for an actively growing cell.

If Rnq1p negatively regulated the availability of certain metabolic intermediates and precursors, this would place an increasing demand on the cell to synthesise these products or find metabolic alternatives, and hence would require an increase in translational processes to achieve this. The depletion of proteins Fas2p and Fas1p, which function together as fatty acid synthetases and are reduced in expression when Rnq1p is increased in abundance (Table 3.3), would cause a decrease in lipid metabolism. Another indicator of reduced lipid biosynthesis when Rnq1p expression was altered from the endogenous wild-type level was the reduction in the conversion of G6P in the pentose phosphate pathway, (Table 3.3), which would normally generate NADPH and biosynthetic precursors for the reductive biosynthesis of lipids (and nucleic acids). Fas2p depletion has also been observed to cause mitochondrial abnormalities (Altman, 2005) and may have therefore been a contributing factor to the decrease in cellular respiration associated with a reduction in Sdh1p and Sdh2p. However, three additional proteins that also decreased may have contributed to mitochondrial abnormalities: Fcj1p, a protein involved in the formation and structure

of mitochondrial crista junctions; Mdm38p, a protein required for the integration of certain proteins into the inner membrane of mitochondria; and Clu1p/Tif1p an eIF3 component with unknown function whose deletion causes defects in mitochondrial organisation – it is possible a reduction in Tif1p expression contributed to this phenotype(Fields *et al.*, 1998) (Fields, 1998).

Since it was observed that the TCA-cycle was up-regulated when Rnq1p levels were varied (Table 3.3), yet the mitochondria were also possibly defective in some way particularly when Rnq1p was over-expressed (Table 3.3), this could indicate that despite up-regulation of many TCA-cycle components, this did not amount to an increase in TCA-cycle output or efficiency. If a reduction in flux through the TCA-cycle was brought about, either by damage to the mitochondria or by an increased siphoning off of TCA-cycle intermediates for the amino acid biosynthetic processes that appear to be up-regulated, the cell may respond to the resulting high ratio between ADP/AMP and NAD^+/NADH by increasing the expression of TCA-cycle components – albeit with little productive effect. A reduction in TCA-cycling would also contribute to a decrease in cellular respiration, since a functional TCA-cycle is required by the respiratory complexes for the provision of NADH and $FADH_2$.

The strains studied here were grown in galactose, and harvested during log-phase, therefore the cells should have been actively fermenting the galactose, with minimal activity from the TCA-cycle. The up-regulation of TCA-cycle components in the *rnq1Δ* and Rnq1 over-expressing strains could indicate a defect in glucose or carbon source sensing possibly brought about by signalling disruption through loss or over-production of Rnq1p.

The increase in proteins associated with translation might also indicate a Rnq1p specific defect in translation, and that the identified proteins are elevated in abundance to counteract the negative effects of Rnq1p on translation: another strategy of which may be to increase ribosome biogenesis.

Given the observed localisation of Rnq1p to both the nucleus and the cytoplasm, it may be that in the cytoplasm, Rnq1p acts at the level of translation and protein

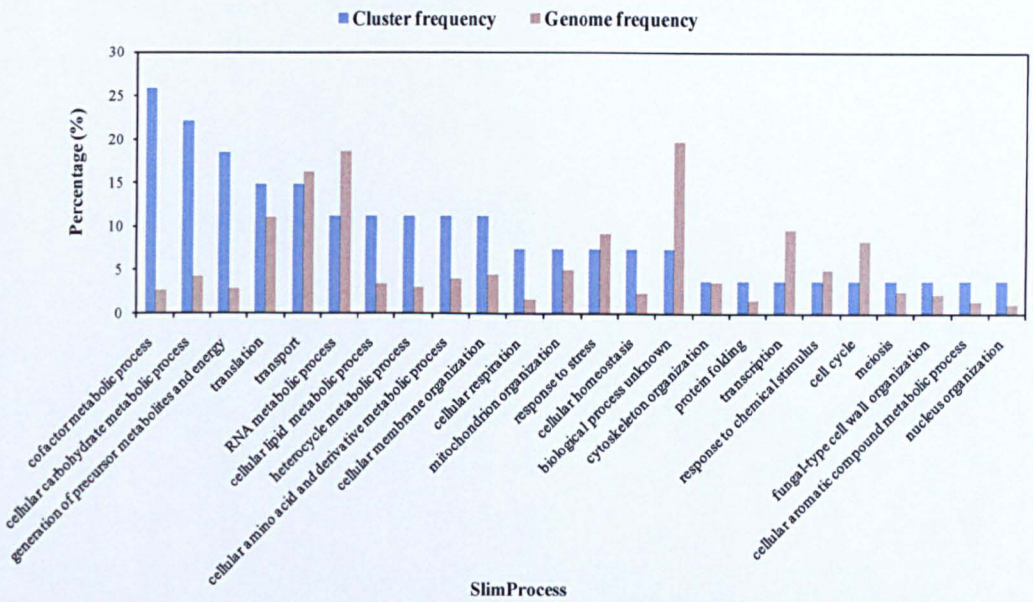

Figure 3.44: Gene ontology process terms associated with the 28 proteins that consistently decreased in expression as Rnq1p expression increased.

The frequency of a term associated with the gene list was plotted against the genome frequency for the term. SlimProcess is an online gene ontology tool available on the *Saccharomyces Genome Database* website (hhtp://www.yeastgenome.org)

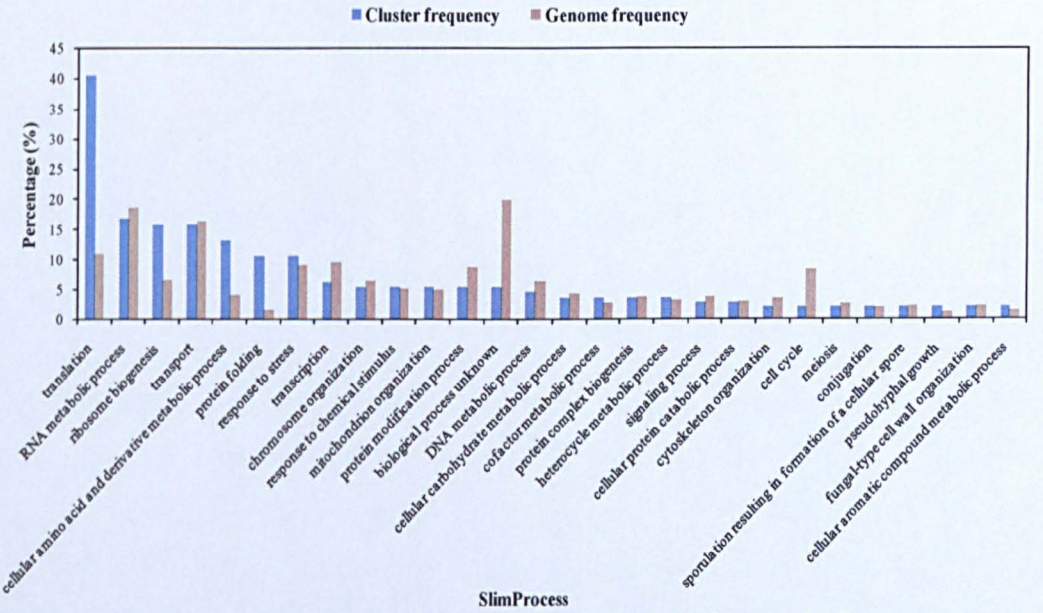

Figure 3.45: Gene ontology process terms associated with the 118 proteins that consistently increased in expression as Rnq1p expression increased.

The frequency of a term associated with the gene list was plotted against the genome frequency for the term. SlimProcess is an online gene ontology tool available on the *Saccharomyces Genome Database* website (hhtp://www.yeastgenome.org).

folding, but in the nucleus can affect transcriptional regulation of certain metabolic processes.

3.4.3.2 Expression Profiles: GO Function

Analysis of the GO function terms associated with the group of proteins that decreased in abundance as Rnq1p was elevated in the cell indicated a very significant decrease in oxidoreductase activity (6.88x more than gf), a decrease in ligase activity (4.11x more than gf), and a decrease in helicase (2.85x more than gf) and lyase activity (2.85x more than gf) (figure 3.46). In contrast, GO functions that were up-regulated when Rnq1p was increased in the cell were structural molecule activity function (5.32x more than gf), RNA binding (1.28x more than gf), protein binding (1.36x more than gf), oxidoreductase (2.32x more than gf), lyase (3.38x more than gf) and isomerase activities (3.89x more than gf) (figure 3.47).

These GO function results were considered in terms of the GO processes previously discussed. The increase in structural molecular activity was likely indicative of the macromolecular assemblies associated with ribosome biogenesis, translation and protein folding. An increase in RNA and protein binding function probably reflected the increasing demand for mRNA processing and the interactions necessary for ribosome biogenesis, translational processes and protein folding.

Oxidoreductase activity involves the reversible change to a molecules oxidation state and is associated with molecular dehydrogenases such as Sdh1p and Adh3p that provide NADPH for reductive anabolic processes or redox reactions important in the protection against oxidative stress. The oxidative branch of the pentose phosphate pathway, the reaction converting G6P to ribulose-5-phosphate, provides ~60% of the cells NADPH requirement, however proteins catalysing these steps were down-regulated in both the *rnq1Δ* and Rnq1p over-expressing strains, suggesting a decrease in the cellular pool of NADPH. In support of this, one of the most significant reductions in protein expression occurred for Ymr315w in the dr:Y pair-wise comparison, i.e. Ymr315w was significantly up-regulated in the *rnq1Δ* strain, and this protein was also up-regulated in the Rnq1p over-expressing strain;

Ymr315w is transcriptionally regulated in response to depleted cellular levels of NADPH.

Proteins that showed a consistent decrease in expression as Rnq1p expression increased were particularly enriched for oxidoreductase activity. The proteins falling into this category included Adh3p, Ara1p, Fas2p, Gpd1p, Nde1p, Oye2p, Sdh1p and Sdh2p, for example. The proteins Sod1p, Ctt1 and Prx1p, involved in cellular protection from oxidative stress, also varied in their expression level as Rnq1p abundance changed but they were not included in this particular GO analysis since their expression levels did not consistently decrease. Instead, Ctt1p, Sod1p and Prx1p levels decreased if Rnq1p levels varied from the endogenous, wild-type levels.

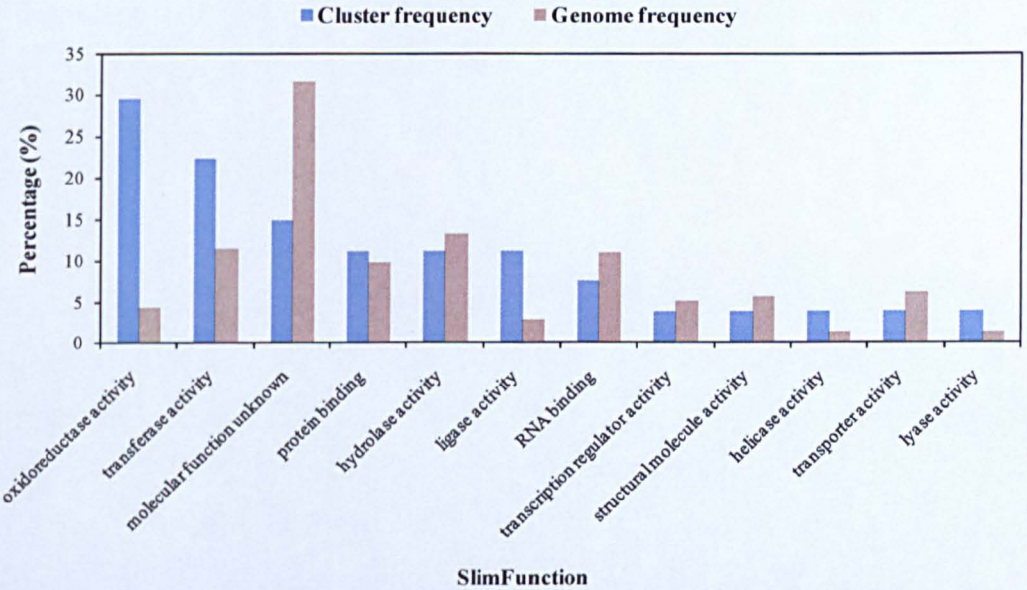

Figure 3.46 Gene ontology function terms associated with the 28 proteins that consistently decreased in expression as Rnq1p expression increased.
The frequency of a term associated with the gene list was plotted against the genome frequency for the term. SlimFunction is an online gene ontology tool available on the *Saccharomyces Genome Database* website (hhtp://www.yeastgenome.org).

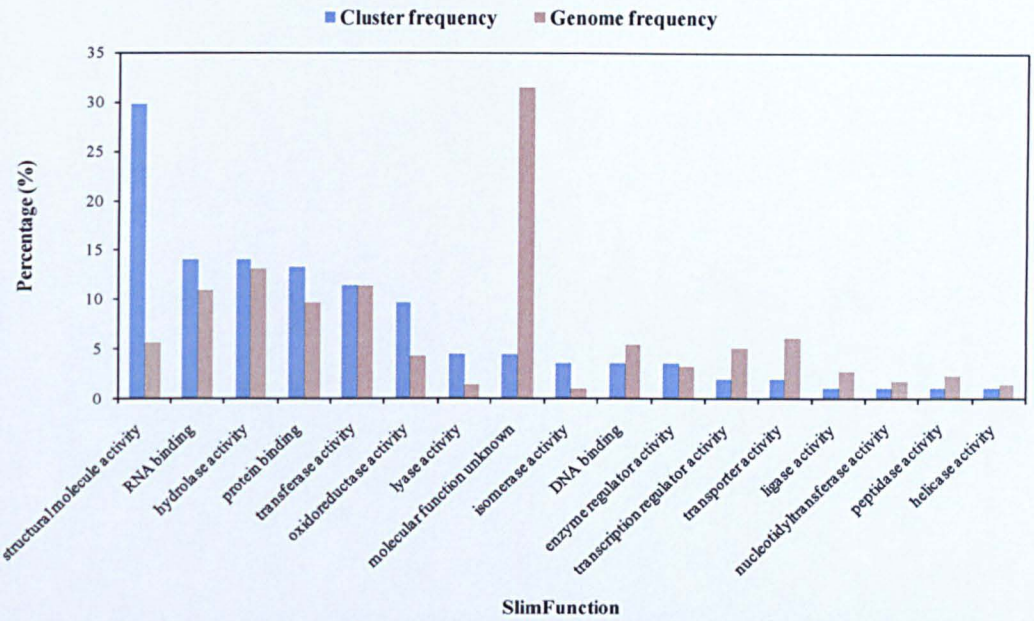

Figure 3.47 Gene ontology function terms associated with the 118 proteins that consistently increased in expression as Rnq1p expression increased.
The frequency of a term associated with the gene list was plotted against the genome frequency for the term. SlimFunction is an online gene ontology tool available on the *Saccharomyces Genome Database* website (hhtp://www.yeastgenome.org).

It was notable that oxidoreductase activity was also up-regulated, although it was not as significant a function for the up-regulated group of proteins as it was for the down-regulated group of proteins. Specifically, 2 of the up-regulated proteins (Ahp1p and Glr1p) are directly involved in glutathione and hydroperoxide reduction, 8 are involved in various metabolic processes such as GMP production (Imd3p) or acetyl-coA production (Pda1p).

3.4.3.3 Expression Profiles: GO Component

The GO component term indicates the organelles or cellular localisations associated with a list of query proteins. The components most affected by the decreased group of proteins were associated with the mitochondrial envelope (4.4x more than genome frequency, 'gf'), peroxisomes (3.7x more than gf) and the mitochondria (2.5x more than gf) (figure 3.48). The components most affected by the increased group of

proteins were the ribosome (6.9x more than gf) and the membrane fraction (2.75x more than gf) (figure 3.49).

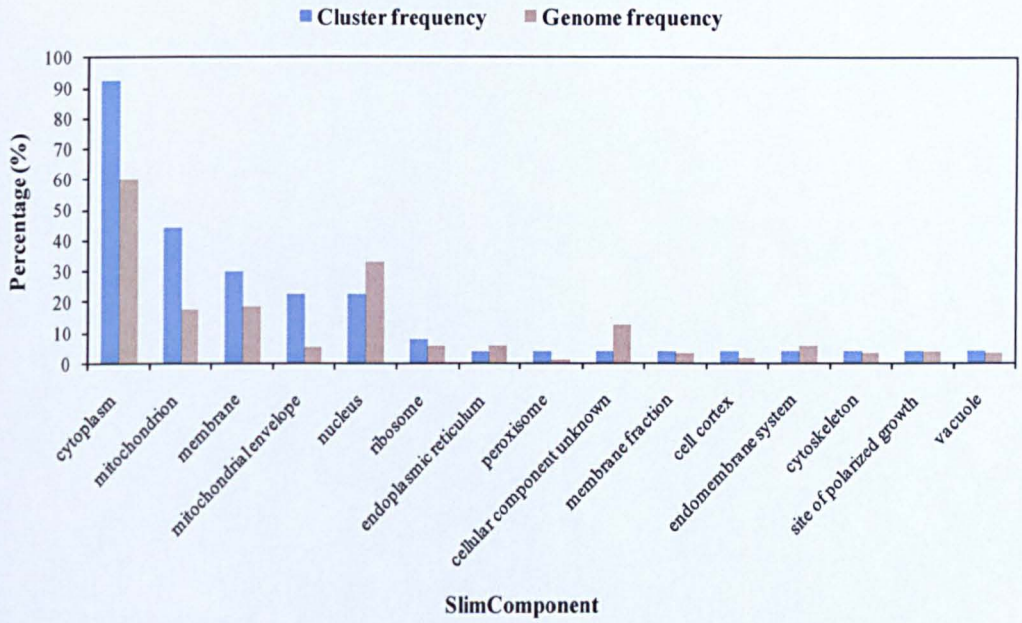

Figure 3.48 Gene ontology component terms associated with the 28 proteins that consistently decreased in expression as Rnq1p expression increased.

The frequency of a term associated with the gene list was plotted against the genome frequency for the term. SlimComponent is an online gene ontology tool available on the *Saccharomyces Genome Database* website (hhtp://www.yeastgenome.org).

Peroxisomes are organelles within the cell involved in oxidative reactions and the oxidation, breakdown and utilisation of fatty acids. Therefore, a decrease in peroxisome activity would be associated with a decrease in lipid metabolism. The increase in the ribosome component was fitting with gene ontology terms so far associated with the group of up-regulated proteins, which have increased ribosome biogenesis and translational processes. The increase in the membrane fraction component was somewhat surprising and it was difficult to reconcile this term with the processes thus far indicated. It pertained to the consistent increase in expression of proteins: Ahp1p, Gas1p, Hom2p, Hsc82p, Imd3p, Met6p, Ras2p, Ssa2p, Ssb2p, and Vps1p, as Rnq1p expression was increased in the cell. Only the function of Gas1p is specific to the cell wall, which serves as a cell wall assembly protein. The Ssb2p protein is a ribosome associated chaperone that works with the J-protein

chaperone Zuo1p, which was also consistently increased in expression as Rnq1p abundance increased. Given the multiple annotations assigned to each protein, the 'membrane fraction' component may not be significant however it should not be entirely disregarded.

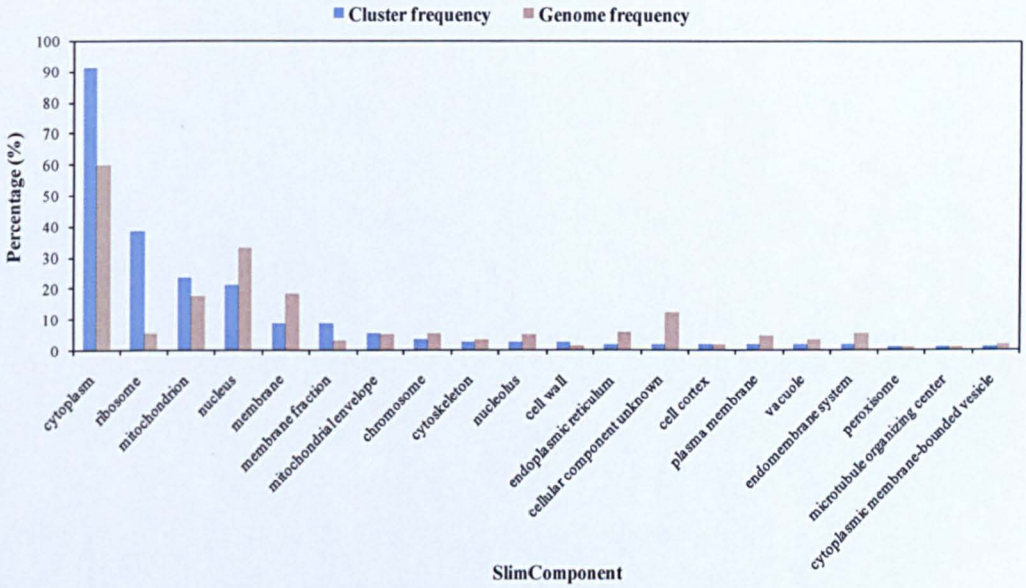

Figure 3.49 Gene ontology component terms associated with the 118 proteins that consistently increased in expression as Rnq1p expression increased.

The frequency of a term associated with the gene list was plotted against the genome frequency for the term. SlimComponent is an online gene ontology tool available on the *Saccharomyces Genome Database* website (hhtp://www.yeastgenome.org).

3.4.4 Validating biological indications of the data set

Results obtained from the proteomics study represent statistically significant changes to the proteome as a consequence of variation in the level of Rnq1p expression. Ideally, one should be able to demonstrate biological events predicted by such a study. In this study, biological indications for Rnq1p have been inferred from changes in the expression level of different proteins therefore, the data presented by the LC/MALDI-MS technique would be further supported in its indications if a second source of evidence existed confirming these changes in protein levels, specifically by quantitative western blots. In addition, the detected functional perturbations brought about by the protein of interest, in this case Rnq1p, should also

be reproducible and verified directly. This validates not only the observations made concerning Rnq1p, but also the utility of the LC/MALDI-MS approach in revealing the biological identity of a given protein.

3.4.4.1 Rnq1p sensitizes the cell to oxidative stress

The proteomics data indicated that as Rnq1p expression was elevated in the cell, both cellular respiration and mitochondrial organisation were down-regulated and a significant decrease in oxidoreductase function was also detected. To determine whether there was a link between Rnq1p and mitochondrial damage or oxidative stress, the effect of an oxidative stress inducing agent, in this case hydrogen peroxide (H_2O_2), was tested on three different strains that differed only in their expression level of Rnq1p creating a gradient of Rnq1p abundance on the galactose-based medium between the three strains, with no Rnq1p protein present in the *rnq1Δ* strain, the wild-type level of Rnq1p protein present in the pYES2 transformed strain, and an elevated level of Rnq1p protein present in the pYES2-*RNQ1* transformed strain. However, on medium other than galactose, the level of Rnq1p should be comparable in the pYES2 and pYES2-*RNQ1* transformed [*pin*$^-$] strains, since there was expected to be minimal induction of Rnq1p from the pYES2-*RNQ1* vector in the absence of galactose.

The strains were grown overnight in a glucose-based selective minimal medium before diluting and spotting onto 2 % raffinose selective minimal media, with or without 3 mM H_2O_2 (figure 3.50). In the absence of 3 mM H_2O_2, the three strains grew similarly on the 2 % raffinose. However, on the 2 % raffinose containing 3 mM H_2O_2 the two [*pin*$^-$] strains showed weaker growth, relative to the *rnq1Δ* strain. This indicated that the absence of Rnq1p conferred a slight growth advantage in the presence of 3 mM H_2O_2.

Cells from colonies on the 2 % raffinose plates with and without H_2O_2 were then used to establish cell dilutions for spotting onto galactose medium, with and without H_2O_2. For example. cells from the 2 % raffinose plate were transferred to 2 % galactose medium and 2 % galactose + 3 mM H_2O_2; similarly, cells from the 2 % raffinose + 3mM H_2O_2 plate were transferred to 2 % galactose medium and 2 %

galactose + 3 mM H_2O_2. The cell suspension used to establish these dilutions was cell number adjusted to ensure all samples contained equivalent numbers of cells.

The three strains grew equally well on 2 % galactose, regardless of whether they had been previously exposed to 3 mM H_2O_2. This indicated 1) that galactose induced over-expression of Rnq1p in the [*pin*$^-$] background was not responsible for any growth defect on 2 % galactose medium, 2) that earlier oxidative stress events did not impair subsequent growth capacity, and 3) that all three strains grew to the same extent on 2% galactose.

However, transfer of these strains from 2 % raffinose to 2 % galactose + 3 mM H_2O_2 resulted in a growth defect that appeared to correlate with the level of Rnq1p being expressed. Specifically, Rnq1p protein appeared to sensitise the cells to oxidative stress induced by H_2O_2. A similar result was observed when the strains were transferred from 2 % raffinose + 3 mM H_2O_2 media to 2 % galactose + 3 mM H_2O_2 media however in this case, there was slightly more growth observed for all three strains, and this is likely to represent the benefit conferred by pre-adaptation to oxidative stress on these cells, allowing for the subsequent slightly improved growth in the presence of the same oxidative stress.

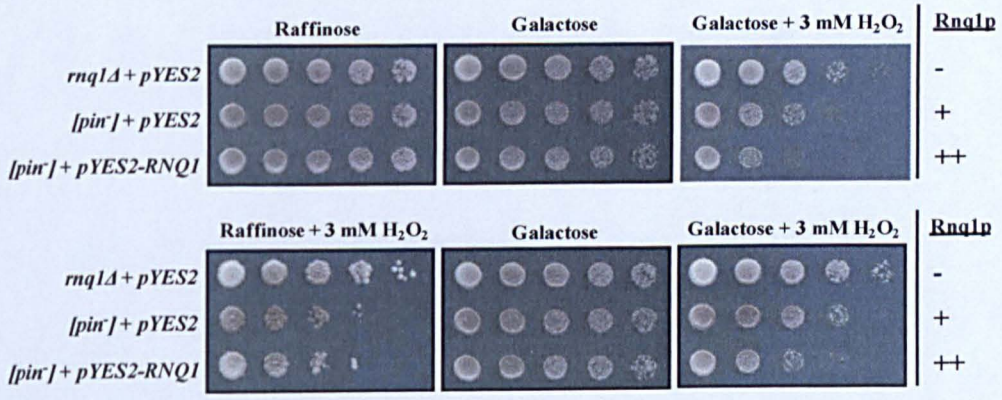

Figure 3.50 Oxidative stress sensitivity as a consequence of changes to Rnq1p abundance.
The growth defect brought about by oxidative stress (hydrogen peroxide, H_2O_2) increased as the cellular abundance of Rnq1p increased. Galactose induced the over-expression of Rnq1p from the pYES2-*RNQ1* vector. Pre-adaptation to oxidative stress allowed for greater growth on subsequent exposure to oxidative stress on galactose, but the effect relationship between sensitivity and Rnq1p expression persisted.

In summary these results appears to support indications from the proteomics data of decreased oxidoreductase activity and perturbations to the mitochondria, since an increase in cellular Rnq1p abundance increased the sensitivity of the cells to oxidative stress.

3.4.4.2 Rnq1p and the TOR pathway: rapamycin exposure

The consequence of altering Rnq1p abundance appeared to impact upon diverse range of processes. Many of the processes that were seemingly altered, ribosome biogenesis, protein synthesis (translation), TCA-cycle components and mitochondrial respiration for example, are also processes that are responsive to Tor1p signalling. Target of rapamycin-1, Tor1p, mediates growth related signalling in response to nutrition or cellular stress; however its activities can be inhibited by exposure to the antibiotic rapamycin. It was therefore decided to determine if there was a genetic interaction between Rnq1p and Tor1p, a BY4741 *rnq1Δ* strain was grown up in YPD-rich medium overnight, serially diluted at 5-fold increments and spotted onto YPD-agar with or without 25 nM rapamycin. At the same time, a *ppq1Δ* strain was also tested along with a double knock out *rnq1Δ ppq1Δ* strain. Ppq1p is a serine/threonine phosphatase (Chen *et al.*, 1993) that enhances the efficiency of nonsense suppression (Vincent *et al.*, 1994) and a *ppq1Δ* strain enhances the frequency of [*PSI*$^{+}$] *de novo* appearance. Additionally, *ppq1Δ* was identified in a high-throughput screen of the Yeast Knock-out Collection to be partially resistant to rapamycin (Chan *et al.*, 2000).

A *ure2Δ* strain is sensitive to rapamycin (Merwe, 2001), and a *gln3Δ* strain which resistant to rapamycin (Merwe, 2001), were included in the study as controls. Both were obtained from the yeast-based BY4741 Yeast Knock-out Collection and all strains were cell-number adjusted prior to serial dilutions and plating.

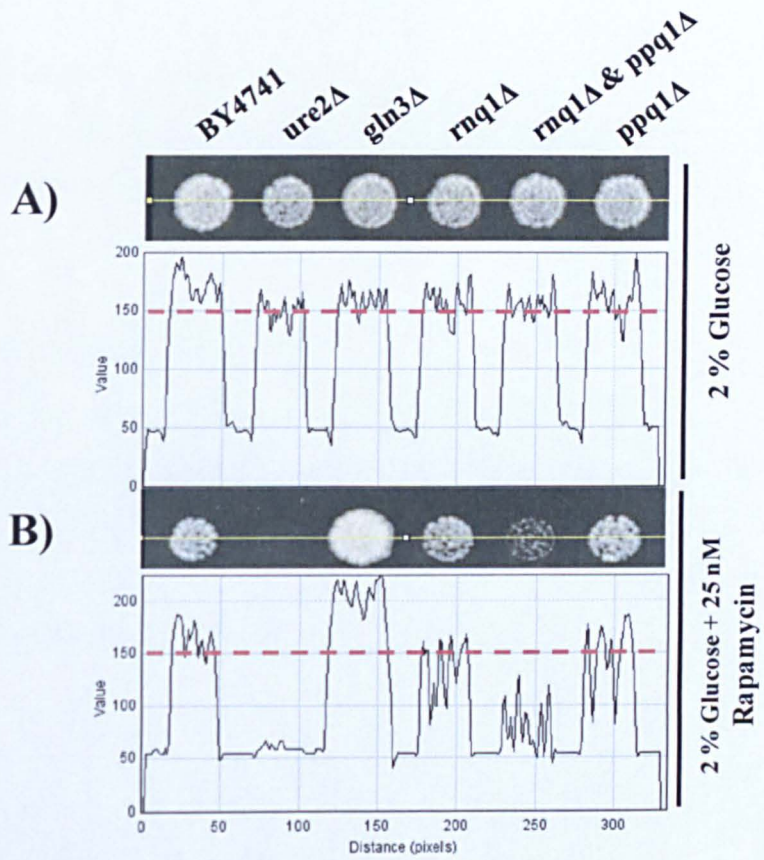

Figure 3.51 Rapamycin phenotype assay of the *rnq1Δ* strain.
There appeared to be no difference in growth for the *rnq1Δ* compared to the parental BY4741 strain on 2 % glucose (panel A) or upon exposure to 25 nM rapamycin in 2 % glucose (panel B). There was however partial sensitivity of a *rnq1Δ* & *ppq1Δ* double-knockout in BY4741, suggestive of Rnq1p's role in a redundant pathway that may be positively regulated by Tor1p or that enhances Tor1p signalling. The *ure2Δ* and *gln3Δ* strains served as growth controls since they are known to be sensitive and resistant, respectively, to rapamycin exposure. The accompanying trace reflects cell density of the colonies.

Comparing growth of the strains on YPD complete agar without rapamycin (figure 3.51A) and with rapamycin (figure 3.51B) all strains except the resistant *gln3Δ* strain exhibited a growth defect, with no growth for the sensitive *ure2Δ* strain at the presented dilution. The *rnq1Δ* strain and the *ppq1Δ* strain grew similarly to the BY4741 parental strain however the double knockout *rnq1Δ&ppq1Δ* showed enhanced sensitivity to rapamycin suggesting a possible interaction between Ppq1p and Rnq1p that is either positively regulated by Tor1p or that enhances Tor1p signalling. That the partial sensitivity phenotype only presented in the combined

absence of Rnq1p and Ppq1p, it may suggests some functional redundancy exists that can substitute for the absence of Rnq1p or Ppq1p, but the redundant components do not work sufficiently well to prevent the onset of partial rapamycin sensitivity when both Rnq1p and Ppq1p are absent.

3.4.4.3 Rnq1p and cell wall defects

The proteomics project indicated that cellular lipid metabolism and fatty acid synthesis were consistently down-regulated as Rnq1p expression was increased, which may have implications for cell wall integrity. If these processes are at their maximal in the absence of Rnq1p protein, it might be predicted that the cell wall is more robust in the absence of Rnq1p.

To address this possibility, the effect on a *rnq1Δ* strain of exposure to cell-wall stress was tested. The same cultures as prepared in section 3.4.4.3 were spotted onto 2 % glycerol + 0.01 % SDS; the detergent SDS is believed to damage cellular membranes but also induce mitochondrial petites, growth on non-fermentative medium therefore selects only for the growth of respiratory competent cells.

Comparing growth of the strains at the same dilution on 2 % glucose, 2 % glycerol and 2 % glycerol + 0.01 % SDS it was observed that the *rnq1Δ* strain exhibited no noticeable growth defect on 2 % glycerol or increased resistance to SDS stress, compared to the BY4741 parental strain (figure 3.52). The *ppq1Δ* showed a slight growth advantage in the presence of SDS, however in the combined absence of *rnq1Δ* & *ppq1Δ* not only was there a slight growth advantage on glycerol compared to all other tested strains, but also a noticeable resistance to SDS. This result links Rnq1p to stress resistance or cell wall integrity; however the absence of Rnq1p was not sufficient to be able to detect this link directly.

Alternatively, the *rnq1Δ* & *ppq1Δ* strain may have enhanced respiratory capacity, since this strain not only grew well on glycerol relative to the other strains, but the impaired growth of the other strains in the presence of SDS may reflect the induction of petites in these strains and therefore a reduction in the number of cells capable of growing on glycerol. The effect of the *rnq1Δ* and *ppq1Δ* mutations may render this

strain less susceptible to petite mutation induction by SDS

Figure 3.52 Phenotypic assay of cell wall integrity in a *rnq1Δ* strain.
Growth on non-fermentative media was not altered in the *rnq1Δ* strain compared to the parental BY4741 strain, and there was no difference in response to SDS between these two strains. There was however increased growth on glycerol of a *rnq1Δ* & *ppq1Δ* double knock-out, and a significant increase in SDS-resistance of the double-knockout strain relative to all other strains tested.

3.4.4.4 The growth response of *rnq1Δ* to different carbon sources

The proteomics data indicated changes to the central metabolic processes, such as the TCA-cycle, that are commonly responsive to carbon source. In the presence of different carbon sources the cell preferentially metabolises the fermentable carbon source, such as glucose, and the TCA-cycle is repressed, only to be derepressed upon exhaustion of the fermentable carbon source and a need to metabolise non-fermentable carbon sources, such as glycerol or ethanol – the latter of which is a by-product of the fermentation process.

The up-regulation of the TCA cycle components simultaneously with glycolysis, following an increase or decrease in Rnq1p abundance relative to the wild-type endogenous level, suggested that Rnq1p might interfere with carbon source signalling, causing the cell to respire where the cell would normally be fermenting the carbon source and repressing respiration. Such an affect of Rnq1p on the cell may amount to growth defects on fermentable carbon sources, or a growth advantage

on non-fermentative carbon sources. To test this, the growth rates of a 74D694 [*pin*$^-$] and *rnq1Δ* strain were determined on different carbon sources.

A 74D694 [*pin*$^-$] and *rnq1Δ* strain were inoculated into a sterile 24-well plate containing 1 mL aliquots of complete media varying in carbon source: 2 % glucose, 2 % galactose, 2 % glycerol or 2 % ethanol. Growth was monitored by changes to OD_{600} over time using a BMG LabTech FLUOstar OPTIMA plate reader, with shaking and incubation at 30 °C. The results obtained were an average of 4 analyses over 2 separate experiments.

No significant differences in growth was discerned between the strains on glucose. On galactose, a subtle growth defect of the *rnq1Δ* strain was observed, and this defect was exaggerated when grown in a glycerol-based medium. Growth rates on ethanol between the two strains were not statistically different, however the maximal doubling time for growth in ethanol was probably not obtained over the time course of the experiment since this value was still decreasing at the end of the experiment.

The results obtained suggest that the up-regulation of the TCA-cycle in the *rnq1Δ* strain is not associated with a defect in glucose up-take or fermentation since there was little difference in growth rate between the *rnq1Δ* and [*pin*$^-$] strains on glucose. However, a growth disadvantage was seen with the *rnq1Δ* strain on both galactose and glycerol.

Galactose is a carbon source that shows a slight increase in respiration relative to glucose, occurring simultaneously with fermentation (albeit to a considerably less degree than fermentation) e.g. fermentation and respiration are not entirely mutually exclusive. Glycerol is a non-fermentable carbon source and therefore can only be metabolised through respiration, hence the ability to utilise glycerol demands respiratory-competent mitochondria. The overlapping error bars for the ethanol-based doubling times undermine the simple conclusion that respiratory activity of the cell accounts for the *rnq1Δ* and [*pin*$^-$] strain growth differences on galactose and glycerol, however it was observed that the maximal doubling time for growth on ethanol was not obtained, and therefore the doubling time result for ethanol may be somewhat less persuasive in its indication. It would be necessary to repeat the growth analysis of ethanol over a longer time period in order to determine the

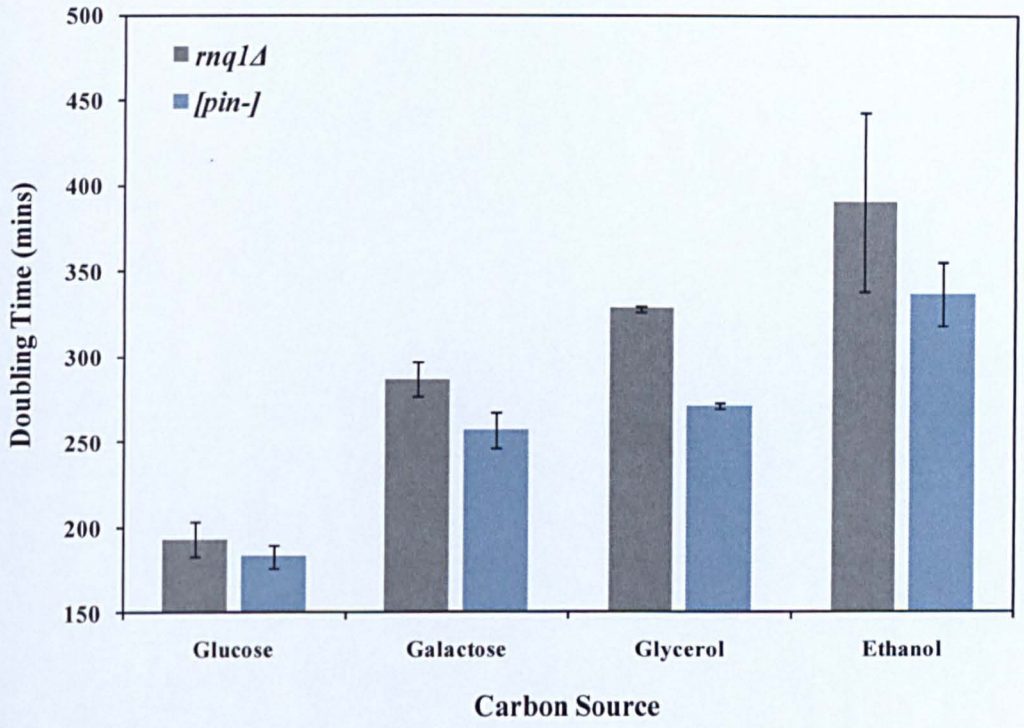

Figure 3.53: Growth analysis of a wild-type (*RNQ1+*) and *rnq1Δ* strain on difference carbon sources.

Comparing the maximal doubling time for the 74D *rnq1Δ* and 74D [*pin*$^-$] strains on each of the listed carbon sources suggests that the *rnq1Δ* strain has a subtle growth defect on galactose and a slightly more significant defect on glycerol.

difference in maximal doubling times between the two strains. However, if the *rnq1Δ* strain does have a respiratory-dependent defect, despite the observed up-regulation of TCA-cycle components, this might indicate a problem with flux through the TCA-cycle in the *rnq1Δ* strain or a reduction in the provision of NADPH, required for cellular respiration, resulting in reduced growth on carbon sources that require respiratory competency. The up-regulation of TCA-cycle components might represent attempts of the cell to increase TCA-cycle activity.

3.4.5 Summary of main findings and conclusions

The cell is not simply a collection of many distinct non-overlapping activities; the direct perturbation of a single function due to changes of a single protein is likely to be accompanied by non-direct perturbations of other cellular functions. Such a plethora of indications are not insignificant since they accurately reflect the cellular influence of the protein in question but it can complicate identification of the specific activity of the protein under test.

The proteomics data provided a means by which to identify functions that were up-regulated or down-regulated in the cell as a consequence of increasing or ablating the expression of Rnq1p. There appeared to be quite distinct functions associated with these up- and down-regulated proteins and the most significant fold-changes in these functions relative to their genome frequency are summarised in table 3.5. There was not however one over-arching indication that identified the function of Rnq1p within the cell but instead it provided important material for hypothesis-driven experiments some of which were undertaken and reported in this chapter.

An almost contradictory assembly of processes were up- or down-regulated with changes in Rnq1p abundance. Given the diversity of proteome-level changes linked to Rnq1p abundance in the cell, it seems likely that Rnq1p is involved directly or indirectly with transcriptional programs pertaining either to the mitochondria or to central metabolism, and that these changes then have downstream consequences on other cellular processes.

Since more proteins increased (than decreased) in expression in both the *rnq1Δ* strain and the over-expression strain, this might indicate that Rnq1p forms a complex with other cellular proteins making the relative stoichiometry, rather than the absolute amount, of Rnq1p important. Again, it is likely that if Rnq1p is involved in one or more complex assemblies, then such a complex must be well placed to affect the rather radical transcriptional choices observed.

In overview, glycolysis was up-regulated in both the *rnq1Δ* and Rnq1p over-expressing strains, while gluconeogenesis was down-regulated in the same strains, as was the oxidative branch of the pentose phosphate pathway and fatty acid

metabolism. The TCA-cycle was up-regulated in the *rnq1Δ* and Rnq1p over-expressing strains, as were components of the electron transport chain.

	decreased		increased	
	xGF	GO term	xGF	GO term
PROCESS	9.59	co-factor metabolic process	7.5	protein folding
	6.37	generation of precursor metabolites	3.67	translation
	5.16	cellular carbohydrate metabolism	3.3	cellular amino acid metabolism
	4.6	cellular respiration	2.4	ribosome biogenesis
	3.7	nucleus organisation	5.32	structural molecule activity
	3.7	heterocycle	3.89	isomerase activity
	3.26	cellular lipid metabolism	3.38	lyase activity
	3.2	cellular homeostasis	2.23	oxidoreductase activity
FUNCTION	6.88	oxidoreductase activity	1.36	protein binding activity
	4.11	ligase activity	1.28	RNA binding activity
	2.85	helicase activity	6.8	ribosome
	2.85	lyase activity	2.75	membrane fraction
COMPONENT	4.4	mitochondrial envelope	1.62	cell wall
	3.7	peroxisome		
	2.5	mitochondrion		

Table 3.5 Summarising cellular processes, functions and components that increased or decreased with increasing Rnq1p abundance.
The proteins that were found to consistently increase or decrease in expression as Rnq1p abundance was increased in the cell were analysed for enrichment of gene ontology terms relative to the genome frequency (xGF) and are summarised in the above table. Consistently decreased proteins n= 28; consistently increased proteins n= 118.

Many proteins involved in oxidoreductase activity were consistently down-regulated, and, possibly due to down-regulation of the oxidative branch of the pentose-phosphate pathway, Ymr315w was increased (particularly in the *rnq1Δ* strain) indicative of a low cellular pool of NADPH. Despite this, amino acid biosynthesis levels were up-regulated, and energy demanding processes such as ribosome biogenesis and translation were also increased.

It is likely that the mitochondria were negatively affected by increases to Rnq1p abundance, since concomitant with this were decreases in proteins required for mitochondrial structure and assembly, such as Mdm38p, Fcj1p, Clu1/Tif1p and Fas2p. Both Fcj1p and Mdm38p were up-regulated in the *rnq1Δ* strain.

It was also interesting that many proteins known to be induced or repressed by zinc-deficiency varied in this manner in the *rnq1Δ* strain. Specifically, Zps1p, induced by low zinc levels, was significantly up-regulated (2.95x) in the *rnq1Δ* strain, along with Hsp26p, Tsa1p, Ade1p, Eno1p, Eno2p, Scw4p, Tdh1p, with Adh1p and Adh3p being repressed, as expected in zinc-deficiency.

Additionally, the Tt1p protein of the ASTRA complex regulating telomeric chromatin was substantially down-regulated in the *rnq1Δ* strain and increased consistently with Rnq1p abundance. In contradiction however, the Rvb2p protein, also a component of the ASTRA component, showed the opposite correlation with Rnq1p, decreasing consistently in abundance as Rnq1p increased. This might indicate for the ASTRA complex at least the regulation of complex activity via stoichiometric control based on feedback from individual subunit abundance.

The benefit of testing the 3 strains *rnq1Δ* + pYES2, [*pin*$^-$] + pYES2 and [*pin*$^-$] + pYES2-*RNQ1*, and their subsequent pair-wise comparison is exemplified by the finding of this alternating response of protein expression in response to Rnq1p levels. Had only the *rnq1Δ* strain and [*pin*$^-$] + pYES2 transformed strain been compared, we might have concluded for example that the TCA-cycle was up-regulated in the *rnq1Δ* strain and our stipulations might have revolved merely around a negative influence of Rnq1p in TCA-cycle activity. However, in the current arrangement of the experiment we have been fortunate to determine that it is the precise level of Rnq1p abundance in the cell that is influential for the central metabolic pathways.

Chapter IV

Analysis of Sequence Polymorphisms in the *RNQ1* Gene of Natural and Laboratory Strains of *Saccharomyces cerevisiae*

4.1 Introduction

Previous work in the Tuite laboratory on a group of 7 different *S. cerevisiae* strains demonstrated that the *RNQ1* gene contained considerable polymorphism at the nucleotide and amino acid level (Resende *et al.*, 2003a). Of the strains examined, 5 were clinical isolates and one a standard laboratory strain (Resende *et al.*, 2003a).

In order to gain a better appreciation for the full repertoire of *RNQ1* gene polymorphisms that might exist in nature, a collection of 15 natural isolates, 16 clinical isolates and 7 laboratory strains of *S. cerevisiae* were assembled. In choosing the natural isolate strains, consideration was given to the influence of spatial and temporal separation as a possible driving force for further sequence polymorphism, and as such the natural isolate collection assembled represented a variety of ecological niches from around the globe.

The initial aim of this work was to determine whether Rnq1p was expressed in these strains and whether Rnq1p existed in the [*pin*$^-$] or [*PIN*$^+$] state. Subsequently PCR was used to isolate the respective *RNQ1* gene for sequencing and polymorphism analysis. The full list of yeast strains studied is provided in the materials and methods Table 2.1

4.1.1 Detection of Rnq1p in strains of *S. cerevisiae*

The Rnq1p protein was readily detected by western blot analysis for most of the strains, although for some strains the signal was faint (figure 4.1). This may be due to differences in extract handling and/or to differences in the expression level of Rnq1p in these strains.

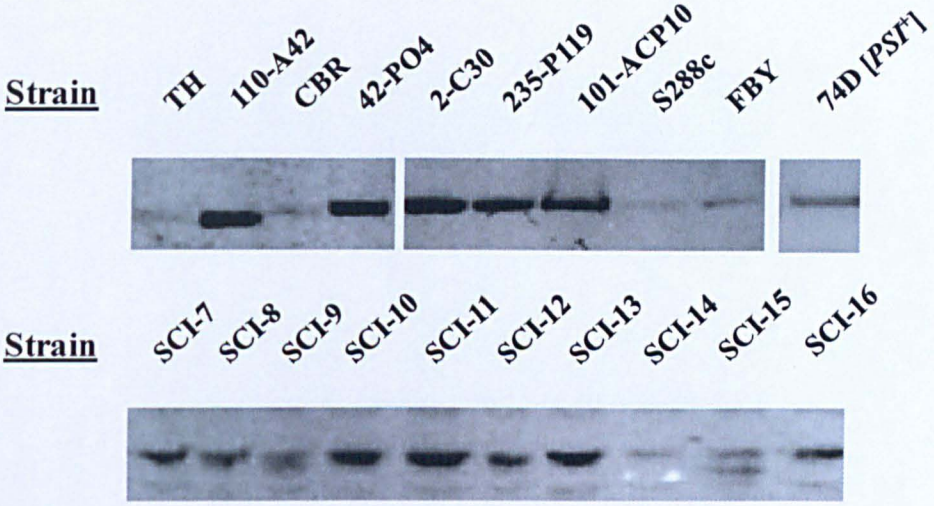

Figure 4.1 Western blot analysis confirms Rnq1p expression in both laboratory and natural strains.

4.1.2 Establishing the [*PIN*$^+$] status of the test strains

To determine whether Rnq1p existed in the [*pin*$^-$] or [*PIN*$^+$] state in these 31 strains, a sedimentation analysis was performed on each. This method relies on differential ultracentrifugation of aggregated and soluble protein. Higher molecular weight, aggregated Rnq1p protein is distributed to the pelleted fraction, with the lower molecular weight, soluble protein remaining in the soluble fraction. Analysis of the non-ultracentrifuged (total) fraction, the soluble fraction and the pellet fraction by SDS-PAGE and subsequent western blot reveals, was used to establish whether Rnq1p was predominantly in the pellet fraction and therefore [*PIN*$^+$] or predominantly in the soluble fraction, and therefore [*pin*$^-$]

While the 17 of the 31 strains were found to be [*pin*$^-$], five clinical isolates and two natural strains were [*PIN*$^+$], along with the five laboratory strains (figure 4.2 and table 4.1).

Figure 4.2 Rnq1p prion status of studied strains
Sedimentation analysis was performed to determine the prion status of Rnq1p in the different *S. cerevisiae* strains.

[*PIN*$^+$] Strains	[*pin*$^-$] Strains	
FBY	*SCI-6*	*SCI-12*
SCI-13	**L1384**	*SCI-15*
SCI-1	2-C30	*SCI-16*
SCI-2	101-ACP10	Y12
SCI-3	*SCI-7*	K11
SCI-4	*SCI-8*	
SCI-5	*SCI-9*	
JSW508	NCYC-361	
JSW512	*SCI-10*	
W303	*SCI-11*	
SDY	TH	
S288c	235-P119	
74D-694	42-PO4	

Table 4.1 A summary of the strains identified as [*PIN*$^+$] or [*pin*$^-$].
Sedimentation analysis of the 31 test strains confirmed whether they harboured Rnq1p in the prion [*PIN*$^+$] state or the soluble [*pin*$^-$] state. Lab strains are indicated in bold (x7), clinical isolates are italicised (15x), and the remainder are the natural strains (x9).

To determine whether duration of growth, the culture OD_{600} or the number of harvested cells might affect the distribution of Rnq1p between the pellet and soluble fractions, an analysis of these parameters with the natural [*PIN*$^+$]strain yeast strain SDY was carried out (figure 4.3). No significant effect on Rnq1p distribution between the fractions was noted until the 6 hr culture and this is likely to do the high cell density of the sample, which possibly compromised protein extraction procedure and resulting a lysate with increased content of cellular debris. Alternatively, the bulk of material in this sample may have saturated the proteases that are required to prevent degradation of Rnq1p in the sample.

Time (hr)	2	3	3 ^{74D}	4	4	5	6
Culture OD_{600}	0.46	0.82	0.53	1.58	1.25	1.92	2.81
Harvest OD_{600}	4.0	4.0	4.0	4.0	10.0	4.0	28.1
Result	T P S	T P S	T P S	T P S	T P S	T P S	T P S

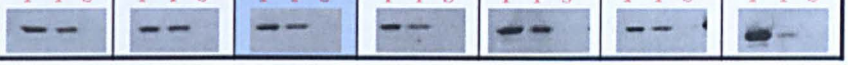

Figure 4.3: The affect on Rnq1p sedimentation analysis of changes to culture and harvest conditions.

The natural strain SDY was cultured and harvested to different indicated OD_{600} densities prior to sedimentation analysis of Rnq1p to determine the impact on Rnq1p distribution across the collected fractions. Isolated fractions are as follows: 'T' is total, 'P' is pellet, and 'S' is soluble.

4.1.3 Cloning of the *RNQ1* gene

The *RNQ1* gene was isolated from the different yeast strains listed in table X of the M&M section by PCR. Trials of primers and sequencing regions were performed before deciding upon the combination of primers presented here. Specific, primers incorporating 46 bp up- and 36 bp down-stream of the ORF were chosen for amplifying the *RNQ1* gene from the different strains. The DNA and sequence of the amplified *RNQ1* genes was performed by DBS Genomics services using the same pair of primers.

Individual isolated *RNQ1* genes were cloned into the pYES2 plasmid for further downstream analyses. The pYES2 plasmid is a 2μ vector with an ampicillin resistance gene, a *URA3* selectable marker and galactose-inducible *GAL1* promoter. The 5' PCR primer incorporated a *Hin*dIII restriction site and the 3' primer an *Xho*I restriction site to enable the ligation of the *RNQ1* PCR fragment into the multiple cloning site of pYES2 (figure 4.4).

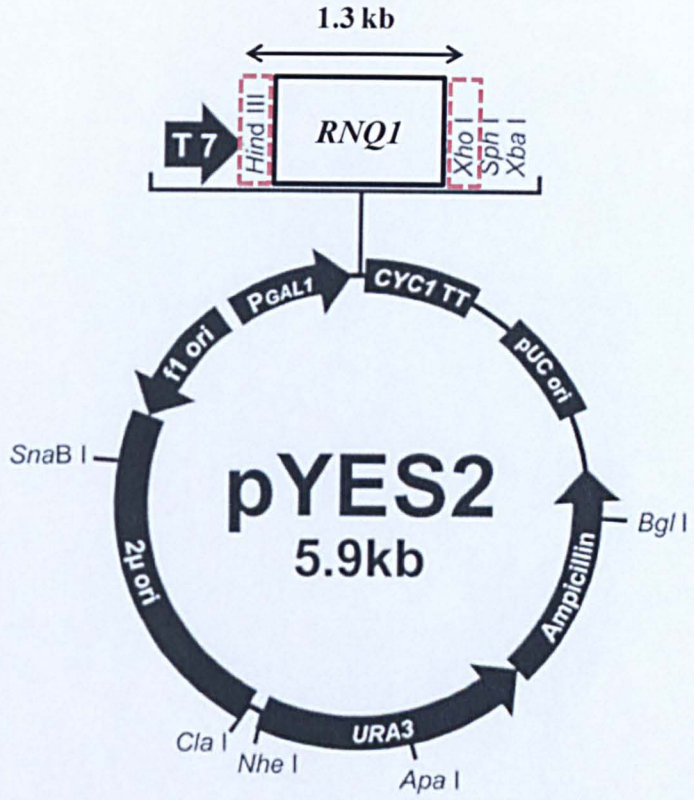

Figure 4.4: The plasmid map for pYES2-*RNQ*1.
The *RNQ1* gene was cloned into the multiple cloning site of pYES2 with via a 5' *Hind*III and a 3' *Xho*I restriction site. The insert was approximately 1.3 kb and was placed under the control of the galactose inducible promoter (P_{GAL1}).

Prior to the ligation reaction, a 1 uL aliquot of the purified PCR product and a diluted aliquot of the vector were checked by agarose gel electrophoreses to determine an appropriate ligation ratio as illustrated in figure 4.5. The ligation reaction mixture was transformed into competent *E. coli* cells which were then selected for by the pYES2-conferred resistance to ampicillin. Plasmid DNA was isolated from the resistant colonies and, to determine which plasmid DNA represented a successful ligation reaction e.g. *RNQ1* ligated to pYES2, an aliquot of the different plasmid preparations was digested with *Hind*III and *Xho*I to visualise release of the ~1.3 kb *RNQ1* insert (figure4.6).

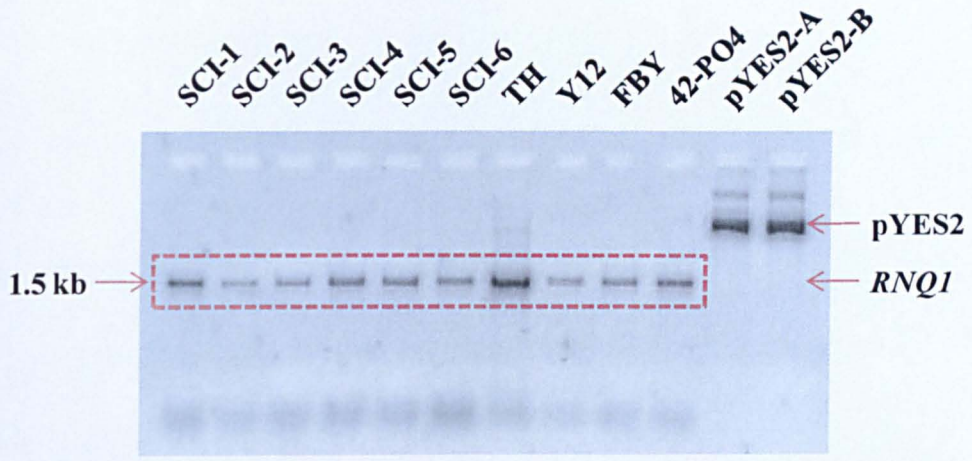

Figure 4.5: Determination of ligation ratio for pYES2 cloning.
Following purification of the PCR amplified *RNQ1* insert from each of the indicated strains, 1 µl was loaded onto an agarose gel alongside an aliquot of pYES2 vector to determine suitable ligation ratios.

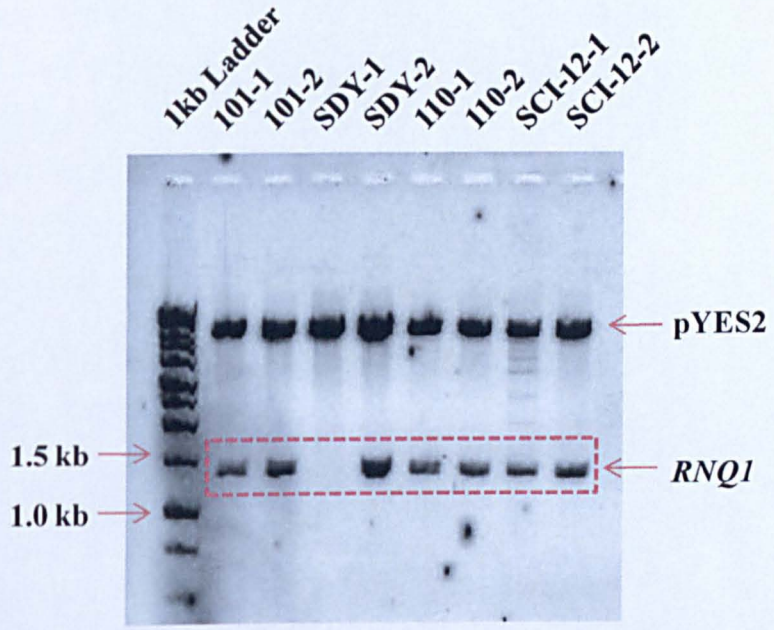

Figure 4.6: The identification of successful ligation reactions between the pYES2 vector and the *RNQ1* gene insert.
Plasmid DNA is isolated from *E. coli* transformants and digested to confirm the presence or absence of *RNQ1* insert in the plasmid. If *RNQ1* has ligated to pYES2, then a digest with restriction enzymes *Xho*I and *Hind*III will liberate a ~1.3 kb band corresponding to the size of the *RNQ1* gene (1218 bp) plus flanking sequences 5' (45 bp) and 3' (36 bp) of the *RNQ1* coding sequence incorporated by the primers.

The *RNQ1* gene was previously shown to be heteroallelic in a number of diploid/triploid strains (Resende *et al.*, 2003a). In such cases the PCR reaction would generate two or three products. To increase the chance of visualising these different alleles from a single strain, multiple constructs representing each strain were generated and the cloned *RNQ1* allele sequenced.

4.1.4 Identifying *RNQ1* Polymorphisms

Forward and reverse sequence reads were aligned against the consensus *RNQ1* sequence in BioEdit to determine the sequence of test constructs. The resulting predicted amino acid sequences for all alleles are given in Appendix 1. Table 4.2 summarises the identified polymorphic residues and the strains that harbour these polymorphisms.

The sequence information was used to generate a referencing system of alleles, where each allele reflects a unique combination of regional variation throughout the *RNQ1* gene (table 4.3). Most of the alleles were detected in only one strain, though there were a few instances where multiple strains possess the same *RNQ1* allele. The sequence originally published for *RNQ1* (considered the consensus, 'non-polymorphic' sequence) is classified as allele-type *RNQ1-1*.

Analysing the positions of the identified Rnq1p polymorphisms (Table 4.7) in terms of the regions assigned by Kadnar *et al.* (Kadnar *et al.*, 2010) (section 1.5), the polymorphisms were seen to scatter across the protein. However, the QG_{10} and QN_1 region appeared to be particular hot-spots for polymorphism, with 20 polymorphisms clustering to a 45 amino acid region. In contrast, immediately adjacent to the QG_{10}/QN_1 region, the QN_2 region also spanning 45 residues, was associated with only 5 polymorphisms.

	Polymorphism		
Residue	From	To	**Strain**
18	N	S	12-a, 12-b, 12-B, 12-C, 12-D
32	S	P	TH-b
39	M	T	SDY-b
		V	13-c
55	D	E	NCYC-90-4
		G	NCYC-361-d
59	G	R	14-a, 14-b, 14-c
62	D	G	16-a
66	D	N	13-b
76	M	K	13-b
77	N	S	16-a
82	D	G	12-E
88	Q	P	W303 W11D
99	T	A	Y12-c
100	V	A	12-b
101	M	V	NCYC-90-D, 16-a
115	D	G	13-b
128	G	S	101-2
130	S	G	SDY-a
132	S	G	Y12-d
143	S	P	2-C3O-a
152-173	$(\Delta QG)_2$		12-A, NCYC-90-4, 12-1
	$(\Delta QG)_4$		1-d, 1-c, 5-c, 7-a, 7-b
	$(\Delta QG)_6$		12-2, 12-D, 12-B, 12-C
	$(\Delta QG)_8$		TH-c, TH-b, TH-d, 10-d
	$(\Delta QG)_{10}$		15-a, 16-d
157	Q	R	15-b
160	G	S	NCYC-361-d
163	Q	R	110-1
165	Q	R	SDY-b
171-172	+QG		Y12-a, Y12-c, Y12-d, 13-d, NCYC-90-D
173	S	P	110-1
174	F	S	110-2
178	A	V	FBY-b
180	L	S	Y12-d
182	S	P	110-c
184	F	S	110-a
185	M	V	TH-b

	Polymorphism		
Residue	From	To	**Strain**
193	Q	X	14-a, 14-b, 14-c
194	G	S	NCYC-361-d
198	S	G	13-c
210	M	T	13-c
211	A	T	16-d
215	M	I	JSW512-a
222	N	S	TH-b
250	Q	R	10-b
264	G	S	13-d
268	S	A	110-c
282	Q	R	W303 W11D
285-308	Δ11		9-c, 2-C30-d (ΔQQGQN/NQQQYQ or ΔNQQQYQ/QQGQN) 15-a, 16-d, 7-a, 7-b (ΔNQQQY/NQQGQN or ΔNQQGQN/NQQQY)
289	Q	R	110-2
305			
311	Q	H	15-a, 16-d
316	Q	R	74D-1b
319	Q	X	BY4741-c
321	H	R	14-a
336	L	P	16-d
357	R	S	12-A
360	Q	H	FBY-d, Y12-a, Y12-c, Y12-d, 12-1, 13-d, 13-c, 9-a, NCYC-90-D, NCYC-90-4, 12-A, 12-E, 15-b, 7-a, 10-d
372	P	L	16-a
372-373	+QHNGQQQSNEYGRP		7-a
		S	12-c
379	N	K	7-b
		D	10-b
382	G	E	7-b
383	Q	H	7a
386	S	P	2-c
387	F	V	12-b, 15-c
390	S	P	2-C30-c, 2-C30-b
401	N	S	12-E

Table 4.2 A summary of the Rnq1p residues identified as polymorphic. The *RNQ1* gene from multiple *S. cerevisiae* strains was sequenced leading to the identification of multiple polymorphic residues, as listed above. The majority are single amino acid changes, however many represent deletion of small tracts (Δ number) or expansions of sequence (+ amino acid).

Allele	Polymorphism (from-to-residue)	Strains	Construct #
RNQ1-1	none	consensus[1], 16-b[2], 101-1[3], SDY-2[4], 110-b[5], 110-d[6], SDY-D[7], 3-b[8], 3-c[9], 3-d[10], 4-b[11], 4-c[12], 4-d[13], 74D-5a[14], L1384-c[15], L1384-b[16], L1384-d[17], 6[18], 8[19], 2-a[20], BY4741-a[21], HIGH-1[22], MED-1[23], LOW-1[24], V.HIGH-3[25], 42-PO4-a[26], 42-PO4-b[27], 42-PO4-d[28], 101-C[29], 101-B[30]	19[1], 10[2], 14[3], 16[4], 22[5], 24[6], 27[7], 63[8], 64[9], 65[10], 66[11], 67[12], 68[13], 76[14], 45[15], 80[16], 81[17], 48[18], 50[19], 60[20], 78[21], 51[22], 53[23], 52[24], 54[25], 56[26], 86[27], 87[28], 28[29], 29[30]
RNQ1-2	s-p-32; Δ8-152-173; m-v-185; n-s-222	TH-b	70
RNQ1-3	d-n-66; m-k-76; d-g-115	13-b	37
RNQ1-4	d-g-62; n-s-77; m-v-101; p-l-372	16-a	9
RNQ1-5	d-g-82; q-h-360; n-s-401	12-E	34
RNQ1-6	q-p-88; q-r-282	W303-W11D	77
RNQ1-7	t-a-99; +qg-171-172; q-h-360	Y12-c	91
RNQ1-8	v-a-100; n-s-18; f-v-387	12-b	2
RNQ1-9	g-s-128	101-2	15
RNQ1-10	g-r-59; q-x-193	14-b[1], 14-c[2]	3[1], 5[2]
RNQ1-11	g-r-59; q-x-193; h-r-321	14-a	4
RNQ1-12	m-t-39; q-r-165	SDY-b	26
RNQ1-13	m-t-39; q-r-165; m-t-210; s-g-198; q-h-360	13-c	38
RNQ1-14	s-g-130	SDY-a	25
RNQ1-15	s-g-132; +qg-171-172; q-h-360; l-s-180	Y12-d	72
RNQ1-16	s-p-143	2-C30-a	41
RNQ1-17	q-r-157;q-h-360	15-b	7
RNQ1-18	q-r-163; s-p-173	110-1	17
RNQ1-19	f-s-174; q-r-289	110-2	18
RNQ1-20	a-v-178	FBY-b	90
RNQ1-21	s-p-182; s-a-268	110-c	23
RNQ1-22	f-s-184	110-a	21
RNQ1-23	g-s-160; g-s-194	NCYC-361-d	47
RNQ1-24	d-e-55; Δ2-152-173; q-h-360	NCYC-90-4	40
RNQ1-25	a-t-211; Δ10-152-173; l-p-336; q-h-311; Δ11-285-308	16-d	12
RNQ1-26	m-i-215	512-a	46
RNQ1-27	q-r-250; n-s-379	10-b	55/82
RNQ1-28	q-r-258; Δ11-285-308	9-c	36
RNQ1-29	g-s-264; +qg-171-172; q-h-360	13-d	39
RNQ1-30	g-s-305; Δ8-152-173; q-h-360	10-d	83
RNQ1-31	q-r-316	74D-1b	74
RNQ1-32	q-x-319	BY4741-c	84
RNQ1-33	r-s-357;q-h-360; Δ2-152-173	12-A	30
RNQ1-34	r-g-357	16-c	11
RNQ1-35	s-p-386	2-c	61
RNQ1-36	n-s-379; n-s-18; Δ6-152-173	12-C	32
RNQ1-37	n-k-379; g-e-382; Δ11-285-308; Δ4-152-173	7-b	85
RNQ1-38	q-h-383; Δ4-152-173; Δ11-285-308; q-h-360; qhngqqqsneygrp-372-373	7-a	49
RNQ1-39	f-v-387	15-c	8
RNQ1-40	s-p-390	2-C30-c[1]; 2-C30-b[2]	43[1], 42[2]
RNQ1-41	n-s-18; Δ6-152-173	12-B[1]; 12-D[2]	31[1], 33[2]
RNQ1-42	n-s-18; Δ6-152-173	12-a	1
RNQ1-43	m-v-101; +qg-171-172; q-h-360	NCYC-90-D	73
RNQ1-44	Δ2-152-173; q-h-360	12-I	x
RNQ1-45	Δ4-152-173	1-d[1], 1-c[2], 5-c[3]	59[1], 58[2], 69[3]
RNQ1-46	Δ8-152-173	TH-c[1], TH-d[2]	88[1], 89[2]
RNQ1-47	Δ6-152-173	12-2	x
RNQ1-48	Δ10-152-173; q-h-311; Δ11-285-308	15-a	6
RNQ1-49	+qg-171-172; q-h-360	Y12-a	71
RNQ1-50	Δ11-285-308	2-C30-d	44
RNQ1-51	q-h-360	9-a[1], FBY-d[2]	35[1], 57[2]
RNQ1-52	a-v-63	2-d	62
RNQ1-53	d-g-55	NCYC-361-b	13

Table 4.3: A summary of *RNQ1* alleles from this study.
Strains harbouring an identical combination of polymorphic residues were clustered together under a *RNQ1* allele number, resulting in the generation of 53 distinct *RNQ1* alleles.

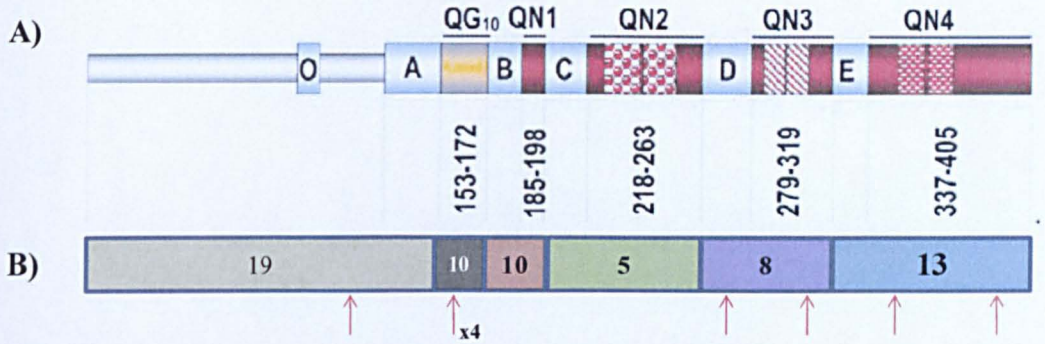

Figure 4.7 The number of polymorphisms detected in each region of Rnq1p, as defined by Kadnar *et al* (Kadnar *et al.*, 2010).
The number within coloured boxes indicates the number of polymorphism within that region. The red arrows indicate regions of the protein where more than one strain harbours the same polymorphic residue, or expansion/contraction of sequence Note that the region indicated 153-172 encapsulates sequence 152-172.

4.1.5 Bioinformatic analysis of the sequences

A phylogenetic tree reflecting inferred evolutionary change between the *RNQ1* amino acid sequences did not reveal environmental or [*PIN*$^+$] prion status specific clustering, suggesting these factors are not the main determinant for *RNQ1* polymorphism.

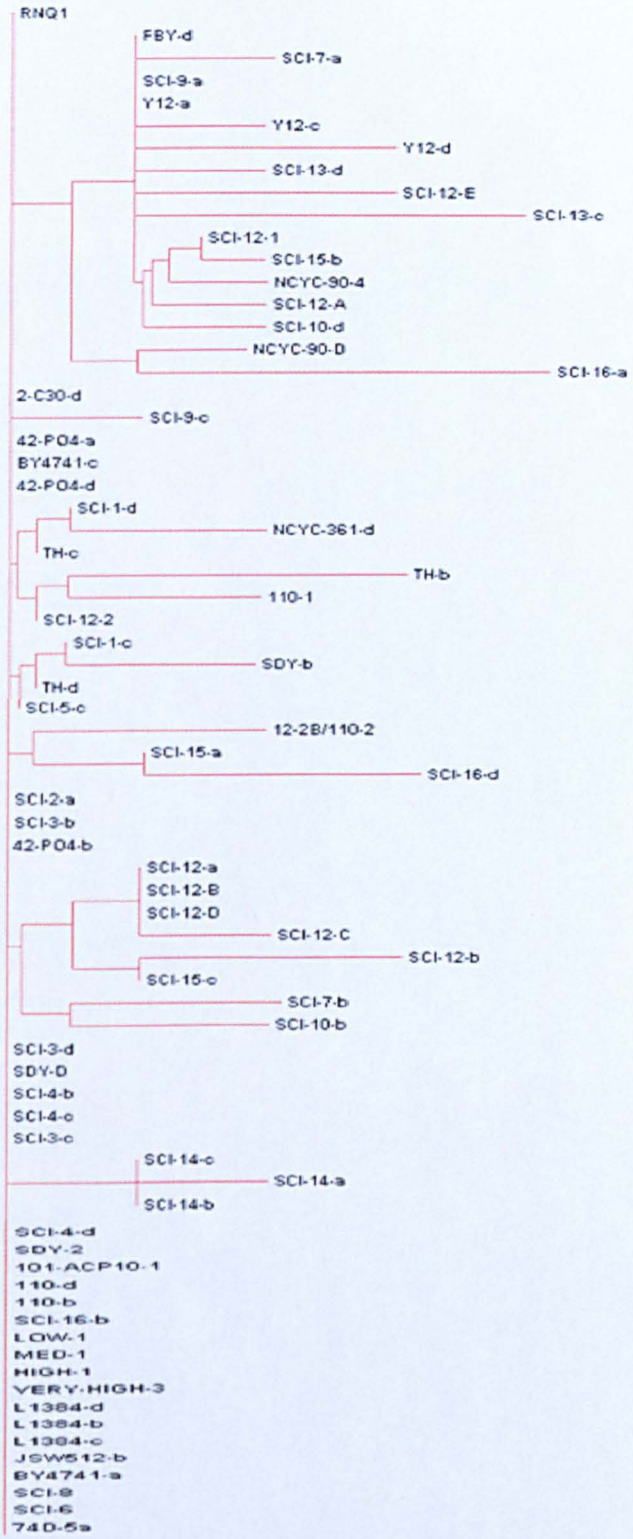

Figure 8: Phylogram tree of all *RNQ1* alleles.
The branching diagram (tree) is an estimate of phylogeny. Branch lengths are proportional to the amount of inferred evolutionary change. The phylogram tree shown was generated by the ClustalW2 program of BioEdit (freeware: http://www.mbio.ncsu.edu/bioedit/bioedit.html).

Chapter V

Understanding the toxic nature of Rnq1p in a [*PIN*$^+$] background

5.1 Analysing the toxicity profile of Rnq1p

Whilst it is well known that over-expression of Rnq1p causes toxicity in a [*PIN*$^+$] background, little information is available about the exact nature of the toxicity phenotype. To date, the toxicity of Rnq1p has been attributed to the accumulation of toxic oligomers, once the capacity for Sis1p to assemble the conformers into protective aggregates has been exceeded (Douglas *et al.*, 2009b). This chapter summarises attempts to further characterise the [*PIN*$^+$]-dependent toxic phenotype of Rnq1p.

5.1.1 Rnq1p over-expression is toxic in a [*PIN*$^+$], but not a [*pin*$^-$], background

In order to commence a study of the toxicity phenotype of Rnq1p, it was important to be able to reproduce the published toxicity phenotype, namely that Rnq1p over-expression is toxic in a [*PIN*$^+$] but not in a [*pin*$^-$] background. To confirm this, a galactose inducible pYES2-*RNQ1* (2μ) plasmid, representing the 74D694 *RNQ1* gene sequence, was over-expressed in the BY4741 [*PIN*$^+$] and [*pin*$^-$] backgrounds. It is important to mention that BY4741 is naturally [*PIN*$^+$] and therefore where BY4741 is mentioned throughout this thesis, the prion status should be assumed to be [*PIN*$^+$] unless specified as [*pin*$^-$]. A growth defect was observed only in the [*PIN*$^+$] background, as expected (figure 5.1). Equivalent growth of both strains on raffinose prior to growth on galactose demonstrated that the growth defect on galactose was specific to the over-expression of Rnq1p.

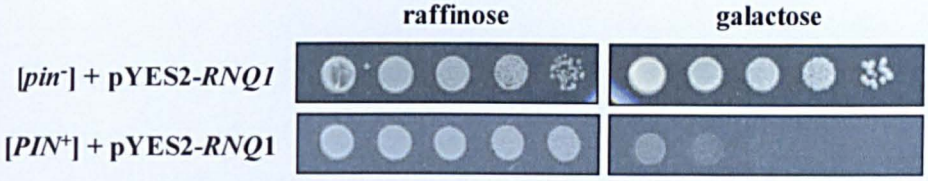

Figure 5.1 Toxicity assay demonstrating that Rnq1p over-expression is toxic in a [*PIN*$^+$] but not in a [*pin*$^-$] background.
Rnq1p (pYES2-*RNQ1*) over-expression is induced by the P_{GAL1} promoter on galactose medium, and causes a growth defect that is specific to the [*PIN*$^+$] background.

The effect of Rnq1p over-expression on growth rate was also determined in the [*PIN*$^+$] BY4741 strain. After 3 hours of galactose induction/Rnq1p over-expression, the growth profiles of the control strain (BY4741 transformed with the empty pYES2 plasmid) and the test strain (BY4741 transformed with pYES2-*RNQ1*) began to deviate (fig.5.2) resulting in a doubling time of 1.64 hrs for control BY4741 strain and 3.62 hrs when Rnq1p was over-expressed in this strain.

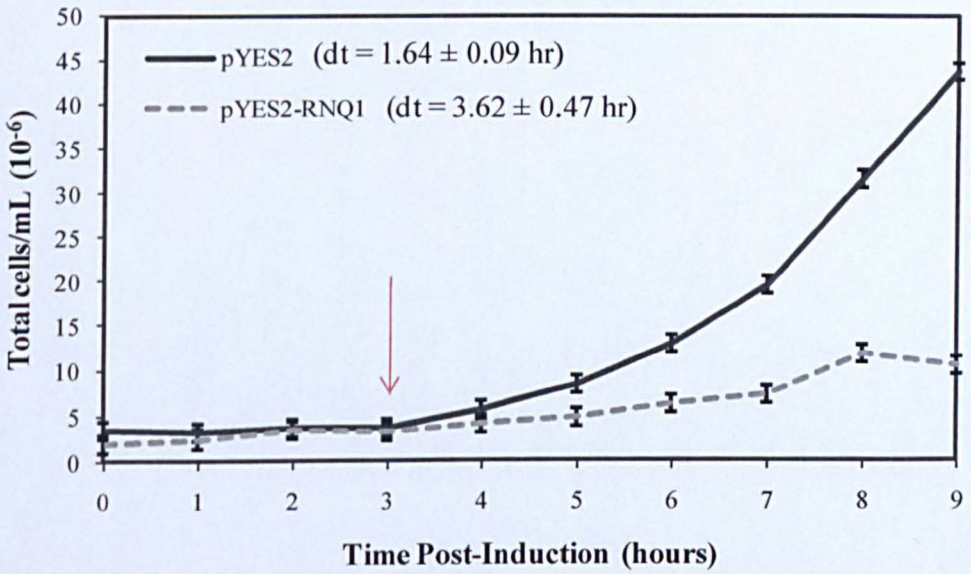

Figure 5.2: Growth profile for BY4741 with (pYES2-*RNQ1*) and without (pYES2) Rnq1p over-expression.
Cell number was determined after regular intervals post-transfer to induction medium (galactose) at t=0 hr. The detrimental effect of Rnq1p over-expression on growth began to emerge 3 hrs after induction (↓). The data was used to calculate doubling time for BY4741 with and without Rnq1p over-expression.

5.1.2 Rnq1p over-expression is not cytostatic, but cytotoxic

Rnq1p over-expression causes a severe growth defect (figures 5.1 & 5.2), however this could be due to a reversible block in cell division (a cytostatic effect), or (a cytotoxic effect (i.e. cell death). To answer this question, aliquots of both control (BY4741 + pYES2) and test (BY4741 + pYES2-*RNQ1*) cells were removed from the culture at regular intervals post-transfer to induction medium, counted, and diluted to obtain a specific number of colonies when plated out onto non-induction medium (glucose-based). If Rnq1p over-expression is cytostatic, the repression of galactose uptake by transfer to glucose medium and therefore the inhibition of further Rnq1p expression from the plasmid, would release the cells from the reversible cell cycle block and the expected number of colonies should not differ considerably from the observed. If Rnq1p over-expression is cytotoxic however, inhibiting further Rnq1p expression by transfer to glucose medium would not reverse the toxic effects suffered by the cells, and therefore one would expect the observed number of colonies to be considerably less than the expected number of colonies.

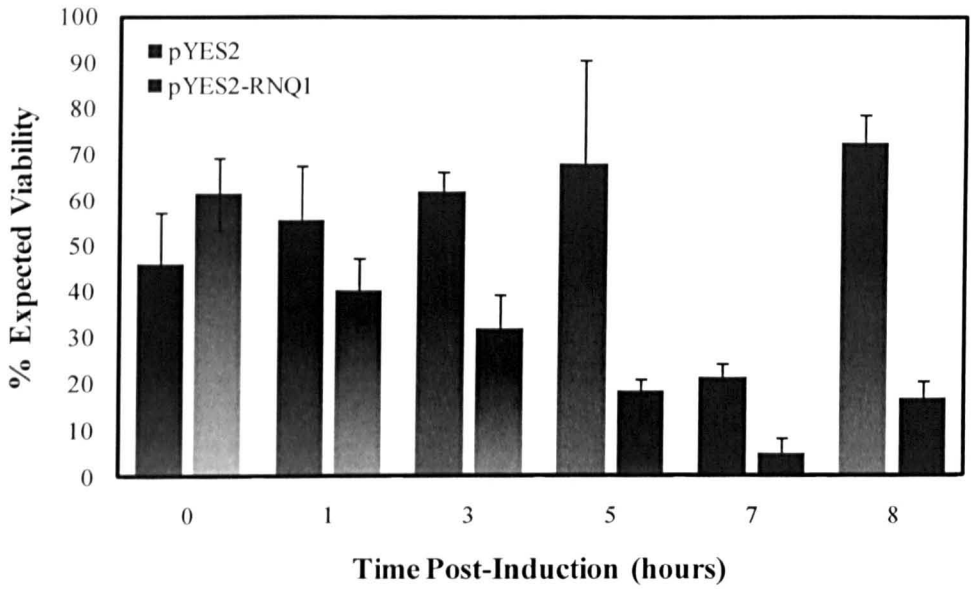

Figure 5.3: The affect of Rnq1p over-expression on cell viability.
Difference between expected and observed colony-forming units, expressed as a percentage, for cells taken from control (BY4741 + pYES2) and test (BY4741 + pYES2-*RNQ1*) cultures at regular intervals post-transfer to induction medium (galactose) and plated onto glucose medium. The longer Rnq1p was over-expressed, the greater the loss in cell viability.

The results of the experiment (figure 5.3) indicate an inverse relationship between duration of Rnq1p over-expression and the number of viable cells. This suggests that Rnq1p is cytotoxic to the cell, and that the observed reduction in cell growth associated with Rnq1p over-expression is due to a toxic effect of Rnq1p on the cell, rendering it non-viable.

5.1.3 Rnq1p over-expression causes an increase in cell size

A control (BY4741+ pYES2) and test strain (BY4741+ pYES2-*RNQ1*) were transferred to induction medium (galactose) so as to over-express Rnq1p from the pYES2-*RNQ1* plasmid present in the test strain. Aliquots were taken from both strains at regular intervals post-transfer to the induction medium.. A gradual increase in cell size was noted (figure 5.4) with the test strain but not with the control strain. After 9 hrs of induction, the cells over-expressing Rnq1p were ~16 % larger than the control strain.

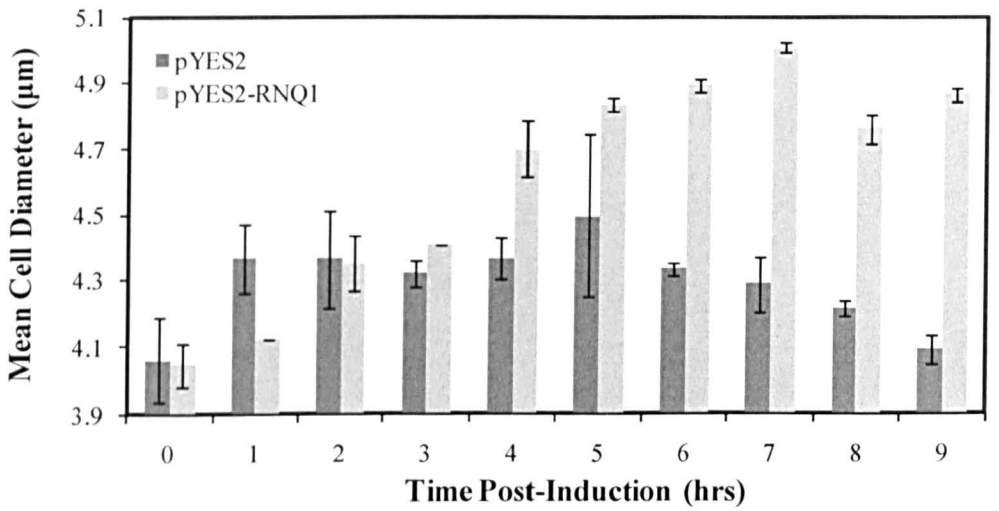

Figure 5.4: The affect of Rnq1p over-expression on cell size.
Average size (µm) of cells taken from control (BY4741 + PYES2) and test (BY4741 + pYES2-*RNQ1*) cultures, following the indicated time since transfer to the induction medium. Rnq1p over-expression results in an increase in cell size with time, differing from the profile of the control strain..

5.1.4 Rnq1p over-expression causes a defect in nuclear migration

When Rnq1p was over-expressed in yeast strain BY4741 via the GAL promoter in plasmid pYES2-*RNQ1* construct (test strain), cells where the nucleus is divided between the mother and daughter cell became over-represented, relative to the pYES2 (control strain) (figure 5.5). This was identified by incubating aliquots of control and test strain with the fluorescent stain 4',6-diamidino-2-phenylindole (DAPI), at regular intervals post-transfer to the pYES2-*RNQ*1 induction medium, galactose. DAPI binds to nucleic material within the cells, and when excited by ultraviolet light fluoresces at 461 nm, allowing both nuclear and mitochondrial DNA to be visualized as a blue colour. The phenotype observed in this experiment indicates that Rnq1p over-expression causes a defect in nuclear migration.

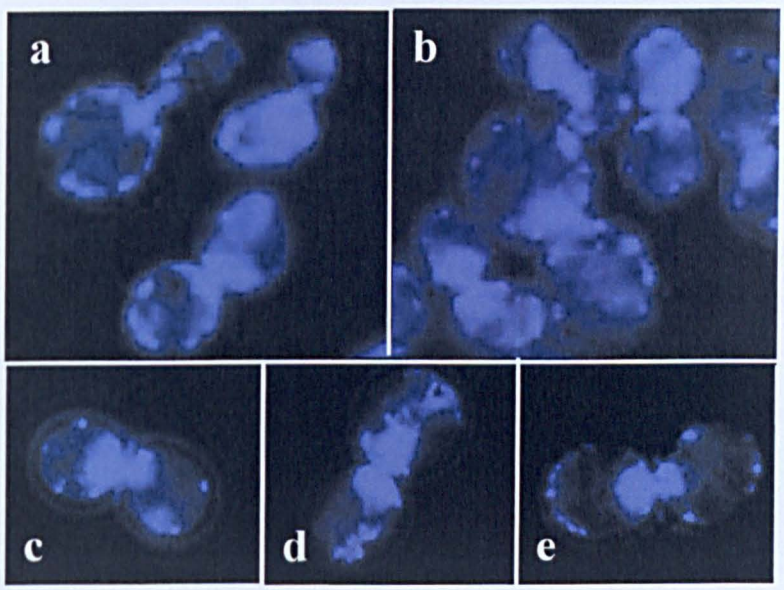

Figure 5.5: Rnq1p over-expression leads to nuclear-migration defects.
Over-expression of Rnq1p in a [*PIN*$^+$] background leads to a defect in nuclear migration (panels a-e), as revealed by DAPI staining. 60X magnification.

5.1.5 Rnq1p over-expression results in Sis1p localising to aberrant structures

The above nuclear migration defect correlated with a terminal phenotype previously published for Sis1p (Luke *et al.*, 1991), whereby depletion of this essential Hsp40 chaperone resulted in a nuclear migration defect that matched that seen with Rnq1p over-expression. Sis1p depletion also resulted in an increase in cell size, as observed

for Rnq1p (figure 5.5). As it is also known that Rnq1p interacts with Sis1p in a [*PIN*$^+$] state (Lopez *et al.*, 2003), an initial hypothesis was formed that the toxicity associated with Rnq1p over-expression in a [*PIN*$^+$] background was due to depletion of the functional pool of Sis1p in the cell, and that toxicity was not observed in a [*pin*$^-$] background because Rnq1p does not bind and therefore could not deplete Sis1p in this background.

To investigate further, a Sis1-Gfp strain was analysed to see whether the protein behaved aberrantly when Rnq1p was over-expressed. Prior to Rnq1p over-expression, the Sis1-Gfp protein was distributed between the nucleus and the cytoplasm, often with multiple small mobile foci, or more rarely with 1 or 2 larger immobile foci (figure.5.6). There existed slight differences between the control (+pYES2) and test (+pYES2-*RNQ1*) strains prior to galactose induction, and this may be due to leaky expression of the *RNQ1* gene in raffinose and thus Rnq1p was slightly elevated in the test strain prion to galactose induction. Specifically, multiple small foci were more common in the test strain at t = 0 hr, than in the control strain. In a minority of test cells at t=0 hr, Sis1-Gfp appeared to coalesce into a structure similar in size to the nucleus, but which did not overlay the nuclear signal.

With increased duration of Rnq1p over-expression, cells started to exhibit the nuclear migration defects. Unique to these cells was the formation of two large aberrant structures, one each in the mother and daughter cell. The large aberrant structures did not co-localise with the nuclear signal of the cells. It is possible that the Sis1-Gfp structures formed earlier on in the induction time-course represent an earlier stage in the development of the larger aberrant structures. This might suggest that such early observable changes in Sis1-Gfp behaviour commit the cell to a fate of defective nuclear migration.

Additionally, at t=3 hr in the test strain, a number of cells appeared to contain ring-like structures of Sis1-Gfp (figure 5.7). These structures were not detected in the control strain, or at any other time point of the test strain. It is possible that Sis1-Gfp is localised to the nuclear envelope or endoplasmic reticulum in these cells, since there were instances where the ring-structure did not appear to encircle the nucleus.

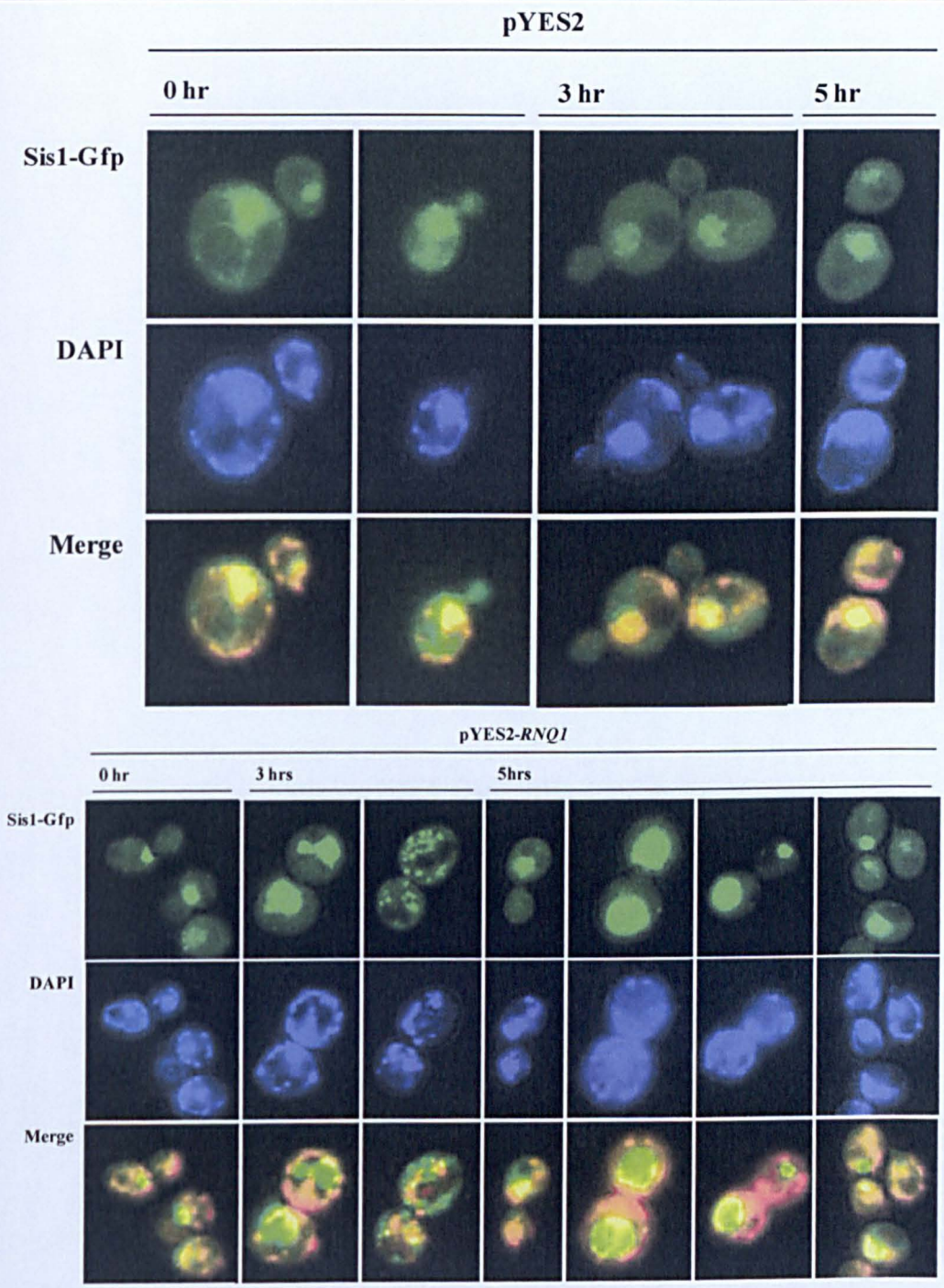

Figure 5.6 Sis1-Gfp displays a dynamic and aberrant behaviour following Rnq1p over-expression.

BY4741 strain with *GFP* fused to the endogenous *SIS1* open-reading frame was transformed with pYES2 (control) and pYES2-*RNQ1* (test) to determine the effect of Rnq1p over-expression on Sis1-Gfp behaviour. Images were captured at indicated times post induction. DNA was stained with DAPI. The merged images reveal regions where Sis1-Gfp co-localises with the nucleus. 60X magnification.

It was noted that between t=0 hr and t=3 hr, Sis1-Gfp foci in the test strain became more numerous with increasing expression of Rnq1p, but that after 5 hrs of Rnq1p over-expression, these foci returned either to a normal distribution or formed the large aberrant structures previously mentioned. No change in foci number was observed in the control strain.

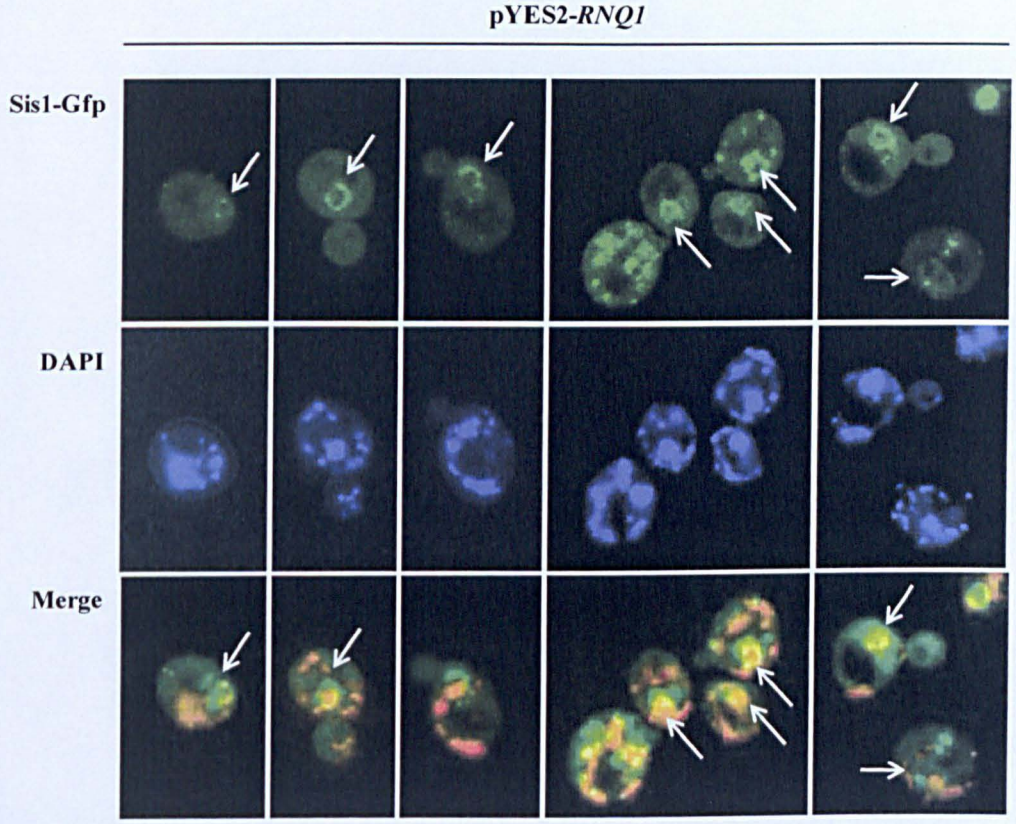

Figure 5.7 Sis1-Gfp formed a ring-structure in cells over-expressing Rnq1p.
Images presented here represent t=3 hr post pYES2-*RNQ1* induction in the Sis1-Gfp test strain (green). Cells were stained with DAPI to co-visualise DNA within the cell (blue). Images were merged to reveal any co-localisation pattern between Sis1-Gfp and DNA. The ring structures indicated by the white arrow may represent Sis1-Gfp localisation to the nuclear envelope or the endoplasmic reticulum.

It is possible that the altered Sis1-Gfp localisation associated with the 'large structures' represents the vacuole, as large vacuoles have been reported as a Sis1p depleted phenotype (Luke *et al.*, 1991), though Sis1p localisation to the vacuole itself has not been reported. Such a co-localisation could be confirmed by the use of vacuole specific dyes. If Sis1p is redirected to the vacuole with increasing Rnq1p

abundance within the cell, it may represent an event equivalent to a rapid depletion in the functional pool of Sis1p available within the cell.

Sis1p depletion may not be only source of Rnq1p toxicity, since (Douglas *et al.*, 2009a) Douglas *et al* reported continued toxicity of Rnq1p in a [*PIN*$^+$] cell when the predicted Sis1p binding site on Rnq1p was mutated, such that the strength of the interaction between Rnq1p:Sis1p was impaired. If the initial hypothesis were correct, then reducing the interaction between Rnq1p and Sis1p would be expected to alleviate or reduce the toxicity. Therefore, while the altered localisation and dynamic behaviour of Sis1p in the presence of elevated Rnq1p *may* contribute to Rnq1p toxicity, this has not been proven here. To discount the contribution of Sis1p to Rnq1p toxicity entirely, it would be necessary to inhibit Sis1p binding to Rnq1p for example by deletion of the entire Sis1p binding site. However, the loss of Sis1p interaction would need to be confirmed, perhaps by co-immunoprecipitation, in case Rnq1p possessed additional, currently unidentified, Sis1p binding sites. Further to this, while a direct physical interaction has been demonstrated for Rnq1p and Sis1p (Lopez *et al.*, 2003a), it is possible that they also impinge upon each other by an indirect route e.g, via shared interactions or downstream processes, and as such a mutational approach may not be conclusive either.

5.1.6 Rnq1p over-expression may cause mitochondrial dysfunction

It was of interest to determine whether Rnq1p over-expression triggered oxidative stress in the cell or compromised the function of the mitochondria. Loss of mitochondrial function is associated with an inability to grow on non-fermentable carbon sources, such as glycerol, since mitochondria are required for respiratory growth. Therefore, if Rnq1p over-expression compromised mitochondrial function, then these cells would be impaired in their ability to grow on a non-fermentative carbon source such as glycerol.

After growth of the control (BY4741 + pYES2) and test (BY4741 + pYES2-*RNQ1*) strains in glucose-based broth overnight, followed by growth on raffinose agar, and then induction of pYES2-*RNQ1* on galactose agar, it was found that subsequent growth on glycerol was not impaired (fig.8). However, it was reasoned that if the

effect of Rnq1p on mitochondrial was subtle, then a reduction in the total pool of functional mitochondria prior to Rnq1p over-expression may assist in observing any such phenotype. Thus, the assay was repeated but a low dose of ethidium bromide was added during growth in the glucose-broth. The result was impaired growth on glycerol for the strain that had over-expressed Rnq1p, where the control strain showed no such growth defect on glycerol, despite both strains being pre-exposed to the same low dose of ethidium bromide.

To investigate petite mutants (lacking mitochondria) of the strains were generated by successively growing the cells in the presence of a higher dose of ethidium bromide prior to use in the assay. Their petite status was initially confirmed by DAPI staining, which revealed the presence of only nuclear signal in the treated cells. Over-expression of Rnq1p in the petite mutants induced toxicity, but in this case neither the control nor test strains were able to grow on glycerol, consistent with and further confirmation of, their petite status.

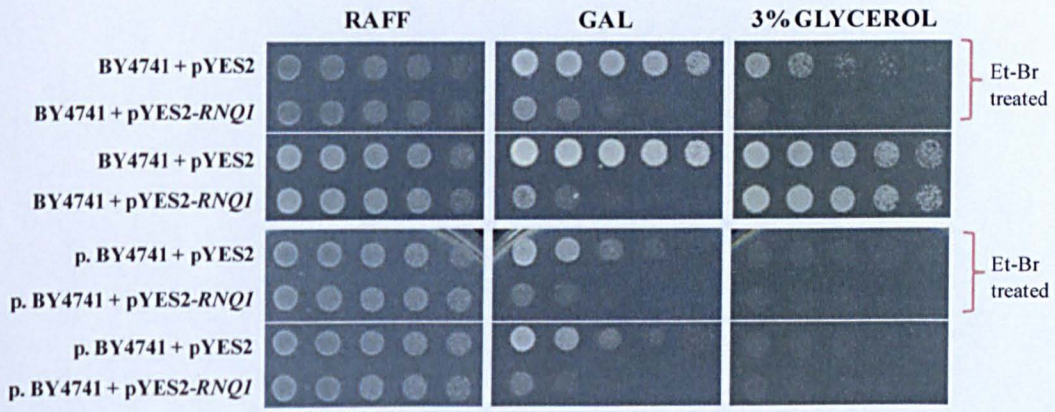

Figure 5.8 Rnq1p over-expression causes a mild mitochondrial dysfunction.
Rnq1p over-expression in BY4741 does not affect subsequent growth on glycerol unless the pool of functional mitochondria is first slightly depleted by low dose exposure to ethidium bromide (EtBr), before the proteotoxicity assay. Rnq1p toxicity does not require functional mitochondria however, since Rnq1p over-expression continues to be toxic in a petite strain . Petite strains indicated with 'p.' prefix.

These results suggest that whilst Rnq1p over-expression may have a subtle effect on mitochondrial function, the impairment of mitochondrial function is not the source

of Rnq1p's toxicity, since in the absence of mitochondria the toxicity associated with Rnq1p over-expression is still observed (figure 5.8).

It would be of interest to determine whether the mitochondrial dysfunction was specific to Rnq1p over-expression in the [*PIN*$^+$] state, and therefore linked to its toxicity, or whether the same phenotype would also be observed in the [*pin*$^-$] background, thus indicating that this phenotype is linked to a cellular function of Rnq1p.

5.1.7. Rnq1p co-localises with foci formed by the P-body marker Dcp2p

The similarity between Rnq1p foci formed in a [*PIN*$^+$] state and the behaviour and appearance of P-body foci was commented on by a colleague (C. Campbell).. P-bodies are cytoplasmic foci formed by accumulations of untranslating mRNA that are associated with translation-repression and mRNA-decay proteins: the mRNA stored in P-bodies will either return to translation or be degraded.

Rnq1p localisation to P-bodies had not previously been demonstrated, so to determine whether Rnq1p was associated with P-body foci, co-localisation studies between Rnq1p-DsRed (pAG425-*RNQ1-DsRED*) and Dcp2-GFP (BY4741 ORF-GFP fusion collection) were performed (Figure 5.9). Dcp2-Gfp is an mRNA decapping protein that is used as a marker for P-bodies within the cell.

The co-localisation of Rnq1p with Dcp2p foci (Figure 5.9) suggests that Rnq1p has a function in P-body dynamics or mRNA degradation. Additionally, it may be that the QN-rich property of Rnq1p is used to mediate mRNP assembly. The role of Rnq1p in P-bodies will be explored further, in particular to determine whether the prion state of Rnq1p affects the number of observable P-bodies capable of forming within the cell.

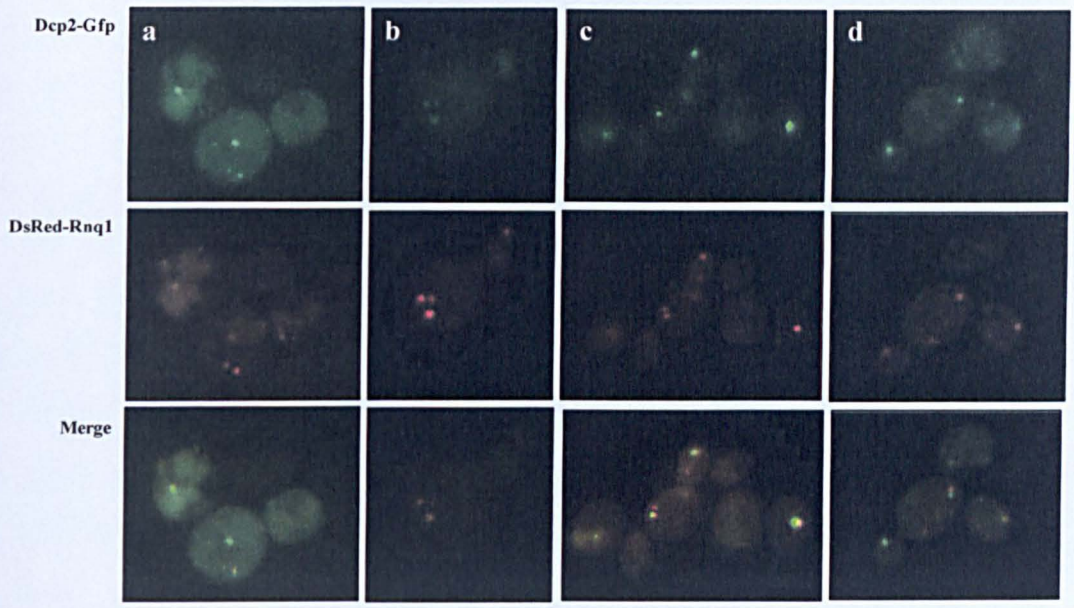

Figure 5.9: Rnq1p co-localises with Dcp2p to cytoplasmic foci.

Expression of Rnq1-DsRed in a BY4741 Dcp2-GFP strain (GFP-tagged ORF collection) showed co-localisation between the P-body marker and Rnq1p. Image (a) produced by C. Gourlay

5.1.8. A summary of the Rnq1p toxicity profile

An analysis of Rnq1p toxicity in this study reproduced the [*PIN*$^+$] specificity of Rnq1p toxicity reported by Douglas *et at* (Douglas *et al.*, 2009c) however whether the growth defect associated with Rnq1p over-expression in a [*PIN*$^+$] background was cytostatic or cytotoxic was unclear. In this study we find that a release from Rnq1p over-expression, by transferring cells from inducing to non-inducing medium, was not associated with a recovery of growth and therefore Rnq1p is cytotoxic. In fact increased duration of Rnq1p expression was inversely correlated with cell viability. It was also observed that over-expression of Rnq1p resulted in an increase in cell size. Most notably however was the detection of a nuclear migration defect in cells over-expressing Rnq1p; cells with this defect started to appear as differences in cell growth rate between the pYES2 control and pYES2-*RNQ1* test strain were becoming detectable, suggesting that the nuclear migration defect correlated with cell toxicity.

An analysis of Sis1p localisation in the cell as Rnq1p was over-expressed revealed dynamic changes in its distribution, and culminated in the formation of two structures simultaneous with the nuclear migration defect; these structures may represent Sis1p localisation to the vacuole although this remains to be determined. Additionally, approximately 3 hrs after Rnq1p induction (when negative effects of Rnq1p over-expression begin to manifest) ring-structures of Sis1p were observed, and may represent Sis1p localisation to the ER/nuclear envelope. The significance of this is yet to be addressed.

Rnq1p over-expression also appeared to cause a defect in mitochondrial respiratory capacity, though was only be observed when the mitochondrial function was pre-compromised, for example by ethidium bromide. However Rnq1p toxicity proceeded in the absence of mitochondria, indicating that the dysfunction is a secondary consequence of Rnq1p over-expression.

5.2 Sequence determinants

Rnq1p is a highly polymorphic protein. The isolation and sequencing of many *RNQ1* alleles in this project presented an opportunity to ask whether any of the polymorphisms were functionally significant. With no cellular function known for Rnq1p and only a short list of potentially assayable phenotypes, the phenotype of toxicity was chosen since this might indicate naturally occurring polymorphisms of Rnq1p that affected Rnq1p toxicity. The ultimate aim was to identify non-toxic alleles and [*PIN*$^+$]-independent toxic alleles, again the purpose being to reveal significant sequence features required for the toxicity of Rnq1p. While some of the pYES2-*RNQ1* constructs possessed identical *RNQ1* sequences, all constructs were screened individually and therefore reference is made to the construct number rather than a designated *RNQ1* allele.

5.2.1 The principle of the proteotoxicity assay

The utility of the toxicity assay relies upon the fact that Rnq1p over-expression in a [*PIN*$^+$] background results in a severe growth defect, but no growth defect is seen when Rnq1p is over-expressed in a [*pin*$^-$] background (figure 5.10). Each pYES2-based construct that was generated in this project was used to assay for Rnq1p toxicity in the yeast BY4741 [*PIN*$^+$] strain. The transformed strains were subsequently 'cured', eliminating the [*PIN*$^+$] prion, and re-assayed for toxicity in the [*pin*$^-$] state. Notable results therefore would be Rnq1p constructs permitting growth in a [*PIN*$^+$] state, and Rnq1p constructs that showed growth defects in the [*pin*$^-$] state.

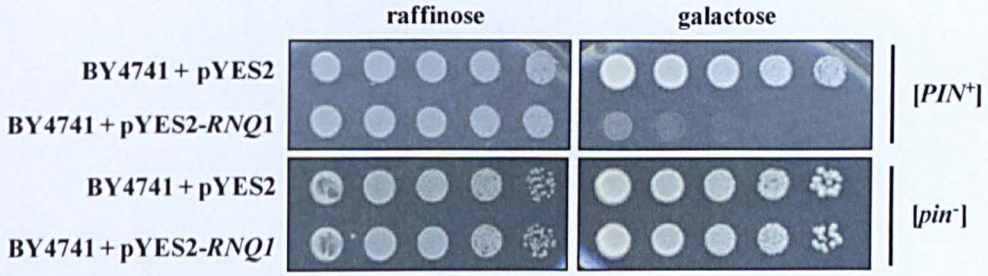

Figure 5.10 The proteotoxicity assay shows [*PIN*$^+$] specific toxicity associated with Rnq1p over-expression.
A strain transformed with either pYES2 or pYES2-*RNQ1* will grow similarly on raffinose medium but on galactose, if Rnq1p over-expression is toxic, there will be a pYES2-*RNQ1* specific growth defect. The consensus *RNQ1* allele is toxic in the [*PIN*$^+$] background.

5.2.2 Proteotoxicity screen of multiple *RNQ1* alleles

In total, 90 different *RNQ1* were tested for their ability to induce the toxicity phenotype (1-74, 76-91) together with the pYES2 vector as a control. In the [*PIN*$^+$] state, four levels of growth were noted: strong, weak, faint and none growth, where 'strong' represents a non-toxic allele and 'none' represents a normal, toxic allele. In the [*pin*$^-$] state, interpretation was less clear and possible subtle differences will be described later. The results presented for [*PIN*$^+$] and [*pin*$^-$] capture the 3rd or 5th position, respectively, in a five-fold dilution series (crude, 1/5, **1/25**, 1/125, **1/625**) (fig.2)

The *RNQ1* constructs of interest in the [*PIN*$^+$] background are indicated in Table 5.1, and those of interest in the [*pin*$^-$] background in Table 5.2. Only one obvious toxicity

phenotype was associated with over-expressing the constructs in a [*pin*$^-$] background, and this was with construct #82, the other constructs listed in Table 5.2 are those that appear to have manifested only a slightly adverse effect on growth in the [*pin*$^-$] state. Additionally, no growth was present for construct #73 however this was due to a plating error.

For the difficulty in discerning information about [*pin*$^-$] toxicity from the single colony snap-shots presented in figure 5.11, the listed constructs are further presented in their entirety alongside an ImageJ generated dynamic profile which reflects in peak size and area the growth intensity of colonies in their respective position (figure 5.12).

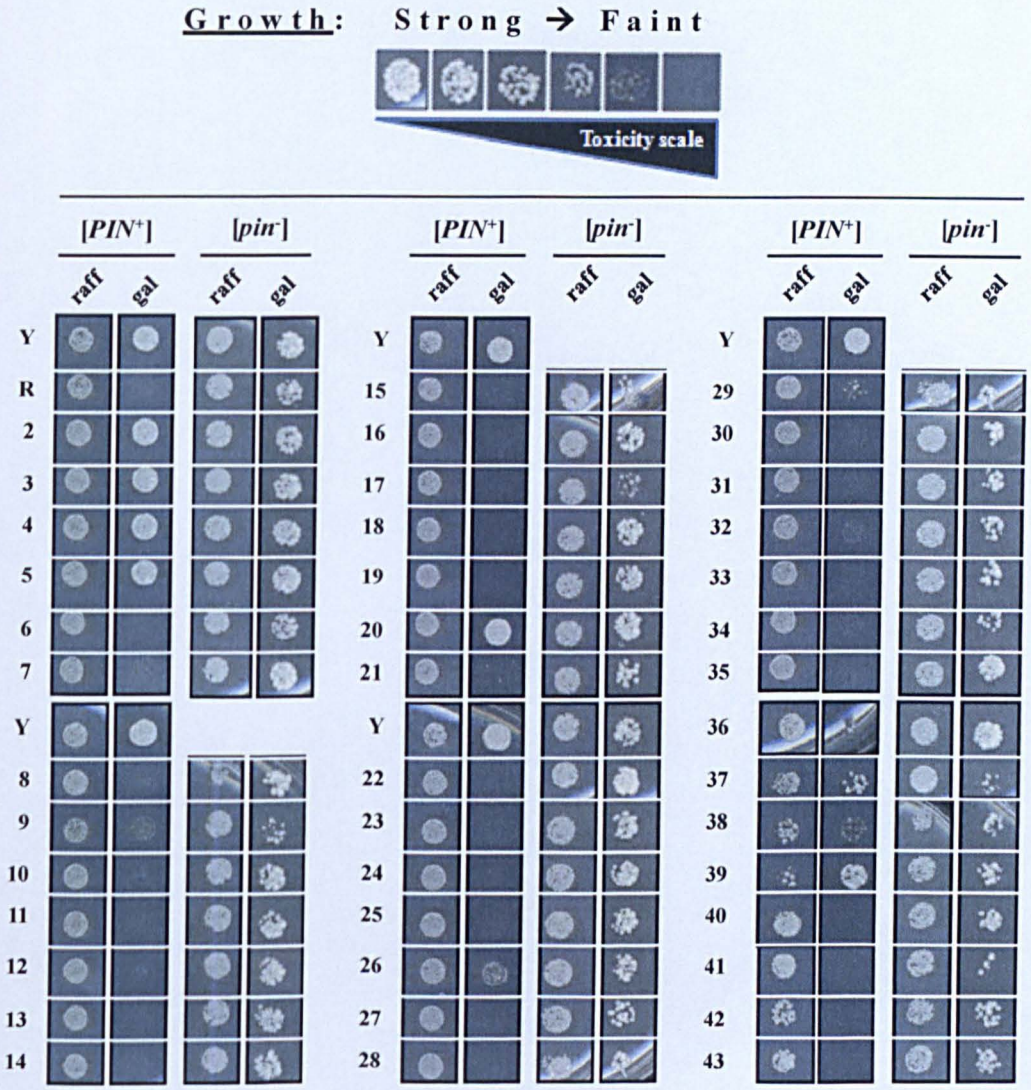

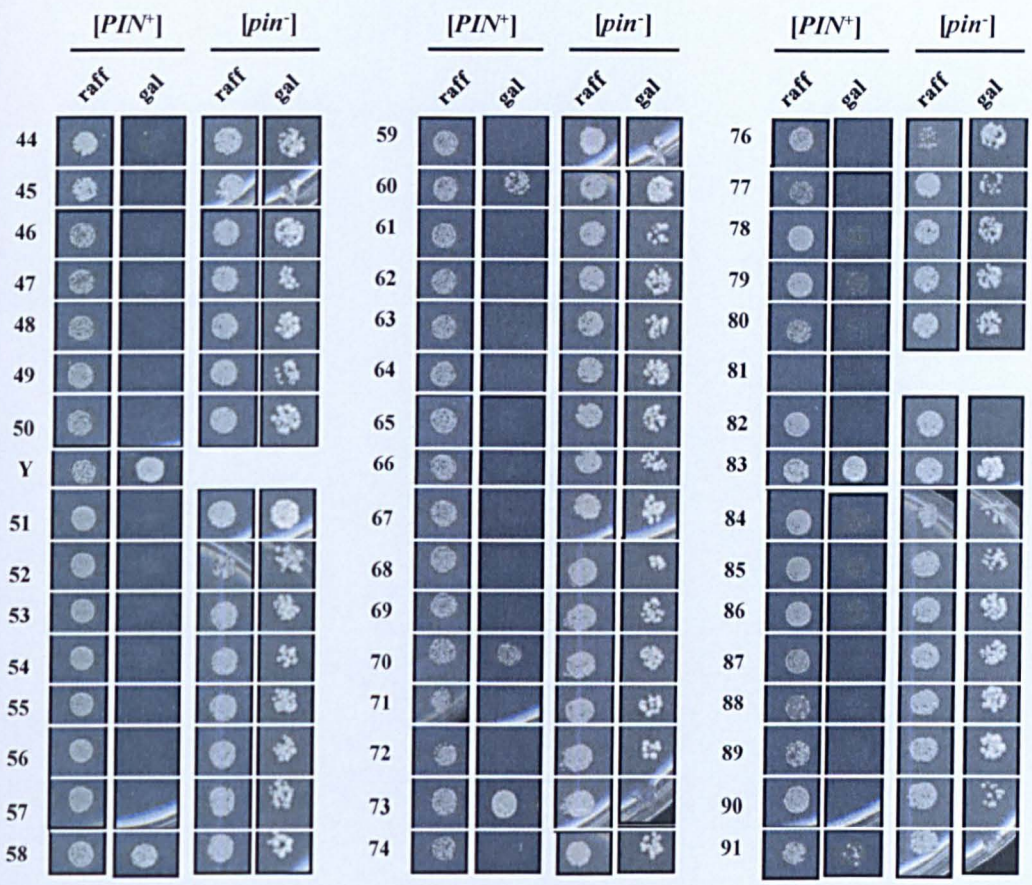

Figure 5.11 Proteotoxicity assay of the multiple pYES2-*RNQ1* constructs in the BY4741 [*PIN*$^+$] and [*pin*$^-$] strains.

The [*PIN*$^+$] results are captures of the $^1/_{25}$ dilution on both raffinose and galactose. The [pin$^-$] results are captures of the $^1/_{625}$ dilution on both raffinose and galactose medium. 'Y' is the internal control (pYES2 vector backbone). The provided scale indicates the range of growth defects associated with Rnq1p toxicity.

		Constructs
Growth	Strong	2, 3, 4, 5, 20, 37, 39, 58 73, 83
	Weak	9, 26, 38, 60, 70, 91
	Faint	32, 36, 79

Table 5.1 pYES2-*RNQ1* constructs associated with reduced growth defects.

Over-expression of Rnq1p from the listed constructs resulted in a reduced toxicity phenotype in the [*PIN*$^+$] background.

Phenotype	Constructs
Toxic	82
Possible subtle growth defect	17, 41, 77

Table 5.2 pYES2-*RNQ1* constructs associated with increased growth defects.
Over-expression of Rnq1p from the listed constructs resulted in impaired growth, as indicated, in the [*pin*$^-$] background.

For the difficulty in discerning information about [*pin*$^-$] toxicity from the single colony snap-shots presented in figure 5.11, the listed constructs are further presented in their entirety alongside an ImageJ generated dynamic profile which reflects in peak size and area the growth intensity of colonies in their respective position (figure 5.12).

From this profile, it can be seen that the 'references' (the pYES2 control (+Y), the consensus allele of *RNQ1* (+R) and a further construct that represents natural growth variation (#49)) are well defined with variability appearing above the arbitrary value of 150. In contrast, the peaks of the query constructs #17, #41, #77 and #82 mostly fall below the 150 value and show a greater inconsistency in the peak area. This indicates that the reference colonies are denser in cell number than the query colonies, suggesting that there is reduced growth of the query colonies brought about by the harboured construct. Indeed, even in the $^1/_{25}$ dilution position on galactose this difference in cell density between the reference and query colonies can be appreciated by close inspection.

5.2.3 Independent evaluation of a toxic and non-toxic construct

Two constructs, #70 and #89, a non-toxic and toxic construct respectively, where derived from the same source strain (a brewing strain isolated from, Theakston's Bitter), and were chosen for further growth and microscopic investigation in the [*PIN*$^+$] background.

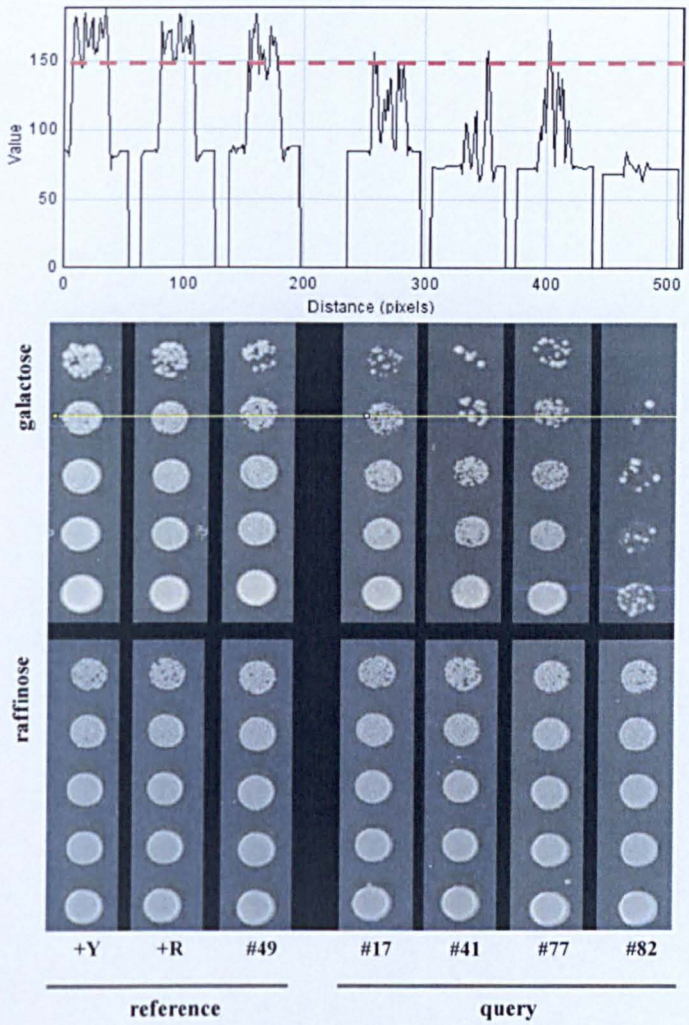

Figure 5.12 Colony profiling of the enhanced toxicity pYES2-*RNQ1* constructs. The pYES2-*RNQ1* constructs that showed a growth defect when over-expressed in the [*pin*$^-$] background, and further identified in table 2, were analysed by dynamic profiling, which reflects the cell density within a colony.

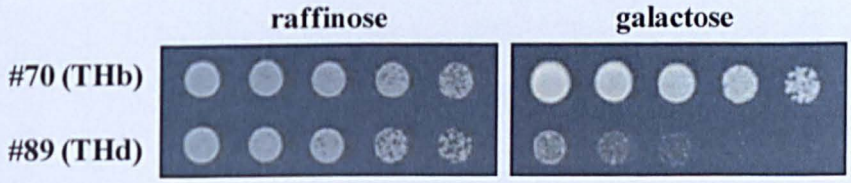

Figure 5.13 An independent evaluation of the toxicity phenotypes associated with the expression of constructs #70 and #89. Constructs #70 and #89 were derived from the same source strain, 'TH' or (Theakston's Ale). The analysis confirmed the results shown in figure 2: construct #70 was non-toxic, construct #89 showed toxicity.

While the entire assay of the constructs was repeated by undergraduate project students to show reproducibility of the results, the constructs #70 and #89 were also repeated in isolation and found to be reproducible (figure 5.13).

Growth analysis of strains expressing the constructs in selective 2% galactose/1 % raffinose medium revealed a similar growth profile to that obtained when comparing a Rnq1p control (+pYES2) and test (pYES2-*RNQ1*) strain (figure.5.14). Namely, a growth defect was apparent in the strain expressing the toxic allele (#89), but no defect was observed in the strain expressing the non-toxic construct (#70).

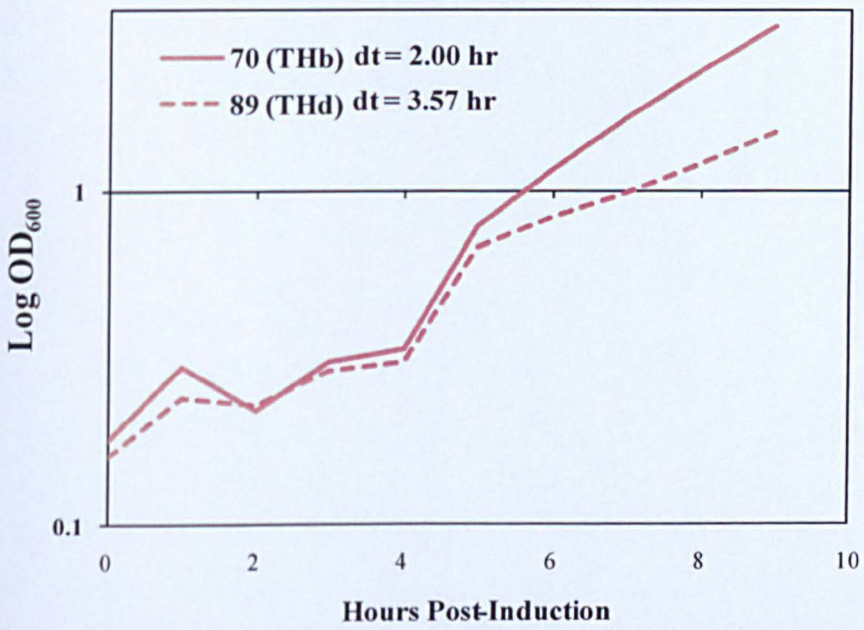

Figure 5.14 Growth profile for BY4741 expressing pYES2-*RNQ1* construct #70 or #89 as indicated.
The OD_{600} value was determined at regular intervals post-transfer to induction medium (galactose) at t=0 hr. The growth defect associated with Rnq1p over-expression was not observed with construct #89 until after t=5 hrs. The data was used to calculate doubling time for BY4741 expressing construct #70 and #89.

It was of interest to determine whether the nuclear migration defect associated with Rnq1p over-expression would correlate only with the toxicity phenotype of construct #89 or whether it would also be over-represented in cells expressing a non-toxic form of Rnq1p (#70) e.g. was the nuclear defect synonymous with toxicity.

Therefore, aliquots of culture from #70 transformed and #89 transformed cells were removed at regular intervals post-induction (galactose inducible pYES2-vector), and stained with DAPI to visualise the nucleic acids. The nucleus is very mobile within any given cell (Morris,2000), but most pertinent to the phenotype of interest were those cells whose nucleus was either 1) located at the bud neck, 2) 'trapped' mid-way between the mother and daughter cell, or 3) could not be seen but whose cell size was notably large (figure 5.15). To compare the toxic and non-toxic alleles, cells from each culture were counted and recorded for the positioning of the nucleus if it fell into one of the three categories listed above. This distribution was expressed as a percentage of the total cells counted for the respective culture (figure 5.15).

Although a nucleus at the bud neck or between the mother and daughter cell does not represent an anomalous event in itself, an enrichment of cells whose nucleus is trapped between the mother and daughter does represent an atypical event. As the nucleus at the bud neck should precede this event, an enrichment of these cells may also be indicative of a defective cell.

Those cells expressing the toxic form (#89) of Rnq1p were found more likely to display nuclear migration defects compared with cells expressing a non-toxic form (#70) of Rnq1p. Specifically, in cells over-expressing a toxic form of Rnq1p, the nucleus was 2.4 fold more likely to be at the bud neck, 11.2 fold more likely to be trapped between the mother and daughter cell, and 4.37 fold more likely to have no nuclear signal, concurrent with a large cell size. This result indicates that the nuclear migration defect is a phenotype specific to the toxic form of Rnq1p, possibly as a consequence of differential cellular interactions, aggregation propensity or conformation permitted by the toxic form of Rnq1p but absent in the non-toxic form of Rnq1p.

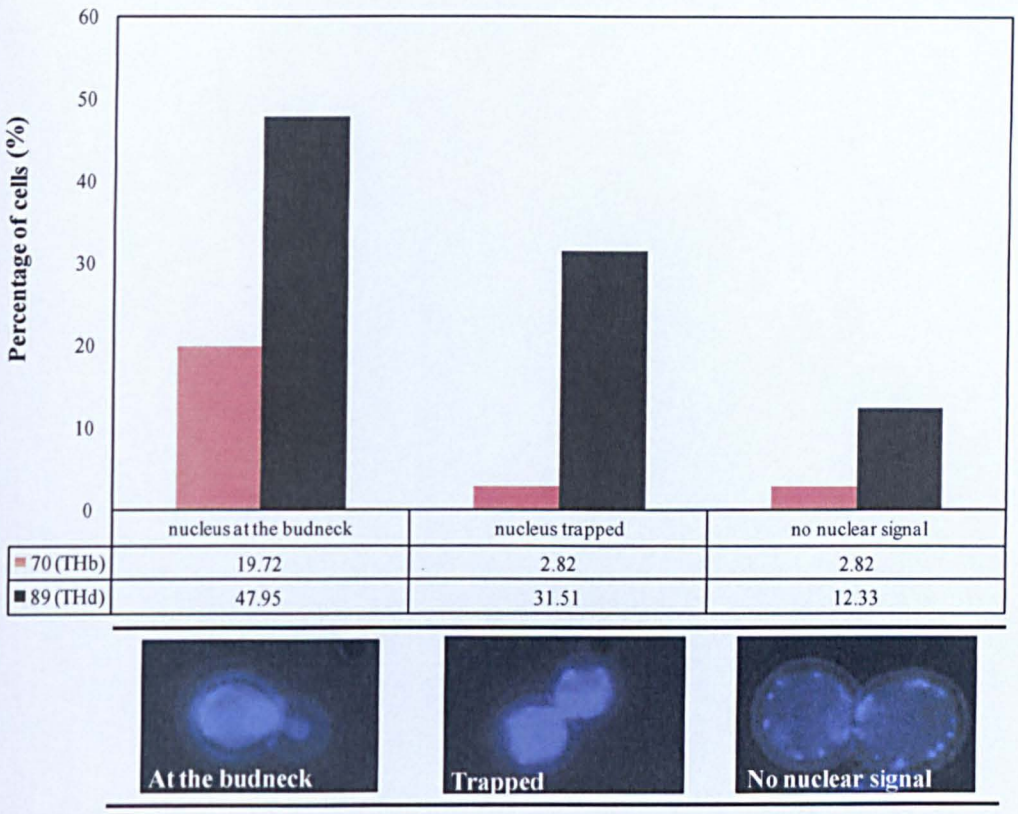

Figure 5.15 Nuclear-migration defects correlate with Rnq1p toxicity.
The distribution of the nucleus to three positions: bud neck, trapped and absent, for cells expressing either toxic Rnq1p (#89, n=73) or non-toxic Rnq1p (#70, n=71) was determined by DAPI staining of the DNA.

5.2.4 Most of the [*PIN*$^+$] toxicity results correlate with Rnq1p expression level

Before commencing a bioinformatics analysis of the constructs to identify sequence features that may be required for Rnq1p toxicity, it was important to verify that the results obtained were due to differences in Rnq1p sequence and not to differences in expression level of Rnq1p from the different constructs. Select *RNQ1* constructs were therefore expressed in BY4741 [*PIN*$^+$] and quantitative western blots performed to identify any differences in the steady state levels of Rnq1p post-induction.

Clear differences in the steady state level of Rnq1p from the pYES2-vectors, relative to the consensus construct, #19 (figure.5.16) were detected. A pattern was noted when the constructs were ordered by their expression level of Rnq1p, whereby the low-expressing constructs were less toxic as determined by the plate assay, and the

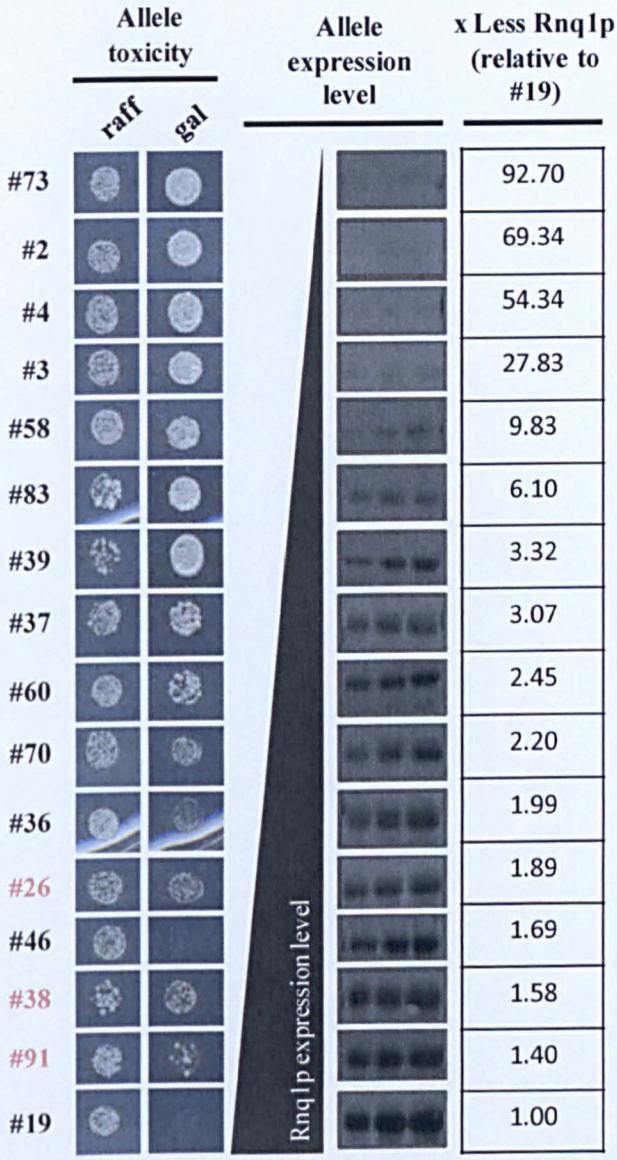

Figure 5.16 Rnq1p toxicity is linked to increased Rnq1p abundance.
Quantitative western blot analysis of Rnq1p expression from the constructs revealed an inverse relationship between the proteotoxicity result of each construct and the construct's expression level.

high-expressing constructs showed a greater degree of toxicity in the plate assays. This would suggest that many of the 'non-toxic' constructs identified were non-toxic simply due to low-expression of Rnq1p. Toxicity appeared to manifest itself when Rnq1p over-expression was no less than 2-3x fold lower than the construct expressing the consensus Rnq1p sequence. There were however a few outliers from

the general trend: constructs #26 and #38 show more growth than #36, #46 and #19, and slight growth was also seen for #91. These constructs can be studied for any shared sequence features; however for the majority of the constructs it has not been possible to determine the toxic nature of the encoded Rnq1p protein due to inconsistencies in expression from the galactose-inducible *GAL1* promoter.

5.2.5 Rnq1p toxicity is modulated by the prion status of a strain

To determine shared sensitivities of yeast strains BY4741 and 74D694 to Rnq1p over-expression, and the effect of [PIN$^+$] prion background on Rnq1p toxicity, a select few constructs were transformed into the yeast strain 74D694 differing in the specific combination of prions harboured ([*pin*$^-$][*psi*$^-$], [*PIN*$^+$][*psi*$^-$], [*PIN*$^+$][*PSI*$^+$], or the Sup35p PNM mutant), plus a 74D *rnq1Δ* strain. Employing the plate toxicity assay, constructs #12, #36, #49, #70 and #71 were tested. All except #70 were previously found to be toxic in BY4741, although #36 was also slightly less toxic.

In the 74D [*PIN*$^+$][*psi*$^-$] strain, as in BY4741, all constructs except #70 were toxic (fig.9). These growth defects were more pronounced when over-expressed in the 74D [*PIN*$^+$][*PSI*$^+$] background, with even mild toxicity apparent from the construct #70. This would suggest that the [*PSI*$^+$] prion or the cellular context as altered by the presence of the [*PSI*$^+$] prion exacerbates Rnq1p toxicity.

As expected, none of the constructs were toxic in the 74D [*pin*$^-$][*psi*$^-$] strain. However, in the 74D strain carrying a deletion of the *RNQ1* gene, while construct #71 and #70 (latter not shown) were non-toxic, both construct #49 and #36 showed increased toxicity: This is surprising since the toxicity associated with over-expression of Rnq1p is believed to be [*PIN*$^+$]-dependent and further, toxicity for these constructs was not seen in the [*pin*$^-$] state. Repeating this assay demonstrated reproducibility of the result, though in the second instance #49 and #36 were more similar in their toxicity effect, growing as #36 in the assay shown.

The expression level of the non-toxic construct #70 in BY4741 *rnq1Δ* was ~ 2.2x lower than the consensus construct #19 (figure 5.16), whereas the toxic construct was ~ 2 x less than the consensus construct – it is unlikely that such a slight change in expression level could account for this difference in Rnq1p toxicity, assuming

equivalent levels of expression in BY4741 and 74D-694. It would be interesting to determine whether the consensus construct is toxic in the 74D *rnq1Δ* background, where it is not in BY4741 *rnq1Δ* background. If Rnq1p over-expression were toxic in a 74D *rnq1Δ* but not in a BY4741 *rnq1Δ* background, this would indicate either: differential interactions for Rnq1p in these backgrounds that determine whether Rnq1p is directed down a toxic or non-toxic route; or that deletion of *RNQ1* allows for the conversion of a different prion protein to its prion state, which is capable of serving as a [*PIN*$^+$] factor.

A second interesting outcome from these experiments was the finding with the 74D PNM strain, which possibly contains unstable [*PSI*$^+$] aggregates. As per usual, construct #70 was not toxic, although in a [*PSI*$^+$] strain this construct was associated with mild toxicity. Similar to the [*PSI*$^+$] strain though, all other constructs were toxic, albeit less than in the [*PIN*$^+$][*PSI*$^+$] strain, with constructs #12 and #71 seemingly more toxic than constructs #36 and #49. This is curious since construct #49 had consistently shown the greatest degree of toxicity in instances where toxicity was to be found. This result may indicate that shared interactions of Rnq1p/[*PIN*$^+$] and Sup35p/[*PSI*$^+$] are altered by subtle differences in the primary sequence of Rnq1p and Sup35p, affecting either binding motifs or conformational diversity, thus modulating the degree of toxicity associated with Rnq1p over-expression.

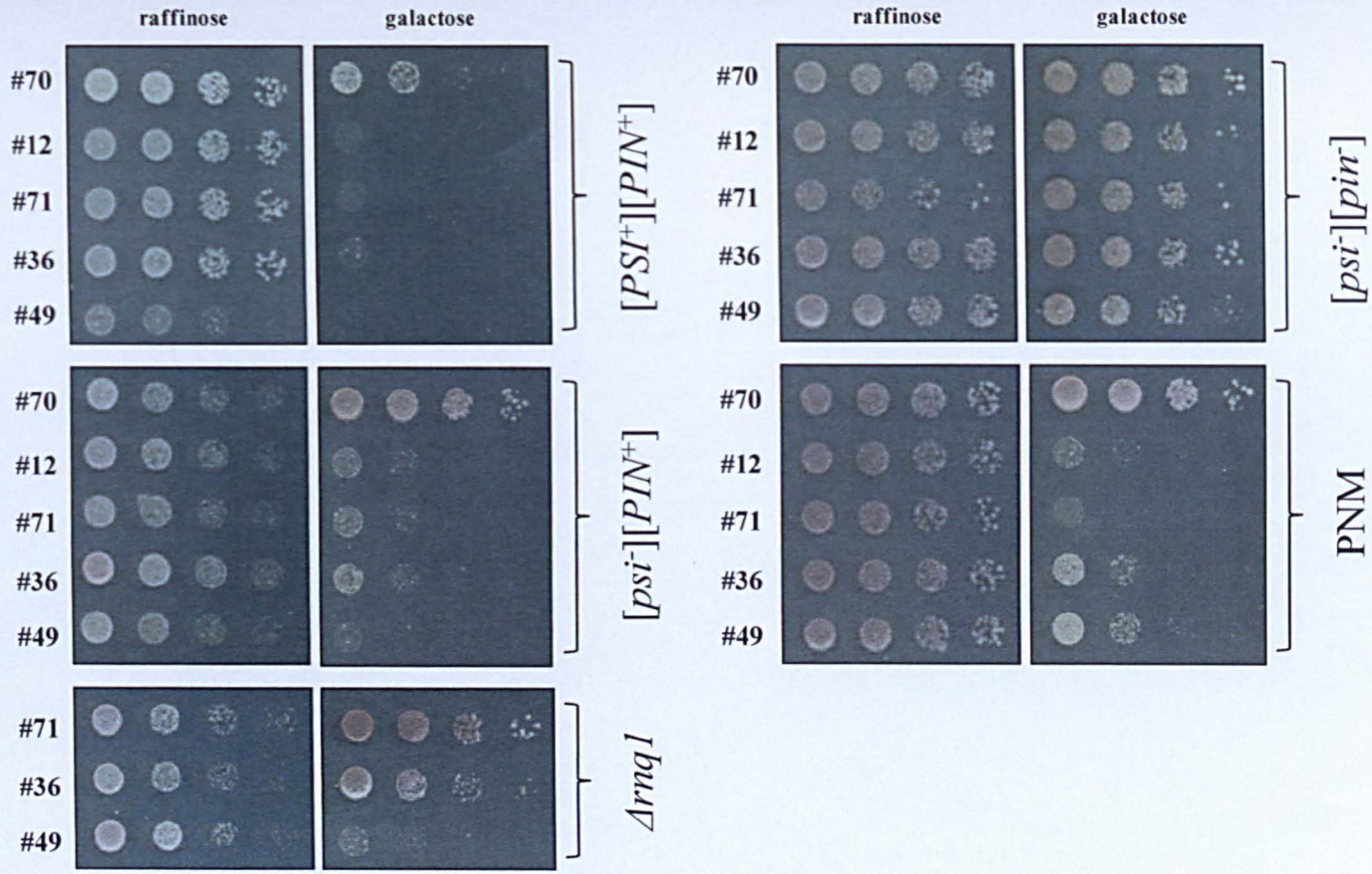

Figure 5.17 The toxicity of multiple pYES2-*RNQ1* constructs is influenced by the prion background of the 74D-69D strain.
Constructs #70, #12, #71, #36, and #49 were assayed for proteotoxicity in the 74D-694 strains [*PSI*$^+$][*PIN*$^+$], [*psi*$^-$][*PIN*$^+$], [*psi*$^-$][*pin*$^-$], *rnq1Δ* and Sup35p *PNM* ('*Psi-no-more*') mutant G58Y.

5.2.6 Analysis of the amino acid sequences of the Rnq1p constructs

5.2.6.1 Constructs from the [*PIN*$^+$] study

Initially, 19 constructs were identified that demonstrated reduced toxicity of Rnq1p when over-expressed in a [*PIN*$^+$] background. However, subsequent analysis of these constructs revealed that the majority were expressing Rnq1p at, significantly, reduced levels. Therefore, at this time it is not known whether any of these constructs would be non-toxic if expressed at levels equivalent to the levels in the control strain expressing the consensus construct. Consequently, only those few constructs that gave both high Rnq1p expression level and showed reduced toxicity were analysed i.e. constructs #26, #38, and #91. Alignment of these 3 constructs against each other and the consensus sequence for *RNQ1*, revealed no single polymorphism shared by all constructs, relative to the consensus sequence (figure.5.18).

Analysis of the amino acid sequences of the three constructs revealed that construct #26 had 2 polymorphisms, construct #38 has 4 polymorphisms and construct #91 had 3 polymorphisms. Table 3 summarises the polymorphisms associated with these constructs, the amino acid change representing the polymorphism, the source of the construct and whether any of the other constructs tested possess polymorphism at the same or a nearby residue.

The polymorphism was residue 39 is unique to constructs #26 and #38. To determine whether this polymorphism was likely responsible for the loss of toxicity in these constructs, it will be necessary to look at the other polymorphisms they possess, and whether any of these cluster with other toxic or non-toxic alleles. This strategy for identifying significant residues can also be applied to the third non-toxic construct #91. Table 5.4 lists those constructs identified in table 5.3 that share similar residue polymorphism as the 3 non-toxic constructs. By using information from these two tables a number of conclusions can be made.

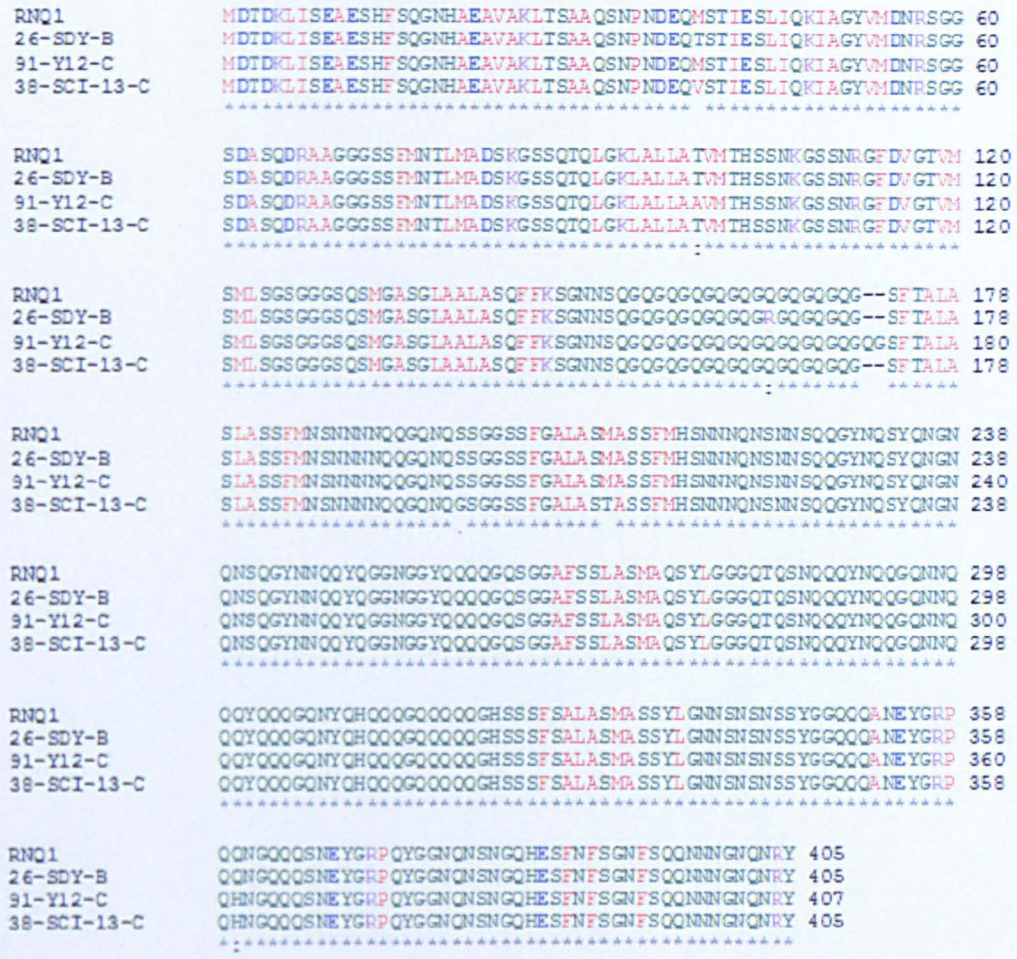

Figure 5.18 Alignment of the *RNQ1* DNA sequence from reduced toxicity constructs reveals no shared polymorphism. The constructs #26, #91 and #38 are associated with reduced Rnq1p toxicity in the [*PIN*$^+$] background. The *RNQ1* DNA sequences of these constructs were compared to identify a shared sequence feature that might account for the reduced toxicity phenotype.

Polymorphism (amino acid)		Construct #	Construct name	Shared or Nearby Polymorphism
39	M→T	**26**	SDY-B	none
	M→V	**38**	SCI-13-c	
99	T→A	**91**	Y12-c	aa101(#73); aa100(#2); aa101(#9)
165	Q→R	**26**	SDY-B	aa163(#17); aa157(#7); aa160(#47)
153-172	+QG	**91**	Y12-c	(#39); (#71); (#72); (#73)
198	S→G	**38**	SCI-13-c	aa194(#47)
210	M→T	**38**	SCI-13-c	aa211(#12)
360	Q→H	**91**	Y12-c	(#7);(#30);(#34);(#35);(#38);(#39);(#40)
	Q→H	**38**	SCI-13-c	;(#49);(#57);(#71);(#72);(#73);(#83)

aa=amino acid; (#x) = construct number

Table 5.3 Polymorphisms associated with the reduced toxicity pYES2-*RNQ1* constructs.

Details of the Rnq1p polymorphisms encoded by constructs #26, #38 and #91 and whether shared or proximal polymorphisms are harboured by other constructs.

Construct#	Tally with non-toxic polymorphisms	Toxicity	x less expression than consensus allele	Similar to polymorphism of interest (amino acid)
2	1	NT	69.34	**99**
7	2	T	n.d.	165, 360
9	1	LT	n.d.	**99**
12	1	T	n.d.	210
17	1	T	n.d.	165
30	1	T	n.d.	360
34	1	T	n.d.	360
35	1	T	n.d.	360
39	2	NT	3.32	**153-172, 360**
40	1	T	n.d.	360
47	2	T	n.d.	165, 198
49	1	T	n.d.	360
57	1	T	n.d.	360
71	2	T	n.d.	153-172, 360
72	2	T	n.d.	153-172, 360
73	3	NT	92.7	**99, 153-172, 360**
83	1	NT	6.1	**360**

n.d. = no data

Table 5.4: Analysis of constructs harbouring similar Rnq1p polymorphisms to those present in the non-toxic constructs.

The polymorphic residues of reduced toxicity constructs #26, #38, and #91 (table 3) are present in or similar to the polymorphisms of the above listed constructs.

First, the second polymorphism of construct #26 at residue 165, is also found in construct #26 however nearby polymorphisms in other constructs at residues 157 (#47), 160 (#7) and 163 (#17) did not reduce the toxicity of Rnq1p, therefore this residue appeared to be less relevant to the toxicity phenotype compared to the polymorphism at residue 39.

Second, construct #38 possessed 3 further polymorphisms, 2 of which are at residues 198 and 210 and other constructs possessing nearby polymorphisms at residue 194 (#47) and 211 (#12) are not associated with reduced toxicity either. The final polymorphism of construct #38 detected was at residue 360, and this is common to toxic and non-toxic constructs alike (fig.11), thereby giving further support that the polymorphism at residue 39 is responsible for loss of toxicity of Rnq1p in constructs #26 and #38.

Third, the remaining non-toxic construct, #91, had three polymorphisms: residue 99, a QG expansion between region 152-173, and residue 360. The latter polymorphism was discussed in the previous paragraph and appears not to be significant for changes in Rnq1p toxicity. The QG expansion between residues 152-173 was found in 4 other constructs, 2 of which were toxic (i.e. #71, #72), with the other 2 being non-toxic (i.e. #39, #73). However, one of the non-toxic constructs (#73) expressed very little Rnq1p protein and therefore whether this construct is toxic or non-toxic remains to be evaluated. The other non-toxic constructs with a QG expansion, #39, was expressed at levels approximately 3-fold less than the consensus, and may be below the level required for Rnq1p toxicity phenotype to manifest. In summary, it is not likely that the QG expansion is responsible for the reduced toxicity observed with construct #91, since the QG expansion is also associated with toxic constructs (#71 and #72). The final polymorphism found in this construct was at residue 99 and was proximal to 3 the other polymorphisms at residues 100 (#2), 101 (#9) and 101 (#73). All of these constructs were found to be non-toxic. However, both construct #2 and #73 were also found to give very little expression of Rnq1p. The only indication that this residue might be linked to reduced toxicity was that construct #9 showed only reduced toxicity, suggesting that it is expressed more readily yet does not cause the same degree of toxicity associated with Rnq1p. Construct #91 also showed reduced, but not complete loss of toxicity, with a high expression level. It is also notable that residue 99 is immediately adjacent to the predicted Sis1p binding

site (residues 91-98), and nearby residues such as 100 and 101 may also influence Sis1p binding if they alter the conformation or accessibility of the binding motif. Therefore while it is not conclusive which residue is responsible for the reduced toxicity of construct #91, the evidence is obtained point to residue 99 as being the sequence determinant feature associated with reduced toxicity. These leads could be easily addressed by site-directed mutagenesis experiments, recapitulating the same polymorphisms either at residue 99 or incorporating a QG expansion between region 152-173.

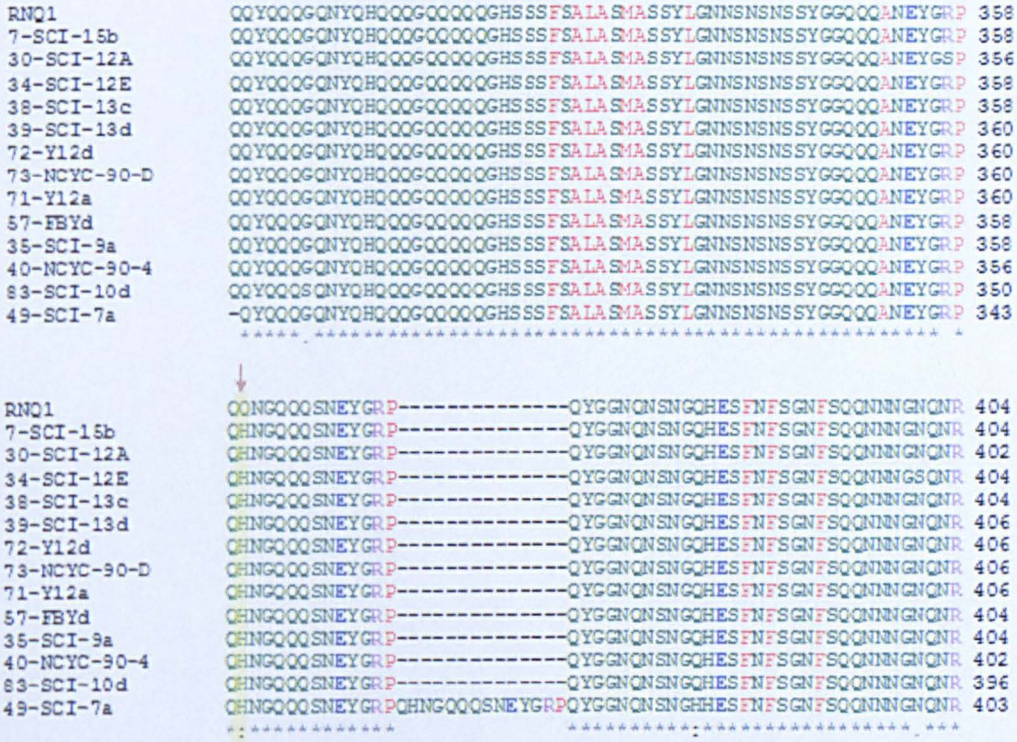

Figure 5.19: The Q360H polymorphism is present in toxic and non-toxic constructs.
Alignment of the *RNQ1* DNA sequence from toxic and non-toxic constructs, the red arrow (↓) indicates the position of the Q360H polymorphism.

5.2.6.2 Constructs from the [*pin*$^-$] study

The construct #82 was derived from strain SCI.10, and differed considerably in sequence from the second construct sourced from this strain (#83) in that construct #82 contained only a single amino acid change, the mutation N379D, rather than

multiple changes relative to the *RNQ1* consensus sequence (construct #19). However, by fortuitous coincidence discovered after the event, construct #82 is also the construct #55, and construct #55 did not cause a growth defect in the [*pin*$^-$] background. This suggests that the sequence of construct #82 cannot be used to infer a special toxicity status, and further, analysis of other construct sequences revealed that 2 further constructs (#32 and #85) harbour polymorphism at this residue, albeit with a different residue at this position, and neither presented with a toxicity phenotype in the [*pin*$^-$] state (fig.12). Therefore construct #82 can be discounted from further sequence analysis.

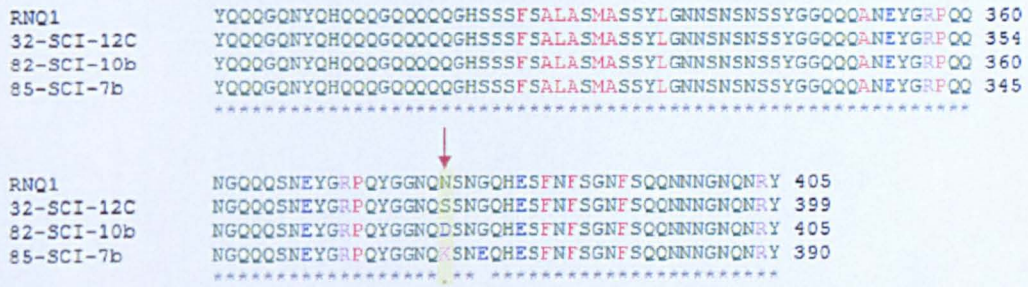

Figure 5.20 Polymorphism at 379 is not associated with enhanced toxicity of Rnq1p.
Toxic construct #82 possesses one polymorphism, N379D indicated by red arrow (↓), however this polymorphism was present in non-toxic constructs and therefore invalidates this residue as conferring enhanced toxicity.

The remaining constructs, #17, #41 and #77, were found to have 2, 1 and 3 polymorphisms, respectively (table 5). The single polymorphism in construct #41 at residue 143 was not found in any other construct and therefore may represent an important residue modulating Rnq1p toxicity or behaviour in the [*pin*$^-$] cell.

Construct #17 had 2 polymorphisms, however while these polymorphisms were unique to construct #17, these constructs also possess polymorphisms at nearby residues, specifically constructs #26, #47 and #18. The implications of this are that any acquired toxic behaviour of construct #17 crucially relies on the mutations that have occurred at the residue 163 or 167.

Finally, construct #77 harbours 3 polymorphisms: one of these, residue 184, was shared by a non-toxic construct #21 and therefore is likely to be insignificant as a residue altering the toxic properties of Rnq1p. Either of the remaining 2 polymorphisms, at residues 88 and 282, could be important for the increased toxicity of Rnq1p seen in strains expressing these constructs. No other constructs possessed polymorphisms associated with these residues or residues nearby.

Again, the contribution of these polymorphisms to the behaviour of Rnq1p in a [*pin*$^-$] background could be determined by recapitulating the mutations with a site-directed mutagenesis strategy.

Polymorphism (amino acid)		Construct #	Construct name	Shared or Nearby Polymorphism
88	Q→P	**77**	W303-W1:1D	none
143	S→P	**41**	2-C3O-a	none
163	Q→R	**17**	110-1	aa165(#26); aa160(#47); aa168(#18)
167	S→P	**17**	110-1	aa165(#26); aa160(#47); aa168(#18)
184	F→L	**77**	W303-W1:1D	(#21); aa182(#23); aa185(#70)
282	Q→R	**77**	W303-W1:1D	none

Table 5.5: Polymorphisms associated with enhanced toxicity constructs #17, #41 and #77.
The polymorphisms associated with constructs showing [*pin*$^-$] growth defects were analysed non-toxic constructs sharing similar or proximal polymorphisms were noted.

5.2.7 Sequence determinants summary

A number of constructs were identified as causing a loss of or a reduction in Rnq1p toxicity when over-expressed in a [*PIN*$^+$] background. However, quantitative western blots revealed that most of the non-toxic constructs were also expressing very low levels of Rnq1p from the pYES2-based vectors. Constructs #26, #38 and #91 (*RNQ1-12*, *RNQ1-13* and *RNQ1-7*, respectively) can be considered as non-toxic constructs since their expression was sufficiently high to otherwise manifest toxicity. Analysis of these constructs revealed that residues 39 and either residue 99 or a QG expansion between region 152-173 may impact upon the toxicity of Rnq1p (i.e. reduction of toxicity).

In the [*pin*$^-$] background, 4 constructs were identified as causing mild growth defects however #82 was excluded from this list since it was duplicated in the study and in the duplicate was not toxic. Analysis of the remaining 3 constructs, #17, #41 and #77 (*RNQ1-18*, *RNQ1-16* and *RNQ1-6*, respectively), revealed that residues 143, 88 or 282, and 163 or 167, had a negative impact on Rnq1p behaviour in the cell, increasing Rnq1-associated toxicity, albeit only very slightly. The reasons for this have not been addressed experimentally, however one might predict that these constructs have a higher propensity to form toxic aggregates, undergo *de novo* formation to [*PIN*$^+$], or that they more efficiently mediate interactions that promote the toxic phenotype of Rnq1p.

As determined in the [*PIN*$^+$] study a non-toxic (#70) and toxic construct (#89) (*RNQ1-2* and *RNQ1-46*, respectively), were use as a means to identify toxicity specific phenotypes. It appeared that growth defects and nuclear migration defects were correlated only with a toxic Rnq1p construct, however quantitative western blots revealed that construct #70 (*RNQ1-2*) was expressed at level of Rnq1p that may be borderline for non-toxicity (x 2.2 less than the consensus). Therefore, it cannot be confidently concluded that the observed nuclear migration defects were specific to toxic Rnq1p expression, although it is logical to assume this is the case.

Surprisingly, Rnq1p over-expression from constructs #36 and #49 (*RNQ1-28* and *RNQ1-38*, respectively) in a 74D *rnq1Δ* strain was toxic, although these constructs were not toxic in the 74D [*pin*$^-$] strain. The consensus sequence (construct #19) Rnq1p was not toxic in BY4741 *rnq1Δ* or [*pin*$^-$]. However it remains to be determined whether the consensus sequenced/construct of Rnq1p is toxic in 74D *rnq1Δ* or whether constructs #36 and #49 are toxic in BY471 *rnq1Δ*. Analysis of the constructs #36 and #49 reveal an 11 amino acid deletion between residues 285 and 308 (fig.13). Deletion in this region is also observed for constructs #44, #6, #12 and #85. It would be interesting to determine whether these 4 constructs are also toxic in 74D *rnq1Δ* or BY4741 *rnq1Δ*. Expressing construct #12, while construct #12 was in the 74D *rnq1Δ* strain, would be useful for determining whether deletion in the 285-308 region causes Rnq1p to be toxic in a *rnq1Δ* background.

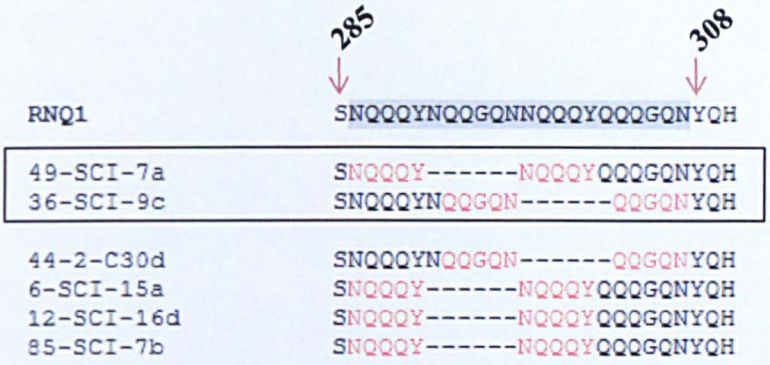

Figure 5.21 Analysis of encoded Rnq1p sequence from constructs toxic in the 74D-694 *rnq1Δ* strain.

The constructs #36 and #49 were toxic in the 74D-694 *rnq1Δ* strain. Both constructs differ from the consensus sequence (RNQ1) by an 11 amino acid deletion between residues 285-308. Due to the repetitive nature of the Rnq1p amino acid sequence it was not possible to determine the precise position of the deletion within this region, however the left- and right-hand red characters reflect opposing presence or absence, along with the dashed lines. Four other constructs (#44, #6, #12 and #85) have a deletion in the same region.

5.3 The [*PIN*$^+$] Variants

There is a greater complexity to the prion form of Rnq1p, [*PIN*$^+$], and this is its ability to establish different 'variants' of [*PIN*$^+$]. As described in section 1.5., [*PIN*$^+$] the 'variants' represent distinct heritable forms of Rnq1p that can induce [*PSI*$^+$] appearance at differing frequencies, and is attributed to the stability of the [*PIN*$^+$] prion in a range of conformations. While it has been reported that Rnq1p over-expression is toxic in a [*PIN*$^+$] background (Douglas *et al.*, 2009b), it is not known whether Rnq1p toxicity is modulated differentially by the different [*PIN*$^+$] variants.

5.3.1 The [*PIN*$^+$] variants are not the result of *RNQ1* gene polymorphism

Since the variants had been isolated in the same strain background, they were believed to have resulted from conformational shifts rather than DNA mutation. However, given the polymorphic nature of the Rnq1p it was important to confirm that changes in [*PIN*$^+$] behaviour were not due to polymorphism of the *RNQ1* gene. Therefore the *RNQ1* gene was isolated from each of the 4 variants, cloned into the

pYES2 vector according to the method previously described (section 4.1.3) and sequenced. The *RNQ1* gene from the [*PIN*$^+$] variants strains was indeed identical to each other and to the consensus allele of *RNQ1* (fig. 5.22)

5.3.2 Rnq1p over-expression is not toxic in all variant [*PIN*$^+$] backgrounds

Rnq1p over-expression is toxic in a [*PIN*$^+$] background; however it was of interest to determine whether the variant of [*PIN*$^+$] present would affect the toxicity phenotype associated with Rnq1p over-expression. To test this, the 74D-694 variant [*PIN*$^+$] strains along with the 74D-694 [*pin*$^-$] strain were transformed with pYES2-*RNQ1* and the pYES2 vector backbone, and Rnq1p toxicity was assayed according to the standard toxicity assay protocol. As expected, Rnq1p over-expression was not toxic in the [*pin*$^-$] strain however, while toxicity was observed in the low and high [*PIN*$^+$] variants, Rnq1p over-expression appeared less toxic in the medium [*PIN*$^+$] variant, and was not toxic in the very high [*PIN*$^+$] variant (fig.2).

The degree of Rnq1p toxicity in the different [*PIN*$^+$] variant strains shows no relationship with the amount of soluble Rnq1p present in the variants or with the ability of the variants to induce [*PSI*$^+$]. This suggests that the interaction between [*PIN*$^+$] and Sup35p, and the mechanism by which [*PIN*$^+$] stimulates Sup35p conversion to a prion, is fundamentally different to the interaction between soluble Rnq1p protein and [*PIN*$^+$] assemblies that result in Rnq1p toxicity.

This variable relationship between Rnq1p protein and the different [*PIN*$^+$] variants would be interesting to explore with the different Rnq1p alleles.

```
RNQ1        MDTDKLISEAESHFSQGNHAEAVAKLTSAAQSNPNDEQMSTIESLIQKIAGYVMDNRSGG 60
LOW-1       MDTDKLISEAESHFSQGNHAEAVAKLTSAAQSNPNDEQMSTIESLIQKIAGYVMDNRSGG 60
MED-1       MDTDKLISEAESHFSQGNHAEAVAKLTSAAQSNPNDEQMSTIESLIQKIAGYVMDNRSGG 60
V.HIGH-3    MDTDKLISEAESHFSQGNHAEAVAKLTSAAQSNPNDEQMSTIESLIQKIAGYVMDNRSGG 60
HIGH-1      MDTDKLISEAESHFSQGNHAEAVAKLTSAAQSNPNDEQMSTIESLIQKIAGYVMDNRSGG 60
            ************************************************************

RNQ1        SDASQDRAAGGGSSFMNTLMADSKGSSQTQLGKLALLATVMTHSSNKGSSNRGFDVGTVM 120
LOW-1       SDASQDRAAGGGSSFMNTLMADSKGSSQTQLGKLALLATVMTHSSNKGSSNRGFDVGTVM 120
MED-1       SDASQDRAAGGGSSFMNTLMADSKGSSQTQLGKLALLATVMTHSSNKGSSNRGFDVGTVM 120
V.HIGH-3    SDASQDRAAGGGSSFMNTLMADSKGSSQTQLGKLALLATVMTHSSNKGSSNRGFDVGTVM 120
HIGH-1      SDASQDRAAGGGSSFMNTLMADSKGSSQTQLGKLALLATVMTHSSNKGSSNRGFDVGTVM 120
            ************************************************************

RNQ1        SMLSGSGGGSQSMGASGLAALASQFFKSGNNSQGQGQGQGQGQGQGQGQGQGSFTALASL 180
LOW-1       SMLSGSGGGSQSMGASGLAALASQFFKSGNNSQGQGQGQGQGQGQGQGQGQGSFTALASL 180
MED-1       SMLSGSGGGSQSMGASGLAALASQFFKSGNNSQGQGQGQGQGQGQGQGQGQGSFTALASL 180
V.HIGH-3    SMLSGSGGGSQSMGASGLAALASQFFKSGNNSQGQGQGQGQGQGQGQGQGQGSFTALASL 180
HIGH-1      SMLSGSGGGSQSMGASGLAALASQFFKSGNNSQGQGQGQGQGQGQGQGQGQGSFTALASL 180
            ************************************************************

RNQ1        ASSFMNSNNNNQQGNQSSGGSSFGALASMASSFMHSNNNQNSNNSQQGYNQSYQNGNQN 240
LOW-1       ASSFMNSNNNNQQGNQSSGGSSFGALASMASSFMHSNNNQNSNNSQQGYNQSYQNGNQN 240
MED-1       ASSFMNSNNNNQQGNQSSGGSSFGALASMASSFMHSNNNQNSNNSQQGYNQSYQNGNQN 240
V.HIGH-3    ASSFMNSNNNNQQGNQSSGGSSFGALASMASSFMHSNNNQNSNNSQQGYNQSYQNGNQN 240
HIGH-1      ASSFMNSNNNNQQGNQSSGGSSFGALASMASSFMHSNNNQNSNNSQQGYNQSYQNGNQN 240
            ************************************************************

RNQ1        SQGYNNQQYQGGNGGYQQQQGQSGGAFSSLASMAQSYLGGGQTQSNQQQYNQQGQNNQQQ 300
LOW-1       SQGYNNQQYQGGNGGYQQQQGQSGGAFSSLASMAQSYLGGGQTQSNQQQYNQQGQNNQQQ 300
MED-1       SQGYNNQQYQGGNGGYQQQQGQSGGAFSSLASMAQSYLGGGQTQSNQQQYNQQGQNNQQQ 300
V.HIGH-3    SQGYNNQQYQGGNGGYQQQQGQSGGAFSSLASMAQSYLGGGQTQSNQQQYNQQGQNNQQQ 300
HIGH-1      SQGYNNQQYQGGNGGYQQQQGQSGGAFSSLASMAQSYLGGGQTQSNQQQYNQQGQNNQQQ 300
            ************************************************************

RNQ1        YQQQGQNYQHQQQGQQQQQGHSSFSALASMASSYLGNNSNSNSSYGGQQQANEYGRPQQ 360
LOW-1       YQQQGQNYQHQQQGQQQQQGHSSFSALASMASSYLGNNSNSNSSYGGQQQANEYGRPQQ 360
MED-1       YQQQGQNYQHQQQGQQQQQGHSSFSALASMASSYLGNNSNSNSSYGGQQQANEYGRPQQ 360
V.HIGH-3    YQQQGQNYQHQQQGQQQQQGHSSFSALASMASSYLGNNSNSNSSYGGQQQANEYGRPQQ 360
HIGH-1      YQQQGQNYQHQQQGQQQQQGHSSFSALASMASSYLGNNSNSNSSYGGQQQANEYGRPQQ 360
            ************************************************************

RNQ1        NGQQQSNEYGRPQYGGNQNSNGQHESFNFSGNFSQQNNNGNQNRY 405
LOW-1       NGQQQSNEYGRPQYGGNQNSNGQHESFNFSGNFSQQNNNGNQNRY 405
MED-1       NGQQQSNEYGRPQYGGNQNSNGQHESFNFSGNFSQQNNNGNQNRY 405
V.HIGH-3    NGQQQSNEYGRPQYGGNQNSNGQHESFNFSGNFSQQNNNGNQNRY 405
HIGH-1      NGQQQSNEYGRPQYGGNQNSNGQHESFNFSGNFSQQNNNGNQNRY 405
            *********************************************
```

Figure 5.22: The *RNQ1* gene in each [*PIN*$^+$] variant strain is identical.
Sequencing of the *RNQ1* gene from each of the [*PIN*$^+$] variant strains confirms that their phenotypic differences are not the result of changes at the DNA level of the *RNQ1* gene.

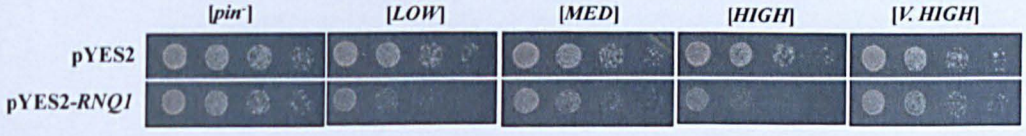

Figure 5.23 Rnq1p toxicity is influenced by the [*PIN*$^+$] variant.
Rnq1p over-expression in the different [*PIN*$^+$] variant backgrounds reveals differing degrees of Rnq1p toxicity depending on the variant of [*PIN*$^+$] present. Rnq1p over-expression was not toxic in a [*pin*$^-$] strain, but it also appeared not to be toxic in the very high [*PIN*$^+$] variant. In contrast, Rnq1p over-expression wa toxic in the low and high [*PIN*$^+$] variants, and showed slightly reduced toxicity in the medium [*PIN*$^+$] variant.

5.4 Expressing Rnq1p in *Drosophila melanogaster*

5.4.1 Introduction: *Drosophila melanogaster*

The function of the [*PIN*$^+$] prion in catalysing the conformational conversion and misfolding of aggregation prone proteins has been well documented. In the yeast Huntington's disease model, expression of the expanded exon 1 (103Q) construct requires the presence of [*PIN*$^+$] for aggregation and toxicity: this raises the question of whether other proteins serve equivalent roles to [*PIN*$^+$] in mammalian cells that show mutant huntingtin toxicity in the absence of Rnq1p/[*PIN*$^+$]. It was of interest to determine whether Rnq1p might similarly aggregate in non-yeast cells, perhaps seeded by an elusive mammalian [*PIN*$^+$] factor. Additionally, the genetic modifiers study (Chapter 6) had identified a deletion strain (*upf1Δ*) that suppressed Rnq1p and 103Q toxicity, and Upf1p was subsequently identified as a modulator of mutant huntingtin toxicity in *Drosophila* by a high-throughput RNAi screen (7200 genes screened identifying 404 candidates) (Doumanis, 2009). Thus, it was particularly interesting to identify whether Rnq1p was toxic in *Drosophila*, and if it was, to subsequently identify whether a *UPF1* mutant would also suppress Rnq1p toxicity in *Drosophila*.

5.4.2 The *Drosophila melanogaster GAL4-UAS* system

There are a number of factors to consider when planning to express a protein of interest in *Drosophila*. In the case of Rnq1p, these included: where to express Rnq1p, when to express it, and at what intensity. The availability of a highly tractable promoter system called *GAL4-UAS* allows for such temporal and spatial precision in *Drosophila* .

The product of the *GAL4* gene, the Gal4p protein, is a transcriptional activator that binds to a promoter element known as an *UAS* (Upstream Activating Sequence). A large number of fly lines have been engineered each containing a different tissue-specific promoter upstream of the *GAL4* gene; therefore Gal4p is only produced in a subset of fly tissues in each of these lines. For example, the actin promoter upstream of the *GAL4* gene results in ubiquitous expression of Gal4p throughout the fly since actin is expressed in all tissues. Conversely, the Hsp70 promoter would be

responsive to heat-shock and therefore Gal4p expression would only be induced in these instances. Since the *UAS* is only activated by the presence of Gal4p, *UAS* activity will also be tissue-specific. A gene of interest cloned downstream of the *UAS* promoter element will result in tissue specific expression of the protein of interest.

The gene of interest, under the control of the *UAS* element, is often referred to as the 'responder'. To activate transcription of the responder, in this case the *RNQ1* gene, the responder line of flies is crossed to a particular *GAL4* 'driver' line of flies, which will determine the expression pattern of the responder. Thus, the two units of this system are brought together by a specific breeding strategy, as illustrated in figure 5.24.

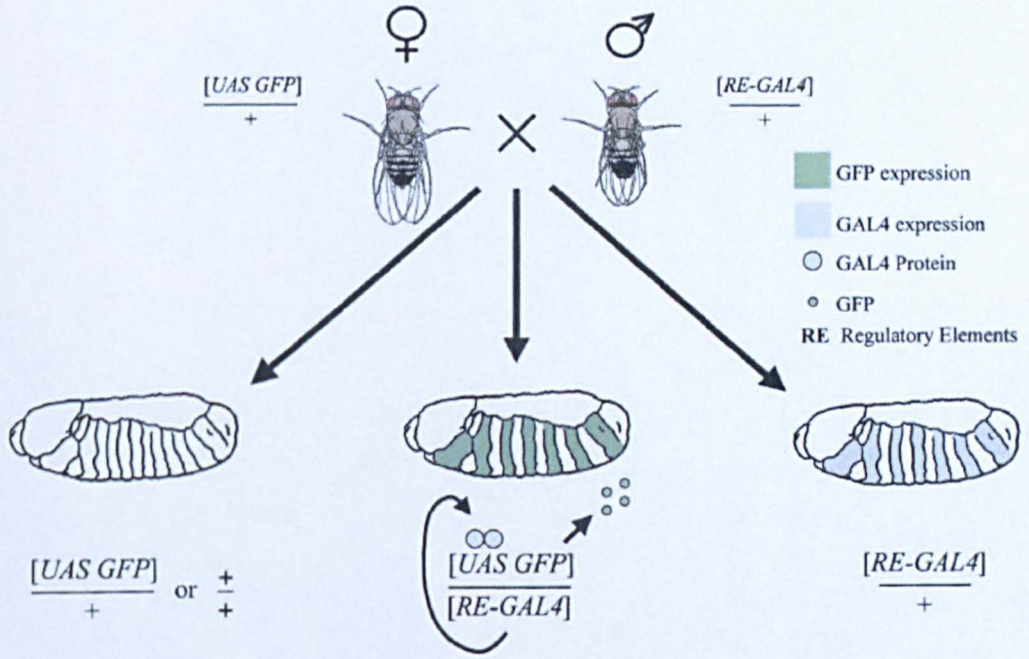

Figure 5.24 Demonstrating the mating strategy for the two-component *GAL4-UAS* promoter system.
Mating of a female *UAS-GFP* responder line to a male *GAL4*-driver line results in progeny carrying both the *UAS-GFP* element and the *GAL4*-driver element. The progeny will have tissue specific activation of Gal4p and thus tissue-specific expression of the Gfp responder. Image from Duffy *et al* (Duffy,2002).

5.4.3 Construct generation for larval injection

The full-length *RNQ1* gene cloned into a Gateway entry clone was recombined with a Gateway destination vector adapted for use in *Drosophila*: an untagged pTW vector with a *UASt* promoter (figure.5.25).

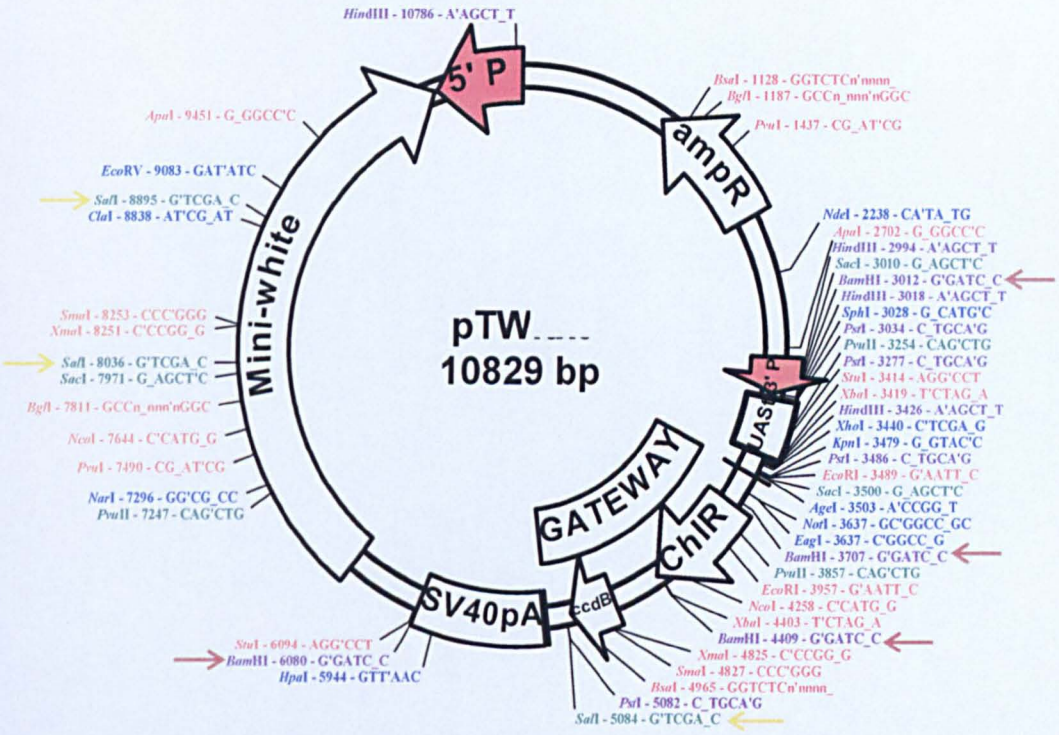

Figure 5.25 The plasmid map for the pTW Gateway destination vector. An LR-recombination reaction between the pTW vector and the *RNQ1*-bearing entry clone results in expulsion of the *ccdB* and chloramphenical resistance gene (ChlR) and insertion of the *RNQ1* gene at this position. External red arrows indicate positions of *Bam*HI restriction sites. Orange arrows indicate *Sal*I restriction sites.

For further confidence in the identity of the expression clones, 3 were selected for further examination. A digest with restriction enzyme *Sal*I should liberate an 859 bp fragment if the 'gateway' region of the vector has been recombined out, otherwise a third restriction site for this enzyme would remain in the 'gateway' region, generating 3 bands. For all 3 potential expression vectors tested, the 859 bp fragment was observed following *Sal*I digestion of an aliquot of the respective plasmid DNA

Various ratio amounts of entry clone and destination vector were tested in an LR reaction to generate the desired *RNQ1*-bearing expression clone. Those reactions that when transformed into *E. coli* gave rise to ampicillin resistant colonies were cultured further to isolate plasmid DNA. The putative clones were digested with the

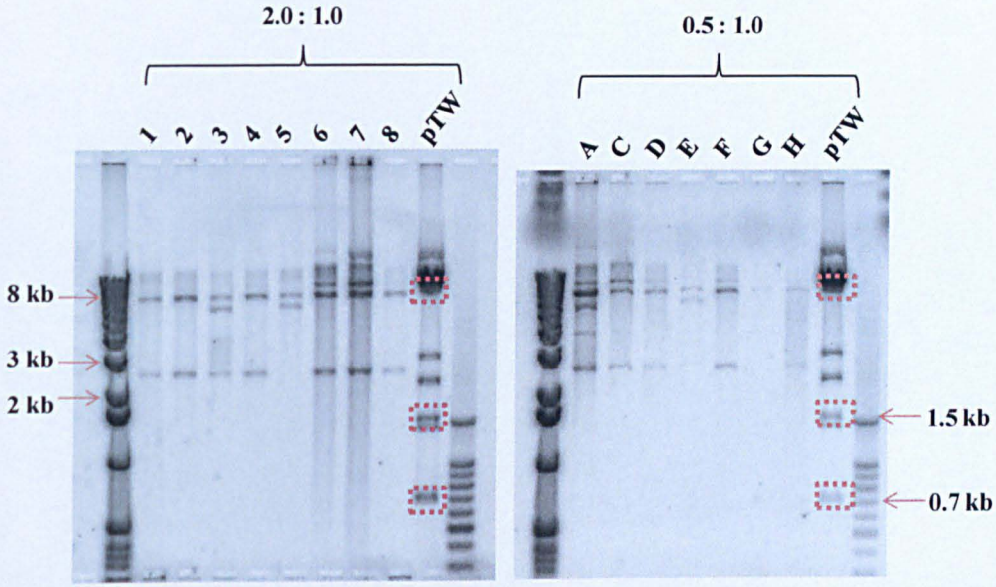

Figure 5.26: Agarose gel analysis of *Bam*HI restriction digest products of potential expression clones.
The two gels represent different ratios of pTW vector to entry clone used. Samples 1 through to 8 and A through to H were tested as potential expression clones. Most samples contain the 2500-2700 bp and 7761 bp fragments expected for successful integration of *RNQ1* into the pTW vector. The pTW vector backbone liberated the 695/702 bp doublet, the 1671 bp and 7744 bp fragments as expected (indicated in dashed red squares).

restriction enzyme *Bam*HI to determine if any reactions had generated an expression clone (figure 5.26). Such a *Bam*HI digest of the pTW backbone should liberate 4 DNA fragments of sizes: 695 bp, 702 bp, 1671 bp and 7744 bp. These were observed along with 2 additional bands at ~ 2800 bp and 3500 bp, that most likely were partial digest products (figure.5.26). If the *RNQ1*gene recombined with the pTW destination vector, then 2 bands should be observed, one ~ 7761 bp and the other ~2500 – 2700 bp. Fortunately, there were a number of apparently successful reactions (figure.5.27).

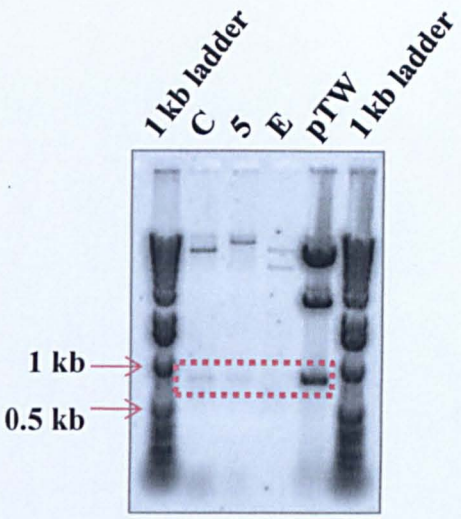

Figure 5.27: Agarose gel analysis of a *SalI* restriction digest of potential RNQ1 expression clones.

Plasmids C, 5 and E, along with the pTW backbone as a positive control, were digested with the restriction enzyme *Sal*I. A *Sal*I digest should liberate a 859 bp fragment from the pTW vector (indicated with dashed red square) and any pTW-*UAS-RNQ1* vectors, confirming identity of the pTW vector.

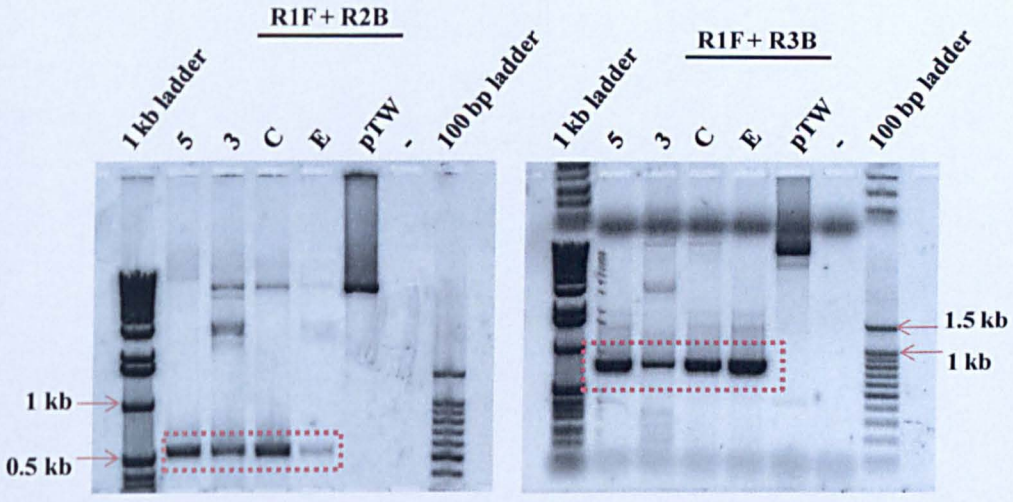

Figure 5.28 PCR confirmation of successful pTW-*RNQ1* expression clones.

Agarose gel analysis of *RNQ1*-specific PCR reactions testing potential expression clones 5, 3, C, E and the pTW vector as negative control. The two PCR reactions amplify two differently sized internal *RNQ1* fragments (573 bp for primer pair R1F+R2B; 793 bp for primer pair R1F+R3B). This result confirms presence of the *RNQ1* gene in the pTW expression vectors tested. Primer sequences can be found in materials and methods section 2.7.

PCR analysis of the potential expression clones for the presence of the *RNQ1* gene was also performed (figure 5.28). The PCR reactions were performed independently and the pTW backbone was also analysed with the same primers to ensure non-specific amplification of vector sequence did not lead to false-positive identification of inserts. A positive result for *RNQ1* gene presence was detected for all tested expression constructs, but absent in the pTW vector backbone sample

5.4.4 Sequencing of the constructed expression clones

Constructs 5 and C were sent off for sequencing to ensure correct integration of the *RNQ1* gene downstream of the *UAS* element. A forward primer binding upstream of the UAS element were used for sequencing, along with a reverse primer binding within the *RNQ1* gene coding sequence. Figure 6 shows how both constructs 5 and C contain sequence reads identical to that of the pTW vector until nucleotides AGC, corresponding to the AGC of the 3' residual attR1 site of the destination vector (indicated in figure 5.29), after which point the sequence corresponds to residual attL1 sequences of the entry clone – indicating successful recombination between the pTW destination vector and the *RNQ1*-bearing entry clone.

The overall sequence of the pTW-*UAS-RNQ1* expression vector that was confirmed by sequencing (excluding additional 3' *RNQ1* coding sequence) is shown in figure 7. Construct 5 was chosen for use in the study noting however that it contained a SNP in the hsp70 TATA sequence, resulting in an A → G residue polymorphism.

A)

B)

>pTW-UAS-RNQ1

TCGGATCCAAGCTTGCATGCCTGCAGGTCGGAGTACTGTCCTCCGAGCGGAGTACTGTCCTCCGAGCGGATACTG
TCCTCCGAGCGGAGTACTGTCCTCCGAGCGGAGTACTGTCCTCCGAGCGGAGACTCTAGCGAGCGCCGGAGTATA
AATAGAGGCGCTTCGTCTACGGAGCGACAATTCAATTCAAACAAGCAAAGTGAACACGTCGCTAAGCGAAAGCTA
AGCAAATAAACAAGCGCAGCTGAACAAGCTAAACAATCTGCAGTAAAGTGCAAGTTAAAGTGAATCAATTAAAAG
TAACCAGCAACCAAGTAAATCAACTGCAACTACTGAAATCTGCCAAGAAGTAATTATTGAATACAAGAAGAGAAC
TCTGAATAGGGAATTGGGAATTATCGAGGCCTGTCTAGAGAAGCTTGTTCGAATCTCGAGTGCGCGCTTCCGGAG
GTATACACCTAGGCGGTACCACTGCAGTGAATTCGGAGCTCTACCGGTATACAAGTTTGTACAAAAAAGCAGGCT
CCGCGGCCGCCCCCTTCACCATGGATACGGATAAGTTAATCTCAGAGGCTGAGTCTCATTTTTCTCAAGGAAACC
ATGCAGAAGCTGTTGCGAAGTTGACATCCGCAGCTCAGTCGAACCCCAATGACGAGCAAATGTCAACTATTGAAT

..... = UAS (5 GAL4 binding sites
..... = residual attR1 of destination vector
..... = hsp70 TATA
..... = residual attL1 of entry clone
A = SNP occurring in construct 5, A→G
..... = *RNQ1*

Figure 5.29 Sequencing of pTW-*RNQ1* expression clones.
A) Sequence alignment of a specific region of the pTW vector against the same region of the pTW-*UAS-RNQ1* expression clones 5 and C, confirming recombination between destination vector attR1 and entry clone attL1 sequences. B) The DNA sequence of the pTW-*UAS-RNQ1* expression construct 5, as determined by sequencing. The relevant regions of the pTW-*UAS-RNQ1* vector are colour coded to the key provided.

5.4.5 Screening of the transgenic flies and identifying *RNQ1* integration site

Following a midi-prep of the selected pTW-*UAS-RNQ1* expression construct, 80 µg of the purified vector DNA was sent to Genetic Services Inc (USA) for larva injection. Approximately 65 adults were isolated from the injected batch.

The DNA is injected in such a way that it becomes incorporated into the germ line cells of the embryos, therefore it is not immediately possible to identify successful exogenous DNA integrants in the flies that develop from the injected embryos. Identification relies on transfer via the germ line of a genetic marker. Specifically, the injected embryos, instead of having wild-type red eyes, were white-eyed mutants that co-inherited with the exogenous DNA in this case *RNQ1*, the "mini-white" gene (figure 5.25) allowing for partial rescue of the white mutant and resulting in orange

eyes for subsequent progeny that inherit the transgene. Thus, it was necessary to mate the injected generation of flies (generation 0, or 'G0') and isolate any of the resulting progeny (generation 1, or 'G1' flies) that had orange eyes.

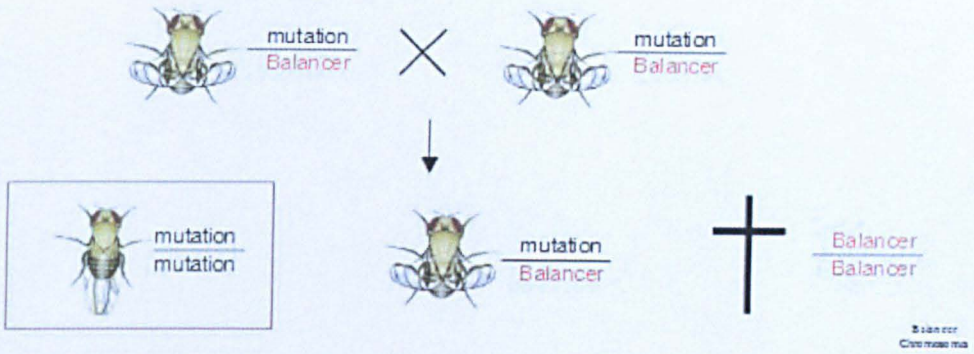

Figure 5.30 *Drosophila melanogaster* double-balancer chromosomes. Illustrating the use of balancer chromosomes in visually identifying offspring carrying a mutation, which has downstream utility in further breeding strategies. Any offspring that inherit two copies of the balancer are non-viable. Copied from http://www.scribd.com/doc/6125010/Drosophila-as-a-Model-Organism.

Since it is often necessary to identify where the exogenous DNA has integrated, the G0 and G1 flies were mated to 'double balancer' flies. These flies double balancer have a dominant marker on each arm of chromosomes 2 and 3, that serves to stabilise the integrated DNA through continued selection of the associated marker phenotypes.. Additionally, the markers are also recessive lethal, reducing the number of viable but non-desirable offspring (figure 5.30).

The double balancers flies used had white eyes (w^-); on the second chromosome their carried *CyO* (curly wings) and *Sco* (hairless); and on their third chromosome *Hu* (extra shoulder bristles, also called *TM6B*) and *Sb* (short thick bristles called stubble, also known as *MRKS*). See figure 5.31 for examples. The *RNQ1* integration site was determined by sequential mating with the double balancers and in combination with selecting flies that had only orange/red eyes, eventually results in the absence of only one balancer phenotype, which must be due to *RNQ1* integration at that particular position. Figure 5.3.2 represents a possible breeding pattern, in the case where

RNQ1 integrated into the 2nd chromosome- at the stage of analysing the G2 flies, *RNQ1* could be detected on the 2nd chromosome because the *Cyo* and *Sco* balancers would never appear together in any of the red eyed G2 flies.

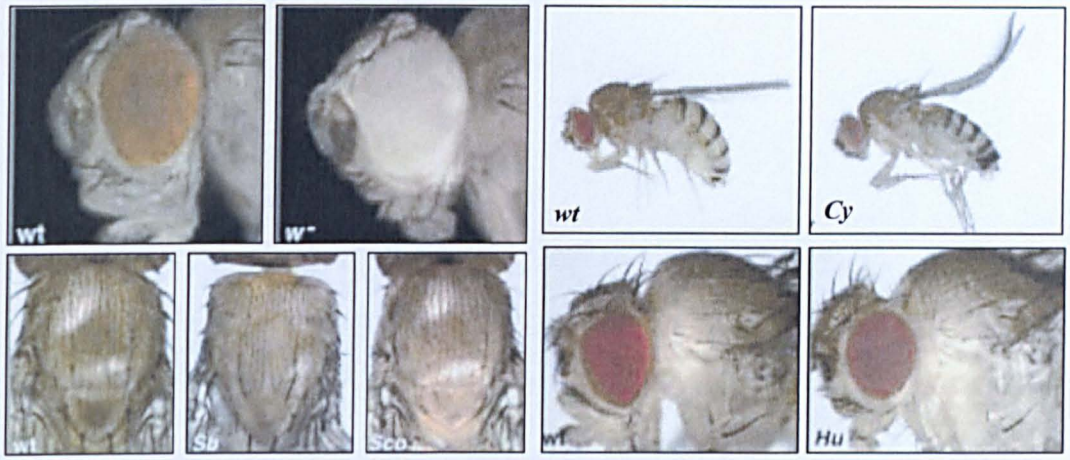

Figure 5.31 Images showing the phenotypes associated with the balancer chromosomes used in this study.
Top row left to right: '*wt*' wild-type red eyes and '*w*-' mutant white eyes, '*wt*' wild-type straight wings and '*Cy*' mutant curly wings. Bottom row left to right: '*wt*' wild-type bristles on xxx, '*Sb*' stubble on the xxx, '*Sco*' or hairless on the xxx, '*wt*' wild-type for shoulder hair, '*Hu*' or humeral, with extra hair on the shoulders. Copied from http://www.drosophila-images.org/images-2006/14c-slide-F.htm.

In this particular experiment, 65 injected larva eclosed and the adult G0 flies were crossed with double balancers. The offspring were screened for the presence of an orange eye indicating a transgenic line. Of ~4000 screened, 6 transgenic lines were identified, representing G0 lines #2, #23, #30 (x2), #33 and #60 (Table 5.6).

The relatively low efficiency of successful transgenics in combination with a generally pale eye colour for all transgenic flies was taken as a possible indication of Rnq1p toxicity, since some leaky expression of transgenes can occur without Gal4p mediated activation, particularly in transcriptionally active areas. If Rnq1p was toxic in the transgenic flies, any successful integration of *RNQ*1 into such active areas would cause some degree of cellular toxicity or loss of viability of the developing embryos. The pale eye colour of the transgenic flies indicated that in all of these flies *RNQ1* was integrated into transcriptionally silent areas.

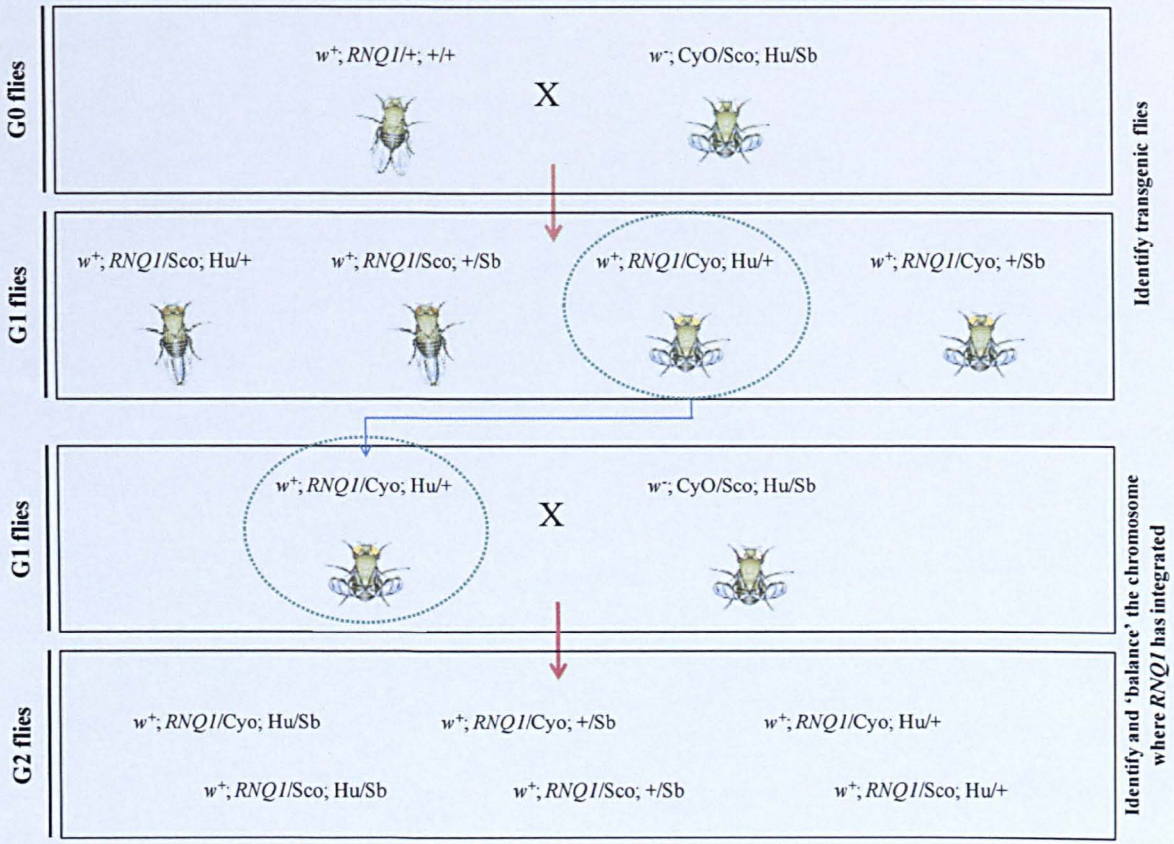

Figure 5.3.2: Example breeding strategy to identity integration chromosome of the *RNQ1* gene.
G0 flies were mated with double balancers; *RNQ1* transgenic flies will have orange/red eyes. The G1 flies are mated with double balancers to identify and 'balance' the chromosome where the *RNQ1* gene has integrated.

Line	Genotype
2	*x? Y?; +/+; +/+*
23	*RNQ1/w; +/+; +/+*
30	*(a) w; RNQ1/Cyo; +/+* *(a,b) w; RNQ1-a/Cyo; RNQ1-b/TM6B*
33	*w; +/+ ; RNQ1/TM6B*
60	*w; RNQ1/Cyo; +/+*

Table 5.6 Transgenic *UAS-RNQ1* lines of *D. melanogaster* created in this study.
RNQ1 is represented on the second chromosome (lines 30a), on the second and third chromosome (line 30a-30b), on the third chromosome (line 33), on the Y chromosome (line 23) and on either the X or the Y chromosome (line 2).

5.4.6 *UAS-RNQ1* X *GAL4*-driver lines

It was decided that expression of Rnq1p in the following tissues, as determined by the relevant *GAL4*-driver lines, were chosen to provide a reliable indication as to whether Rnq1p was toxic or not:

sev-GAL4 : the enhancer of the *sevenless* gene, drives strong expression of Gal4p in photoreceptor precursor cells and precursor cone cells of the ommatidium (*Drosophila* eye).

da-GAL4 : the promoter of the transcription factor *daughterless* is involved in developmental pathways and drives ubiquitous expression of Gal4p in tissues throughout the fly.

elav-GAL4 : the promoter of the *embryonic lethal abnormal vision* gene, results in panneural distribution of Gal4p. This particular driver can also be temporally controlled, since the tissue-specific promoter can be activated by systemic exposure to the ligand RU486 (mifepristone). Therefore, *elav-GAL4* allows for both temporal and spatial control of Gal4p expression.

gmr-GAL4 : the promoter element of the *glass multiple receptor* gene expresses Gal4p in all photoreceptor neurons of the eye.

Visual inspection of the different *GAL4-/UAS-RNQ1* offspring indicated that Rnq1p was not toxic in the constructed transgenic flies. No eye deformity was observed and no changes to mobility or activity were noted. However, Rnq1p expression level remains to be determined all of the transgenic flies. Further, examination only occurred a few days after eclosion of the *GAL4/UAS-RNQ1* flies, which may not have been sufficient time for toxicity phenotypes to manifest themselves. It was also not known at the time of the experiments that *GAL4*-lines are temperature sensitive, and unfortunately the flies were stored at both 26 °C and 18 °C with only the former temperature being ideal for activity of Gal4p.

Therefore, at this stage it is not possible to confidently comment on the toxicity of Rnq1p expression in *Drosophila melanogaster* and this analysis remains to be completed.

Chapter VI

Genetic Modifiers of Toxicity

6.1 The toxicity relay

The ability of each protein to fulfil its allotted function in the cell is intricately dependent on the ability of other proteins to fulfil their own function, and on the ability of proteins to interact appropriately; both temporally and spatially. Similarly, toxicity caused by a particular protein is not an isolated, independent event, but it is embedded in a network of interactions that allow the toxicity to propagate throughout the cell. It stands to reason that those proteins involved in the propagation of a toxicity phenotype are also the best positioned to modulate the toxicity phenotype, however it is likely that only those proteins in close proximity to the initial toxic event are capable of blocking damage before it becomes too wide-spread and the cell irrecuperably damaged. Therefore, the toxicity of Rnq1p should be susceptible to modulation by those proteins working in close proximity to Rnq1p, either by way of functional pathways or spatial arrangement. Screening for genetic modifiers of Rnq1p toxicity, looking for alterations in Rnq1p toxicity due to the absence of individual proteins/genes, should be informative not just of terms of identifying proteins responsible for propagating Rnq1p toxicity, but also those that are functionally and spatially related to Rnq1p in the cell, helping to identify possible cellular functions for Rnq1p.

6.1.1 Rnq1p and huntingtin-103Q are not toxic in a *upf1Δ* strain

The initial objective was to identify modulators of Rnq1p toxicity since they may inform us of possible functions for Rnq1p. The *rnq1Δ* and *hsp104Δ* strains were included in the initial screen for such modulators, since they served as positive controls for the assay (suppression of toxicity). The *ctt1Δ* strain and *sod2Δ* strains,

absent of catalase-1 and Sod2p, respectively, which otherwise protect against oxidative damage were tested since variable growth defects of the [*PIN*$^+$] variants, [*pin*$^-$] and a *rnq1Δ* strain had been observed upon exposure to hydrogen peroxide, indicating a possible link between Rnq1p and oxidative stress/damage. A *upf1Δ* strain was also tested since Upf1p, one of three proteins forming the nonsense-mediated decay (NMD) complex that recognise premature stop-codons in mRNA transcripts at the ribosome, was a common factor to both Rnq1p's interaction with Sup35p, where both Sup35p and Upf1p are ribosomal, and also to Rnq1p's co-localisation with P-bodies, where Upf1p is responsible for shuttling mRNA transcripts containing premature stop codons to P-bodies for their degradation. Thus, Upf1p may be functionally related to Rnq1p and important for Rnq1p interactions in the cell.

A toxicity assay of the deletion strains was carried out in both the [*PIN*$^+$] and [*pin*$^-$] backgrounds (figure 6.1). While Rnq1p over-expression was toxic in both the *ctt1Δ* and *sod2Δ* [*PIN*$^+$] strains, as in the parental BY4741 [*PIN*$^+$] strain, there was also a slight toxicity phenotype associated with Rnq1p over-expression in the *sod2Δ* [*pin*$^-$] strain. The most significant result however was suppression of Rnq1p toxicity in the *upf1Δ* [*PIN*$^+$] strain.

Since it was possible that the *upf1Δ* strain had naturally, or due to the deletion, converted to a [*pin*$^-$] strain, the [*PIN*$^+$] status of the *upf1Δ* strain was confirmed (figure 6.2). To determine whether the suppression of Rnq1p toxicity was specific to the absence of the Upf1p protein, or to the function of the nonsense-mediated decay (NMD) complex, the deletion strains *upf2Δ* and *upf3Δ* were also tested for their [*PIN*$^+$] status (figure 6.2) in preparation for further downstream analyses.

Sedimentation analysis of the deletion strains *upf1Δ*, *upf2Δ* and *upf3Δ* confirmed that all three strains were [*PIN*$^+$] (figure 6.2), therefore the suppression of Rnq1p toxicity by delta *upf1Δ* was indicative of a significant genetic interaction between Upf1p and Rnq1p.

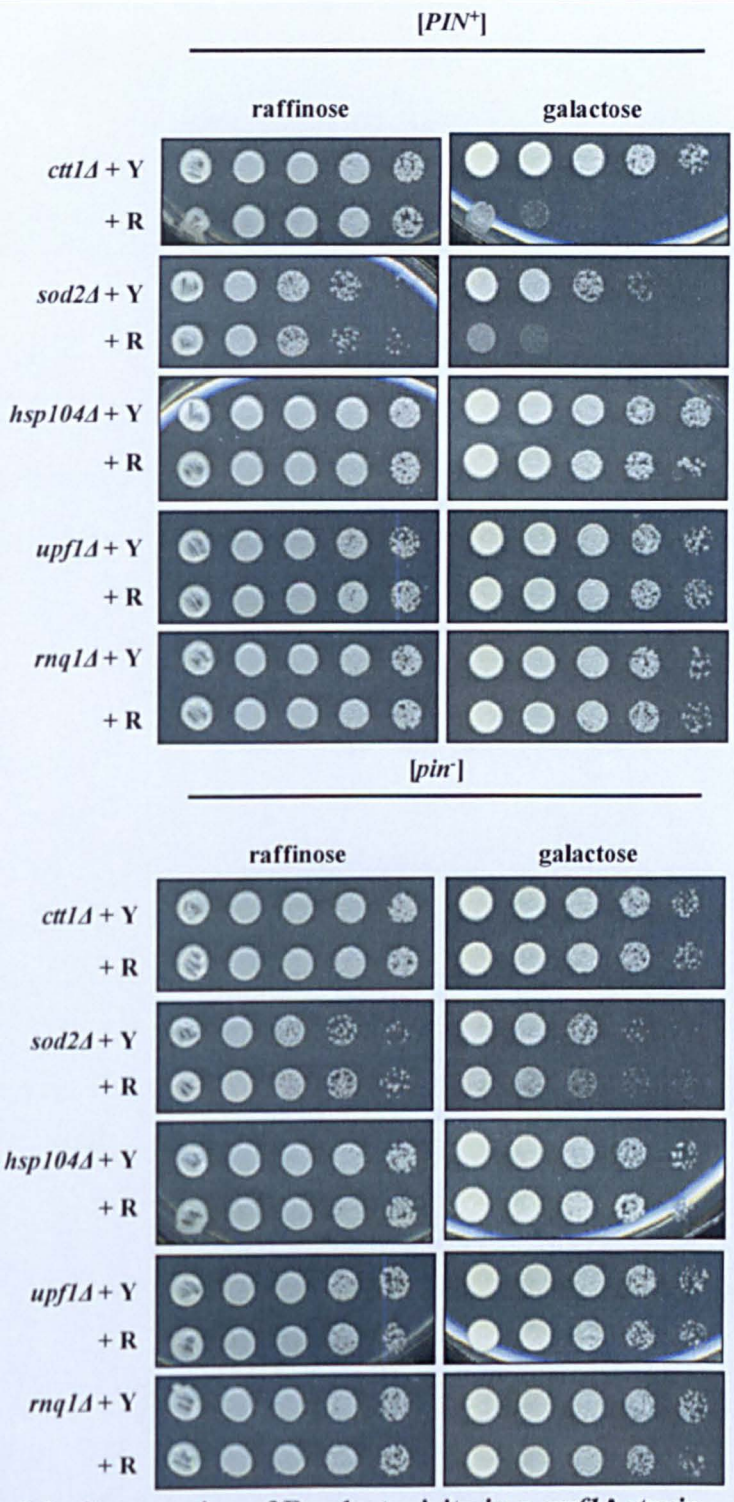

Figure 6.1 Suppression of Rnq1p toxicity in a *upf1Δ* strain.
An initial screen to identify genetic modifiers of Rnq1p toxicity examined the effect on growth of galactose induced pYES2-*RNQ1* (+R) over-expression in deletion strains *ctt1Δ*, *sod2Δ*, *upf1Δ*, *hsp104Δ* and *rnq1Δ*, compared to their pYES2 (+Y) control equivalents. The *upf1Δ* strain suppressed the toxicity normally associated with Rnq1p over-expression in a [*PIN*$^+$] background.

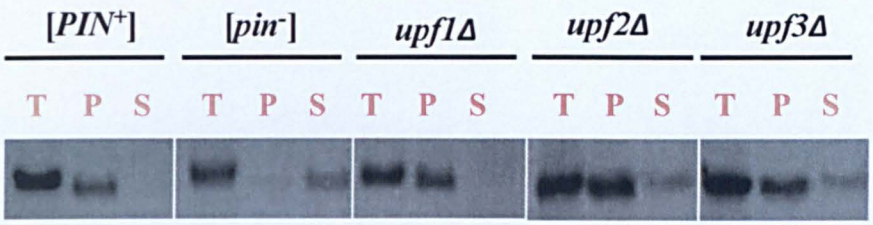

Figure 6.2 Sedimentation analysis of BY4741 deletion strains *upf1Δ*, *upf2Δ* and *upf3Δ*.
To determine the prion status of Rnq1p in the *upf1Δ*, *upf2Δ* and *upf3Δ* deletion strains, sedimentation analysis of these strains was performed. BY4741 [*PIN*$^+$] and [*pin*$^-$]strains were included in the analysis as controls. In a [*PIN*$^+$] strain, more Rnq1p protein is found in the pellet (P) fraction relative to the soluble (S) fraction; the reverse is true for a [*pin*$^-$] strain. All three deletion strains appear to be [*PIN*$^+$].

As Rnq1p is a polyglutamine rich protein whose over-expression induces cell toxicity, it was of interest to determine whether the suppression of Rnq1p toxicity by the *upf1Δ* strain was specific to Rnq1p, or whether it would suppress polyglutamine toxicity in general. Therefore it the Huntingtin 103Q construct used in the yeast Huntington disease model was be tested for toxicity in this deletion background. Additionally to establish whether suppression of toxicity was due to the absence of Upf1p or due to the function of the NMD complex, the deletion strains *upf2Δ* and *upf3Δ* were assayed.

The 103Q and 25Q plasmids obtained from Y. Chernoff (Meriin *et al.*, 2002), were analysed by restriction digest (figure 6.3) and the expected difference in fragment size released by 25Q and 103Q was ~234 nt (i.e. a difference of 78 amino acids) and this was the approximate size difference observed.

In contrast to what was observed with *upf1Δ*, toxicity of Rnq1p was not suppressed by *upf2Δ* or *upf3Δ* (figure 6.4) although there was a slight reduction in Rnq1p toxicity in the *upf2Δ* strain.

Over-expression of the 103Q construct in BY4741 was less toxic than Rnq1p over-expression in BY4741. The *upf1Δ* suppressed 103Q-associated toxicity, and while 103Q was toxic in *upf3Δ*, it appeared not to be toxic in *upf2Δ (*figure 6.4)

It was possible that the difference in the degree of toxicity associated with Rnq1p over-expression, compared to the much reduced toxicity of 103Q, could account for *upf2Δ* suppressing 103Q toxicity, but only slightly reducing Rnq1p toxicity e.g. the effect of *upf2Δ* may be essentially the same, but due to the different degree of toxicity associated with the two proteins in question, gives rise to an apparent suppression for one (103Q) and reduction for the other (Rnq1p). If this were true, the result still implicates both Upf1p and Upf2p in the toxicity of these polyglutamine-rich proteins, suggesting that it is not the activity of the NMD complex *per se*, since the NMD complex requires Upf3p (He *et al.*, 1997), whose deletion did not suppress Rnq1p or 103Q toxicity.

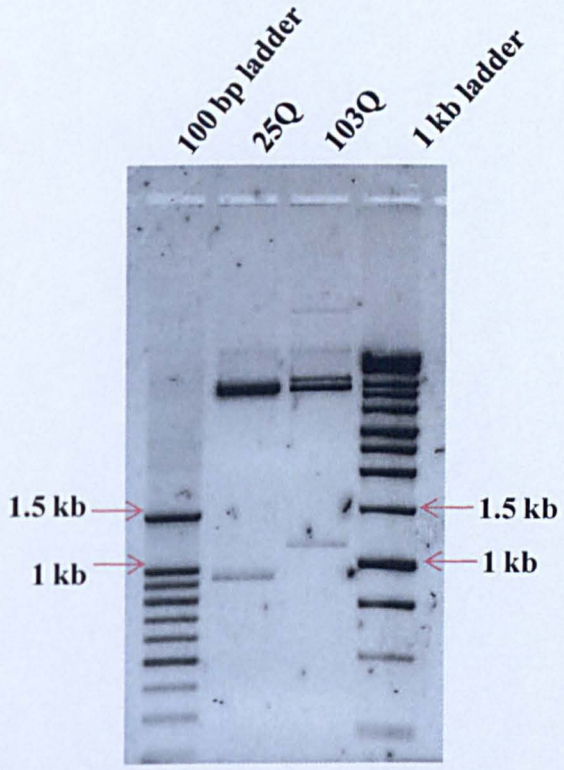

Figure 6.3 Confirming pYES2-25Q and pYES2-103Q insert size.
Agarose gel analysis of products from a restriction digest of the pYES2-25Q and pYES2-103Q plasmids. To confirm that these plasmids contained the correct sized insert, restriction enzyme *Bam*HI was used to release the respective fragments. The difference in size between the 25Q derived and 103Q derived fragment as shown here was equivalent to 78 amino acids, as expected. Plasmids provided by Y. Chernoff.

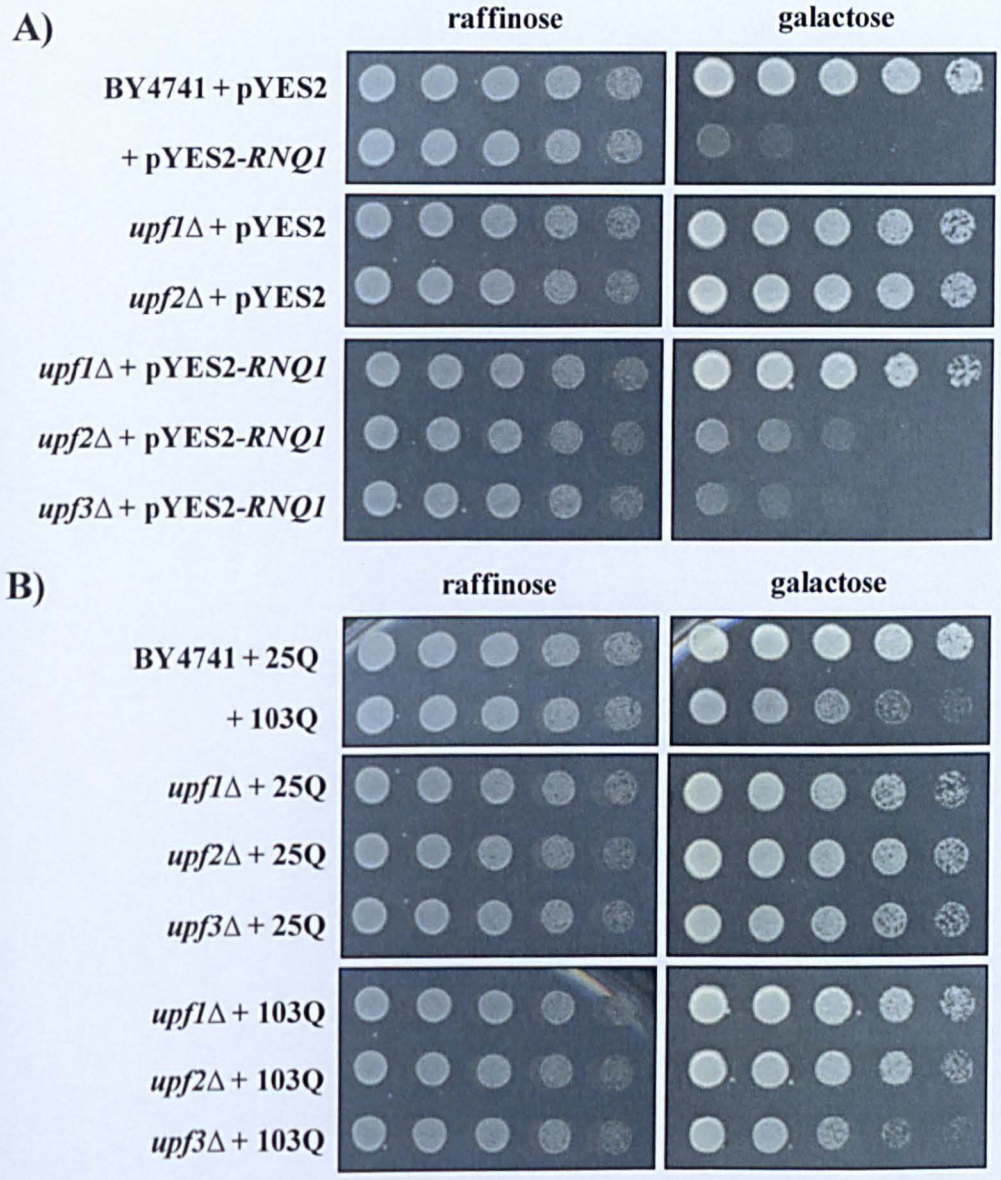

Figure 6.4 The *upf1Δ* strain suppresses the [*PIN*$^+$]-dependent toxicity of Rnq1p and 103Q over-expression.

The induction of Rnq1p (panel A) and 103Q (panel B) over-expression from the galactose inducible pYES2-*RNQ1* and pYES2-103Q vectors, respectively, by transfer to a galactose-based medium demonstrated a toxicity phenotype associated with over-expression of both of these proteins in BY4741, relative to their controls (the pYES2 vector backbone for Rnq1p and pYES2-25Q for 103Q).

To further validate the specificity of the *UPF1* deletion to the suppression of Rnq1p toxicity, the *UPF1* gene on a Gateway entry clone was recombined with a centromeric destination vector (pAG415) to determine whether Upf1p expression in the *upf1Δ* strain would restore toxicity of Rnq1p over-expression. The destination vector backbone was included in the study as a negative control.

The presence of the vector backbone or the expression of Upf1p via this plasmid in BY4741 was without consequence, as expected (figure 5.5). The over-expression of Rnq1p in the *upf1Δ* strain in the presence of the vector backbone resulted in suppression of toxicity, also as expected. However, over-expression of Rnq1p in a *upf1Δ* strain that was also expressing Upf1p from a plasmid resulted in Rnq1p toxicity. This result confirmed that the suppression of Rnq1p toxicity in the *upf1Δ* strain is specific to the absence of Upf1p, since restoring expression of Rnq1p in the *upf1Δ* background results in restoration of toxicity.

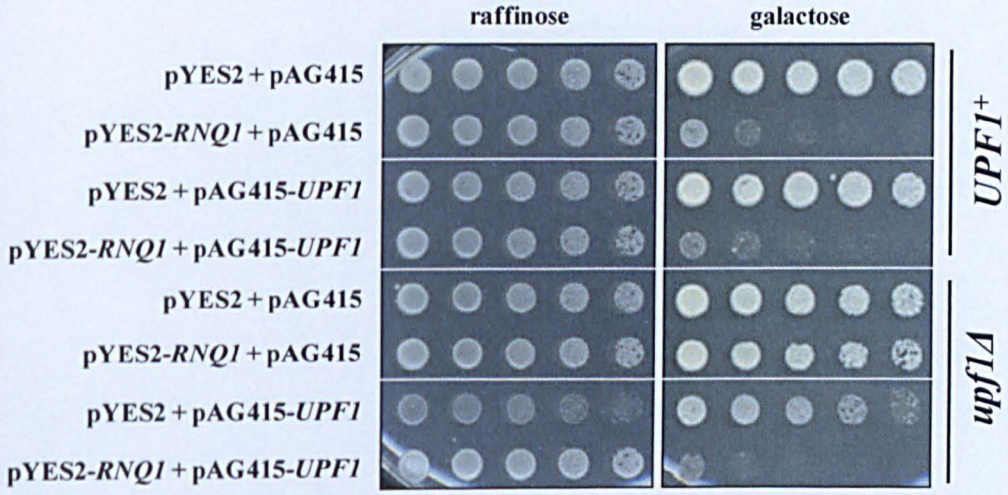

Figure 6.5 Suppression of Rnq1p toxicity in a *upf1Δ* strain is specific to the absence of the *UPF1* gene.
To determine whether the absence of Rnq1p toxicity in the *upf1Δ* strain was due to the deletion of the *UPF1* gene, its expression was restored via pAG415-*UPF1*. The BY4741 and *upf1Δ* strains were co-transformed with the following plasmid pairs: pYES2 and pAG415; pYES2 and pAG415-*UPF1*; pYES2-*RNQ1* and pAG415; and pYES2-*RNQ1* and pAG415-*UPF1*.

6.1.2 103Q over-expression may cause mitochondrial dysfunction

That Upf1p could modulate the toxicity of both Rnq1p and 103Q suggested the respective toxicity pathways of Rnq1p and 103Q had some degree of overlap. Having previously identified that Rnq1p over-expression, resulted in reduced mitochondrial function (section 5.1.6), it was of interest to determine whether 103Q over-expression resulted in the same phenotypic consequence.

As previously observed for Rnq1p (section 5.1.6), 103Q over-expression alone did not affect cell growth on a non-fermentative carbon source such as glycerol (figure 6.6). However, when the cellular pool of mitochondria were partially depleted by exposure to a low dose of ethidium bromide (EtBr), over-expression of 103Q resulted in a subsequent growth defect on glycerol where the 25Q control did not, indicating that 103Q expression had a negative effect on the mitochondrial population, since cells over-expressing 103Q after EtBr exposure were unable to respire sufficiently for growth on glycerol.

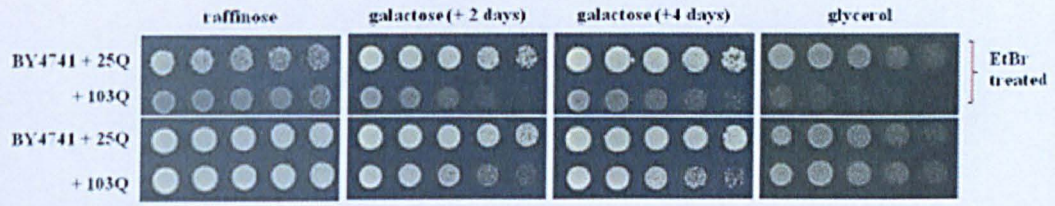

Figure 6.6 Over-expression of 103Q induces mild mitochondrial dysfunction.
The over-expression of 103Q, induced by galactose, causes a toxicity phenotype in BY4741 where no toxicity is observed on galactose for the 25Q control construct. Transfer of these strains to glycerol does not indicate any respiratory defect associated with 25Q or 103Q over-expression. Partial depletion of mitochondrial function by low dose ethidium bromide (EtBr) exposure prior to the proteotoxicity assay however results in a 103Q specific respiratory defect, as indicated by an inability of the 103Q strain to grow on non-fermentative, glycerol-based medium.

This result was also observed for Rnq1p (section 5.1.6), suggesting that over-expression of the polyglutamine rich proteins caused a slight mitochondrial dysfunction in the cell. The pre-requisite of a depleted pool of mitochondria for the

appearance of this phenotype may suggest, in terms of Huntington's disease, that those harbouring mitochondrial defects with either a genetic or environmental basis, could be more vulnerable to the damaging effects of expanded Huntingtin protein.

Alternatively, a reduction in mitochondrial activity may result in a change to the toxicity profile of the polyglutamine-rich proteins. It may be that the activity of the mitochondria or the specific homeostasis of proteins in the presence of a certain threshold of mitochondrial number or activity directs toxicity down one particular cellular pathway, but when this homeostasis or the mitochondria activity level is disrupted, toxicity takes a different route with greater detriment to the remaining mitochondria.

6.1.3 Growth analysis of Rnq1p over-expression in the *upf1Δ* strain

As described in chapter 5. Three particular cellular effects of Rnq1p over-expression were investigated: cell doubling time, cell size, and cell viability. This analysis was repeated in the *upf1Δ* strain.

The pYES2 backbone and the pYES2-*RNQ1* constructs were transformed into the *upf1Δ* strain. Transformants were grown up overnight (approximately 16 hr) in 5 mL glucose-based selective minimal media, sub-cultured for a second night (approximately 16 hr) in 10 mL 2 % raffinose-based selective minimal media, and an equal number of cells from the pYES2 transformant and pYES2-*RNQ1* transformant cultures used to inoculate 50 mL 2% raffinose 2 % galactose selective minimal media. Time of inoculation into the galactose containing medium was taken as t = 0 hr.

The results show fold differences in cell number between a particular strain expressing pYES2 relative to the same strain expressing pYES2-*RNQ1*, at specific times as indicated post-induction (figure 6.7). The BY4741 data is included to provide context for the *upf1Δ* strain result. For BY4741, cell number in the BY4741 + pYES2 (control) and BY4741 + pYES2-*RNQ1* (test) cultures were essentially the same after 2 hrs of growth, however the difference in cell number increased continually until t = 9 hrs when there were 4.1 x as many cells in the BY4741 control strain relative to the BY4741 test strain. In the *upf1Δ* strain, a difference in cell

number was also observed between the control and test cultures however the difference in cell number was not as extreme and at t = 9 hrs there were ~ 1.9 x as many cells in the *upf1Δ* control strain relative to the test strain over-expressing Rnq1p.

Thus, it appears that Rnq1p over-expression does manifest a negative effect on cell growth however since the *upf1Δ* suppressed Rnq1p toxicity, the negative effect that Rnq1p had on cell number was not significant.

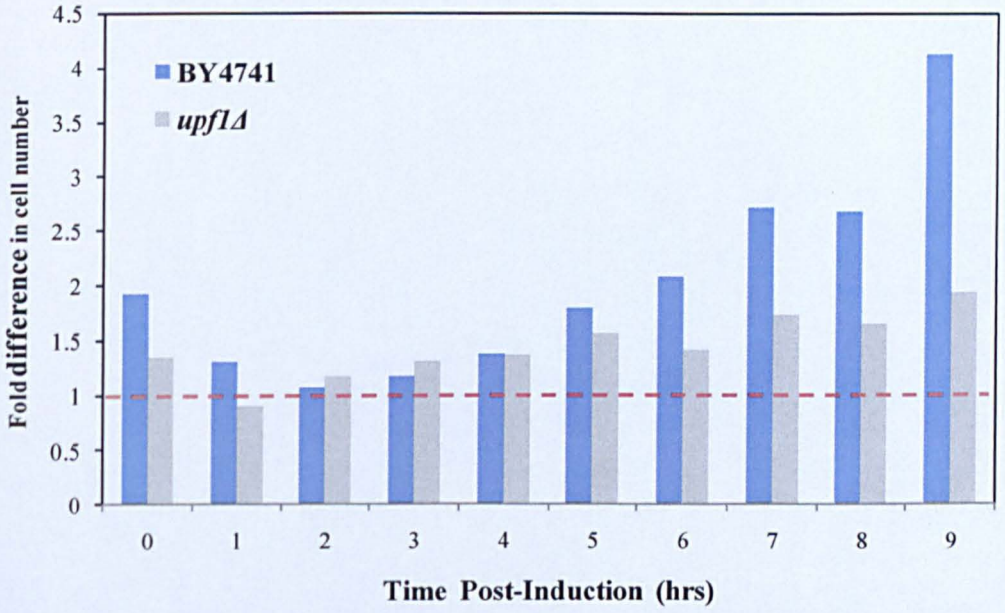

Figure 6.7 Rnq1p over-expression causes a greater growth defect in *UPF1*$^+$ compared to a *upf1Δ* strain.
The fold difference in cell number of a BY4741(*UPF1*$^+$) strain transformed with either pYES2 (control) or pYES2-*RNQ1* (test) is plotted alongside the fold difference in cell number for a *upf1Δ* control and test strain, with cell number determined at the indicated times. At t=9 hrs, the BY4741 strain has ~4.1 x fold more cells in the control relative to the test strain. At t= 9hrs in the *upf1Δ* strain the effect is less severe and amounts to ~ 1.9 x fold increase in cell number for the pYES2 control strain relative to the test strain over-expressing Rnq1p.

The same aliquots were also analysed for cell size differences. Previously it was shown that Rnq1p over-expression caused an increase in cell size relative to the cell size seen in the pYES2 control strain (section 5.1.3). The relationship between

Rnq1p over-expression and cell size seen in the *upf1Δ* strain was very different to that seen in the parental *UPF1*$^{+}$ BY4741 strain (figure 6.8). The *upf1Δ* showed a large cell phenotype, since cell size increased throughout the experiment for the *upf1Δ* + pYES2 control strain. Thus relative to the behaviour of the *upf1Δ* control strain, Rnq1p over-expression did not result in an increase in cell size.

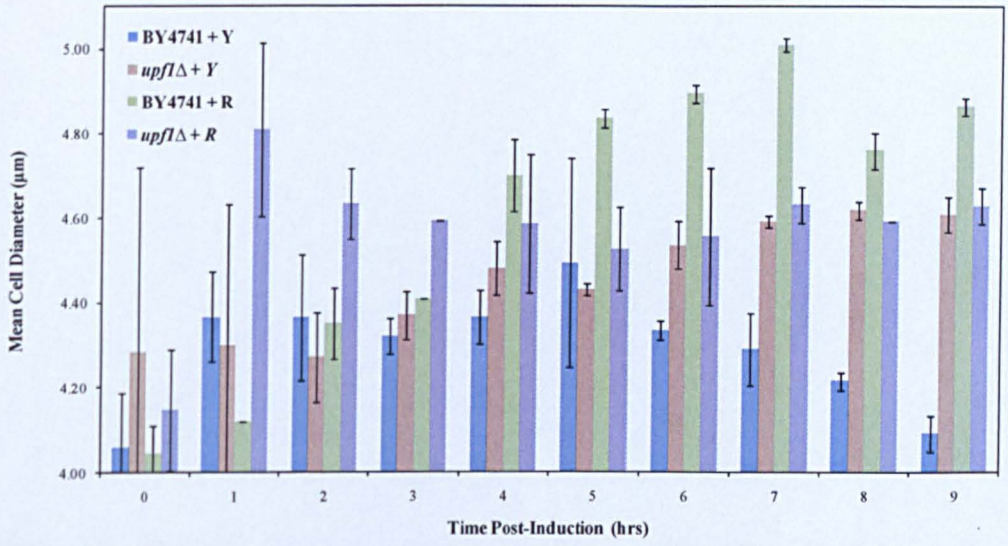

Figure 6.8 Rnq1p over-expression in a *upf1Δ* strain does not result in an increase of cell size.
At the indicated times following pYES2-*RNQ1* induction, the effect of Rnq1p (+R) over-expression on cell size is determined in the BY4741 parental and *upf1Δ* strain, relative to their respective pYES2 (+Y) transformed control strains. While Rnq1p over-expression in BY4741 increases cell size, there is no effect on cell size in the *upf1Δ* strain. It is notable that the cell size of the control *upf1Δ* strain appears to be larger than that seen for the control BY4741 strain.

In addition, cells were taken from each of the obtained aliquots, counted, diluted and transferred to a glucose-based selective minimal medium to obtain an expected number of colony forming units. The purpose of this assay was to establish whether Rnq1p over-expression was cytotoxic to the cell, in which case the difference between expected and observed colonies on the plates would increase with each time point, or whether Rnq1p was cytostatic, in which case the difference between expected and observed colonies on the plate would remain relatively constant throughout the experiment.

Compared to the results obtained previously for Rnq1p over-expression in BY4741, there was no loss of cell viability with Rnq1p over-expression in the *upf1Δ* strain. Thus, despite Rnq1p appearing to negatively affect cell growth, albeit it considerably less so than in the BY4741 parental strain, this did not reflect a loss of cell viability, as seen in BY4741 (figure 6.9).

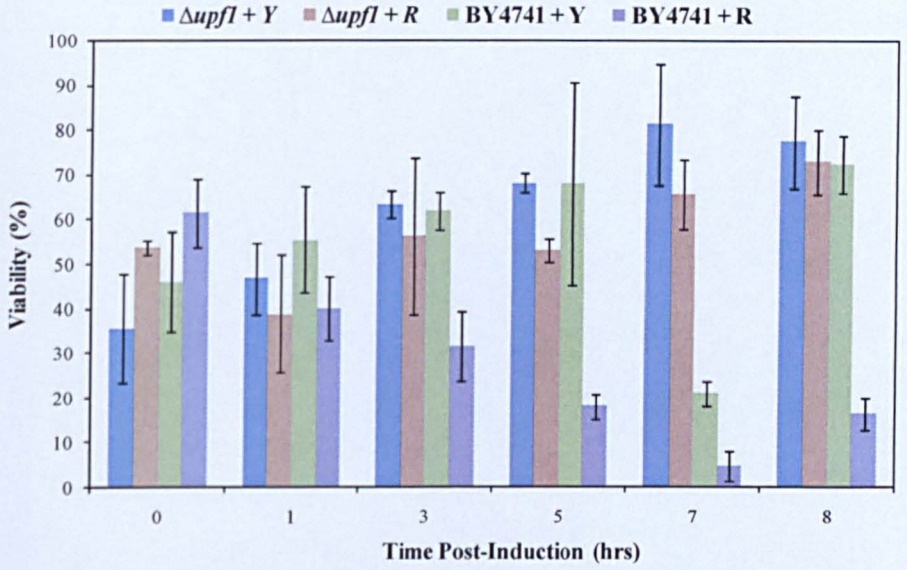

Figure 6.9 Rnq1p over-expression in a *upf1Δ* strain does not result in reduced cell viability.

The effect of Rnq1p (+R) over-expression on cell viability in the BY4741 and *upf1Δ* strain was tested by counting, diluting and plating aliquots taken from the control (+Y) and test (+R) cultures at the indicated times post Rnq1p induction. The difference between the expected and observed number of colony forming units (CFU) is plotted as a percentage. Rnq1p over-expression in the BY4741 strain results in an increasing loss of cell viability with duration of Rnq1p induction. There appears to be no change in cell viability associated with Rnq1p over-expression in the *upf1Δ* strain.

6.2 Genetic modifiers of Rnq1p and 103Q toxicity

The potential for overlapping components in the Rnq1p and 103Q toxicity pathways was suggested by (a) the suppression of both Rnq1p and 103Q toxicity by the *upf1Δ* strain (discussed in section 6.1), (b) by a shared detrimental effect of both Rnq1p and 103Q over-expression on mitochondrial respiratory capacity, and (c) by the unifying

features of being glutamine rich and nucleocytoplasmic proteins. Thus, with the publication of 28 gene deletions (Table 6.1) that suppressed 103Q toxicity it was of great interest to identify whether any of the same deletions would also suppress Rnq1p toxicity(Giorgini *et al.*, 2005).

6.2.1 Identifying potential genetic modifiers Rnq1p and 103Q toxicity

Most of the 28 deletion strains identified in the Giorgini study (Giorgini *et al.*, 2005), with the exception of *yir454wΔ* and *ymr082cΔ*, were transformed with the pYES2 (control) vector backbone and the pYES2-*RNQ1* (test) vector to determine the toxicity of Rnq1p within these deletion strains. The *hsp104Δ* and *rnq1Δ* deletion strains were not included in this screen since their suppression of Rnq1p toxicity is well established.

Of the 24 deletion strains tested, 11 were found to suppress Rnq1p toxicity (figure 6.1), and a further 2, *def1Δ* and *arg7Δ*, showed reduced toxicity of Rnq1p. Following completion of this toxicity screen, a study of [*PIN*$^+$] presence in the Yeast Knock-out Collection was published (Manogaran *et al.*, 2010). Cross-referencing the list of strains identified as [*pin*$^-$] by the Liebman/Manogaran study with those presented as suppressors of 103Q toxicity in the (Giorgini *et al.*, 2005)Giorgini study revealed that 13 of the original 28 strains were [*pin*$^-$].

Since presence of the [*PIN*$^+$] prion is a pre-requisite for 103Q toxicity in yeast (Meriin, 2002), the 13 identified [*pin*$^-$] deletion strains were no longer informative in terms of understanding mechanisms of 103Q toxicity in the cell. Those strains identified as [*pin*$^-$] are indicated in table 6.1.

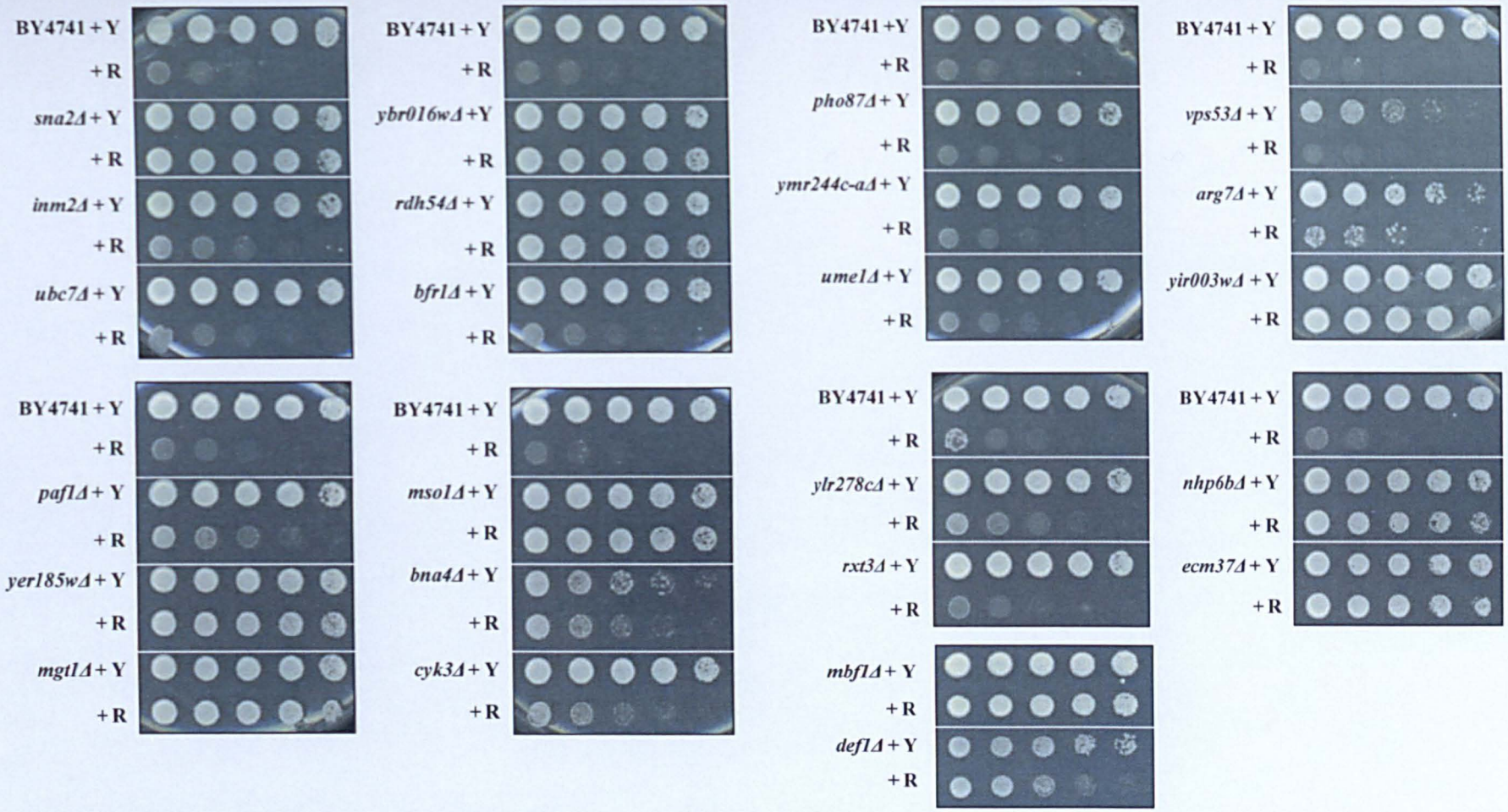

Figure 6.10: Proteotoxicity screen for genetic modifiers of Rnq1p toxicity.

Deletion strains previously identified as suppressing 103Q toxicity were screened for their effects on Rnq1p-mediated toxicity. Abbreviations: R = pYES2-*RNQ1*; Y = pYES2.

Deletion	Systematic Name	Liebman screen
bfr1Δ	YOR198C	
cyk3Δ	YDL117W	[*pin*$^-$]
def1Δ	YKL054C	
mso1Δ	YNR049C	[*pin*$^-$]
sna2Δ	YDR525W-A	[*pin*$^-$]
vps53Δ	YJL029C	
mbf1Δ	YOR298C-A	[*pin*$^-$]
nhp6bΔ	YBR089C-A (90C-A)	[*pin*$^-$]
paf1Δ	YBR279W	
rxt3Δ	YDL076C	
ume1Δ	YPL139C	
rnq1Δ	YCL028W	[*pin*$^-$]
arg7Δ	YMR062C	
bna4Δ	YBL098W	

Deletion	Systematic Name	Liebman screen
ecm37Δ	YIL146C	[*pin*$^-$]
hsp104Δ	YLL026W	[*pin*$^-$]
mgt1Δ	YDL200C	[*pin*$^-$]
pho87Δ	YCR037C	
rdh54Δ	YBR073W	[*pin*$^-$]
inm2Δ	YDR287W	mixed
pug1Δ	YER185W	[*pin*$^-$]
smy2Δ	YBR172C	
aim21Δ	YIR003W	[*pin*$^-$]
Δ	YIR454W	
Δ	YMR082C	mixed
Δ	YMR244C-A	
Δ	YLR278C	
Δ	YBR016W	[*pin*$^-$]

Table 6.1: Deletion strains identified as [*pin*$^-$].
Deletion strains from the Giorgini study (Giorgini *et al.*, 2005) that were identified as [*pin*$^-$] in the Manogaran/Liebman study (Manogaran *et al.*, 2010) indicate that only 13(±2) of the 28 are biologically significant.

Additional to the 13 deletion strains that were identified as [*pin*$^-$], 2 further deletion strains were identified as containing a mixed population of cells (Manogaran *et al.*, 2010) – meaning that some cells harboured the [*PIN*$^+$] prion while others were [*pin*$^-$], and therefore an analysis of these particular strains was likely to have variable consequences. The mixed deletion strains are also indicated in table 6.1.

Consequently, of the 11 (of 24 tested) deletion strains that were found to suppress Rnq1p toxicity, 10 were [*pin*$^-$] (Table 6.2). Since Rnq1p toxicity, like 103Q, requires the presence of the [*PIN*$^+$] prion, these 10 deletion strains cannot be used to infer knowledge about Rnq1p function or toxicity. The remaining 1 deletion strain, *bna4Δ* (of the original 11), was the only clear suppressor of Rnq1p toxicity that was not also identified as [*pin*$^-$]. Thus, this study identified 1 suppressor of Rnq1p toxicity, *bna4Δ*, and two deletion strains where Rnq1p toxicity was reduced: *arg7Δ* and *def1Δ*.

Of the 13 deletion strains identified in Table 6.1 as [*pin*$^-$], only 10 of these strains have thus far been referred to since they were among the 11 found to suppress Rnq1p toxicity (only 1 of the 11 suppressors was actually [*PIN*$^+$]); the remaining 3 [*pin*$^-$] deletion strains include the *rnq1Δ* and *hsp104Δ* strains and the deletion strain *cyk3Δ*. In this study, *cyk3Δ* did not suppress Rnq1p toxicity, though it did suppress 103Q

toxicity. Therefore, if *cyk3Δ* is [*pin*$^-$], it suggests that Rnq1p toxicity is enhanced by this deletion strain, such that Rnq1p toxicity becomes [*PIN*$^+$]- independent. Alternatively, if the *cyk3Δ* strain is [*PIN*$^+$], it suggests this strain is a suppressor of 103Q toxicity.

Non-toxic and predicted [*pin*$^-$]	Toxic and predicted [*pin*$^-$]
sna2Δ, yer185wΔ, ecm37Δ, ybr016wΔ, mgt1Δ, yir003wΔ, nhp6bΔ, mbf1Δ, mso1Δ, rdh54Δ	*cyk3Δ, inm2Δ**
Non-toxic, presumed [*PIN*$^+$]	**Toxic, presumed [*PIN*$^+$]**
bna4Δ	*bfr1Δ, paf1Δ, pho87Δ, ymr244c-aΔ, ume1Δ, vps53Δ, arg7Δ*, ylr278cΔ, rxt3Δ, def1Δ**
Not tested	
yir454wΔ, ybr082cΔ	

Table 6.2: Summary of deletion strains and their interaction with Rnq1p. The *bna4Δ* was the only [*PIN*$^+$] strain found to suppress Rnq1p toxicity. The [*pin*$^-$].*cyk3Δ* strain enhanced Rnq1p toxicity.

Finally, of the two deletion strains found to contain a mixed population of cells, one was not tested (*ybr082cΔ*) while Rnq1p was found to be toxic in the other (*inm2Δ*). Since the *inm2Δ* strain also showed suppression of 103Q toxicity in the Giorgini study (Giorgini *et al.*, 2005), it is possible that the *inm2Δ* strain isolate used in this study was [*PIN*$^+$] and the *inm2Δ* strain isolate used in the Giorgini study (Giorgini *et al.*, 2005) was [*pin*$^-$].

6.2.2 Extended analysis for potential Rnq1p and/or poly-Q toxicity modulators

Following on from this study, a large number of deletion strains were selected for screening either due to a predicted or confirmed functional link to Rnq1p, or due to their identification in a screen for modulators of expanded Huntingtin toxicity in *Drosophila* (Zhang, 2010). The latter selection of deletion strains were of particular interest since any deletion strain capable of suppressing both Huntingtin toxicity in

Drosophila and Rnq1p toxicity in yeast would indicate the existence of conserved proteins or pathways with a general role in handling toxic amyloid or polyglutamine toxicity within the eukaryotic cell. Additionally, all deletion strains tested were cured to the [*pin*$^-$] state by consecutive passages on plated with 5 mM GdHCl and the assay repeated. The utility of this was to reveal modulators of toxicity whose effect could be masked by the presence of the [*PIN*$^+$] prion.

[*PIN*$^+$] Deletion Strains

Not Toxic		Less Toxic	
Rnq1p	103Q	Rnq1p	103Q
bna4	*tor1*	*arg7*	*nhp6b*
ecm37	*hsp104*	*def1*	*paf1*
get2	*ybr016*	*hrp1*	*pde1*
get3	*mso1*	*hsp82*	*mbf1*
hsp104	*smy2*	*lsm7*	*ubc1*
mbf1	*sna2*	*ptc2*	*isy1*
mgt1	*ecm37*	*tor1*	*get4*
mso1	*bna4*	*upf2*	*nup84*
nhp6b	*yer185w*	*paf1*	*sod2*
rdh54	*rdh54*	*ylr278c*	
rnq1	*yir003w*	*sfp1*	
sna2	*arg7*	*ppz1*	
upf1	*atp5*	*dcp2*	
ybr016w	*snf2*		
yir003w	*upf1*		
yer185w	*upf2*		
	dcp2		
	shs1		
	nup170		
	kar2		
	mgt1		
	stp22		
	bfr1		
	not1		
	grx2		
	tom1		
	end3		
	rnq1		

[*pin*$^-$] Deletion Strains

Toxic		Slightly Toxic	
Rnq1p	103Q	Rnq1p	103Q
atp5	*bna4*	*arg7*	*aat2*
bna4	*bub3*	*get2*	*ume1*
ccr4	*ccr4*	*dnm1*	*wwm1*
swi3	*sfp1*	*end3*	*snf2*
pop2	*swi3*	*nth1*	*get1*
sfp1	*xrn1*	*sod2*	*nup170*
snf2	*ypt31*	*sse1*	*nup84*
ymr082c	*zap1*	*ume1*	*ppn1*
	rxt3	*nup170*	*rpn10*
	atp5	*nhp6b*	*vps53*
	get3	*ycr051w*	*bub1*
			get2

Shared [*PIN*$^+$] Deletion Strains

Not Toxic	Less Toxic	MIX
bna4	*paf1*	*tor1*
upf1		*upf2*
		dcp2

Shared [*pin*$^-$] Deletion Strains

Toxic	Slightly Toxic	MIX
atp5	*ume1*	*snf2*
bna4	*nup170*	
ccr4		
swi3		
sfp1		

Table 6.3: Genetic modifiers of Rnq1p and 103Q toxicity.
Summary of deletion strains identified as either suppressing [*PIN*$^+$] dependent toxicity of Rnq1p and 103Q or causing [*pin*$^-$] toxicity of Rnq1p and 103Q. The inset table lists deletions with overlapping effects on Rnq1p and 103Q toxicity.

The full list of deletion strains tested is given in Appendix 1. Those deletion strains that either suppressed or enhanced Rnq1p or 103Q toxicity are summarised in table

6.3, and the results of the screen were analysed in terms of their gene ontology classifications.

Since the tested deletion strains were chosen based on their identification as modifiers of aggregation and toxicity or due to a possible functional link with Rnq1p, rather than any means based on protein abundances, the frequency of gene ontology terms associated with the suppressors or enhancers were deemed directly significant and were not considered according to the genome frequency of those terms. However, the frequency of terms associated with the suppressors/enhancers can be considered relative to the frequency of terms associated with the entire group of tested deletion strains, and deviations from the expected distribution would be considered increasingly significant, since this represents enrichment within an already non-random group.

6.2.3 Suppressors of Rnq1p and Huntingtin toxicity

After excluding those genes identified in the Liebman/Manogaran study (Manogaran *et al.*, 2010) as [*pin*$^-$], only two deletion strains of the 113 tested (Appendix 1) showed full suppression of Rnq1p toxicity in the [*PIN*$^+$] state, and these were previously mentioned: *bna4Δ* and *upf1Δ* (Table 6.3). There is no functional overlap between the products of these two genes, therefore the GO analysis of Rnq1p suppressors includes both the two toxicity-suppressing deletion strains and the 13 deletion strains (*arg7Δ, def1Δ, hrp1Δ, hsp82Δ, lsm7Δ, ptc2Δ, tor1Δ, upf2Δ, paf1Δ, ylr278cΔ, sfp1Δ, ppz1Δ* and *dcp2Δ*) that showed a reduction in Rnq1p toxicity.

Suppressors of 103Q toxicity in the [*PIN*$^+$] background were greater in number than that seen for Rnq1p. Discovered in this study were 13 deletion strains that suppressed 103Q toxicity (*tor1Δ, atp5Δ, snf2Δ, upf1Δ, upf2Δ, dcp2Δ, shs1Δ, nup170Δ, kar2Δ, stp22Δ, not1Δ, grx2Δ, tom1Δ*, and *end3Δ*), and 6 further deletion strains showed a reduction in 103Q-toxicity (*pde1Δ, ubc1Δ, isy1Δ, get4Δ, nup84Δ*, and *sod2Δ*) (Table 6.3). Interestingly, of the original 28 deletion strains found to suppress 103Q toxicity (Giorgini *et al.*, 2005), while 13 were [*pin*$^-$] and 2 were mixed [*PIN*$^+$]/[*pin*$^-$] as mentioned, 6 were found not to suppress 103Q toxicity in this study (*vps53Δ, rxt3Δ, ume1Δ, pho87Δ, 244Δ* and *278Δ*), 4 were confirmed in

their suppression of 103Q (*arg7Δ, bfr1Δ, smy2Δ, paf1Δ,* and *bna4Δ*), one showed partial suppression of toxicity (*paf1Δ)* and 4 were not tested for 103Q toxicity (*ymr244c-aΔ, ymr082cΔ, def1Δ* and *inm2Δ*). Therefore in total, 18 suppressors of 103Q toxicity and 7 partial suppressors of toxicity were identified.

The deletion strains that reduced and fully suppressed Rnq1p toxicity were analysed for enrichment of particular gene ontology ('GO') terms, as were those deletion strains that reduced and fully suppressed the toxicity of 103Q toxicity.

6.2.3.1 Suppressors of Rnq1p and 103Q [*PIN*$^+$] toxicity: GO Process

The GO processes represented by the suppressors of Rnq1p and 103Q toxicity are identified in figure 6.11. There are a number of processes enriched in both sets, which are also enriched relative to the genome frequency (gf): RNA metabolic process (gf=18.6%) is the most significant term for suppressors of both Rnq1p and 103Q toxicity, response to stress (9.2%) and transcription (gf=9.6%) are also highly enriched along with ribosome biogenesis (gf=6.5%), and protein modification process (gf=8.7%).

Individually, chromosome organisation appears to be uniquely significant for Rnq1p (gf=6.2%), and DNA metabolic process is also enriched (gf=6.3%). For suppressors of 103Q toxicity, the process of transport (gf=16.3%) is particularly enriched, followed by processes such as cell cycle (gf=8.3%), response to chemical stimulus (gf=5%), cellular membrane organisation (gf=4.4%), vesicle mediated transport (gf=5.6%) and nucleus organisation (gf=1%).

Therefore, there exist processes that appear similarly important for both Rnq1p and 103Q toxicity mechanisms, but there are also processes unique to each protein, that may reflect differences in upstream events prior to a general toxicity mechanism, or possibly relate to the cellular functions of the proteins

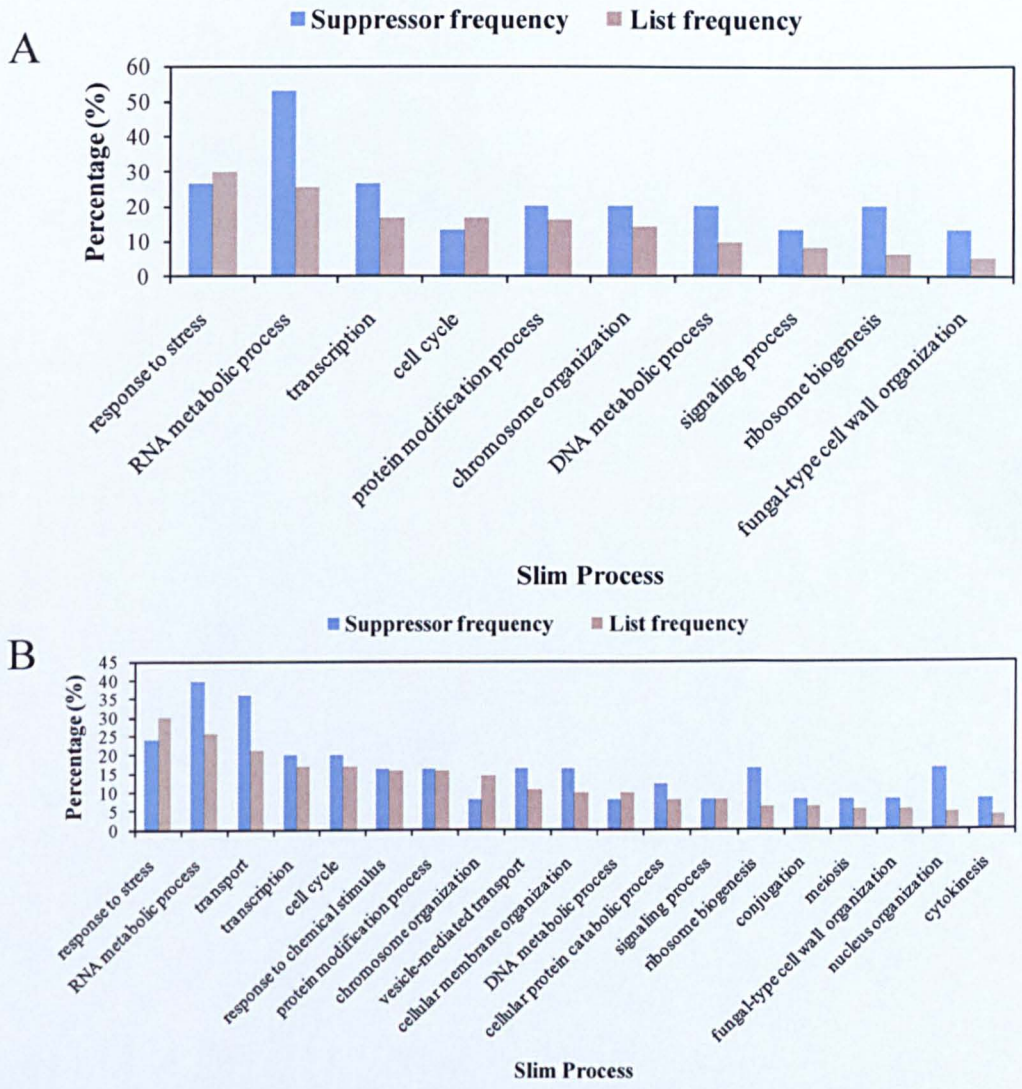

Figure 6.11: Gene ontology SlimProcess analysis of Rnq1p and 103Q toxicity suppressors.
A) Rnq1p specific suppressors, 15 genes. B) 103Q-specific suppressors, 25 genes.

6.2.3.2 Suppressors of Rnq1p and 103Q [*PIN*$^+$] toxicity: GO Functions

The GO function terms that are enriched for both the suppressors of Rnq1p and the suppressors of 103Q (figure.6.12) include: hydrolase activity (gf=13.1%), protein binding (gf=9.7%) and transferase activity (gf=11.4%).

GO function terms that are significant for suppressors of Rnq1p toxicity include RNA binding (gf=10.9%), DNA binding (gf=5.4%), transcription regulator (gf=5%)

and phosphoprotein phosphatase activity (gf=0.8%). The GO function terms that are significant for suppressors of 103Q toxicity are oxidoreductase activity (gf=4.3%) and structural molecule activity (gf=5.6%).These functions may therefore play roles in mediating the toxicity of Rnq1p and/or 103Q since a deterioration in these activities resulted in suppression of Rnq1p and/or 103Q toxicity.

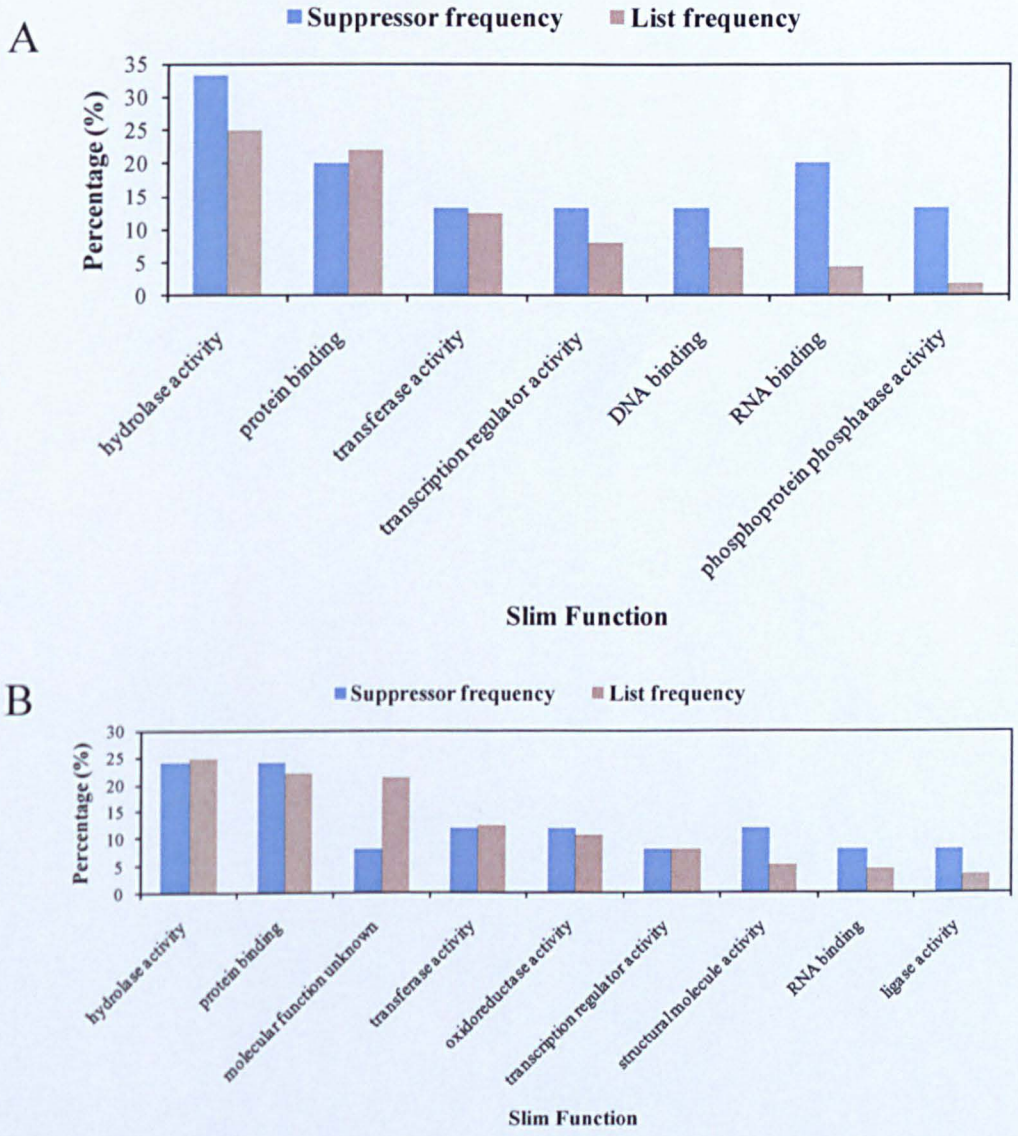

Fig 6.12 Gene ontology SlimFunction analysis of Rnq1p and 103Q toxicity suppressors

A) Rnq1p specific suppressors, 15 genes. B) 103Q-specific suppressors, 25 genes

6.2.3.3 Suppressors of Rnq1p and 103Q [*PIN*$^+$] toxicity: GO Components

The GO component term most represented by the suppressors of both Rnq1p and 103Q (figure 6.13) toxicity was cytoplasm (gf=60%). The nucleus component (gf=32.8%) is more abundant for Rnq1p suppressors at 66.7 % than it was for 103Q suppressors, at 36 %. Additionally, the membrane component was more abundant for suppressors of 103Q toxicity, at 30 %, than it was for suppressors of Rnq1p toxicity, at 20 %. The mitochondria (gf=17.7%) and the plasma membrane (gf=4.5%) are

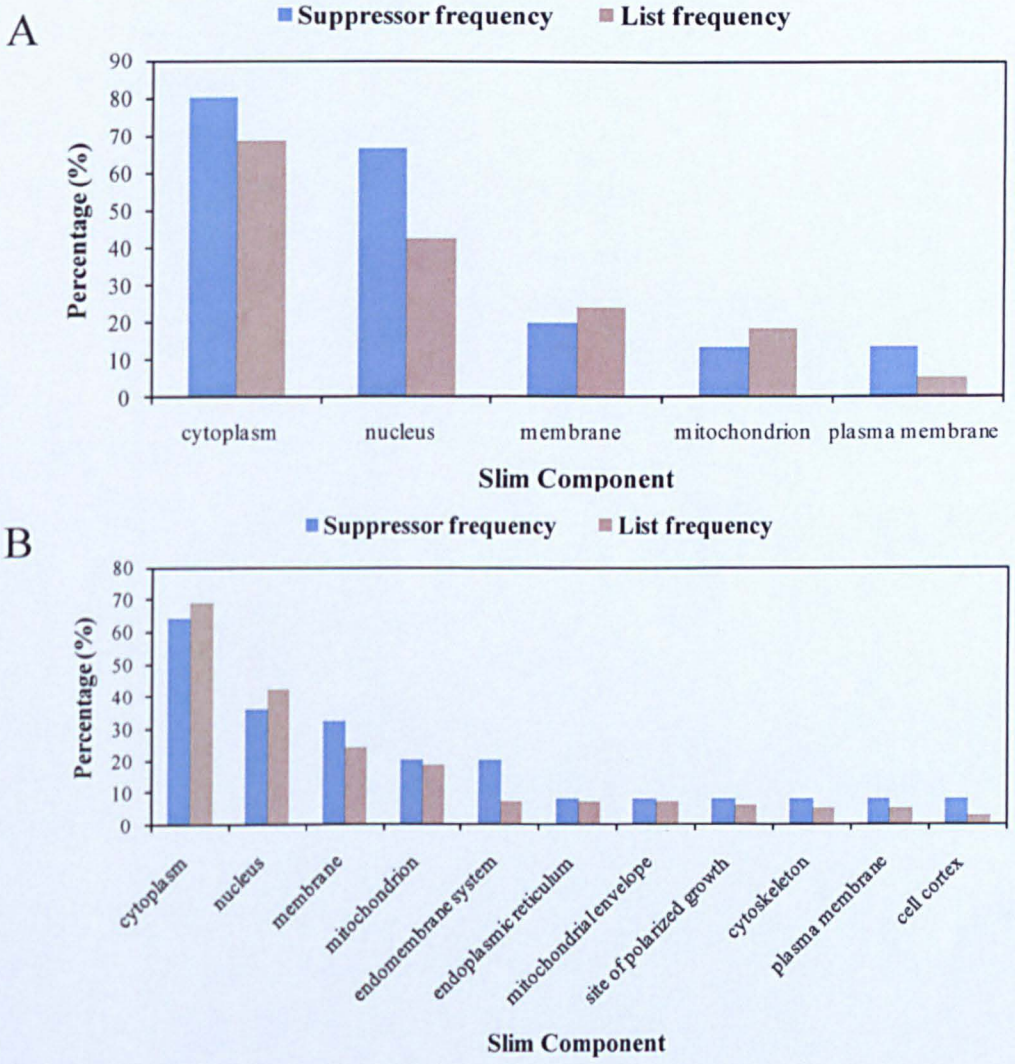

Fig 6.13: Gene ontology SlimComponent analysis of Rnq1p and 103Q toxicity suppressors
A) Rnq1p specific suppressors, 15 genes. B) 103Q-specific suppressors, 25 genes

represented GO component terms of both Rnq1p and 103Q suppressors, though the mitochondrial component was more significant for 103Q suppressors, as was the endomembrane component term which was unique and highly enriched in the 103Q suppressors.

6.2.4 Enhancers of Rnq1p and Huntingtin toxicity

The yeast strain BY4741 is a [*PIN*$^+$] strain, and since this is also the strain in which all of the gene deletions tested here were made, they should also be [*PIN*$^+$]. However, as revealed by the study of Manogaran/Liebman (Manogaran *et al.*, 2010), some of the deletion strains were identified as [*pin*$^-$]. The significance of this for the current study is that the toxicity of Rnq1p and 103Q depends upon the presence of the [*PIN*$^+$] prion (Meriin *et al.*, 2002; Douglas *et al.*, 2009b) and therefore in strains that are [*pin*$^-$], toxicity would not occur and the consequences of such deletions on [*PIN*$^+$]-mediated Rnq1p and 103Q toxicity would remain undetermined. Yet in some deletion strains that are [*pin*$^-$], toxicity was observed when Rnq1p and 103Q were over-expressed, suggesting that 1) cellular changes can give rise to [*PIN*$^+$] 'substitutes' that serve as [*PIN*$^+$], or 2) removal of certain cellular components that would otherwise serve as barriers to aggregation or protein toxicity lead to these events, or 3) destabilising the toxic protein by removal of interacting partners can lead to [*PIN*$^+$]-independent aggregation of the toxic protein. Thus, since toxicity of Rnq1p and 103Q in the [*pin*$^-$] state was another source of information about the toxicity mechanism of Rnq1p and 103Q, the deletion strains were also tested in the cured, [*pin*$^-$] state.

Surprisingly, there were more deletion strains that enhanced the toxicity of Rnq1p and 103Q in the [*pin*$^-$] state then there were deletion strains that suppressed or reduced the toxicity of Rnq1p and 103Q in the [*PIN*$^+$] state. This suggests that many phenotypes associated with gene deletions, at least in terms of protein aggregation pathways, were masked by the presence of the [*PIN*$^+$] prion.

Two levels of toxicity enhancers were noted, those that enhanced toxicity causing a growth defect similar to that observed when Rnq1p is over-expressed in a [*PIN*$^+$] background, and those that enhanced toxicity to cause a slight growth defect when

Rnq1p or 103Q was over-expressed. Since the number of enhancer strains causing toxicity or slight toxicity of Rnq1p was greater than the number of suppressors of Rnq1p, it was possible to analyse the enhancer group independently of the slight toxicity enhancers; this had not been possible for suppressors of Rnq1p since only 2 deletion strains showed full suppression and therefore suppressors and less toxic [*PIN*$^+$] deletion strains were analysed together.

6.2.4.1 Enhancers of Rnq1p and 103Q toxicity: GO Processes

Analysis of the set of gene deletions that significantly enhanced the toxicity of Rnq1p and 103Q (figure.6.14, panel A and B respectively) (i.e. [*PIN*$^+$]-independent toxicity) revealed many of the same GO terms that had also been abundant in the deletion group for [*PIN*$^+$] toxicity suppressors. Specifically, RNA metabolic process and transcription were the two process terms most represented by the enhancer deletions, as had been observed for the suppressor deletions (section 6.2.3.1). However, while RNA metabolic process was of similar abundance for both the suppressor and enhancer deletions, the transcription term was 2-3x more abundant for the enhancers than it was for the suppressors.

As observed for the Rnq1p toxicity suppressors, chromosome organisation and DNA metabolic GO process terms were enriched for the enhancer deletions. Similarly, the cell cycle process term was enriched in the 103Q enhancers set as it had been in the suppressors set, however also enriched for the 103Q enhancers was signalling process (gf=3.7%).

6.2.4.2 Enhancers of Rnq1p and 103Q toxicity: GO Functions

The GO function terms associated with the enhancer deletion strains showed overlapping significance with the suppressor deletion strains for hydrolase activity.

Common to both Rnq1p and 103Q (figure 6.15, panel A and B respectively) toxicity enhancers were the function terms transcription regulator activity, DNA binding and molecular function unknown.

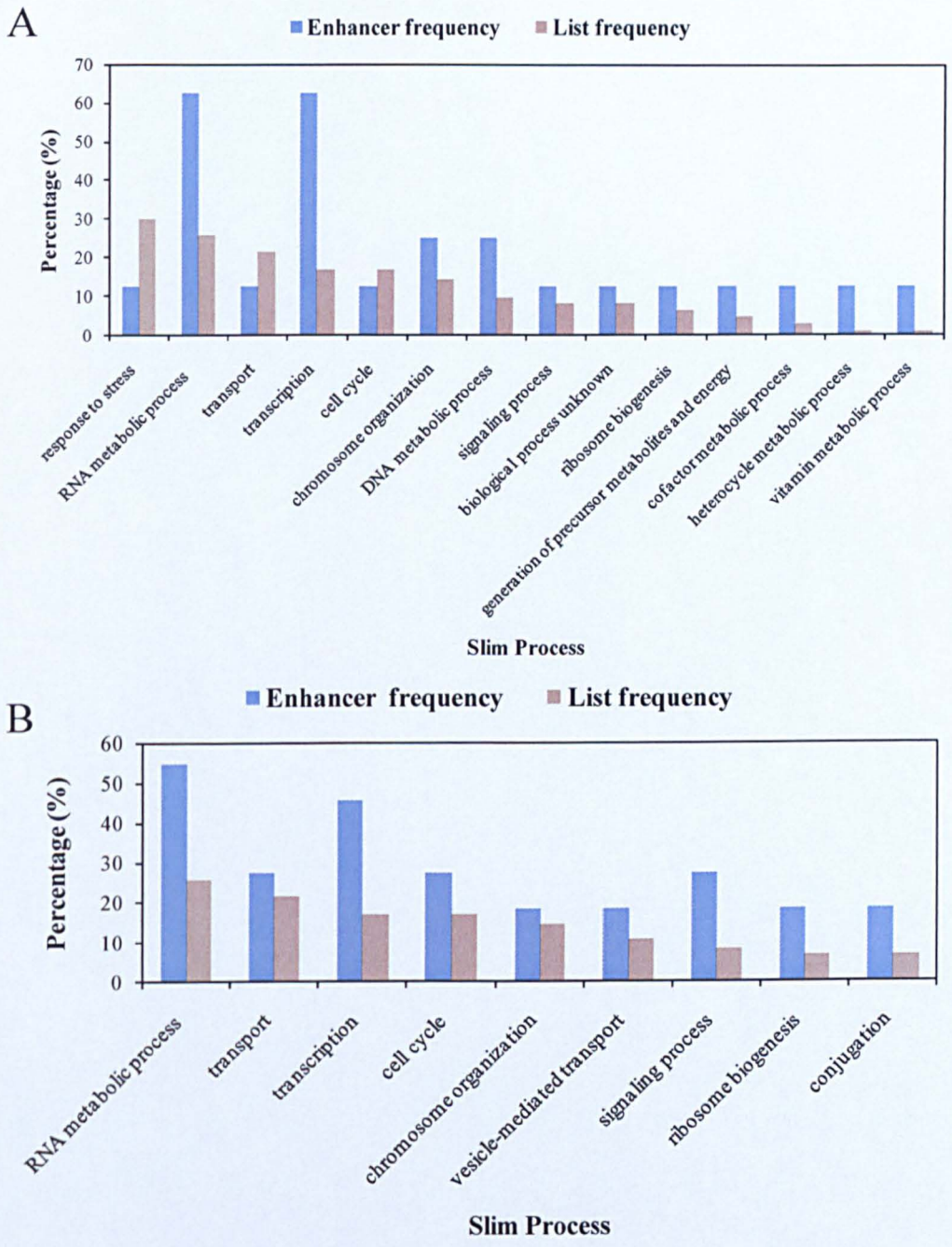

Figure 6.14: Gene ontology SlimProcess analysis of Rnq1p and 103Q toxicity enhancers

A) Rnq1p specific enhancers, 8 genes. B) 103Q-specific enhancers, 11 genes.

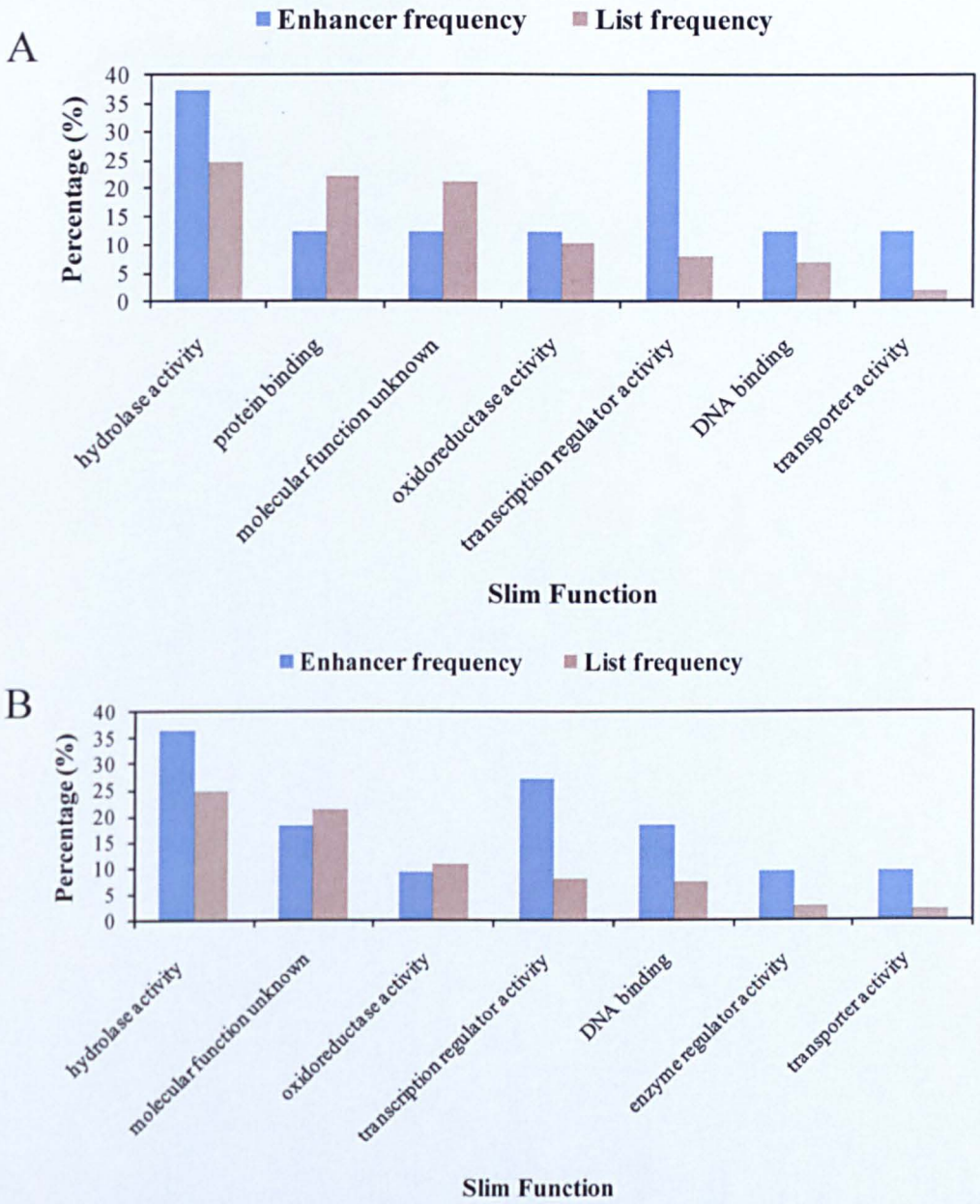

Figure 6.15: Gene ontology SlimFunction analysis of Rnq1p and 103Q toxicity enhancers

A) Rnq1p specific enhancers, 8 genes. B) 103Q-specific enhancers, 11 genes.

6.2.4.3 Enhancers of Rnq1p and 103Q toxicity: GO Components

GO component terms for the enhancer deletions of Rnq1p (figure 6.16, panel A) and 103Q (figure 6.16, panel B) showed significant overlap: the cytoplasm and nucleus each ~ 60 % abundant for both Rnq1p and 103Q enhancer sets. Additionally, the membrane, mitochondrion and mitochondrion envelope were each ~ 25 % abundant for both the Rnq1p and the 103Q suppressors.

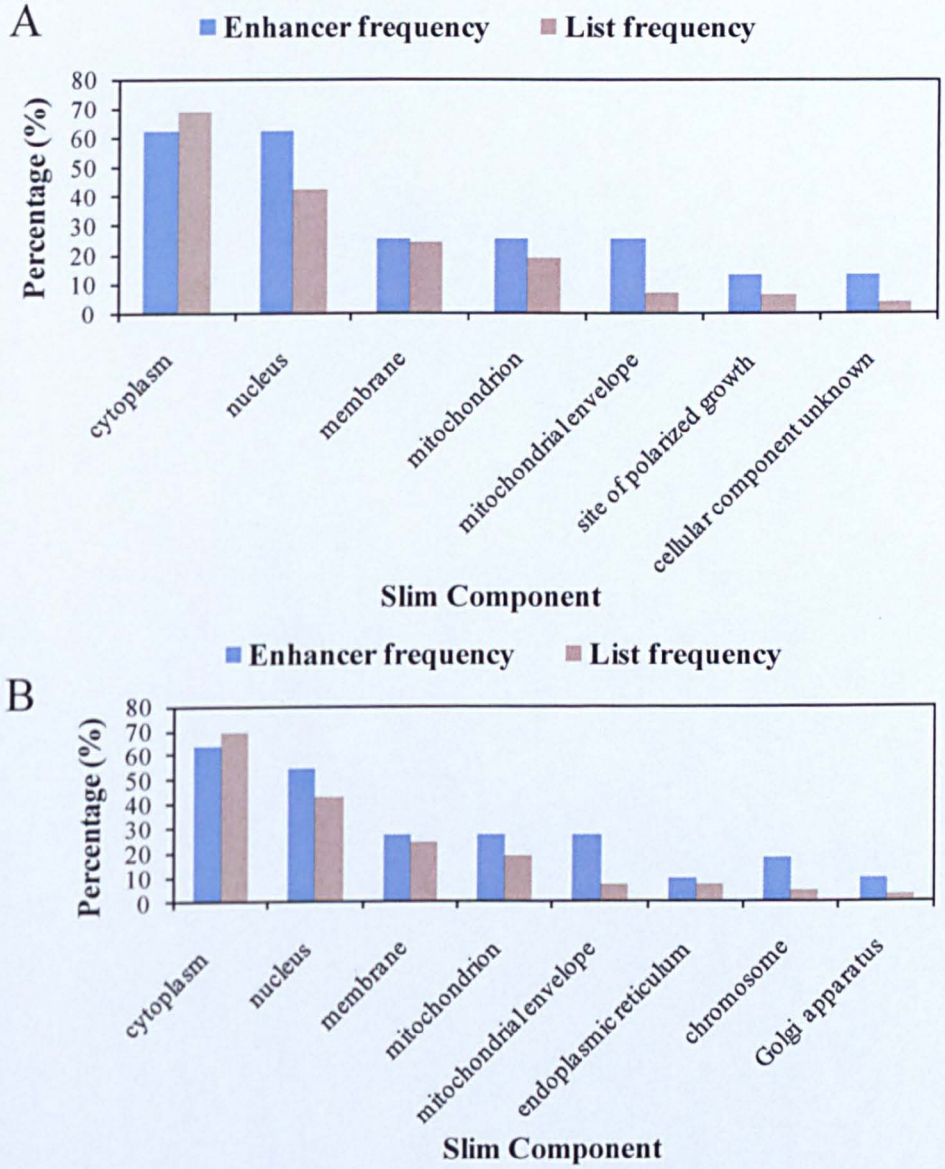

Figure 6.16 Gene ontology SlimComponent analysis of Rnq1p and 103Q toxicity enhancers

A) Rnq1p specific enhancers, 8 genes. B) 103Q-specific enhancers, 11 genes.

6.2.5 Pathway prediction: 103Q toxicity and the GET pathway

The GET proteins are a group of 5 proteins, (Get1p - Get5p), which target tail-anchored (TA) proteins for integration into the endoplasmic reticulum membrane (figure 6.17) (Rabu *et al.*, 2009). Get3p is a cytoplasmic protein that is believed to form a transmembrane-segment recognition complex with Get4p and Get5p, Get3p then shuttles the bound tail-anchored proteins to the heterodimer receptor formed by Get1p and Get2p located in the ER membrane. The precise role of Get4p and Get5p is not known but these proteins appear to form a complex that acts upstream of Get3p, and may involve transfer of certain TA-proteins to Get3p(Schuldiner *et al.*, 2005; Auld *et al.*, 2006; Schuldiner *et al.*, 2008; Chartron *et al.*, 2010).

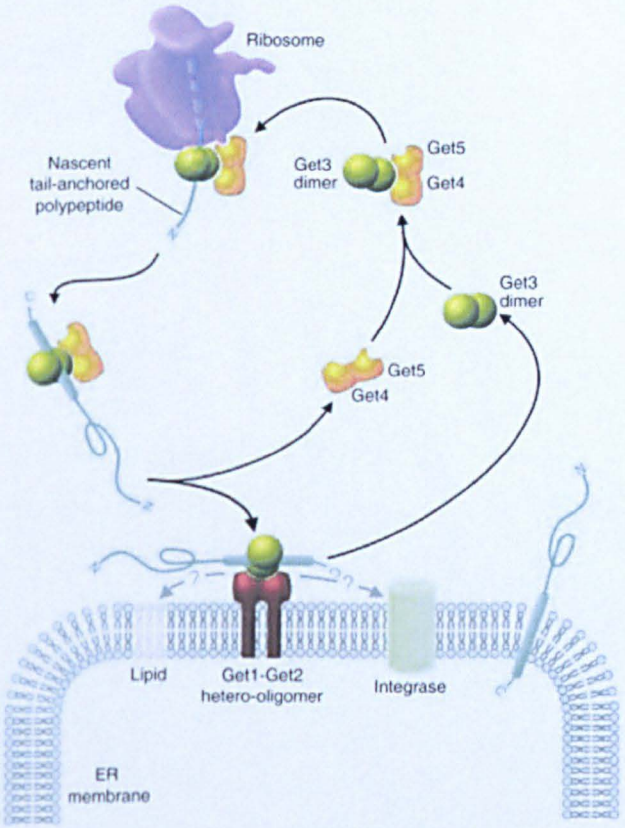

Figure 6.17: Activities and localisation of Get protein components of the GET pathway.
Get4p and Get5p associate with a Get3p dimer in the binding of tail-anchored proteins, which are then shuttled by Get3p to the ER-localised Get1p-Get2p receptor complex. Image from Rabu *et al* (Rabu *et al.*, 2009).

Two deletion strains, *get2Δ* and *get3Δ*, showed suppression of Rnq1p toxicity. After referring to the Manogaran *et al* (Manogaran *et al.*, 2010) list of identified [*pin*$^-$] strains, *get2Δ* and *get3Δ* were found to be amongst the [*pin*$^-$] population of deletion strains. Therefore, *get2Δ* and *get3Δ* would be expected to show suppression of Rnq1p toxicity, and 103Q toxicity, since the toxicity of Rnq1p and 103Q require the presence of the [*PIN*$^+$] prion (ref). Yet, the [*pin*$^-$] status of *get2Δ* and *get3Δ* did not result in suppression of 103Q toxicity, though 103Q was slightly rather than fully toxic in the *get2Δ* strain. This result would suggest that the [*pin*$^-$] *get2Δ* and *get3Δ* strains mediate some degree of 103Q [*PIN*$^+$]-independent toxicity.

Unfortunately, the *get2Δ* and *get3Δ* strains were not processed (passage on guanidine hydrochloride) and tested in the [*pin*$^-$] study, which would have confirmed the enhanced toxicity phenotype of *get2Δ* and *get3Δ*. However, if they are indeed [*pin*$^-$] then the *get2Δ* and *get3Δ* strains can be considered enhancers of 103Q toxicity. Further support for their [*pin*$^-$] status is the fact that when cured, *get1Δ* showed slight toxicity of 103Q. In contrast however, *get4Δ* was found to slightly reduce the toxicity of 103Q in a [*PIN*$^+$] state.

Overall, this result suggests that the absence of *get1Δ*, *get2Δ* and *get3Δ* leads to [*PIN*$^+$]-independent aggregation events allowing for 103Q toxicity. Additionally, since in the [*PIN*$^+$] state a *get4Δ* deletion reduces 103Q toxicity – it may suggest that Get4p has an important role in 'sorting' substrates for the GET pathway, redirecting into or away from the GET pathway as necessary. One could speculate that Get4p preferentially directs an unidentified substrate (possibly 103Q itself) away from the ER membrane possibly to the mitochondrial membrane (Ocampo *et al.*, 2010) and that this activity positively correlates with 103Q toxicity. Thus when Get4p is removed, the substrate can associate with Get3p to enter the GET pathway resulting in a reduction of 103Q toxicity. However, when Get1p, Get2p and Get3p are removed, the substrate is increasingly less likely to reach the ER membrane, and thus results in enhanced 103Q toxicity.

Little is known about the GET pathway and so the potential of the Fitness Database for identifying common interaction partners of GET proteins was explored. As described in material and methods section 2.16.2., chemical sensitivity profiles of gene deletions can be used to identify genes that encode proteins involved in similar

functions. By examining the common partners of each member of the GET pathway, it was possible to expand this pathway to include proteins immediately peripheral to the GET proteins (figure 6.18). The analysis identified Yer084w as a potential candidate for by-passing Get4p in delivering the hypothesised substrate (possibly 103Q) to Get3p in the absence of Get4p. Alternatively, Sgt2p has recently been shown to interact with Get4p/Get5p and also Ssa1p/Ydj1p for the transfer of TA-proteins to the ER membrane (Chang *et al.*, 2010); possibly Sgt2p cargo could be transferred to Get3p in the absence of Get4p. Interactions of Yer084w and Ypr170c with the GET pathway have yet to be examined.

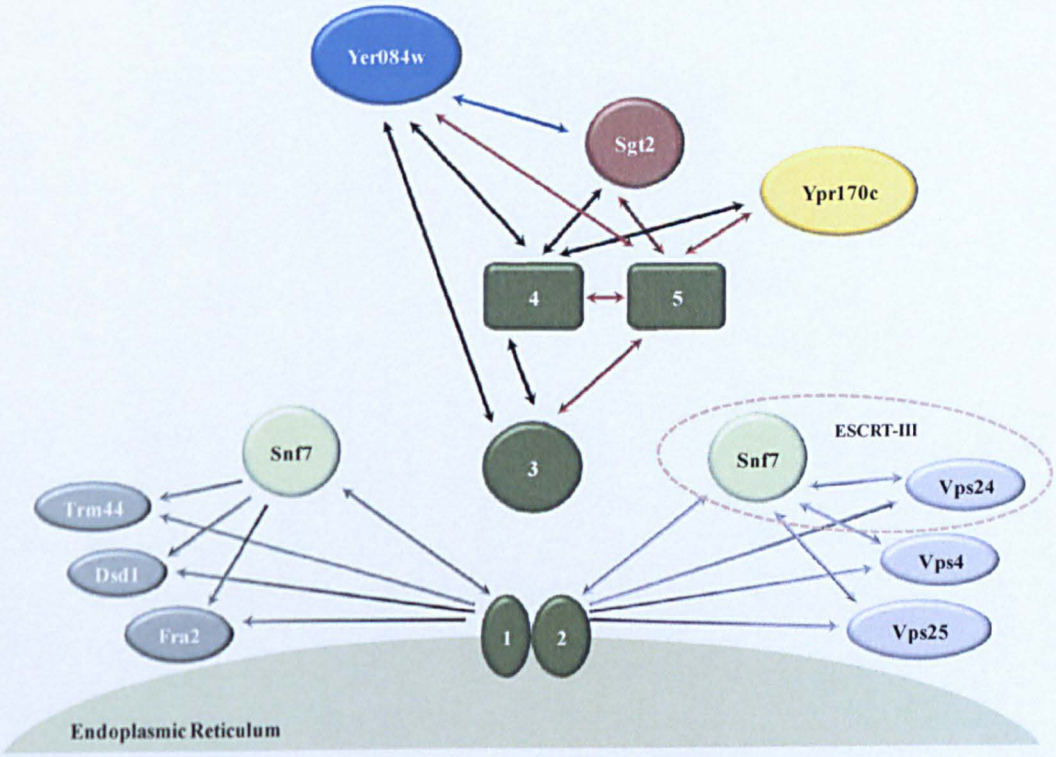

Figure 6.18: Extrapolated interaction pathway from Fitness Database interogation .

Pathway construction based on similarities in deletion strain chemical sensitivity profiles. Reciprocal clustering of genes indicated by bidirectional arrows, otherwise the arrow head points to the interactor, from the query gene. Protein encoded by YER084W shows significant interactions with the GET pathway and pathway outliers also identified through FD interrogation.

6.2.6 Genetic Modifiers Summary: Suppressors

The over-expression of Rnq1p or the Huntingtin (Htt) 103Q protein leads to proteotoxicity in yeast in a [*PIN*$^+$]-dependent manner (Meriin *et al.*, 2002). In this study, gene deletions that suppressed or reduced this toxicity were identified, along with gene deletions that enhanced the toxicity of Rnq1p and 103Q, such that these proteins became toxic in a [*pin*$^-$] background.

The deletion strain *bna4Δ* has previously been shown to suppress 103Q toxicity in yeast (Giorgini *et al.*, 2005). Bna4p encodes an enzyme of the mitochondrial kynurenine pathway (KP), which is required for tryptophan metabolism and is the major pathway in the cell for synthesis of NAD^+. Deletion of *BNA4* abolishes production of KP intermediates that are implicated in the pathology of Huntington disease (HD)(Giorgini *et al.*, 2005). The expression of mutant Htt appears to up-regulate KP by transcriptional dysregulation and therefore increases production of neurotoxic KP intermediates (Giorgini *et al.*, 2005)(Giorgini *et al.*, 2008). In this study, we discovered that *bna4Δ* not only also suppresses Rnq1p toxicity, but in a [*pin*$^-$] strain where over-expression of Rnq1p and 103Q is usually non-toxic, the absence of Bna4p in a *bna4Δ* strain resulted in toxicity of both Rnq1p and 103Q.

Similarly, deletion of *ATP5*, which encodes a subunit of the mitochondrial F1F0 ATP synthase and is required for ATP synthesis, also suppressed 103Q toxicity in a [*PIN*$^+$] strain but caused 103Q toxicity in a [*pin*$^-$] strain. The *atp5Δ* strain also enhanced Rnq1p toxicity in a [*pin*$^-$] strain, though it did not result in suppression of Rnq1p toxicity in a [*PIN*$^+$] strain.

The essential requirement for NAD^+ in the cell includes its use 1) as a contributor to energy (ATP) production, 2) as a cofactor for NAD^+ glycohydrolases for regulation of intracellular calcium, and 3) as a substrate for DNA-nick sensing polymerases and the class III histone deacetylases (HDAC), also known as sirtuins (Braidy *et al.*, 2009). The suppression of 103Q toxicity in the *bna4Δ* and *atp5Δ* strain may indicate a role for energy imbalance in HD. Specifically, it may be that the toxicity associated with up-regulated KP may not be limited to neurotoxic properties of KP intermediates, but may also be due to increased ATP production brought about by increased NAD^+ production. A reduction in KP activity in a *bna4Δ* strain would result in decreased availability of NAD^+ for ATP production, and ATP production

would also be impaired in an *atp5Δ* strain; in both instances suppression of 103Q toxicity is associated with a decrease in total cellular ATP. It has been observed that an early event in otherwise pre-symptomatic Huntington's Disease patients is the presence of a hyper-metabolic state (Mochel *et al.*, 2007); one could speculate that over-production of ATP might sustain or be causal for this condition and that a reduction in ATP availability would counter progression of HD.

Additionally, analysis of the *bna4Δ* and *atp5Δ* deletion strains in the Fitness Database (http:\\www.fitdb.stanford.org/) reveals that amongst the top 10 deletions strains showing similar chemical sensitivity profiles to *bna4Δ* and *atp5Δ* are components of the mitochondrial ribosome.

That the *bna4Δ* strain suppressed and enhanced Rnq1p toxicity as it did for 103Q toxicity suggests some overlap in the toxicity mechanism of Rnq1p and 103Q; it would be interesting to determine whether *bna4Δ* can suppress the toxicity of other disease associated polyglutamine proteins.

It is not clear however why the *bna4Δ* strain would suppress and enhance toxicity. One could speculate that when Rnq1p and 103Q are over-expressed in a [*pin*$^-$] cell, they may misfold, but there is no template to direct amyloid-specific misfolding and so the conformation they adopt is easily manageable for cellular chaperones. However, in low ATP conditions, chaperone activity may be limited and therefore Rnq1p and 103Q may overwhelm the capacity of the cell to degrade them, leading to disruption of proteohomeostasis and toxicity. In contrast, in a [*PIN*$^+$] cell, in the presence of an efficient template ([*PIN*$^+$] amyloid), both Rnq1p and 103Q form amyloid – this would serve the purpose of self-sequestering the protein avoiding proteotoxicity. However, in a [*PIN*$^+$] cell, chaperone activity is linked to the generation of toxic oligomers but in an ATP depleted cell, while amyloid fibrils would self-assemble there would also be limited activity of chaperones and therefore limited production of toxic oligomers. The flaw in this hypothesis is how a [*PIN*$^+$] state would be sustained when the generation of heritable amyloid seeds, which relies on chaperone activity, is also impaired.

In the study reported here gene deletions that compromised processes such as RNA metabolism, the response to stress and transcription were found to suppress the toxicity of both Rnq1p and 103Q, as did compromised functions such as hydrolase

activity and protein binding, and components of the cytoplasm, nucleus and membrane.

It is interesting that deletions of genes encoding proteins associated with P-bodies (i.e. *dcp2Δ, hrp1Δ* and *lsm7Δ*) and proteins similarly involved in directing mRNA to P-bodies (*upf1Δ/nam7Δ* and *upf2Δ/nmd2Δ*) were capable of suppressing or reducing Rnq1p and 103Q toxicity, suggesting the mRNA degradation pathway may contribute to the toxicity mechanism of Rnq1p and 103Q. It is known that proteins rich in glutamine and asparagine are integral to P-body assembly(Decker *et al.*, 2007) and it could therefore be possible that P-bodies inadvertently serve as additional seeding factors to enhance the rate of aggregation of Rnq1p and 103Q, both of which require QN-rich foci for their aggregation and toxicity(Meriin *et al.*, 2002)(Douglas *et al.*, 2009c) . When P-body formation in the cell is reduced, this may slow down the rate of Rnq1p or 103Q aggregation such that the cell is able to degrade or refold Rnq1p/103Q to a non-toxic state. Only the *dcp2Δ* and *upf1Δ* strains, of those listed at the beginning of the paragraph, fully suppressed both Rnq1p and 103Q toxicity; Dcp2p forms a complex with Upf1p(Lykke-Andersen,2002) , and so it may be the absence of this specific complex in the *dcp2Δ* or *upf1Δ* strain that prevents Rnq1p or 103Q toxicity. Alternatively, it may be that Rnq1p and 103Q expression levels are altered in these deletion strains accounting for apparent suppression that is actually due to reduced expression; this would be easily verified by quantitative western blots.

Suppressor terms specifically significant for Rnq1p toxicity were chromosome organisation, DNA metabolic process, RNA binding, DNA binding, transcription regulator activity, phosphoprotein phosphatase activity, the mitochondria, and plasma membrane - the nucleus was abundant for both Rnq1p and 103Q though it was more significant for the Rnq1p suppressors. This might indicate that the aggregation of Rnq1p in a [*PIN*$^+$] background mediates toxicity via nuclear processes and aberrant interactions therein. Since these terms are more significant for Rnq1p than 103Q toxicity, these terms may be indicative of toxicity events linked to protein function.

Suppressor terms specifically significant for 103Q toxicity included the highly enriched transport process, in addition to the cell cycle, nucleus organisation,

vesicle-mediated signalling and cell membrane organisation. Function terms such as structural molecule activity and oxidoreductase activity were noted, with the mitochondrion, membrane and endomembrane components also significant for suppressors of 103Q toxicity. There is a strong degree of overlap between these indications and the proposed cellular roles and localisation of Htt (Nasir *et al.*, 1995; Cattaneo *et al.*, 2001)(Gutekunst *et al.*, 1995; Rigamonti *et al.*, 2001) which include vesicle-trafficking, endocytosis, neuronal transport, membrane enrichment and nucleocytoplasmic shuttling. Again, since these terms are significant for 103Q compared to Rnq1p, it supports the possibility that unique suppressor terms reflect protein function. Further, it would seem that intervening with the disease-protein function may contribute to the prevention of toxicity, either by blocking the intended end point of protein activity or interfering with interactions that initiate a cascade of disease phenotypes.

6.2.7 Genetic Modifiers Summary: Enhancers

The deletion strains that enhanced both Rnq1p or 103Q toxicity in a [*PIN*$^+$]-independent manner were enriched for transcription and RNA metabolic processes, as had been found for the [*PIN*$^+$] suppressor deletions, however only one P-body component, *xrn1Δ*, was included in the enhancers group, though *ccr4Δ* was also in this group and is involved in mRNA processing, as was *pop2Δ*, a component of the Ccr4-Not complex (Tucker *et al.*, 2002). In contrast, the *not1Δ* strain had been found to suppress 103Q [*PIN*$^+$]-toxicity. It would appear that the remaining members of the RNA metabolic process term (*rxt3Δ, sfp1Δ, swi3Δ, snf2Δ* and *zap1Δ*) associated with the enhancer set lend themselves more directly to the transcriptional process term. Hydrolase activity, transcriptional regulator activity, DNA binding and 'molecular function unknown' were also significant function terms associated with the deletions that enhanced both Rnq1p and 103Q toxicity, as were the component terms cytoplasm, nucleus, membrane, mitochondrion and mitochondrial envelope.

There was more overlap in the enhancer deletion GO terms for Rnq1p and 103Q than was seen in the suppressor deletion terms. One might speculate that this is due to continued activity of the proteins in a [*PIN*$^+$] state, for example amyloid-specific misfolding may allow for persisted activity since it appears misfolding mainly

encompasses the aggregation-prone region, rather than the whole protein. In contrast, in a [*pin*$^-$] strain where loss of a certain gene product triggers a destabilisation of Rnq1p or 103Q, the misfolding would not be amyloid-templated and may be expected to disrupt overall structure of the protein including the functional regions of the protein. However, certain GO terms specific to Rnq1p and 103Q in the suppressor set were present in the enhancer set, specifically chromosome organisation and DNA metabolism for Rnq1p, and transport and cell cycle for 103Q. In addition, the term signalling appeared in the 103Q enhancer set, and represented the only term not also associated in the suppressors.

Just as the *atp5Δ* strain had been found to both suppress 103Q toxicity in a [*PIN*$^+$] strain and enhance 103Q toxicity in a [*pin*$^-$] strain, so the *sfp1Δ* strain was seen to both suppress and enhance the toxicity of Rnq1p. Also analogous to the *atp5Δ* strain, which enhanced but did not suppress the toxicity of Rnq1p, so too the *sfp1Δ* strain enhanced but did not suppress 103Q toxicity. The protein Sfp1p was discussed in section 1.3.5 since it is a yeast prion protein, forming the [*ISP*$^+$] prion (Rogoza *et al.*, 2010). It was also noted Rnq1p toxicity was enhanced by a deletion of the gene encoding Ppz1p phosphatase, which in complex with Hal3p influences the manifestation of the Sfp1p [*ISP*$^+$] prion (Aksenova *et al.*, 2007). It would therefore be interesting to determine the nature of the interaction between Rnq1p and Sfp1p.

The toxicity of Rnq1p and 103Q was also enhanced in the *swi3Δ* and *snf2Δ* strains, both of which are components of the SWI/SNF remodelling complex (section 1.3.3). Deletions abolishing members of the SWI/SNF complex, with each resulting in the same phenotype (i.e. toxicity), suggest that the loss or impairment of SWI/SNF complex activity can cause toxicity of Rnq1p and 103Q.

Finally, Swi1p and Sfp1 have recently been identified as yeast prion proteins, and are rich in glutamine residues, as expected for yeast prion proteins. It was interesting to determine whether this abundance of glutamine was a common feature of the deletion strains that enhanced Rnq1p toxicity. The N-terminus of Ccr4p contains a 3 and a 10 residue glutamine tract, in addition to a 2, a 3 and a 15 residue asparagine tract. The Pop2p protein contains a 3, a 7, an 11, and a 15 residue glutamine tract. Similarly, Snf2p contains a glutamine rich region with 20 glutamines present in a 33 residue stretch in the N-terminus. Glutamine is also the most abundant protein in

Swi3p. In all cases, the most abundant residues in these proteins is glutamine, asparagine, leucine and serine. However, while 5/8 proteins whose absence enhances Rnq1p toxicity were glutamine or asparagine rich, none of those that enhanced 103Q toxicity were noticeably rich in these residues.

Thus, an analysis of the activities associated with the deleted genes that impacted on Rnq1p or poly-Q-mediated proteotoxicity has implicated a number of cellular processes, functions, complexes and components underlying the mechanisms of Rnq1p and 103Q toxicity. The terms and proteins that have been identified as modulators of both Rnq1p and 103Q may indicate core activities in the cell that exacerbates protein misfolding, amyloid toxicity or polyglutamine toxicity.

Chapter VII

Discussion

7.1 Summary

With an increasingly dependent, aged population, comes a mounting sense of urgency to dissect the currently inseparable parallels between ageing, neurodegeneration and dementia. At the molecular level, a unifying feature of these 'events' appears to be the misfolding of proteins and a failure of the cell to effectively manage and contain the consequences of misfolding, particularly in an aged or genetically vulnerable cell. Presently, models of neurodegenerative disease and proteinopathies indicate that while there exist many opportunities for therapeutic intervention, our understanding of the mechanisms leading to proteotoxicity continues to be very limited. As has been touched upon in this thesis, there appear to be many similarities between the toxicity causing proteins of the central nervous system. However, it is also clear that the function, localisation, interaction network and additional sequence features of the disease causing protein are also important to the pathogenesis profile.

In this thesis I have examined the yeast Rnq1p prion protein in order to elucidate the cellular function of Rnq1p; to further characterise the toxicity associated with Rnq1p over-expression; to identify the impact of natural polymorphisms on Rnq1p toxicity; and to identify overlapping mechanisms of toxicity between Rnq1p, a glutamine rich, amyloid forming prion protein, and the amyloid forming, polyglutamine expanded mutant Huntingtin protein, as used in the yeast model of Huntington's disease.

The work presented in Chapter 3 demonstrates that Rnq1p is a negative regulator of translation termination and that Rnq1p co-localises to mRNA processing-bodies (P-bodies). Furthermore, evidence for metabolic remodelling and a role in stress

response indicate a possible transcription regulation activity for Rnq1p. In Chapter 4, an analysis of the *RNQ1* gene from multiple *S. cerevisiae* strains identified fifty-three distinct alleles that, in Chapter 5, lead to the identification of sequence features impacting upon Rnq1p toxicity. In Chapter 6, genetic modifiers of both Rnq1p and mutant Huntingtin toxicity were identified, including multiple components of the P-body and mRNA degradation pathways.

.

7.2 Review of Experimental Results

7.2.1 Rnq1p as a regulator of translation termination

Translation termination in yeast is mediated primarily by two eukaryotic release factors, Sup35p (eRF3) and Sup45p (eRF1)(Stansfield *et al.*, 1995), and their termination activity releases newly synthesised polypeptides from the ribosome. Sup45p comprises three domains, each with a role in the termination process: stop-codon recognition is mediated by the N-domain (Bertram *et al.*, 2000; Song *et al.*, 2000; Chavatte *et al.*, 2001), the peptidyl-transferase activity of the highly conserved GGQ motif is present within the M domain (Frolova *et al.*, 1999), and interactions with Sup35p and the phosphatase Pp2ap are mediated by the C-domain (Stansfield *et al.*, 1995)(Andjelkovic *et al.*, 1996). Sup35p requires only its C-domain for translation termination, which is essential for viability and carries the GTPase activity (Frolova *et al.*, 1996), believed to stimulate efficient release of the polypeptide from the ribosome (Salas-Marco *et al.*, 2004; Alkalaeva *et al.*, 2006). The N-domain of Sup35p is prionogenic and dispensable for viability and translation termination activity however its absence is associated with a decrease in Sup35p stability and functionality (Kodama *et al.*, 2007) . Specifically, binding partners of Sup35p appear capable of modulating Sup35p participation in the termination process by interacting with the N-domain of Sup35p (Kodama *et al.*, 2007).

The signal for translation termination, a stop codon, is recognized at differing efficiencies by the Sup35p:Sup45p complex depending on factors such as the sequence context of the stop codon (Salser *et al.*, 1969; Fluck *et al.*, 1980), the competition with near-cognate transfer RNAs (tRNAs) (Engelberg-Kulka *et al.*,

1981), but also other cellular factors interacting either directly or indirectly with the termination process (Kodama *et al.*, 2007).

In chapter 3 of this thesis, evidence for the role of Rnq1p in the termination process is presented. Specifically, Rnq1p over-expression increased the frequency of stop-codon read-through at all three stop codons, with a ~7x fold decrease in termination efficiency at the UGA stop codon mediated by full-length Rnq1p, and a ~3x fold decrease in UGA recognition by the N-terminus of Rnq1p (amino acids 1-152). Further, it was demonstrated that over-expression of Rnq1p in the presence of the *sup45-2* allele (associated with normal growth but elevated stop-codon read-through) (Stansfield *et al.*, 1997) manifested growth defects that were absent in an otherwise isogenic strain: this would be consistent with Rnq1p acting as an allosuppressor i.e. an enhancer of nonsense suppression and thus exacerbating the *sup45-2* termination defect.

Additional support for the role of Rnq1p as a regulator of translation termination comes from unpublished data generated within the Tuite and von der Haar labs demonstrating 1) a strong physical interaction between the C-domain of Sup45p and Rnq1p as detected by yeast-2-hybrid analysis (Tobias von der Haar), 2) the pull-down of a Sup45:Sup35:Rnq1p complex via Rnq1-TAP (Nadia Koloteva-Levine) and Sup35-TAP (Tobias von der Haar), and 3) additional genetic interaction data analogous to the *sup45-2* result, where mutant *sup35* alleles with termination defects also show severe growth defects or synthetic lethality when shuffled into a *RNQ1*$^{+}$ strain, as opposed to an otherwise isogenic *rnq1Δ* strain (Tobias von der Haar). This latter finding was also supported by work in this thesis, which showed that a deletion of the *RNQ1* gene corrected a slight growth defect associated with a strain expressing Sup35p with an N-terminal truncation (*SUP35ΔN*). Surprisingly, Rnq1p over-expression was shown to be toxic in both the *SUP35ΔN and the SUP35ΔN rnq1Δ* strain. The [*PIN*$^{+}$] prion is a prerequisite for Rnq1p toxicity, yet in the *SUP35ΔN rnq1Δ* strain, the [*PIN*$^{+}$] prion would be absent, suggesting a possible role for the N-terminal domain of Sup35p in suppressing [*PIN*$^{+}$]-independent Rnq1p toxicity.

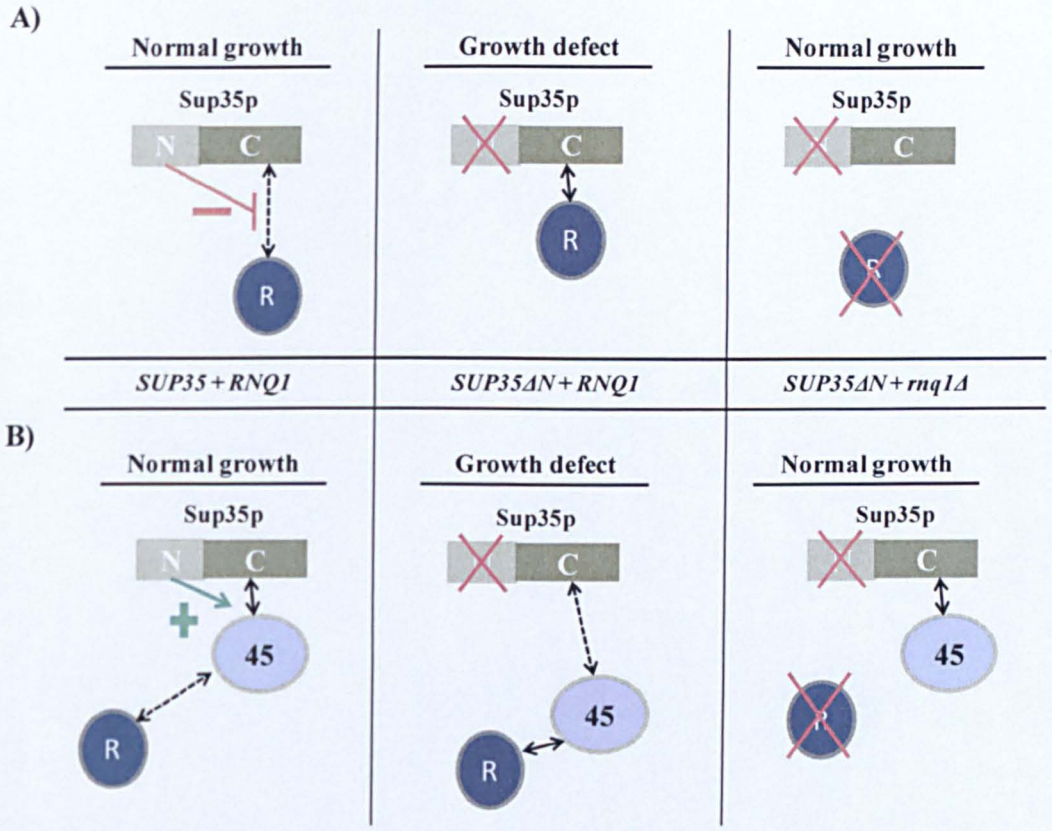

Figure 7.1: Rnq1p negatively regulates the activity of the translation termination complex.
The Sup35p N-domain appears to play an essential role in modulating Rnq1p's suppressor activity, and may do so A) by limiting the interaction of Rnq1p with the C-domain of Sup35p, or B) by limiting the interaction of Rnq1p with Sup45p's C-domain.

It is possible to envisage the role of Rnq1p in translation termination (figure 7.1). For example, Rnq1p may competitively interact with Sup45p, reducing the availability of Sup45p for translation termination activity. The N-domain of Sup35p may have a role in reducing the interaction between Rnq1p and Sup45p, either by increasing the affinity of Sup35p C-domain for Sup45p, or by physically blocking or impairing the interaction between Rnq1p and Sup45p. Thus, in the absence of the Sup35p N-domain (*SUP35ΔN*), the interaction between Rnq1p and Sup45p is increased resulting in a slight growth defect. When Rnq1p is over-expressed in the strain carrying the *sup45-2* allele, the increased association of Sup45p with Rnq1p further impairs the termination activity of Sup45p. When Rnq1p is over-expressed in the *SUP35ΔN* strain, Rnq1p is able to freely associate with Sup45p, causing severe

termination defects that lead to loss of cell viability. It is also possible that the Sup35p N-domain blocks interactions of Rnq1p with Sup35p's C-domain (figure 1, panel A)

It is important to note that the transition of Rnq1p between [*PIN*$^+$] and [*pin*$^-$] states does not affect translation termination (unpublished, Tobias von der Haar). It is also unlikely that Rnq1p contributes to the termination defects associated with [*psi*$^-$] conversion to [*PSI*$^+$], since despite the conformational change of the N-domain of Sup35p to the prion state which may reduce its ability to limit Rnq1p and Sup45p interactions (or Rnq1p and Sup35p interactions), Sup35p is ~ 6 x more abundant than Rnq1p (unpublished, Tobias von der Haar) and a growth defect is not observed in [*PSI*$^+$] cells, as occurs in the *SUP35ΔN* strain.

The role of Rnq1p in translation is particularly interesting in the context of its status as a prion protein, since multiple prion proteins now appear to converge at the level of translation termination: Sup35p/[*PSI*$^+$], Rnq1p/[*PIN*$^+$] and Sfp1/[*ISP*$^+$]. If prions do serve a biological purpose, perhaps translation termination is the ideal mechanism for epigenetic regulation. For example, [*PSI*$^+$]-mediated read-through of stop codons generates phenotypic variability that is believed to account for the observed growth advantage of [*PSI*$^+$] strains relative to isogenic [*psi*$^-$] strains, when exposed to different stress-inducing conditions (True *et al.*, 2000). The cell is able to explore previously hidden genetic variability with the production of C-terminally extended polypeptides, and particularly in a stressful environment, the risk associated with exploring erroneous protein production may be countered 1) by the immediacy of the associated changes that ultimately have a finite lifetime (protein and mRNA can be degraded), and 2) by the magnitude of change that can be introduced, which in the short-term at least, could probably not be paralleled by genetic changes.

Developing the link between Rnq1p and translational processes further, it was also shown in Chapter 3 that Rnq1p co-localises with the mRNA-decapping protein Dcp2p at discrete cytoplasmic foci referred to as processing-bodies (P-bodies). P-bodies are formed by accumulations of untranslating mRNA that are associated with translation-repression and mRNA-decay proteins, and as such the mRNAs in P-bodies will either return to translation or be degraded . The minimal unit of a P-body is the mRNP (messenger ribonucleoprotein) and the microscopically observable P-

bodies typically represent aggregations of mRNPs. While the composition of P-bodies has not been completely determined, proteins that are important for P-body assembly appear to be rich in glutamine (Q) and asparagine (N) residues, which are proposed to serve as molecular 'glue' (Reijns *et al.*, 2008)(Decker *et al.*, 2007). It is possible that the Q/N-richness of Rnq1p makes it ideal for such a role. Close to half of the 107 proteins in yeast that contain QN-rich domains are involved in RNA metabolism, translation or degradation (Buchan *et al.*, 2009). It remains to be determined what impact, if any, conversion of Rnq1p between the [*pin*$^-$] and [*PIN*$^+$] state has on P-body formation.

Additionally, RNA granules within *Drosophila melanogaster* neurons transport and translationally control mRNAs, and they contain many components also found in P-bodies, such as Upf1p, Xrn1p and Dhh1p (Barbee *et al.*, 2006). This suggests that P-bodies and RNA granules in neurons are related and that both may also function in the degradation of mRNAs(Buchan *et al.*, 2009) . This apparent conservation of P-body and RNA granule function is particularly interesting, since the Huntingtin protein has also recently been found to co-localise with P-bodies in HeLa cells (Savas *et al.*, 2008), and with neuronal RNA granules in dendrites (Savas *et al.*, 2008).

The apparent localisation of both Rnq1p and Huntingtin to P-bodies gives further confidence to the identification, in this study, of P-body and mRNA degradation pathways as modifiers of both Rnq1p and mutant Huntingtin toxicity. Specifically, the absence of Upf1p, Upf2p, Dcp2p, Lsm7p, Hrp1p, Not1p, Xrn1p, Ccr4p and Pop2p either suppressed or enhanced toxicity of Rnq1p or 103Q. Of these, the suppressing effect of a *upf1Δ* strain on Rnq1p and 103Q was specifically validated with further study.

An intriguing observation along this particular line of study is that over-expression of 103Q, used to model Huntington Disease in yeast, and which like Rnq1p requires the presence of the [*PIN*$^+$] prion for toxicity, was also toxic in the *SUP35ΔN* and *SUP35ΔN Δrnq1* strains. This raises the question of whether Huntingtin/103Q, like Rnq1p, has a more direct role in translation, or that maybe the role of Rnq1p and Huntingtin within P-bodies is linked to an activity at the ribosome that affects translation termination. Similar to the investigation of Rnq1p and its role in

translation termination, it would be interesting to determine whether Huntingtin too was associated with a defect in translation termination, although such an activity for Huntingtin has not been reported in the literature.

7.2.2 Rnq1p may have a role in transcriptional regulation

The proteomics investigation of Rnq1p-specific perturbations in the cell revealed many changes involving metabolic pathways, protein translation, protein folding, ribosome biogenesis, energy generation, and cellular respiration (Chapter 3). Of the 483 proteins that were reproducibly altered in their abundance as a consequence of changes to the expression level of Rnq1p, 235 proteins were observed to either increase or decrease regardless of whether Rnq1p abundance was increased or abolished. Such a requirement for a precise abundance of Rnq1p might suggest that Rnq1p participates in a functional complex that makes the stoichiometry rather than the absolute amount of Rnq1p important. Further, given the spectrum of changes precipitated by an altered abundance of Rnq1p, it is possible that such a complex has a transcriptional role in the cell. For example, one could imagine a role for Rnq1p in complex assembly: in the absence of Rnq1p, the complex would not form, but when Rnq1p is present in excess, Rnq1p may saturate the interaction sites of the complex components such that they do not form required functional associations (figure 7.2). In both cases, absence or over-expression of Rnq1p, there would be no activity or a reduced activity of the complex, respectively.

The most likely sub-cellular localisation for Rnq1p to exert transcriptional control would be in the nucleus, and Rnq1p is indeed observed in both the cytoplasm and the nucleus. Additionally, Rnq1p has been identified as a protein phosphorylated in response to the DNA mutagen methane methylsulfonate (MMS) (Albuquerque *et al.*, 2008), with a separate study reporting sensitivity of a *rnq1Δ* strain to MMS treatment (Begley *et al.*, 2002b). These findings might support a role for Rnq1p in the transcriptional response to certain stresses or cellular signals. Indeed, the homozygous interaction network generated for Rnq1p in Chapter 3 using chemical-genetic information from the yeast Fitness Database (http://www.fitdb.stanford.org/) clustered the *rnq1Δ* strain with gene deletions that are otherwise involved in the

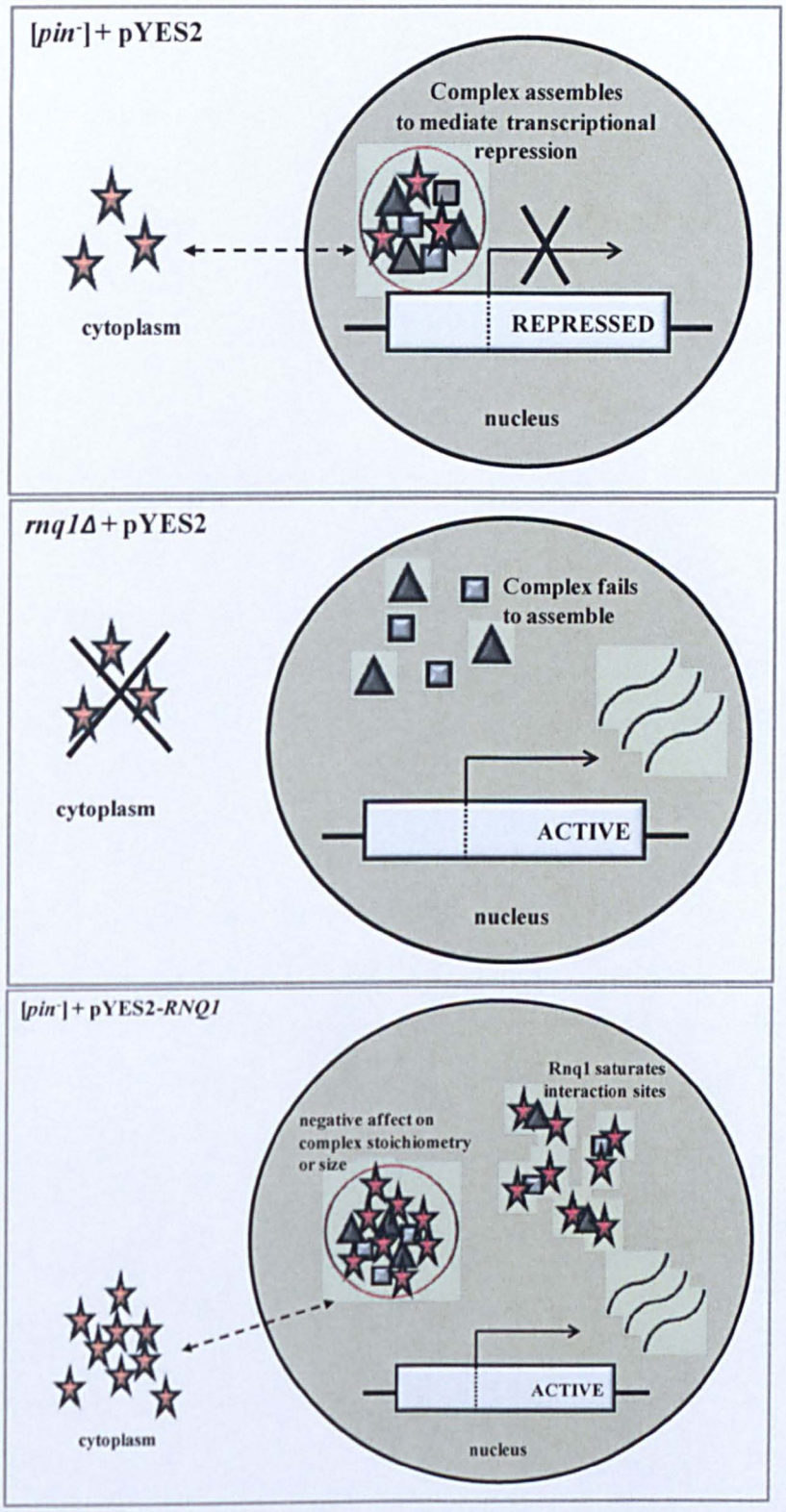

Figure 7.2: A precise abundance of Rnq1p may be important for complex assembly.

The absence or over-expression of Rnq1p could prevent or impair the assembly of a transcriptional complex.

response to chemical stress, signal transduction, the cell cycle, RNA metabolic processes, the response to stress, and cellular amino acid and metabolic processes. The prediction of an FHA-domain in the N-terminus of Rnq1p (section 3.2.2), associated with proteins involved in signalling, cell cycle checkpoints, DNA repair and transcriptional regulation, may therefore be valid.

7.2.3 Toxic Rnq1p over-expression results in a nuclear migration defect

An interesting question arising from the connection between Rnq1p and nuclear activities is whether such an activity of Rnq1p could also be responsible for the nuclear migration defect observed in Chapter 5 when Rnq1p is over-expressed. The N-terminus of Rnq1p is where the FHA-domain is predicted to reside and it is the serine-143 residue that is phosphorylated in response to DNA stress however, as shown in Chapter 3, over-expression of the N-domain (residues 1-152) of Rnq1p alone does not cause toxicity. Indeed, Rnq1p toxicity is only observed when the [*PIN*$^+$] prion is present, suggesting that the nuclear migration defect could for example be due to an indirect consequence of toxic-oligomer accumulation in the cell, or in the [*PIN*$^+$] form, due to nucleocytoplasmic shuttling proteins that functionally interact with Rnq1p becoming sequestered by Rnq1p in the cytoplasm.

Alternatively, the nuclear migration defect may be linked to the divergently transcribed *BIK1* gene, whose regulatory sequences overlap the coding region for *RNQ1*, and vice versa. It has been shown that deletion of *RNQ1* or *BIK1* has a significant negative effect upon the expression level of the other (True *et al.*, 2000). Bik1p is a microtubule-associated protein required for the positioning of spindles, and for spindle-pole body duplication during mitosis (Berlin *et al.*, 1990); its absence in a *bik1Δ* strain leads to chromosome instability and nuclear migration and positioning defects (Berlin *et al.*, 1990). Additionally, over-expression of Bik1p results in the arrest of cell division due to the loss of microtubule structures (Berlin *et al.*, 1990). However, True *et al* (True *et al.*, 2000) reported that it was a requirement only for the regulatory sequence of each gene, present in the other, that

allowed for wild-type levels of expression; expression of wild-type levels of Rnq1p via a plasmid required the presence of the *BIK1* gene, also.

Divergently paired genes are a common feature of eukaryotic genes (Yang *et al.*, 2009), and the co-regulation that is achieved is believed to have functional relevance. It is possible that Rnq1p activity in the cell is somehow related or functionally relevant to that of

Bik1p. It may even be possible that the requirement of Rnq1p to achieve wild-type levels of expression through the presence of Bik1p, and vice versa, occurs not just at the DNA level but also at the protein level, whereby a reduction in Rnq1p protein might lead to a reduction of Bik1p protein. Such an intimate connection between Rnq1p and Bik1p might explain why Rnq1p over-expression results in a nuclear migration defect that is also observed by over-expressing Bik1p.

The over-expression of Rnq1p in a *bik1Δ* strain would confirm whether the nuclear migration defect was a consequence of elevated Bik1p levels. However if the defect is specific only to the over-expression of Rnq1p impacting upon the cellular level of Bik1p, then the prion state should be inconsequential, but in fact toxicity is only observed in the [*PIN*$^+$] state.

The reduced level of Bik1p that is demonstrated in a *rnq1Δ* strain has implications for the interpretation of *rnq1Δ* phenotypes. Indeed, the yeast Fitness Database (http://www.fitdb.stanford.org/) clustered *rnq1Δ* and *bik1Δ* together, and they also shared 5 other genes in common, representing a 60 % overlap in chemical-genetic profiling in the first neighbour instance, the remaining 4 genes of *rnq1Δ* and *bik1Δ* do appear in the second neighbour instance however, appearing on the lists of the first neighbour genes. Overall there is a significant overlap between *rnq1Δ* and *bik1Δ* phenotypes.

The contribution of Sis1p to the nuclear migration defect was also considered, since Luke *et al* (Luke *et al.*, 1991) had reported that depletion of Sis1p resulted in the same nuclear migration defect and cell size increase as reported in Chapter 3 of this thesis. This appeared to be a promising lead since binding to Sis1p by Rnq1p occurs only in a [*PIN*$^+$] cell, and toxicity of Rnq1p is specific to the [*PIN*$^+$] state, however

Douglas *et al* (Douglas *et al.*, 2009b) demonstrated that an impaired interaction between Rnq1p and Sis1p still resulted in toxicity somewhat negated this idea.

The nuclear migration defect caused by toxic over-expression of Rnq1p may represent a significant difference between the end-point of Rnq1p and 103Q toxicity. A nuclear migration defect associated with 103Q over-expression was not was not observed in my own studies, however this may be due to the time-scale on which toxicity of the two proteins presents: a difference in growth rate through Rnq1p over-expression was observed after 3 hrs in this thesis (Chapter 5), but Sokolev *et al* (Sokolov *et al.*, 2006) did not observe a difference in growth rate through 103Q over-expression (relative to 25Q) for approximately 6 hrs. In neurons, the expression of expanded huntingtin protein results in aggregate formation, followed by cell death with apoptotic markers Sokolov *et al* (Sokolov *et al.*, 2006) demonstrated that in yeast, expression of the 103Q construct also presented with nuclear localised aggregate formation, nuclear fragmentation and death with apoptotic markers. Nuclear fragmentation following Rnq1p over-expression was not observed, however again, it is possible that the time-course of the analysis was not of sufficient duration to observe these changes. Specifically, an analysis of DNA content, in cells over-expressing 103Q, by Fluorescent Activated Cell Sorting (FACS) revealed an accumulation of less than 1C DNA, consistent with an apoptotic event, and an increase of 2C DNA content relative to 1C DNA content, which may indicate a cell cycle delay (Sokolov *et al.*, 2006). The authors concluded that apoptosis was not triggered directly by 103Q expression but appeared to be an indirect consequence of 103Q toxicity.

It is possible that 103Q and Rnq1p lead to different terminal phenotypes, and that the non-overlapping genetic modifiers for Rnq1p and 103Q toxicity identified in Chapter 6 reflect these differences in the toxicity pathway. However, it is interesting to speculate whether, just as Rnq1p is conformationally altered in the [*PIN*$^+$] variants, whether the conformation of the expanded polyglutamine of huntingtin exon 1 is similarly altered when seeded by [*PIN*$^+$] in yeast, as opposed to the conformation adopted in mammalian cells, and that it is this transmission from [*PIN*$^+$] to 103Q of structurally similar features that make both susceptible to the same genetic modifiers of toxicity, and why they might also lead to a similar or shared terminal phenotype. If the similarities between Rnq1p and 103Q toxicity were

due to the transmission of a Rnq1p-specific structural feature to the 103Q conformer, then this may negate the relevance of the identified genetic modifiers to studies of huntingtin in other (non-yeast) systems.

Additionally, just as Rnq1p over-expression was shown in Chapter 5 to be differentially toxic in the different [*PIN*$^+$] variants, it would be interesting to determine whether 103Q toxicity is also modulated by the structural differences in the [*PIN*$^+$] variants.

7.2.4 A link between Rnq1p and metabolism

An observation from the proteomics investigation described in Chapter 3 was the effect of Rnq1p abundance on the levels of proteins with integral roles in the central metabolic pathways (glycolysis, the TCA cycle, and the pentose phosphate pathway). The TCA cycle and glycolysis were both up-regulated, and the pentose phosphate pathway was down-regulated, following deviation of Rnq1p abundance from the wild-type level. In yeast, in the presence of a hexose sugar such as glucose, anaerobic fermentative metabolism is used to generate ATP. In the absence of a hexose sugar, the cell will use aerobic oxidative metabolism via the TCA cycle and electron respiratory chain to produce ATP. Fermentation is chosen preferentially by yeast for rapid growth, and upon exhaustion of the fermentable carbon source, metabolism is remodelled such that fermentative glycolysis is down-regulated and the TCA cycle and components for oxidative phosphorylation are up-regulated. This transition between the two metabolic states is referred to as the diauxic shift. If both the TCA cycle and fermentative glycolysis pathway are simultaneously up-regulated, it may be indicative of a deficit in ATP production – which in this case, would be caused by a deviation in the abundance of Rnq1p from wild-type levels.

If ATP production was impaired, this might arise from an event that has reduced the coupling between electron transfer through the respiratory chain to the generation of ATP. The TCA cycle supplies the respiratory chain with NADPH and $FADH_2$, reducing equivalents that are oxidised to generate electrons and hydrogen ions (H^+). The electrons are shuttled through the respiratory complexes, which simultaneously pump H^+ ions into the intermembrane space of the mitochondria, thus creating a H^+

ion (or electrochemical) gradient that is used by the ATP synthase complex to couple the re-entry of protons into the mitochondrial matrix with the generation of ATP.

A number of mitochondrial proteins decreased in abundance as a consequence of changes to the abundance of Rnq1p (Chapter 3). Some of these, such as Fcj1p, Mdm38p, Tif1p and Fas2p, have been associated with defects in mitochondrial morphology, membrane organisation and membrane integration of proteins (Fields *et al.*, 1998)(Altman *et al.*, 2005); these changes might account for a reduction in electron transport chain coupling to ATP production. Notably, the Atp5p protein, a component of the ATPase synthase responsible for utilising the energy of the electrochemical gradient for ATP production, was one of the 12 proteins showing the most significant decrease in expression: this occurred between the *rnq1Δ* and wild-type strain, with Atp5p being 2.55 x more abundant in the *rnq1Δ* strain than in the wild-type strain, and Atp5p was also 2.13 x more abundant in the Rnq1 over-expressing strain, compared to when Rnq1p was present at wild-type levels. Thus, Atp5p is elevated when Rnq1p abundance varies from that of the wild-type level, and may indicate efforts by the cell to sustain ATP production with dysfunctional mitochondria. In addition, Rnq1p over-expression was shown to be toxic in a [*pin*$^-$] *atp5Δ* strain (Chapter 6). Since Atp5p was increased to a similar if not greater level in the *rnq1Δ* strain, it would be interesting to determine whether synthetic lethality occurs in an *atp5Δ rnq1Δ* double-knockout. This would provide further support to the requirement of a precise level of Rnq1p in the cell, as indicated by the proteomics data set of Chapter 3.

Interestingly, the *atp5Δ* strain was also observed to enhance the toxicity of 103Q such that it too was toxic in a [*pin*$^-$] state. Similarities between the expanded exon 1 of huntingtin protein and Rnq1p have thus far been limited to aspects of their toxicity in the [*PIN*$^+$] background. The toxicity of both Rnq1p and 103Q in a [*pin*$^-$] *atp5Δ* strain may indicate that these proteins are able to form toxic aggregates in the absence of Atp5p: this could be easily determined with microscopic analysis of Rnq1-GFP or 103Q-GFP distribution in a *atp5Δ* strain. An energy-deficient cell may be less able to effectively dispose or refold excess Rnq1p or 103Q in the cell, due to impaired ATP-dependent chaperone activities.

The link between mitochondrial dysfunction and over-expression of Rnq1p and 103Q was indicated in Chapter 5 and Chapter 6, respectively, when it was shown that over-expression of Rnq1p or 103Q alone did not cause respiratory deficiency, but that a concurrent reduction in mitochondrial activity by exposure to low dose ethidium bromide did result in respiratory deficiency. The detrimental effect of Rnq1p and 103Q on mitochondria therefore appears to be subtle, or at least the cell is able to compensate or mask the negative effect of Rnq1p and 103Q by up-regulating Atp5p, for example. When mitochondrial function is already partially compromised, Atp5p up-regulation may not be sufficient to sustain the cell. Since mutant huntingtin protein causes mitochondrial defects in mammalian cells this might indicate that people with compromised mitochondrial function might be increasingly susceptible to mutant huntingtin toxicity. However, Rnq1p over-expression is still toxic in a petite strain (depleted of mitochondrial respiratory capacity) suggesting that mitochondrial dysfunction is a secondary effect of Rnq1p toxicity and not the source of Rnq1p-induced cell death. This does not negate the finding though that impaired mitochondrial activity in combination with Rnq1p or 103Q over-expression is sufficient for toxicity.

Interpretation of the role played by Atp5p in modulating Rnq1p and 103Q is complicated somewhat by the finding, in Chapter 6, that the *atp5Δ* strain also suppressed 103Q toxicity in a [*PIN*$^+$] strain, though it does not suppress Rnq1p [*PIN*$^+$]-dependent toxicity. One might speculate that this reflects differences in the toxicity pathways of Rnq1p and 103Q in the [*PIN*$^+$] state. Since both Rnq1p and 103Q over-expression were toxic in the [*pin*$^-$] *atp5Δ* strain this might, as mentioned, indicate that toxic aggregation is occurring in this [*pin*$^-$] strain and may not necessarily be linked to the cellular functions or Rnq1p or 103Q. The differential role of *atp5Δ* in modulating Rnq1p and 103Q toxicity between the two prion states may suggest that in a [*pin*$^-$] *atp5Δ* strain, aggregates of Rnq1p and 103Q are more similar, either structurally, or by the involved toxicity pathways. For example, the Rnq1p L94A mutation in the study of Douglas *et al* (Douglas *et al.*, 2009a) resulted in the formation of toxic aggregates of Rnq1p in a [*pin*$^-$] background, however these aggregates were found not to be amyloid or accessible to Sis1p, two properties central to [*PIN*$^+$] toxicity of Rnq1p (Douglas *et al.*, 2009a).

Thus, in a [*pin*$^-$] background, genetic modifiers that induce aggregation could give rise to toxic aggregates that are structurally distinct from the toxic aggregates formed in a [*PIN*$^+$] background, since only in a [*PIN*$^+$] background is there an efficient template for amyloid-specific conformational conversion, and further, that aggregates formed in a [*pin*$^-$] background may be more similar to each other than are aggregates formed in a [*PIN*$^+$] background. This would of course imply then that the 103Q-amyloids formed in the *atp5Δ* [*PIN*$^+$] background are different to the Rnq1p-amyloids formed in a the same background, and hence why the *atp5Δ* strain could modulate toxicity of both proteins in the [*pin*$^-$] state but only one protein (103Q) in the [*PIN*$^+$] state. This however is quite a complex interpretation, and it does not account for why Atp5p levels increase in both a *rnq1Δ* strain and a [*pin*$^-$] strain over-expressing Rnq1p: this fact alone suggests that the consequence of changes to Rnq1p abundance on mitochondrial function instigates the increase in Atp5p abundance in the cell, and that this increase in Atp5p is required to sustain the cell.

If Rnq1p is involved in transcriptional regulation and a precise abundance of Rnq1p is required for stoichiometric assembly of a transcriptional complex, then the absence or reduced activity of this complex may lead to aberrant transcriptional programmes that are detrimental to the mitochondria and subsequently ATP supply for the cell, resulting in an up-regulation of the TCA cycle, glycolysis and production of the Atp5p protein, for example, to restore ATP levels. That over-expression of Rnq1p in an *atp5Δ* strain is sufficient for toxicity suggests that the Atp5p response of the cell is critical when Rnq1p is misregulated.

Further analysis of the relationship between Rnq1p, Atp5p and 103Q is needed to confirm the suggestions made here. In particular, with reference to table 1, one might predict that Rnq1p and 103Q would be toxic when over-expressed in a [*pin*$^-$] strain pre-treated with ethidium bromide. Particularly informative however will be the double knock-out of *atp5Δ* and *rnq1Δ*, which one might expect to be synthetically lethal, as mentioned.

		[*PIN*$^+$]	[*pin*$^-$]	
mitochondrial stress	EtBr	t	?	Rnq1p
	EtBr	t	?	103Q
	atp5Δ	t	t	Rnq1p
	atp5Δ	nt	t	103Q
	Petites	t	?	Rnq1p
	Petites	?	?	103Q

note: *rnq1Δ*, Atp5p ↑; o/e Rnq1p, Atp5p ↑

Table 7.1: Interactions between Rnq1p, 103Q , mitochondrial respiratory capacity and energy generation.
Rnq1p and 103Q over-expression does not detectably reduce the respiratory capacity of cells unless mitochondrial respiratory capacity is first partially depleted by ethidium bromide exposure or by deletion of the Atp5p component of ATP synthase.(t) toxic; (nt) not toxic; (?) not tested.

7.2.5 What can toxicity tell us about protein function

As described in Chapter 6, there is an overlap between the identified roles of huntingtin in higher eukaryotic cells, and the identity of the gene deletions that are capable of suppressing or enhancing 103Q toxicity. In particular, the process of transport was the most significant gene ontology term associated with the suppressors of 103Q toxicity, along with vesicle-mediated signalling, cell membrane organisation, nuclear organisation, mitochondrion, membrane and endomembrane components: these are all consistent with proposed roles for huntingtin in vesicle-trafficking, endocytosis, neuronal transport, membrane enrichment and nucleocytoplasmic shuttling . In addition, multiple P-body and mRNA degradation components were identified as modifiers of Rnq1p and 103Q toxicity, and both have now been shown to localise to P-bodies, and also RNA granules in neurons in the case of huntingtin (Savas *et al.*, 2008; Savas *et al.*, 2010). Further, Rnq1p is a negative regulator of translation termination (Chapter 3) and two other proteins, Upf1p and Sfp1, which are also regulators of translation termination (Leeds *et al.*, 1991; Volkov *et al.*, 2002), were found to modulate Rnq1p toxicity. Such overlap between protein function and the gene deletions that modulate protein toxicity may support the use of toxicity modulators as a means to identify possible functions and interactions for Rnq1p and 103Q in the cell.

A study by Meriin *et al* (Meriin *et al.*, 2003) identified that many mutations affecting endocytosis caused [*PIN*$^+$]-dependent increases in 103Q toxicity in yeast. One of these deletions, *end3Δ*, was tested in this study (Chapter 6) and found in contrast to suppress 103Q toxicity in the [*PIN*$^+$] background. It is possible that the *end3Δ* strain used in this study had converted to a [*pin*$^-$] state, although this was not determined. Meriin *et al* identified that 103Q expression resulted in the inhibition of endocytosis, and that this defect preceded a reduction in growth rate. Thus, the defects in endocytosis caused by the expression of 103Q may be functionally relevant since huntingtin appears to have a role, amongst others, in vesicle trafficking (Truant *et al.*, 2006). Specifically, a study by Hilditch-Maguire *et al* (Hilditch-Maguire *et al.*, 2000) identified dramatic changes in ES cells in the absence of huntingtin protein to nucleoli, transcription speckles, mitochondrial clusters, the endoplasmic reticulum, Golgi complex and vesicle recycling.

Mutant huntingtin has also long been implicated in transcriptional dysregulation, similar to other expanded polyglutamine proteins (Truant *et al.*, 2007)(Helmlinger *et al.*, 2006). In this study deletions that compromise nuclear organisation (*kar2Δ*, *nup170Δ* and *tom1Δ*) suppressed 103Q [*PIN*$^+$]-dependent toxicity, whereas transcription regulator activity and DNA binding (*sfp1Δ*, *swi1Δ* and *zap1Δ*) were associated with the enhancers of 103Q toxicity.

A very speculative prediction that emerges based purely on gene deletion, toxicity and bioinformatic analyses is the possible role of the yeast Get4p protein in distributing mutant huntingtin to the mitochondrial membrane rather than the ER membrane, the former of which would be associated with toxicity and the latter not. The interaction model, presented in Chapter 6, was used to hypothesise that either Ycl084w or Sgt2p could be the proteins responsible, in the absence of Get4p, for directing mutant huntingtin to the GET pathway for ER membrane association. This hypothesis required that there be a purpose to targeting huntingtin to the ER, and studies by Hilditch *et al* (Hilditch-Maguire *et al.*, 2000) and Atwal *et al*, (Atwal *et al.*, 2007) show that huntingtin localises to the ER membrane where it is important for normal functioning of the ER, and in response to stress, huntingtin traffics from the nucleus to the ER membrane in an ATP dependent manner. Further, a point mutation in the N-terminal region (1-18) that is required for the ER-association of

huntingtin, results in increased mutant huntingtin toxicity (Atwal *et al.*, 2007). These observations are functionally compatible with the prediction that increased trafficking of mutant huntingtin to the ER membrane is protective rather than toxic. In addition, an analysis of 103Q-associated proteins in yeast revealed Sgt2p to be one amongst the 16 identified proteins (Wang *et al.*, 2007). Thus, it may be that Sgt2p could, in the absence of Get4p, have a role in targeting mutant huntingtin (103Q) to Get3p for ER association via the residual components of the GET pathway.

Thus, it appears that deletion of proteins that are functionally related to aggregation-prone/disease-associated proteins can significantly modulate the toxicity of the disease-protein, further supporting the contribution of protein function, cellular localisation and interaction partners to the toxicity profile of a protein.

7.2.6 An interaction network of prions?

If prions do serve a biological purpose in yeast cells, and the increasing number of prion proteins identified in yeast along with the diversity of their associated cellular functions might indicate this possibility, then one might expect there to be some degree of communication between the prion proteins that maintains them in a cell-optimal arrangement. One might speculate that Rnq1p serves as 'central communicator' or a molecular pivot-point, a point at which cellular information converges and is acted upon/conveyed in a structural manner to the regulatory level of prion proteins: conversion to [*PIN*$^+$] and induction of other yeast prions, and their antagonistic interactions. The low conversion frequencies of prions may indicate that while Rnq1p conversion (or other equivalents) initiates the cascade of epigenetic events, subsequent prion conversion events (e.g. [*PSI*$^+$] conversion) are still adequately rare enough to allow the cell time to navigate the environmental condition that triggered Rnq1p conversion, with the existing repertoire of proteins/functions in the cell. This theory would require an ability to lose the [*PIN*$^+$] prion faster than the rate at which [*PSI*$^+$], for example, would appear in the [*PIN*$^+$] background. The observation in the proteomics analysis (Chapter 3) that so many central processes seem to shift slightly one way or the other with Rnq1p abundance indicates that Rnq1p could be quite centrally positioned to translate changes in

cellular physiology to an epigenetic signal. Rnq1p conversion to the [*PIN*$^+$] prion may therefore be likened to switching prion epigenetic overlay on cellular physiology from red light to amber.

References

Aguzzi A., and Steele A.D. (2009) Prion topology and toxicity. *Cell* **137:** 994-996.

Aksenova A., Munoz I., Volkov K., Arino J., and Mironova L. (2007) The HAL3-PPZ1 dependent regulation of nonsense suppression efficiency in yeast and its influence on manifestation of the yeast prion-like determinant [ISP(+)]. *Genes Cells* **12:** 435-445.

Alberti S., Halfmann R., King O., Kapila A., and Lindquist S. (2009) A systematic survey identifies prions and illuminates sequence features of prionogenic proteins. *Cell* **137:** 146-158.

Albuquerque C.P., Smolka M.B., Payne S.H., Bafna V., Eng J., and Zhou H. (2008) A multidimensional chromatography technology for in-depth phosphoproteome analysis. *Mol Cell Proteomics* **7:** 1389-1396.

Alkalaeva E.Z., Pisarev A.V., Frolova L.Y., Kisselev L.L., and Pestova T.V. (2006) In vitro reconstitution of eukaryotic translation reveals cooperativity between release factors eRF1 and eRF3. *Cell* **125:** 1125-1136.

Andjelkovic N., Zolnierowicz S., Van Hoof C., Goris J., and Hemmings B.A. (1996) The catalytic subunit of protein phosphatase 2A associates with the translation termination factor eRF1. *EMBO J* **15:** 7156-7167.

Atwal R.S., Xia J., Pinchev D., Taylor J., Epand R.M., and Truant R. (2007) Huntingtin has a membrane association signal that can modulate huntingtin aggregation, nuclear entry and toxicity. *Hum Mol Genet* **16:** 2600-2615.

Auld K.L., Hitchcock A.L., Doherty H.K., Frietze S., Huang L.S., and Silver P.A. (2006) The conserved ATPase Get3/Arr4 modulates the activity of membrane-associated proteins in *Saccharomyces cerevisiae*. *Genetics* **174:** 215-227.

Barbee S.A., Estes P.S., Cziko A.M., Hillebrand J., Luedeman R.A., Coller J.M., *et al.* (2006) Staufen- and FMRP-containing neuronal RNPs are structurally and functionally related to somatic P bodies. *Neuron* **52:** 997-1009.

Baxa U., Speransky V., Steven A.C., and Wickner R.B. (2002) Mechanism of inactivation on prion conversion of the *Saccharomyces cerevisiae* Ure2 protein. *Proc Natl Acad Sci U S A* **99:** 5253-5260.

Beck T., and Hall M.N. (1999) The TOR signalling pathway controls nuclear localization of nutrient-regulated transcription factors. *Nature* **402:** 689-692.

Begley T.J., Rosenbach A.S., Ideker T., and Samson L.D. (2002) Damage recovery pathways in *Saccharomyces cerevisiae* revealed by genomic phenotyping and interactome mapping. *Mol Cancer Res* **1:** 103-112.

Berlin V., Styles C.A., and Fink G.R. (1990) BIK1, a protein required for microtubule function during mating and mitosis in *Saccharomyces cerevisiae*, colocalizes with tubulin. *J Cell Biol* **111:** 2573-2586.

Bertram G., Bell H.A., Ritchie D.W., Fullerton G., and Stansfield I. (2000) Terminating eukaryote translation: Domain 1 of release factor eRF1 functions in stop codon recognition. *RNA* **6:** 1236-1247.

Bradley M.E., and Liebman S.W. (2003) Destabilizing interactions among [PSI(+)] and [PIN(+)] yeast prion variants. *Genetics* **165:** 1675-1685.

Bradley M.E., Edskes H.K., Hong J.Y., Wickner R.B., and Liebman S.W. (2002) Interactions among prions and prion "strains" in yeast. *Proc Natl Acad Sci U S A* **99 Suppl 4:** 16392-16399.

Braidy N., Grant R., Adams S., Brew B.J., and Guillemin G.J. (2009) Mechanism for quinolinic acid cytotoxicity in human astrocytes and neurons. *Neurotox Res* **16:** 77-86.

Buchan J.R., and Parker R. (2009) Eukaryotic stress granules: The ins and outs of translation. *Mol Cell* **36:** 932-941.

Cattaneo E., Rigamonti D., Goffredo D., Zuccato C., Squitieri F., and Sipione S. (2001) Loss of normal huntingtin function: New developments in huntington's disease research. *Trends Neurosci* **24:** 182-188.

Chan T.F., Carvalho J., Riles L., and Zheng X.F. (2000) A chemical genomics approach toward understanding the global functions of the target of rapamycin protein (TOR). *Proc Natl Acad Sci U S A* **97:** 13227-13232.

Chang Y.W., Chuang Y.C., Ho Y.C., Cheng M.Y., Sun Y.J., Hsiao C.D., and Wang C. (2010) Crystal structure of Get4-Get5 complex and its interactions with Sgt2, Get3, and Ydj1. *J Biol Chem* **285:** 9962-9970.

Chartron J.W., Suloway C.J., Zaslaver M., and Clemons W.M.,Jr. (2010) Structural characterization of the Get4/Get5 complex and its interaction with Get3. *Proc Natl Acad Sci U S A* **107:** 12127-12132.

Chavatte L., Frolova L., Kisselev L., and Favre A. (2001) The polypeptide chain release factor eRF1 specifically contacts the s(4)UGA stop codon located in the A site of eukaryotic ribosomes. *Eur J Biochem* **268:** 2896-2904.

Chen M.X., Chen Y.H., and Cohen P.T. (1993) PPQ, a novel protein phosphatase containing a ser + asn-rich amino-terminal domain, is involved in the regulation of protein synthesis. *Eur J Biochem* **218:** 689-699.

Chernoff Y.O., Derkach I.L., and Inge-Vechtomov S.G. (1993) Multicopy SUP35 gene induces de-novo appearance of psi-like factors in the yeast *Saccharomyces cerevisiae*. *Curr Genet* **24**: 268-270.

Chernoff Y.O., Lindquist S.L., Ono B., Inge-Vechtomov S.G., and Liebman S.W. (1995) Role of the chaperone protein Hsp104 in propagation of the yeast prion-like factor [psi+]. *Science* **268**: 880-884.

Chernoff Y.O., Inge-Vechtomov S.G., Derkach I.L., Ptyushkina M.V., Tarunina O.V., Dagkesamanskaya A.R., and Ter-Avanesyan M.D. (1992) Dosage-dependent translational suppression in yeast *Saccharomyces cerevisiae*. *Yeast* **8**: 489-499.

Chernoff Y.O., Newnam G.P., Kumar J., Allen K., and Zink A.D. (1999) Evidence for a protein mutator in yeast: Role of the Hsp70-related chaperone ssb in formation, stability, and toxicity of the [PSI] prion. *Mol Cell Biol* **19:** 8103-8112.

Cohen F.E., Pan K.M., Huang Z., Baldwin M., Fletterick R.J., and Prusiner S.B. (1994) Structural clues to prion replication. *Science* **264**: 530-531.

Coschigano P.W., and Magasanik B. (1991) The URE2 gene product of *Saccharomyces cerevisiae* plays an important role in the cellular response to the nitrogen source and has homology to glutathione s-transferases. *Mol Cell Biol* **11:** 822-832.

Cosson B., Couturier A., Chabelskaya S., Kiktev D., Inge-Vechtomov S., Philippe M., and Zhouravleva G. (2002) Poly(A)-binding protein acts in translation termination via eukaryotic release factor 3 interaction and does not influence [PSI(+)] propagation. *Mol Cell Biol* **22:** 3301-3315.

Cote J., Quinn J., Workman J.L., and Peterson C.L. (1994) Stimulation of GAL4 derivative binding to nucleosomal DNA by the yeast SWI/SNF complex. *Science* **265:** 53-60.

Courchesne W.E., and Magasanik B. (1988) Regulation of nitrogen assimilation in saccharomyces cerevisiae: Roles of the URE2 and GLN3 genes. *J Bacteriol* **170:** 708-713.

Cox B. (1994) Cytoplasmic inheritance. prion-like factors in yeast. *Curr Biol* **4**: 744-748.

Cox, B. S. (1965) [*PSI*], a cytoplasmic suppressor of super-suppressors in yeast. *Heredity* **20**: 505-521.

Dagkesamanskaya A.R., and Ter-Avanesyan M.D. (1991) Interaction of the yeast omnipotent suppressors SUP1(SUP45) and SUP2(SUP35) with non-mendelian factors. *Genetics* **128:** 513-520.

Decker C.J., Teixeira D., and Parker R. (2007) Edc3p and a glutamine/asparagine-rich domain of Lsm4p function in processing body assembly in *Saccharomyces cerevisiae*. *J Cell Biol* **179:** 437-449.

DePace A.H., Santoso A., Hillner P., and Weissman J.S. (1998) A critical role for amino-terminal glutamine/asparagine repeats in the formation and propagation of a yeast prion. *Cell* **93:** 1241-1252.

Derkatch I.L., Bradley M.E., Hong J.Y., and Liebman S.W. (2001a) Prions affect the appearance of other prions: The story of [PIN(+)]. *Cell* **106:** 171-182.

Derkatch I.L., Bradley M.E., Zhou P., Chernoff Y.O., and Liebman S.W. (1997) Genetic and environmental factors affecting the de novo appearance of the [PSI+] prion in *Saccharomyces cerevisiae*. *Genetics* **147:** 507-519.

Derkatch I.L., Uptain S.M., Outeiro T.F., Krishnan R., Lindquist S.L., and Liebman S.W. (2004) Effects of Q/N-rich, polyQ, and non-polyQ amyloids on the de novo formation of the [PSI+] prion in yeast and aggregation of Sup35 in vitro. *Proc Natl Acad Sci U S A* **101:** 12934-12939.

Derkatch I.L., Bradley M.E., Masse S.V., Zadorsky S.P., Polozkov G.V., Inge-Vechtomov S.G., and Liebman S.W. (2000) Dependence and independence of [PSI(+)] and [PIN(+)]: A two-prion system in yeast? *EMBO J* **19:** 1942-1952.

Diaz-Hernandez M., Torres-Peraza J., Salvatori-Abarca A., Moran M.A., Gomez-Ramos P., Alberch J., and Lucas J.J. (2005) Full motor recovery despite striatal neuron loss and formation of irreversible amyloid-like inclusions in a conditional mouse model of huntington's disease. *J Neurosci* **25:** 9773-9781.

DiFiglia M., Sapp E., Chase K.O., Davies S.W., Bates G.P., Vonsattel J.P., and Aronin N. (1997) Aggregation of huntingtin in neuronal intranuclear inclusions and dystrophic neurites in brain. *Science* **277:** 1990-1993.

Dinger M.E., Mercer T.R., and Mattick J.S. (2008) RNAs as extracellular signaling molecules. *J Mol Endocrinol* **40:** 151-159.

Douglas P.M., Summers D.W., Ren H.Y., and Cyr D.M. (2009a) Reciprocal efficiency of RNQ1 and polyglutamine detoxification in the cytosol and nucleus. *Mol Biol Cell* **20:** 4162-4173.

Douglas P.M., Treusch S., Ren H.Y., Halfmann R., Duennwald M.L., Lindquist S., and Cyr D.M. (2008a) Chaperone-dependent amyloid assembly protects cells from prion toxicity. *Proc Natl Acad Sci U S A* **105:** 7206-7211.

Du Z., Park K.W., Yu H., Fan Q., and Li L. (2008) Newly identified prion linked to the chromatin-remodeling factor Swi1 in *Saccharomyces cerevisiae*. *Nat Genet* **40**: 460-465.

Duffy J.B. (2002) GAL4 system in drosophila: A fly geneticist's swiss army knife. *Genesis* **34**: 1-15.

Engelberg-Kulka H. (1981) UGA suppression by normal tRNA trp in escherichia coli: Codon context effects. *Nucleic Acids Res* **9**: 983-991.

Ferreira P.C., Ness F., Edwards S.R., Cox B.S., and Tuite M.F. (2001) The elimination of the yeast [PSI+] prion by guanidine hydrochloride is the result of Hsp104 inactivation. *Mol Microbiol* **40**: 1357-1369.

Fields S.D., Conrad M.N., and Clarke M. (1998) The S. cerevisiae CLU1 and D. discoideum cluA genes are functional homologues that influence mitochondrial morphology and distribution. *J Cell Sci* **111 (Pt 12)**: 1717-1727.

Flanagan J.F., and Peterson C.L. (1999) A role for the yeast SWI/SNF complex in DNA replication. *Nucleic Acids Res* **27**: 2022-2028.

Fluck M.M., and Epstein R.H. (1980) Isolation and characterization of context mutations affecting the suppressibility of nonsense mutations. *Mol Gen Genet* **177**: 615-627.

Frolova L., Le Goff X., Zhouravleva G., Davydova E., Philippe M., and Kisselev L. (1996) Eukaryotic polypeptide chain release factor eRF3 is an eRF1- and ribosome-dependent guanosine triphosphatase. *RNA* **2**: 334-341.

Frolova L.Y., Tsivkovskii R.Y., Sivolobova G.F., Oparina N.Y., Serpinsky O.I., Blinov V.M., *et al.* (1999) Mutations in the highly conserved GGQ motif of class 1 polypeptide release factors abolish ability of human eRF1 to trigger peptidyl-tRNA hydrolysis. *RNA* **5**: 1014-1020.

Gailer C., and Feigel M. (1997) Is the parallel or antiparallel beta-sheet more stable? A semiempirical study. *J Comput Aided Mol Des* **11**: 273-277.

Garrity S.J., Sivanathan V., Dong J., Lindquist S., and Hochschild A. (2010) Conversion of a yeast prion protein to an infectious form in bacteria. *Proc Natl Acad Sci U S A* **107**: 10596-10601.

Giorgini F., Moller T., Kwan W., Zwilling D., Wacker J.L., Hong S., *et al.* (2008) Histone deacetylase inhibition modulates kynurenine pathway activation in yeast, microglia, and mice expressing a mutant huntingtin fragment. *J Biol Chem* **283**: 7390-7400.

Giorgini F., Guidetti P., Nguyen Q., Bennett S.C., and Muchowski P.J. (2005) A genomic screen in yeast implicates kynurenine 3-monooxygenase as a therapeutic target for huntington disease. *Nat Genet* **37**: 526-531.

Glass N.L., and Kaneko I. (2003) Fatal attraction: Nonself recognition and heterokaryon incompatibility in filamentous fungi. *Eukaryot Cell* **2:** 1-8.

Glickman M.H., and Ciechanover A. (2002) The ubiquitin-proteasome proteolytic pathway: Destruction for the sake of construction. *Physiol Rev* **82:** 373-428.

Goldfarb L.G., Brown P., McCombie W.R., Goldgaber D., Swergold G.D., Wills P.R., *et al.* (1991) Transmissible familial creutzfeldt-jakob disease associated with five, seven, and eight extra octapeptide coding repeats in the PRNP gene. *Proc Natl Acad Sci U S A* **88:** 10926-10930.

Green, R.L. and Warren, G.J. (1985) Physical and functional repetition in a bacterial ice nucleation gene. *Nature* **317:** 645-648.

Gutekunst C.A., Levey A.I., Heilman C.J., Whaley W.L., Yi H., Nash N.R., *et al.* (1995) Identification and localization of huntingtin in brain and human lymphoblastoid cell lines with anti-fusion protein antibodies. *Proc Natl Acad Sci U S A* **92:** 8710-8714.

Hake L.E., and Richter J.D. (1994) CPEB is a specificity factor that mediates cytoplasmic polyadenylation during xenopus oocyte maturation. *Cell* **79:** 617-627.

Harjes P., and Wanker E.E. (2003) The hunt for huntingtin function: Interaction partners tell many different stories. *Trends Biochem Sci* **28:** 425-433.

He F., Brown A.H., and Jacobson A. (1997) Upf1p, Nmd2p, and Upf3p are interacting components of the yeast nonsense-mediated mRNA decay pathway. *Mol Cell Biol* **17:** 1580-1594.

Hegde R.S., Mastrianni J.A., Scott M.R., DeFea K.A., Tremblay P., Torchia M. (1998) A transmembrane form of the prion protein in neurodegenerative disease. *Science* **279:** 827-834.

Helmlinger D., Tora L., and Devys D. (2006) Transcriptional alterations and chromatin remodeling in polyglutamine diseases. *Trends Genet* **22:** 562-570.

Higurashi T., Hines J.K., Sahi C., Aron R., and Craig E.A. (2008) Specificity of the J-protein Sis1 in the propagation of 3 yeast prions. *Proc Natl Acad Sci U S A* **105:** 16596-16601.

Hilditch-Maguire P., Trettel F., Passani L.A., Auerbach A., Persichetti F., and MacDonald M.E. (2000) Huntingtin: An iron-regulated protein essential for normal nuclear and perinuclear organelles. *Hum Mol Genet* **9:** 2789-2797.

Hillenmeyer M.E., Fung E., Wildenhain J., Pierce S.E., Hoon S., Lee W., *et al.* (2008) The chemical genomic portrait of yeast: Uncovering a phenotype for all genes. *Science* **320:** 362-365.

Hinnebusch A.G. (2005) Translational regulation of GCN4 and the general amino acid control of yeast. *Annu Rev Microbiol* **59:** 407-450.

Hofman-Bang J. (1999) Nitrogen catabolite repression in *Saccharomyces cerevisiae*. *Mol Biotechnol* **12:** 35-73.

Holliday R., and Pugh J.E. (1975) DNA modification mechanisms and gene activity during development. *Science* **187:** 226-232.

Hu W., Kieseier B., Frohman E., Eagar T.N., Rosenberg R.N., Hartung H.P., and Stuve O. (2008) Prion proteins: Physiological functions and role in neurological disorders. *J Neurol Sci* **264:** 1-8.

Inge-Vechtomov, S. G. and Andrianova, V. M. (1970) Recessive super-suppressors in yeast. *Genetika* 6:103-115.

Jarret, J.T. and Lansbury, P.T. (1993) Seeding "one dimensional crystallisation" of amyloid: a pathogenic mechanism in Alzheimer's disease and scrapie? *Cell* **73**:1055-1058.

Jia M.H., Larossa R.A., Lee J.M., Rafalski A., Derose E., Gonye G., and Xue Z. (2000) Global expression profiling of yeast treated with an inhibitor of amino acid biosynthesis, sulfometuron methyl. *Physiol Genomics* **3:** 83-92.

Jorgensen P., Edgington N.P., Schneider B.L., Rupes I., Tyers M., and Futcher B. (2007) The size of the nucleus increases as yeast cells grow. *Mol Biol Cell* **18:** 3523-3532.

Kawai-Noma S., Pack C.G., Kojidani T., Asakawa H., Hiraoka Y., Kinjo M., *et al.* (2010) In vivo evidence for the fibrillar structures of Sup35 prions in yeast cells. *J Cell Biol* **190:** 223-231.

Kikuchi Y., Shimatake H., and Kikuchi A. (1988) A yeast gene required for the G1-to-S transition encodes a protein containing an A-kinase target site and GTPase domain. *EMBO J* **7:** 1175-1182.

Kimura Y., Koitabashi S., and Fujita T. (2003) Analysis of yeast prion aggregates with amyloid-staining compound in vivo. *Cell Struct Funct* **28:** 187-193.

King C.Y., Tittmann P., Gross H., Gebert R., Aebi M., and Wuthrich K. (1997) Prion-inducing domain 2-114 of yeast Sup35 protein transforms in vitro into amyloid-like filaments. *Proc Natl Acad Sci U S A* **94:** 6618-6622.

Kisselev L.L., and Frolova L.Y. (1995) Termination of translation in eukaryotes. *Biochem Cell Biol* **73:** 1079-1086.

Kodama H., Ito K., and Nakamura Y. (2007) The role of N-terminal domain of translational release factor eRF3 for the control of functionality and stability in S. cerevisiae. *Genes Cells* **12:** 639-650.

Kramer M.L., Kratzin H.D., Schmidt B., Romer A., Windl O., Liemann S., *et al.* (2001) Prion protein binds copper within the physiological concentration range. *J Biol Chem* **276:** 16711-16719.

Landles C., and Bates G.P. (2004) Huntingtin and the molecular pathogenesis of huntington's disease. fourth in molecular medicine review series. *EMBO Rep* **5:** 958-963.

Lauren J., Gimbel D.A., Nygaard H.B., Gilbert J.W., and Strittmatter S.M. (2009) Cellular prion protein mediates impairment of synaptic plasticity by amyloid-beta oligomers. *Nature* **457:** 1128-1132.

Leeds P., Peltz S.W., Jacobson A., and Culbertson M.R. (1991) The product of the yeast UPF1 gene is required for rapid turnover of mRNAs containing a premature translational termination codon. *Genes Dev* **5:** 2303-2314.

Li, L., and Lindquist, S. (2000) Creating a protein-based element of inheritance. *Science* **287:** 661-664.

Li S.H., and Li X.J. (2004) Huntingtin-protein interactions and the pathogenesis of huntington's disease. *Trends Genet* **20:** 146-154.

Liebman S.W., and Sherman F. (1979) Extrachromosomal psi+ determinant suppresses nonsense mutations in yeast. *J Bacteriol* **139:** 1068-1071.

Lopez N., Aron R., and Craig E.A. (2003) Specificity of class II Hsp40 Sis1 in maintenance of yeast prion [RNQ+]. *Mol Biol Cell* **14:** 1172-1181.

Luke M.M., Sutton A., and Arndt K.T. (1991) Characterization of SIS1, a *Saccharomyces cerevisiae* homologue of bacterial dnaJ proteins. *J Cell Biol* **114:** 623-638.

Luthi-Carter R., Hanson S.A., Strand A.D., Bergstrom D.A., Chun W., Peters N.L., *et al.* (2002) Dysregulation of gene expression in the R6/2 model of polyglutamine disease: Parallel changes in muscle and brain. *Hum Mol Genet* **11:** 1911-1926.

Lykke-Andersen J. (2002) Identification of a human decapping complex associated with hUpf proteins in nonsense-mediated decay. *Mol Cell Biol* **22:** 8114-8121.

Madore N., Smith K.L., Graham C.H., Jen A., Brady K., Hall S., and Morris R. (1999) Functionally different GPI proteins are organized in different domains on the neuronal surface. *EMBO J* **18:** 6917-6926.

Magasanik B., and Kaiser C.A. (2002) Nitrogen regulation in *Saccharomyces cerevisiae*. *Gene* **290:** 1-18.

Manogaran A.L., Fajardo V.M., Reid R.J., Rothstein R., and Liebman S.W. (2010) Most, but not all, yeast strains in the deletion library contain the [PIN(+)] prion. *Yeast* **27:** 159-166.

Marion R.M., Regev A., Segal E., Barash Y., Koller D., Friedman N., and O'Shea E.K. (2004) Sfp1 is a stress- and nutrient-sensitive regulator of ribosomal protein gene expression. *Proc Natl Acad Sci U S A* **101:** 14315-14322.

Masino L., and Pastore A. (2002) Glutamine repeats: Structural hypotheses and neurodegeneration. *Biochem Soc Trans* **30:** 548-551.

Masison D.C., and Wickner R.B. (1995) Prion-inducing domain of yeast Ure2p and protease resistance of Ure2p in prion-containing cells. *Science* **270:** 93-95.

Mathur V., Hong J.Y., and Liebman S.W. (2009) Ssa1 overexpression and [PIN(+)] variants cure [PSI(+)] by dilution of aggregates. *J Mol Biol* **390:** 155-167.

Meriin A.B., Zhang X., He X., Newnam G.P., Chernoff Y.O., and Sherman M.Y. (2002) Huntington toxicity in yeast model depends on polyglutamine aggregation mediated by a prion-like protein Rnq1. *J Cell Biol* **157:** 997-1004.

Meriin A.B., Zhang X., Miliaras N.B., Kazantsev A., Chernoff Y.O., McCaffery J.M., *et al.* (2003) Aggregation of expanded polyglutamine domain in yeast leads to defects in endocytosis. *Mol Cell Biol* **23:** 7554-7565.

Michelitsch M.D., and Weissman J.S. (2000) A census of glutamine/asparagine-rich regions: Implications for their conserved function and the prediction of novel prions. *Proc Natl Acad Sci U S A* **97:** 11910-11915.

Miller J., Arrasate M., Shaby B.A., Mitra S., Masliah E., and Finkbeiner S. (2010) Quantitative relationships between huntingtin levels, polyglutamine length, inclusion body formation, and neuronal death provide novel insight into huntington's disease molecular pathogenesis. *J Neurosci* **30:** 10541-10550.

Miyake T., Reese J., Loch C.M., Auble D.T., and Li R. (2004) Genome-wide analysis of ARS (autonomously replicating sequence) binding factor 1 (Abf1p)-mediated transcriptional regulation in saccharomyces cerevisiae. *J Biol Chem* **279:** 34865-34872.

Mochel F., Charles P., Seguin F., Barritault J., Coussieu C., Perin L., *et al.* (2007) Early energy deficit in huntington disease: Identification of a plasma biomarker traceable during disease progression. *PLoS One* **2:** e647.

Moriyama H., Edskes H.K., and Wickner R.B. (2000) URE3] prion propagation in *Saccharomyces cerevisiae*: Requirement for chaperone Hsp104 and curing by overexpressed chaperone Ydj1p. *Mol Cell Biol* **20:** 8916-8922.

Moore R.C., and Melton D.W. (1997) Transgenic analysis of prion diseases. *Mol Hum Reprod* **3:** 529-544.

Morris N.R. (2000) Nuclear migration. from fungi to the mammalian brain. *J Cell Biol* **148:** 1097-1101.

Morris R.J., Parkyn C.J., and Jen A. (2006) Traffic of prion protein between different compartments on the neuronal surface, and the propagation of prion disease. *FEBS Lett* **580:** 5565-5571.

Nasir J., Floresco S.B., O'Kusky J.R., Diewert V.M., Richman J.M., Zeisler J., *et al.* (1995) Targeted disruption of the huntington's disease gene results in embryonic lethality and behavioral and morphological changes in heterozygotes. *Cell* **81:** 811-823.

Natarajan K., Meyer M.R., Jackson B.M., Slade D., Roberts C., Hinnebusch A.G., and Marton M.J. (2001) Transcriptional profiling shows that Gcn4p is a master regulator of gene expression during amino acid starvation in yeast. *Mol Cell Biol* **21:** 4347-4368.

Neely K.E., and Workman J.L. (2002) The complexity of chromatin remodeling and its links to cancer. *Biochim Biophys Acta* **1603:** 19-29.

Nemecek J., Nakayashiki T., and Wickner R.B. (2009) A prion of yeast metacaspase homolog (Mca1p) detected by a genetic screen. *Proc Natl Acad Sci U S A* **106:** 1892-1896.

Newnam G.P., Wegrzyn R.D., Lindquist S.L., and Chernoff Y.O. (1999) Antagonistic interactions between yeast chaperones Hsp104 and Hsp70 in prion curing. *Mol Cell Biol* **19:** 1325-1333.

Norremolle A., Riess O., Epplen J.T., Fenger K., Hasholt L., and Sorensen S.A. (1993) Trinucleotide repeat elongation in the huntingtin gene in huntington disease patients from 71 danish families. *Hum Mol Genet* **2:** 1475-1476.

Nucifora F.C.,Jr, Sasaki M., Peters M.F., Huang H., Cooper J.K., Yamada M., *et al.* (2001) Interference by huntingtin and atrophin-1 with cbp-mediated transcription leading to cellular toxicity. *Science* **291:** 2423-2428.

Ocampo A., Zambrano A., and Barrientos A. (2010) Suppression of polyglutamine-induced cytotoxicity in *Saccharomyces cerevisiae* by enhancement of mitochondrial biogenesis. *FASEB J* **24:** 1431-1441.

Osherovich L.Z., and Weissman J.S. (2001) Multiple Gln/Asn-rich prion domains confer susceptibility to induction of the yeast [PSI(+)] prion. *Cell* **106:** 183-194.

Pan K.M., Baldwin M., Nguyen J., Gasset M., Serban A., Groth D., *et al.* (1993) Conversion of alpha-helices into beta-sheets features in the formation of the scrapie prion proteins. *Proc Natl Acad Sci U S A* **90:** 10962-10966.

Patel B.K., and Liebman S.W. (2007) "Prion-proof" for [PIN+]: Infection with in vitro-made amyloid aggregates of Rnq1p-(132-405) induces [PIN+]. *J Mol Biol* **365:** 773-782.

Patel B.K., Gavin-Smyth J., and Liebman S.W. (2009) The yeast global transcriptional co-repressor protein Cyc8 can propagate as a prion. *Nat Cell Biol* **11:** 344-349.

Patil C.K., Li H., and Walter P. (2004) Gcn4p and novel upstream activating sequences regulate targets of the unfolded protein response. *PLoS Biol* **2:** E246.

Perutz M. (1994) Polar zippers: Their role in human disease. *Protein Sci* **3:** 1629-1637.

Peterson C.L., Dingwall A., and Scott M.P. (1994) Five SWI/SNF gene products are components of a large multisubunit complex required for transcriptional enhancement. *Proc Natl Acad Sci U S A* **91:** 2905-2908.

Prochnow C., Bransteitter R., Klein M.G., Goodman M.F., and Chen X.S. (2007) The APOBEC-2 crystal structure and functional implications for the deaminase AID. *Nature* **445:** 447-451.

Proft M., and Struhl K. (2002) Hog1 kinase converts the Sko1-Cyc8-Tup1 repressor complex into an activator that recruits SAGA and SWI/SNF in response to osmotic stress. *Mol Cell* **9:** 1307-1317.

Prusiner S.B. (1982) Novel proteinaceous infectious particles cause scrapie *Science* **216:** 136-144.

Rabu C., Schmid V., Schwappach B., and High S. (2009) Biogenesis of tail-anchored proteins: The beginning for the end? *J Cell Sci* **122:** 3605-3612.

Rane N.S., Yonkovich J.L., and Hegde R.S. (2004) Protection from cytosolic prion protein toxicity by modulation of protein translocation. *EMBO J* **23:** 4550-4559.

Reijns M.A., Alexander R.D., Spiller M.P., and Beggs J.D. (2008) A role for Q/N-rich aggregation-prone regions in P-body localization. *J Cell Sci* **121:** 2463-2472.

Resende C.G., Outeiro T.F., Sands L., Lindquist S., and Tuite M.F. (2003) Prion protein gene polymorphisms in *Saccharomyces cerevisiae*. *Mol Microbiol* **49:** 1005-1017.

Riggs A.D. (1975) X inactivation, differentiation, and DNA methylation. *Cytogenet Cell Genet* **14:** 9-25.

Rogoza T., Goginashvili A., Rodionova S., Ivanov M., Viktorovskaya O., Rubel A., *et al.* (2010) Non-mendelian determinant [ISP+] in yeast is a nuclear-residing prion form of the global transcriptional regulator Sfp1. *Proc Natl Acad Sci U S A* **107:** 10573-10577.

Rizet, G. (1952) Les phenomenes de barrage chez *Podospora anserina*. *Rev. Cytol. Biol. Veg.* **13:** 51-92.

Salas-Marco J., and Bedwell D.M. (2004) GTP hydrolysis by eRF3 facilitates stop codon decoding during eukaryotic translation termination. *Mol Cell Biol* **24:** 7769-7778.

Salser W., Fluck M., and Epstein R. (1969) The influence of the reading context upon the suppression of nonsense codons. *Cold Spring Harb Symp Quant Biol* **34:** 513-520.

Sanchez Y., and Lindquist S.L. (1990) HSP104 required for induced thermotolerance. *Science* **248:** 1112-1115.

Satpute-Krishnan P., Langseth S.X., and Serio T.R. (2007) Hsp104-dependent remodeling of prion complexes mediates protein-only inheritance. *PLoS Biol* **5:** e24.

Saupe S.J. (2000) Molecular genetics of heterokaryon incompatibility in filamentous ascomycetes. *Microbiol Mol Biol Rev* **64:** 489-502.

Savas J.N., Ma B., Deinhardt K., Culver B.P., Restituito S., Wu L., *et al.* (2010) A role for huntington disease protein in dendritic RNA granules. *J Biol Chem* **285:** 13142-13153.

Savas J.N., Makusky A., Ottosen S., Baillat D., Then F., Krainc D., *et al.* (2008) Huntington's disease protein contributes to RNA-mediated gene silencing through association with argonaute and P bodies. *Proc Natl Acad Sci U S A* **105:** 10820-10825.

Scherzinger E., Lurz R., Turmaine M., Mangiarini L., Hollenbach B., Hasenbank R., *et al.* (1997) Huntingtin-encoded polyglutamine expansions form amyloid-like protein aggregates in vitro and in vivo. *Cell* **90:** 549-558.

Schlumpberger M., Prusiner S.B., and Herskowitz I. (2001) Induction of distinct [URE3] yeast prion strains. *Mol Cell Biol* **21:** 7035-7046.

Schols L., Bauer P., Schmidt T., Schulte T., and Riess O. (2004) Autosomal dominant cerebellar ataxias: Clinical features, genetics, and pathogenesis. *Lancet Neurol* **3:** 291-304.

Schuldiner M., Metz J., Schmid V., Denic V., Rakwalska M., Schmitt H.D., *et al.* (2008) The GET complex mediates insertion of tail-anchored proteins into the ER membrane. *Cell* **134:** 634-645.

Schuldiner M., Collins S.R., Thompson N.J., Denic V., Bhamidipati A., Punna T., *et al.* (2005) Exploration of the function and organization of the yeast early secretory pathway through an epistatic miniarray profile. *Cell* **123:** 507-519.

Schwimmer C., and Masison D.C. (2002) Antagonistic interactions between yeast [PSI(+)] and [URE3] prions and curing of [URE3] by Hsp70 protein chaperone Ssa1p but not by Ssa2p. *Mol Cell Biol* **22:** 3590-3598.

Si K., Lindquist S., and Kandel E.R. (2003) A neuronal isoform of the aplysia CPEB has prion-like properties. *Cell* **115:** 879-891.

Si K., Choi Y.B., White-Grindley E., Majumdar A., and Kandel E.R. (2010) Aplysia CPEB can form prion-like multimers in sensory neurons that contribute to long-term facilitation. *Cell* **140:** 421-435.

Silveira J.R., Raymond G.J., Hughson A.G., Race R.E., Sim V.L., Hayes S.F., and Caughey B. (2005) The most infectious prion protein particles. *Nature* **437:** 257-261.

Smallridge R. (2002) 'ER we go. *Nat Cell Biol* **4**: E193.

Smets B., Ghillebert R., De Snijder P., Binda M., Swinnen E., De Virgilio C., and Winderickx J. (2010) Life in the midst of scarcity: Adaptations to nutrient availability in *Saccharomyces cerevisiae*. *Curr Genet* **56**: 1-32.

Smith R.L., and Johnson A.D. (2000) Turning genes off by Ssn6-Tup1: A conserved system of transcriptional repression in eukaryotes. *Trends Biochem Sci* **25**: 325-330.

Sokolov S., Pozniakovsky A., Bocharova N., Knorre D., and Severin F. (2006) Expression of an expanded polyglutamine domain in yeast causes death with apoptotic markers. *Biochim Biophys Acta* **1757**: 660-666.

Sondheimer N., and Lindquist S. (2000) Rnq1: An epigenetic modifier of protein function in yeast. *Mol Cell* **5**: 163-172.

Sondheimer N., Lopez N., Craig E.A., and Lindquist S. (2001) The role of Sis1 in the maintenance of the [RNQ+] prion. *EMBO J* **20**: 2435-2442.

Song H., Mugnier P., Das A.K., Webb H.M., Evans D.R., Tuite M.F., *et al.* (2000) The crystal structure of human eukaryotic release factor eRF1--mechanism of stop codon recognition and peptidyl-tRNA hydrolysis. *Cell* **100**: 311-321.

Sparrer H.E., Santoso A., Szoka F.C.,Jr, and Weissman J.S. (2000) Evidence for the prion hypothesis: Induction of the yeast [PSI+] factor by in vitro- converted Sup35 protein. *Science* **289**: 595-599.

Speare J.O., Offerdahl D.K., Hasenkrug A., Carmody A.B., and Baron G.S. (2010) GPI anchoring facilitates propagation and spread of misfolded Sup35 aggregates in mammalian cells. *EMBO J* **29**: 782-794.

Stansfield I., Kushnirov V.V., Jones K.M., and Tuite M.F. (1997) A conditional-lethal translation termination defect in a sup45 mutant of the yeast saccharomyces cerevisiae. *Eur J Biochem* **245**: 557-563.

Stansfield I., Jones K.M., Kushnirov V.V., Dagkesamanskaya A.R., Poznyakovski A.I., Paushkin S.V., *et al.* (1995) The products of the SUP45 (eRF1) and SUP35 genes interact to mediate translation termination in *Saccharomyces cerevisiae*. *EMBO J* **14**: 4365-4373.

Steffan J.S., Kazantsev A., Spasic-Boskovic O., Greenwald M., Zhu Y.Z., Gohler H., *et al.* (2000) The huntington's disease protein interacts with p53 and CREB-binding protein and represses transcription. *Proc Natl Acad Sci U S A* **97**: 6763-6768.

Steffen K.K., MacKay V.L., Kerr E.O., Tsuchiya M., Hu D., Fox L.A., *et al.* (2008) Yeast life span extension by depletion of 60s ribosomal subunits is mediated by Gcn4. *Cell* **133**: 292-302.

Taneja V., Maddelein M.L., Talarek N., Saupe S.J., and Liebman S.W. (2007) A non-Q/N-rich prion domain of a foreign prion, [het-s], can propagate as a prion in yeast. *Mol Cell* **27**: 67-77.

Taraboulos A., Scott M., Semenov A., Avrahami D., Laszlo L., and Prusiner S.B. (1995) Cholesterol depletion and modification of COOH-terminal targeting sequence of the prion protein inhibit formation of the scrapie isoform. *J Cell Biol* **129**: 121-132.

Ter-Avanesyan, M.D., Kushnirov, V.V., Dagkesamanskaya, A.R., Didichenko, S.A., Chernoff, Y.O., Inge-Vechtomov, S.G. and Smirnov, V.N. (1993) Deletion analysis of the *SUP35* gene of the yeast *Saccharomyces cerevisiae* reveals two non-overlapping functional regions in the encoded protein. *Mol Microbiol.* 7: 683-692.

Tipton K.A., Verges K.J., and Weissman J.S. (2008) In vivo monitoring of the prion replication cycle reveals a critical role for Sis1 in delivering substrates to Hsp104. *Mol Cell* **32**: 584-591

Truant R., Atwal R.S., and Burtnik A. (2007) Nucleocytoplasmic trafficking and transcription effects of huntingtin in huntington's disease. *Prog Neurobiol* **83**: 211-227.

Truant R., Atwal R., and Burtnik A. (2006) Hypothesis: Huntingtin may function in membrane association and vesicular trafficking. *Biochem Cell Biol* **84**: 912-917.

True H.L., and Lindquist S.L. (2000) A yeast prion provides a mechanism for genetic variation and phenotypic diversity. *Nature* **407**: 477-483.

Tsukada M., and Ohsumi Y. (1993) Isolation and characterization of autophagy-defective mutants of *Saccharomyces cerevisiae*. *FEBS Lett* **333**: 169-174.

Tucker M., Staples R.R., Valencia-Sanchez M.A., Muhlrad D., and Parker R. (2002) Ccr4p is the catalytic subunit of a Ccr4p/Pop2p/Notp mRNA deadenylase complex in saccharomyces cerevisiae. *EMBO J* **21**: 1427-1436.

Tuite M.F., and Cox B.S. (2009) Prions remodel gene expression in yeast. *Nat Cell Biol* **11**: 241-243.

Tuite M.F., Cox B.S., and McLaughlin C.S. (1987) A ribosome-associated inhibitor of in vitro nonsense suppression in [psi-] strains of yeast. *FEBS Lett* **225**: 205-208.

Tuite M.F., Lund P.M., Futcher A.B., Dobson M.J., Cox B.S., and McLaughlin C.S. (1982) Relationship of the [psi] factor with other plasmids of *Saccharomyces cerevisiae*. *Plasmid* **8**: 103-111.

Tuite, M. F., Mundy, C.R. and Cox, B.S. (1981) Agents that cause a high frequency of genetic change from [psi+] to [psi-] in *Saccharomyces cerevisiae*. *Genetics* **98**: 691-711.

Urakov V.N., Valouev I.A., Kochneva-Pervukhova N.V., Packeiser A.N., Vishnevsky A.Y., Glebov O.O., *et al.* (2006) N-terminal region of *Saccharomyces cerevisiae* eRF3 is essential for the functioning of the eRF1/eRF3 complex beyond translation termination. *BMC Mol Biol* **7:** 34.

van der Merwe G.K., Cooper T.G., and van Vuuren H.J. (2001) Ammonia regulates VID30 expression and Vid30p function shifts nitrogen metabolism toward glutamate formation especially when *Saccharomyces cerevisiae* is grown in low concentrations of ammonia. *J Biol Chem* **276:** 28659-28666.

Vey M., Pilkuhn S., Wille H., Nixon R., DeArmond S.J., Smart E.J., *et al.* (1996) Subcellular colocalization of the cellular and scrapie prion proteins in caveolae-like membranous domains. *Proc Natl Acad Sci U S A* **93:** 14945-14949.

Vincent A., Newnam G., and Liebman S.W. (1994) The yeast translational allosuppressor, SAL6: A new member of the PP1-like phosphatase family with a long serine-rich N-terminal extension. *Genetics* **138:** 597-608.

Vishveshwara N., and Liebman S.W. (2009) Heterologous cross-seeding mimics cross-species prion conversion in a yeast model. *BMC Biol* **7:** 26.

Vitrenko Y.A., Pavon M.E., Stone S.I., and Liebman S.W. (2007a) Propagation of the [PIN+] prion by fragments of Rnq1 fused to GFP. *Curr Genet* **51:** 309-319.

Vitrenko Y.A., Gracheva E.O., Richmond J.E., and Liebman S.W. (2007b) Visualization of aggregation of the Rnq1 prion domain and cross-seeding interactions with Sup35NM. *J Biol Chem* **282:** 1779-1787.

Volkov K.V., Aksenova A.Y., Soom M.J., Osipov K.V., Svitin A.V., Kurischko C., *et al.* (2002) Novel non-mendelian determinant involved in the control of translation accuracy in *Saccharomyces cerevisiae*. *Genetics* **160:** 25-36.

Wang Y., Meriin A.B., Costello C.E., and Sherman M.Y. (2007) Characterization of proteins associated with polyglutamine aggregates: A novel approach towards isolation of aggregates from protein conformation disorders. *Prion* **1:** 128-135.

Watts J.C., Drisaldi B., Ng V., Yang J., Strome B., Horne P., *et al.* (2007) The CNS glycoprotein shadoo has PrP(C)-like protective properties and displays reduced levels in prion infections. *EMBO J* **26:** 4038-4050.

Wickner R.B. (1994) URE3] as an altered URE2 protein: Evidence for a prion analog in *Saccharomyces cerevisiae Science* **264:** 566-569.

Williams F.E., Varanasi U., and Trumbly R.J. (1991) The CYC8 and TUP1 proteins involved in glucose repression in *Saccharomyces cerevisiae* are associated in a protein complex. *Mol Cell Biol* **11:** 3307-3316.

Wong B.S., Chen S.G., Colucci M., Xie Z., Pan T., Liu T., *et al.* (2001) Aberrant metal binding by prion protein in human prion disease. *J Neurochem* **78:** 1400-1408.

Yang L., and Yu J. (2009) A comparative analysis of divergently-paired genes (DPGs) among drosophila and vertebrate genomes. *BMC Evol Biol* **9:** 55.

Yun S., Urbanc B., Cruz L., Bitan G., Teplow D.B., and Stanley H.E. (2007) Role of electrostatic interactions in amyloid beta-protein (A beta) oligomer formation: A discrete molecular dynamics study. *Biophys J* **92:** 4064-4077.

Zajchowski L.D., and Robbins S.M. (2002) Lipid rafts and little caves. compartmentalized signalling in membrane microdomains. *Eur J Biochem* **269:** 737-752.

Zhao Y., Sohn J.H., and Warner J.R. (2003) Autoregulation in the biosynthesis of ribosomes. *Mol Cell Biol* **23:** 699-707.

Zhouravleva G., Frolova L., Le Goff X., Le Guellec R., Inge-Vechtomov S., Kisselev L., and Philippe M. (1995) Termination of translation in eukaryotes is governed by two interacting polypeptide chain release factors, eRF1 and eRF3. *EMBO J* **14:** 4065-4072.